MOBILE METAL IONIZATION: EFFECTIVENESS IN GOLD EXPLORATION

By

Tyson Forbush

RECOMMENDED:

Dr. Sarah Hayes

Dr. Paul Layer

Dr. Rainer Newberry
Advisory Committee Chair

Dr. Paul McCarthy, Chair
Department of Geosciences

APPROVED:

Dr. Paul Layer
Dean, College of Natural Science and Mathematics

Dr. John C. Eichelberger
Dean of the Graduate School

24 June 2016

Date

MOBILE METAL IONIZATION: EFFECTIVENESS IN GOLD EXPLORATION

A

THESIS

Presented to the Faculty

of the University of Alaska Fairbanks

in Partial Fulfillment of the Requirements

for the Degree of

MASTER OF SCIENCE

By

Tyson John Forbush, B.S.

Fairbanks, AK

August 2016

Abstract

A series of investigations and tests vetting the proprietary Mobile Metal Ion™ (MMI) technique for its effectiveness specifically in regards to identify Au concentrations in the subsurface. The Marigold Mine, north central NV, and the Gil Prospect, Interior AK, near Fairbanks, provide two site areas under active exploration and development in drastically contrasting environments. MMI has been widely available as an alternative to conventional soil geochemical methods since the 1990's, during which time it has been used successfully to identify several base metal deposits, mostly in arid climates. Criticisms and reluctance from industry to use the method generally stem from the poor understanding of ion migration mechanisms in the subsurface, and the proprietary extractants' undisclosed composition. While MMI has shown promise in the identification of large base metal deposits, Au is significantly less mobile than other metals at the near surface; a detailed investigation of MMI's ability to identify buried Au deposits is yet to be documented. This thesis conducts a critical review of MMI's overall effectiveness at identifying Au in the subsurface through a combination of small studies investigating both its analytical and geological reproducibility, and comparisons of soil anomalies to subsurface Au identified through drilling. Marigold areas tested with MMI (2007-2009, 2012) are currently being mined, allowing best-case scenario comparisons between ore grade and surface response; whereas at Gil investigations compare MMI responses to total organic carbon (TOC) profiles in soil cores, and test the method's usefulness in variably permafrost-rich soils. Both sites provide comparisons to conventional methods illustrating: MMI's advantages over conventional techniques in situations with between 5 to <100 meters alluvial cover; ineffectiveness over deposits with >100 meters alluvial cover; an interesting case where both MMI and conventional methods identified different portions of a deposit but neither method successfully defined it in its entirety; and strange inter-elemental correlations in the MMI data

that appear to be reflecting how metals concentrate in the soils rather than reflecting bedrock metal correlations. Data also identify how some metals (e.g. As, Bi, Co, Fe, and Zn) preferentially concentrate in the A horizon soils, whereas others such as Au and Ba concentrate in the B horizon. Such results question our generally accepted models of how metals concentrate in soils. The A horizon (commonly considered the zone of leaching) is thought to have lower metal concentrations than the B horizon (zone of accumulation). However if these data are representative, then certain elements preferentially concentrate in the A horizon. Such knowledge will have serious implications on sampling protocols and interpretation of geochemical soil surveys in general.

Table of Contents

Page

Page

List of Figures

Page

Page

Page

List of Tables

Page

Page

List of Appendices

Page

Acknowledgements

A special thanks to the Marigold exploration team (especially James Carver and Andrew Smith) and the Kinross Fort Knox (Gil) exploration department, for making data available, allowing access for sample collection, and for covering select analytical costs. Also thanks to Pierrette Prince and SGS for providing MMI analyses for the two high density sample lines collected on the Marigold property.

I would also like to thank my committee, and Dr. Rainer Newberry specifically for being an instructor who goes the extra mile(s) educating his students. And finally thanks to my wife Sally and son Everitt for your undying support of me in this Alaskan endeavor.

Chapter 1: Introduction

1.1 Use of soils in exploration

Collection and analysis of soil samples is an initial step in exploration for covered mineral deposits. Soil is typically a product of bedrock weathering and soil composition ought to mimic that of underlying bedrock. If a soil sample has an anomalously high concentration of a particular metal or group of metals it is likely that underlying bedrock will also have an anomalously high concentration of those metals. However, conventional soil samples are likely to only reflect composition of the immediately underlying bedrock. Use of soil composition data combined with quality geologic mapping increases the probability that trenching and/or drilling will be targeted over mineralization, if that mineralization is close to the weathering surface (Hoffman, 1986a; Hoffman, 1986b).

In this thesis I present data concerning overall effectiveness of Mobile Metal Ion™ (MMI) techniques with regards to Au deposits. I utilize an existing MMI data set from the Marigold mine in north central Nevada. This dataset is compared to existing subsurface data, and supplemental conventional soil data that I have generated. While Marigold is the main focus of the study, the Gil deposit in interior Alaska serves as a second location providing complementary studies of the Gil's MMI, trench, soil, and drilling data.

1.2 Conventional vs. MMI sampling

By "conventional soil sampling" I refer to a range of industry common practices. However, such samples typically target the regolith, that is, the portion of the soil just above bedrock (C horizon, figure 1.1). In most cases the samples are sieved, with only

the fine-grained fraction analyzed (Thompson, 1986). Ore minerals are typically more susceptible to weathering than silicates, and are thus more likely to become fine particles. Further, solubilized ions of ore elements often adsorb onto clay and/or iron-manganese oxide surfaces, increasing their concentration in the fine-grained fraction. The logic behind targeting the soil in the lower C horizon is that this material is almost certainly derived from the immediately underlying bedrock. Soil closer to the surface could, in many cases, represent transported material unrelated to the bedrock. Such is especially the case where wind, water, or hillside creep has transported near-surface material (Hoffman, 1986a).

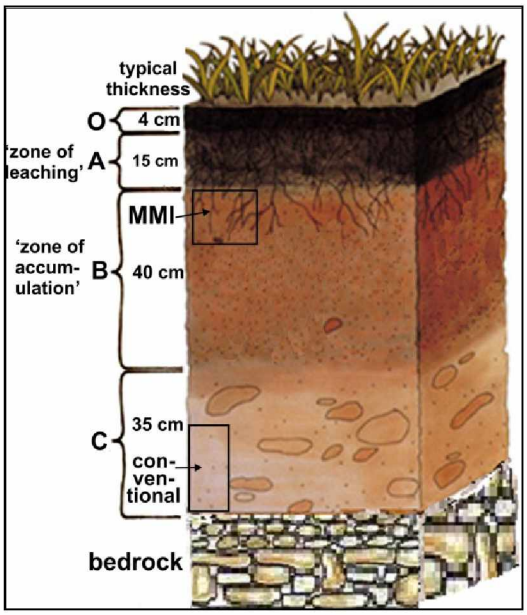

Figure 1.1: Simplified Soil Profile, with typical horizons (O, A, B, C) and thicknesses and also zones targeted by different soil sampling techniques. Modified from Brady (1974).

Once collected and sieved, the samples are usually digested in aqua regia (HCl + HNO_3) or (less commonly) a four acid mix (HCl + HNO_3 + $HClO_4$+ HF). The latter is more expensive, but will cause most minerals to dissolve, including recalcitrant silicate

minerals. Since elements present in silicates are commonly not economically extractible, such 'total digestion' yields information that frequently isn't useful in terms of recoverable resource. After digestion, samples are commonly analyzed using inductively-coupled plasma optical emission spectroscopy (ICP-OES) for lighter elements and inductively-coupled plasma-mass spectrometry (ICP-MS) for heavier elements (Tyler, 2011).

MMI in contrast to conventional soil sampling, does not target regolith, but instead targets the soil B horizon just below the organic rich soil (A horizon, figure 1.1). The underlying logic is that the A horizon, due to low pH associated with decaying organic matter, is the 'zone of leaching'; whereas the B-horizon, with little organic matter is generally the 'zone of accumulation' (Easterbrook, 1999; figure 1.1). MMI is based on the assumption that metal ions released from oxidized ore minerals will migrate up and will be preferentially adsorbed onto clays, Fe-Mn oxides, and lesser organic matter in the 'zone of accumulation'.

Sipos et al. (2008) documented the sorption of Cu, Pb, and Zn in various soil horizons (A, B, C) and found evidence for sorption by organic matter, clay, and Fe-Mn oxides. Mann et al. (2005) documented that MMI-extractable Zn was typically highest in the shallowest (10 cm deep) soil sample (e.g., figure 1.2) but that MMI-extractable Cu, Ag, and Au were highest in the intermediate-depth (20 cm deep) soil. That is, not all elements behave identically, but MMI-extractable concentrations decrease with depth and the 'best' single sample (maximum MMI-extractable concentrations) is typically 10-30 cm below the surface, in the upper B horizon.

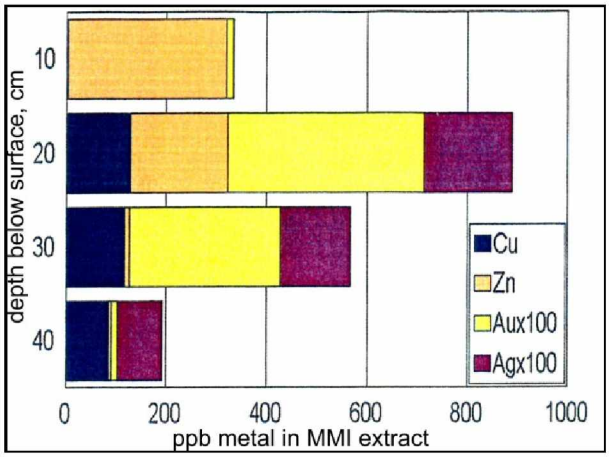

Figure 1.2: MMI-extractable Metals, Cu, Zn, Au, and Ag from soil at variable depth in a single profile from the Hunt Prospect, Manitoba, Canada. Modified from Mann et al. (2005).

Based on studies such as Mann et al. (1995), Mann et al. (1998), Cameron et al. (2004), and Mann et al. (2005), MMI literature recommends using the upper 15 cm of the B horizon (figure 1.1 & 1.2), as this is likely to be most concentrated in mobile (weakly adsorbed) metal ions. During MMI analysis, this fraction of the soil is then digested with a proprietary mix of organic ligands designed to dissolve (by complexing) only the adsorbed ions--without dissolving elements present in solid solution. The goal is to completely leach the adsorbed metal ions but not to dissolve clay, carbonate, oxide, or other minerals present. The solutions generated by this digestion are then analyzed using ICP-MS.

Complications to the soil model presented (figures 1.1 & 1.2) exist in permafrost soils, and those subject to solifluction and cryoturbation; where creep, mixing of soil horizons, and variable depths of soil development can occur due to the formation of ice wedges and freeze-thaw cycles. Bond and Lipovsky (2011) studied soils of the Dawson Range, Canada, and found the distribution and character of permafrost dependent upon

texture of surface material, slope aspect, and topographic position. Further, aqua regia (2-acid) leach profiles of permafrost soils collected near the upper delta of the Lena River, North Eastern Siberia (Antcibor et al., 2014), show peaks in Fe concentration in the A, upper and lower B horizons in the soil; suggesting more complicated metal distribution patterns in permafrost soils than the arid soils for which MMI was developed (Mann et al., 1995). For this reason, the Gil prospect (with soils prone to permafrost and solifluction) provides an excellent trial area for testing MMI's ability to identify subsurface Au in these more complicated soil environments.

1.3 MMI theory and practice

The mobile ions are assumed to be all ions in the oxidized vertical rock column above ore, not merely the oxidizing bedrock immediately under the soil. Mann et al. (2005) argue that the adsorbed ions travel in a more-or-less vertical fashion from the deposit, and thus anomalies produced by MMI truly reflect underlying bedrock to depth. SGS Minerals Services (the proprietor of MMI) thus argues that an MMI survey will produce a sharper and more constrained anomaly than a conventional soil survey.

Several hypotheses have been suggested for the ionic migration responsible for the MMI response, including seismic pumping, convection, and electrochemistry. Goldberg (1998) presented case studies, and experiments exploring mobile ion velocities by diffusion, convection, and electrochemistry. Impressively, Pb and Cu in "damp compacted loam" achieved migration rates of ~2 cm/hour suggesting that under favorable conditions ions could migrate up to 200 m/year (Goldberg, 1998). From the results of several case studies, capillary rise, transpiration, and other hydrological

processes seem to be important variables in the system, at least between the near surface and aquifer dominated zone (Mann et al., 2005). Such is especially the case in arid or semi-arid environments with thick vadose zones, where upward diffusion of dissolved elements is orders of magnitude slower than the downward movement of water films. The only possibilities for the upward transport of elements are mass (advective) transfer of water plus dissolved constituents (Cameron et al., 2004). The responsible mechanisms for any particular environment likely vary. For example, in tectonically active northern Chile, studies suggest that seismic pumping of ground waters is a viable process (Cameron et al., 2004; Leybourne & Cameron, 2007). In situations with thin soils and shallow water tables, capillary rise and transpiration alone are likely sufficient to move mobile metal ion bearing water between the mineral deposit and soil (Mann et al., 2005).

Transportation of ions by the infiltration of rainwater can also create challenges when sampling as the method is prone to changes in response concentrations due to significant levels of precipitation. Figure 1.3 displays MMI Cu responses before and after 40-80 cm of rainfall (SGS Minerals Services, 2009). Note that the concentrations are much lower (half or more) during the second sampling.

Having a method that targets "mobile" ions— those that under appropriate conditions can migrate through tens to hundreds of meters of overburden—is advantageous over conventional methods if searching for deeply buried targets. However, because much of the developmental studies and early successful applications of MMI involved large, disseminated deposits, (Mann et al., 1998) it's unclear how well it works for smaller deposits.

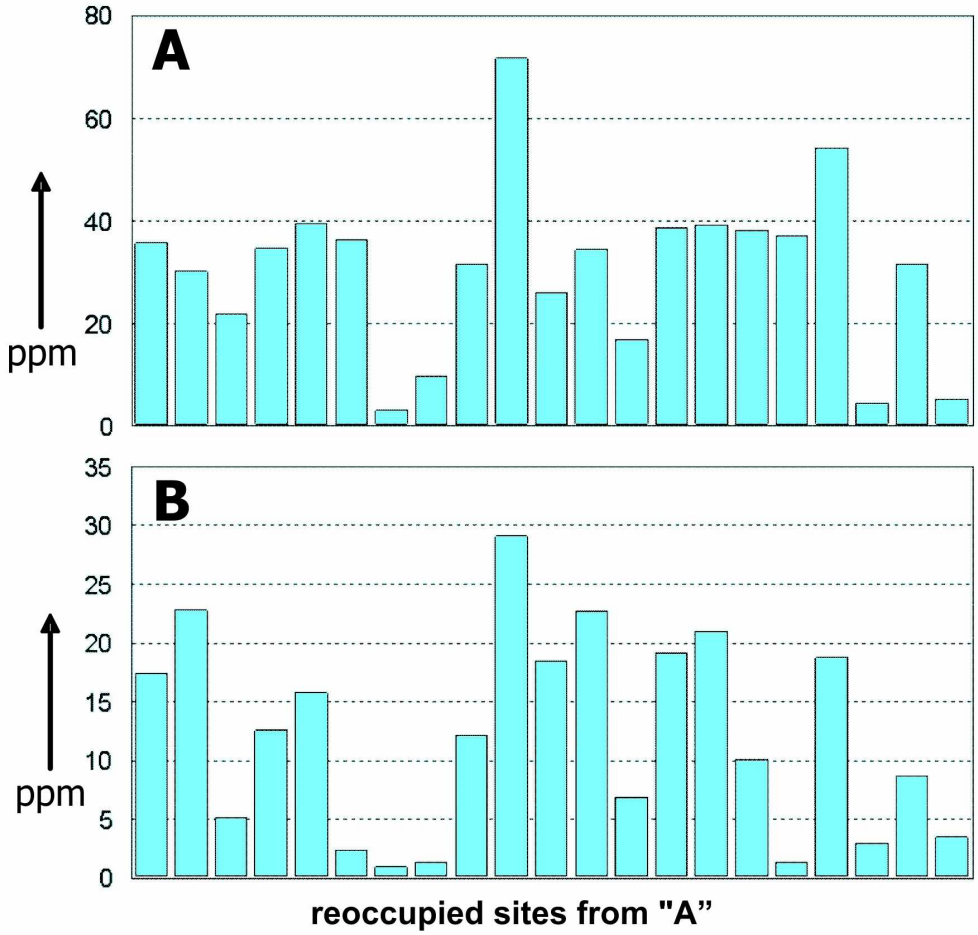

Figure 1.3: MMI Response Before and After Rain, for Cu near Mt. Isa, Queensland, Australia. A- Oct. 2008 (before) and B-Mar. 2009 (after) 40-80 cm of rain. Sample locations relocated to within 5 meters. The large quantities of rain have significantly reduced response magnitudes. Some sites appear to be more affected than others. Modified from SGS Minerals Services, (2009).

MMI has been available commercially since the mid 1990's and has been employed in many regions with variable degrees of success. For example, figures 1.4 and 1.5 present comparisons of MMI and aqua regia (AR, 2-acid) surveys over different ore bodies. Figure 1.4 shows both methods yield largest Cu anomalies that are located >300 m away from (instead of overlying) the main ore body, although the third-highest AR gold anomaly is over the orebody. In this case the AR digest is arguably 'better' than MMI. In contrast, figure 1.5 shows a case where MMI produced a much sharper

anomaly over the ore body than conventional sampling; however, the 'false positive' anomaly at 474250 is also more sharply defined by MMI.

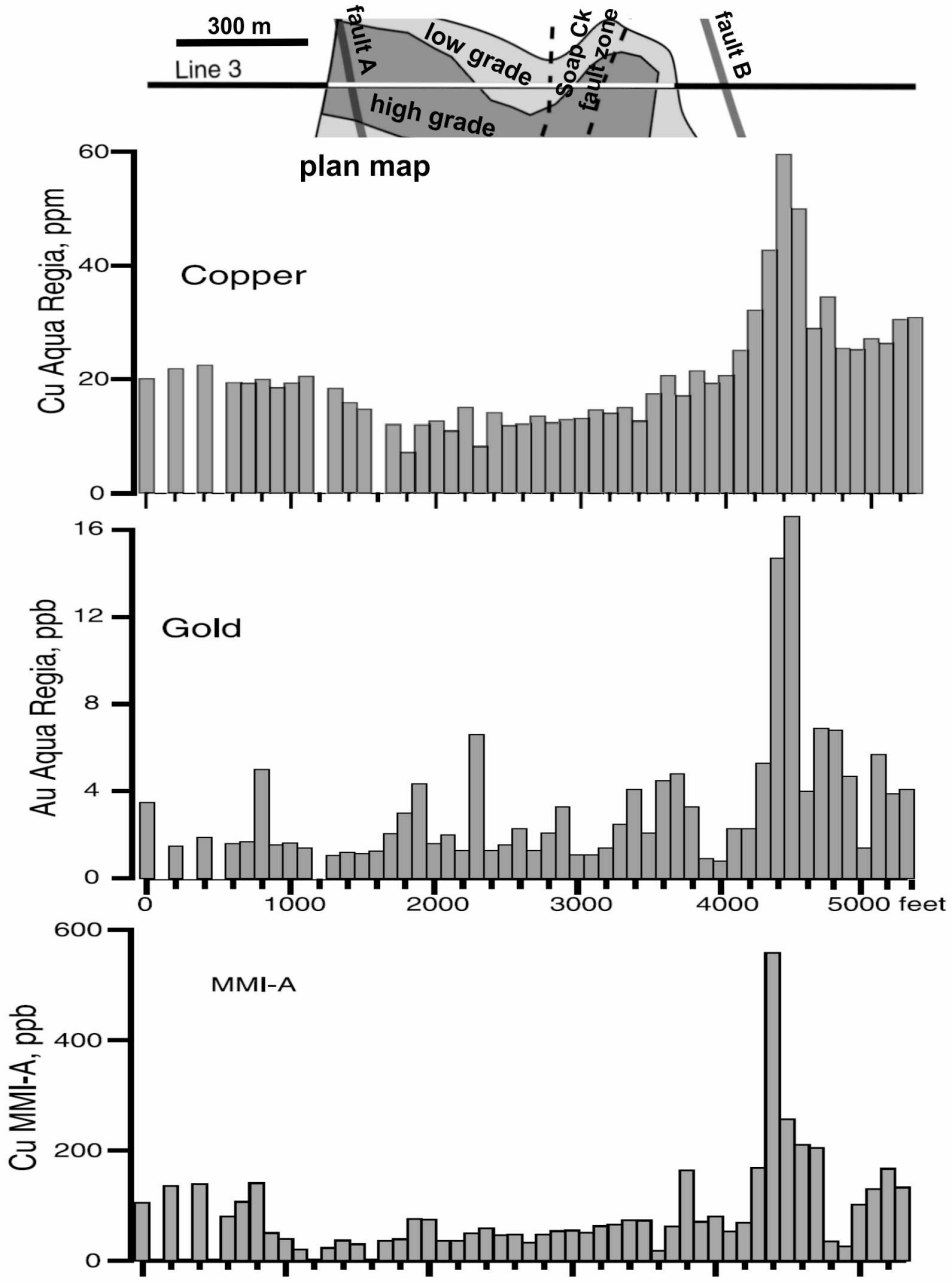

Figure 1.4: Comparison of MMI to aqua regia digested soils-Nevada, digest results for soil samples above the Mike Au-Cu deposit, Nevada. Up to 240 m of unconsolidated sediment overlies the deposit (plan map based on drilling, top). Both digests yield sharp anomalies that are spatially offset from the deposit and known faults. Modified from Cameron et al. (2004).

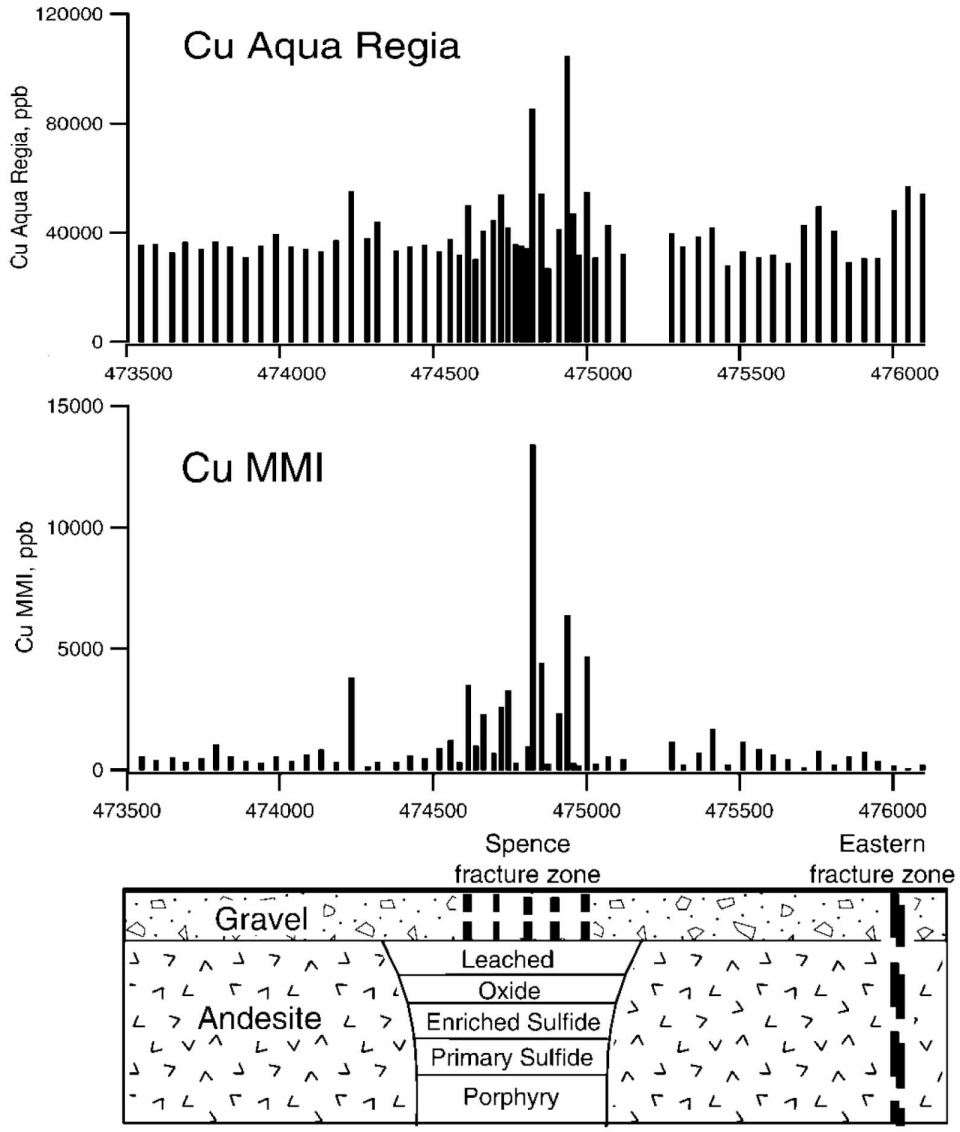

Figure 1.5: Comparison of MMI to aqua regia digested soils-Chile, MMI digest results for soil samples above the Spence Cu deposit, Chile. Cross-section is shown below the soil results. The deposit is covered by 30-180 m of gravel. MMI yields a stronger anomaly and only one false anomaly. Modified from Cameron et al. (2004).

1.4 MMI and other partial extractions

Because the MMI digest is proprietary, the solution composition and pH are not published, making it difficult to predict exactly which chemical species in samples will be dissolved. Cameron et al. (2004) examined overall strength of the MMI digest by comparing total amounts of metal extracted by progressively stronger reagents (figure 1.6). That study showed that the MMI digest targets exclusively the soluble and loosely-bound ions. Concentrations in the MMI solution are 5-20 times higher than that dissolved by de-ionized water; aqua regia dissolves about 50-100 times as much as the MMI solution (figure 1.6).

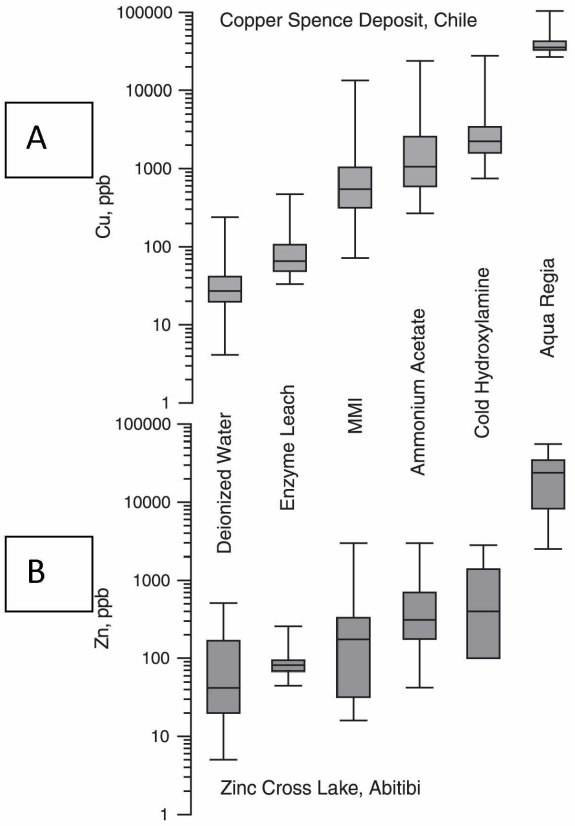

Figure 1.6: Total Metal Extracted by Various Digests, for soils above ore deposits. A= Cu for 63 samples collected over the Spence Cu porphyry deposit, Chile; B =Zn for 54 'B' Horizon soils over the Cross Lake VMS deposit, Ontario. Modified from Cameron et al. (2004).

The MMI extraction is most similar to, although slightly weaker than ammonium acetate, which is commonly used to target sorbed species and carbonate minerals (Dold, 2003).

Conventional soil surveys are complicated by the problem that some metals form negatively charged oxyanions (e.g., AsO_4^{3-}, SbO_4^{3-}, WO_4^{2-}), which are typically not adsorbed onto clay surfaces, and that some elements (e.g., Sn, Ti, Zr, Nb, Ta) do not dissolve appreciably even in 2 or 4 acid digests. Elements of the former group can be adsorbed onto fine-grained iron oxide particles; elements of the latter group will simply not yield ppm-level anomalies in soils even if the underlying bedrock is anomalous in the element. Barium dissolution is complicated by the very low solubility of barite ($BaSO_4$ $K_{sp}=10^{-10.0}$); if significant sulfate is present in either the raw soil or the soil digest after oxidation, it will quantitatively precipitate Ba in solution as $BaSO_4$. Conversely, X-ray Fluorescence (XRF) analysis—which does not depend on dissolving the sample-- gives the total Ba present in a sample. Hence Ba anomalies depend on the analytical techniques employed; for standard acid digests the measured Ba concentrations reflect both the abundance of Ba and digestion conditions.

The MMI technique shares some of the above problems—e.g., oxyanions are not as strongly adsorbed by organic matter as are cations. Similarly, recalcitrant minerals that don't dissolve (e.g., rutile, TiO_2) should not yield MMI anomalies, as the minerals don't appreciably dissolve under natural conditions to form ions. However TiO_2 in another mineral (e.g., biotite) undergoing decomposition by weathering will potentially yield 'mobile' Ti^{4+} ions that might be soluble in partial digests.

In particular, Au is one such low-solubility element/mineral. Because the mineral gold is commonly present as tiny (100 micron to <1 micron) grains, it will be present in

the fine-grained fraction of the soil. Further, because the mineral gold is a Au-Ag solid solution and the Ag is leached out during weathering, larger Au grains form sponge-like masses in an oxidizing environment; these masses are easily broken by physical processes such as freeze-thaw cycles. Finally, gold is soluble in aqua regia due to the formation of Au-chloride complexes and thus can be quantitatively extracted from soil samples. However, extremely low pH and high Eh conditions are required to dissolve significant Au into water with low Cl^- and CN^- concentrations (Garrels & Christ, 1965; figure 1.7). In contrast, typical base metals have solubilities of $\geq 10^{-6}$ molar at near-neutral pH and high Eh (figure 1.7). That is, elemental Au yields extremely tiny concentrations of mobile ions under normal weathering conditions.

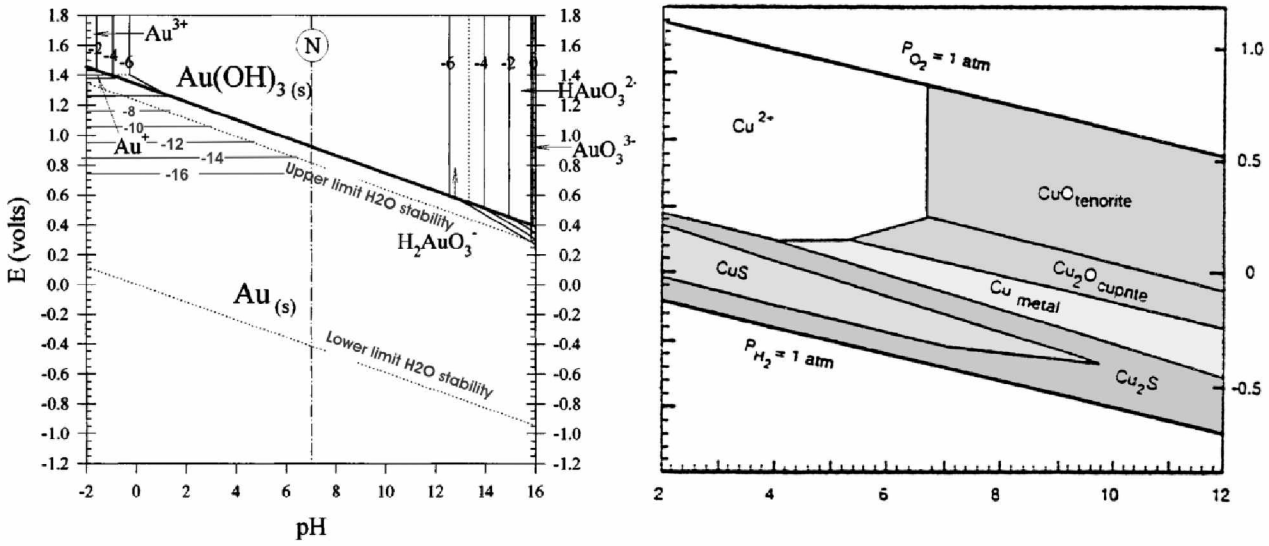

Figure 1.7: Eh-pH diagrams for Au and Cu, Au (left, modified from Marsden & House, 2006) and Cu (right, modified from Garrels & Christ, 1965) in water lacking significant amounts of Cl^-, CN^-, and other common complexing agents. Total S = .01 m and total Cu = 10^{-6} m.

The concentration of Au in a ground water (at saturation) ought to be about 10^{-16} molar (figure 1.7) or 10 billion times smaller than that of base metals in the absence of organic complexing agents. However, if organic species like CN^- are present, Au should be dissolved to a much greater extent. Although organic matter strongly adsorbs Au, the concentration of 'mobile' Au ions in the soil is both a function of the amount of water moving upward and its Au content.

In sum, although the MMI digest is of unknown composition, it is apparently strong enough to dissolve adsorbed metals from soils. If 'mobile' ions truly migrate upward through bedrock and soil, then significant MMI concentrations should be seen in near-surface soils.

1.5 Key considerations for sorption reactions in soils

The vertical migration and subsequent concentration of mobile ions in the upper "B" horizon of the soil through sorption reactions is the fundamental requirement for the success of MMI. Additionally the Marigold ore deposit has had a complex history involving oxidation, re-precipitation, and re-distribution of elements. Thus it is only appropriate to provide a basic overview of sorption reactions.

Sorption is controlled by four primary parameters: 1) particle size and surface area of the sorbents, 2) surface charge of the sorbents and sorptives, 3) concentration, and 4) pH. Two general types of sorption reactions are absorption and adsorption. In the first sorptives are incorporated into the sorbent as a solid solution whereas in the second they adhere to the surface of the sorbent at the sorbent/solution interface (Thompson & Goyne, 2012; figure 1.8). The MMI digest is designed to be weak, thus targeting only adsorbed or more correctly "weakly adsorbed" ions (Mann et al., 1998;

Cameron et al., 2004; Fabris et al., 2009a). Thus parameters controlling these reactions in particular are the most relevant to MMI. Sorbents (in this case, soil particles) that have micro fractures and/or micro pores have a greater surface area than those without (figure 1.8). Additionally, particles with a greater textural or geometric complexity (e.g. from microcrystalline intergrowths) have a greater number of potential adsorptive sites (Ziólkowska et al., 2016).

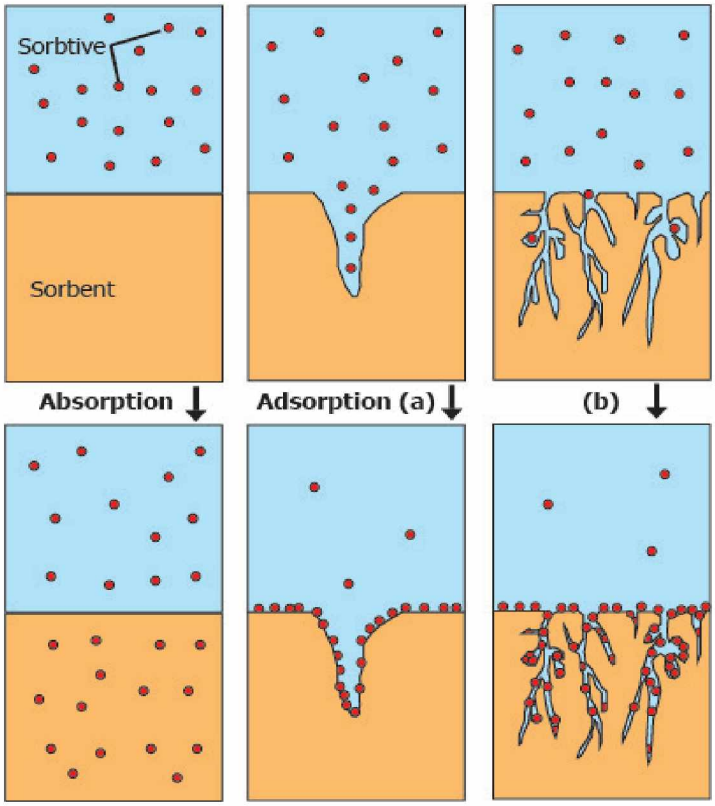

Figure 1.8: Absorption vs. Adsorption, also illustrating the effect of micro fractures/porosity on available surface area and adsorptive sites. Based on principles described by Zumdahl & Zumdahl (2007) and Thompson & Goyne (2012).

In addition to texture, particle size can have a significant effect on surface area. Simply put, the finer the particles the greater the surface area. In particular, Table 1.1 (modified from Langmuir, 1997), shows the increase in area relative to decrease in particle size. If a cubic centimeter was pulverized to 0.01 μm particles, the new surface area would be about that of the floor of a large classroom. For such particles (Table 1.1) approximately 12% of the atoms would be at the surface available for bonding.

Table 1.1: Surface area vs. particle size, modified from Langmuir (1997).

Cube length	Number of Cubes	Area (m^2)	Mol % on surface*
1 cm	1	0.00011	0.00012
10^{-4} cm (1 μm)	10^{12}	1.1	.12
10^{-6} cm (0.01 μm)	10^{18}	110	12

*calculated for hematite

The surface charge of a sorbent will have a significant effect on what it will adsorb. In the case of clays such as kaolinite, the surface charge is predominantly a result of broken bonds at mineral surfaces. As a result, most of the cation exchange capacity (CEC) for kaolinite will be at the particle/solution interface where these broken bonds are present. Other types of clay (such as illite) get most of their CEC from interior lattice charge imbalances. Due to this contrast, clays like kaolinite will have a larger increase in CEC as particle size decreases than those like illite. However, substances for which the bulk of the surface charge comes from broken bonds at edges of mineral surfaces will have CECs that change with pH. As pH decreases, protons in solution will

more effectively compete for sites on the particle surfaces than metal cations. Conversely, materials with a surface charge resulting from interior lattice charge imbalances will maintain a permanent charge and will experience little variation in CEC with change in pH. Table 1.2 (modified from data in Langmuir, 1997) lists some commonly observed substances in soils and their CEC dependence on pH.

Table 1.2: Cation exchange characteristics of common soil constituents*

Substance	Cation Exchange Capacity (CEC) Meq/100 g	pH dependence
Kaolinite	3-15	Strong
Glauconite (green sand)	11-12	Slight
Illite & Chlorite	10-40	Slight
Smectite-montmorillonite	80-150	Absent or negligible
Vermiculite	100-150	Negligible
Organics in soils, humic materials	100-740	Strong
Mn(IV) & Fe(III) oxyhydroxides	290-1020	Strong

*source data: Grim (1968), Brady (1974), Mumpton (1977), Bodek et al. (1988), and Lide (1995)

The total CEC of a soil is caused by: 1) clay minerals, 2) Fe and Mn oxy-hydroxide minerals, 3) carbonate minerals, and 4) organic acids, commonly carboxyl groups (COOH), which deprotonate in the pH ranges of most natural waters. Trace elements can be adsorbed (loosely held on surfaces) by all and absorbed (more tightly held in the crystal lattice) for the first three. In most natural soils an increase in pH will cause both adsorption and absorption of most trace elements, especially cations. Absorption of trace elements during pH increase occurs as ions co-precipitate with major

ions within carbonate and (or) Al, Fe (III), and Mn (IV) oxy-hydroxide mineral lattices (Langmuir, 1997).

CEC's tend to be higher in the A and (especially) B horizons of most soils, resulting from the increased concentrations of clay and organic matter in the upper horizons (Thurman, 1985). Different organic materials will complex to varying degrees with different metals. Metals which are more appreciably complexed with organic matter tend to be the same cations that are readily complexed by CO_3^{2-} and OH^-; for example, Hg^{2+}, Cu^{2+}, and Pb^{2+} (Stumm & Morgan, 1996).

Time and temperature also constitute additional variables in sorption reactions. Carmen & McBride (1998) found sorbed cations to be more strongly sorbed to Fe-oxides after aging and thermal treatment.

In sum, the cumulative effects of all the above parameters dictate the degree and extent of the sorption reactions. Such reactions in soils are responsible for the distribution of the majority of elements sampled by MMI techniques. An understanding of these principles is also relevant to the oxidation and subsequent mobilization and re-precipitation of elements from ore bodies, as is the case with the Marigold study area.

1.6 Geologic summary of the Marigold deposits, Nevada

The Marigold Mine is located three miles south of Valmy, near I-80 in North-Central Nevada (figure 1.9). The geology at Marigold (figure 1.10) is dominated by three Paleozoic packages: the Ordovician Valmy formation, the Pennsylvanian-Permian Antler Sequence (Edna Mountain, Antler Peak, and Battle formations), and the Mississippian to Permian Havallah sequence (Graney & McGibbon, 1991; McGibbon, 2004).

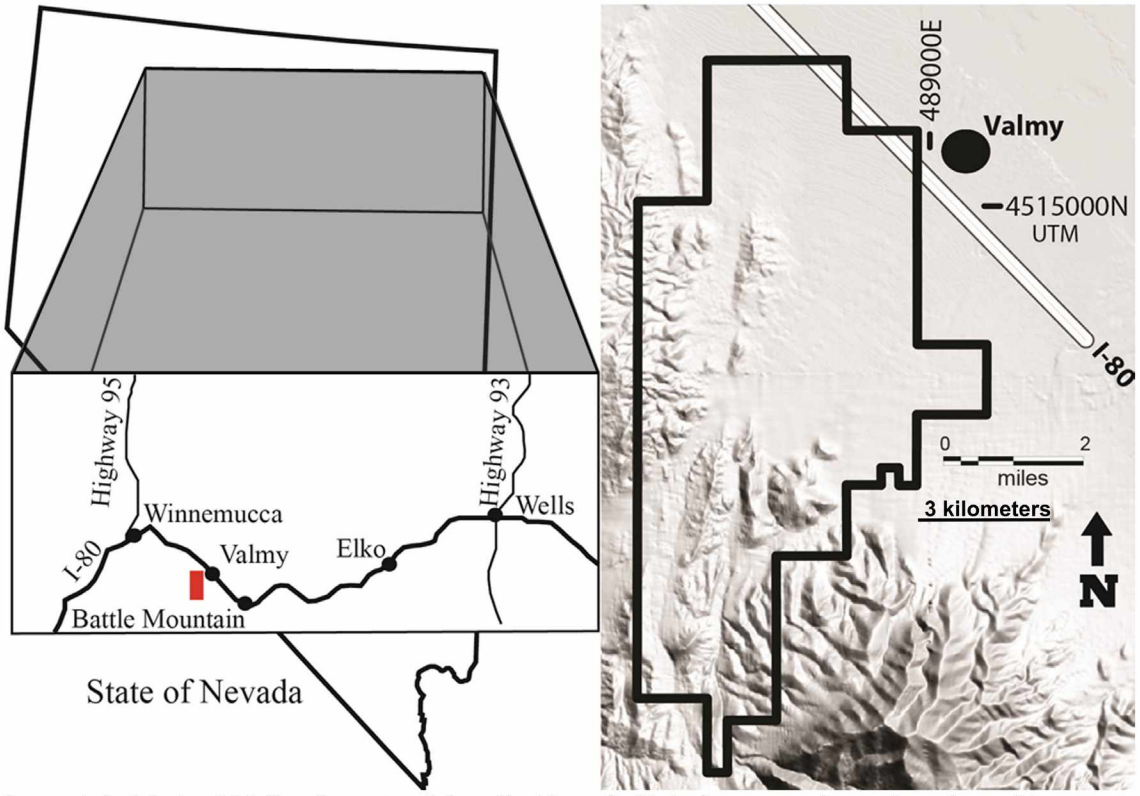

Figure 1.9: Marigold Mine Location Map. Red box (left) is the approximate location of the shaded relief map (right), which shows claim boundaries (thick black lines). Coordinates are NAD83 UTMs in meters.

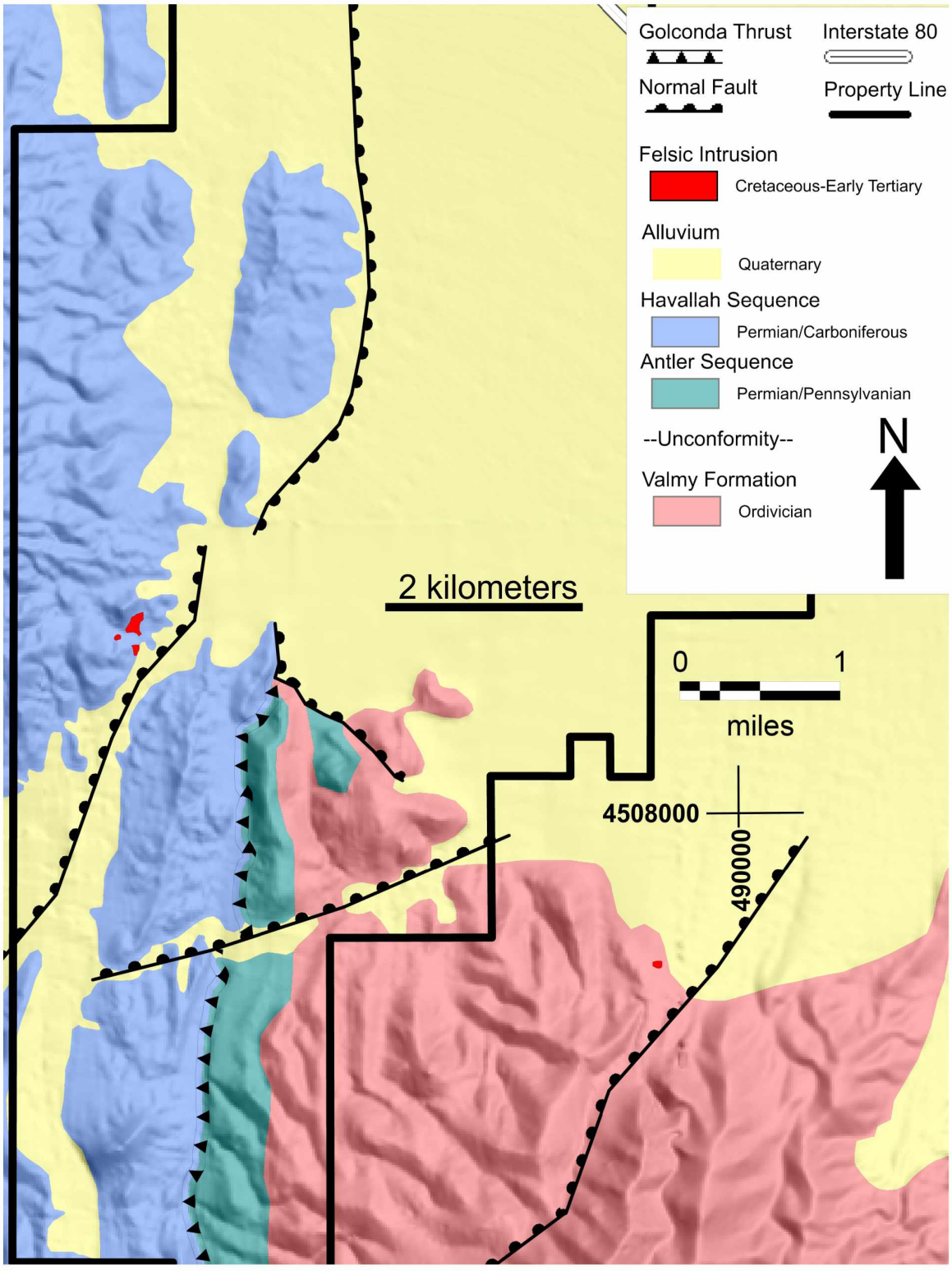

Figure 1.10: Geological Map of the Marigold Mine Area, compiled from unpublished Marigold data. Solid black lines are claim boundaries, as shown on figure 1.9.

The Valmy formation consists of quartzite, chert, and meta-volcanic rocks; the Antler sequence of marine sandstone and shale; and the Havallah of argillite, chert, shale, and meta-volcanic rocks (Graney & McGibbon, 1991). The Antler and Havallah sequences were thrust over the Valmy formation during the Antler and Sonoma orogenies. The bulk of ore is in fractured Valmy quartzite and Antler sequence calcareous sandstone (Smee, 1998; figure 1.11). Regionally, mineralization rarely occurs in Havallah sequence rocks (above the Golconda Thrust); none of the deposits in this study are hosted in the Havallah Sequence (Carver et al., 2014; figure 1.11).

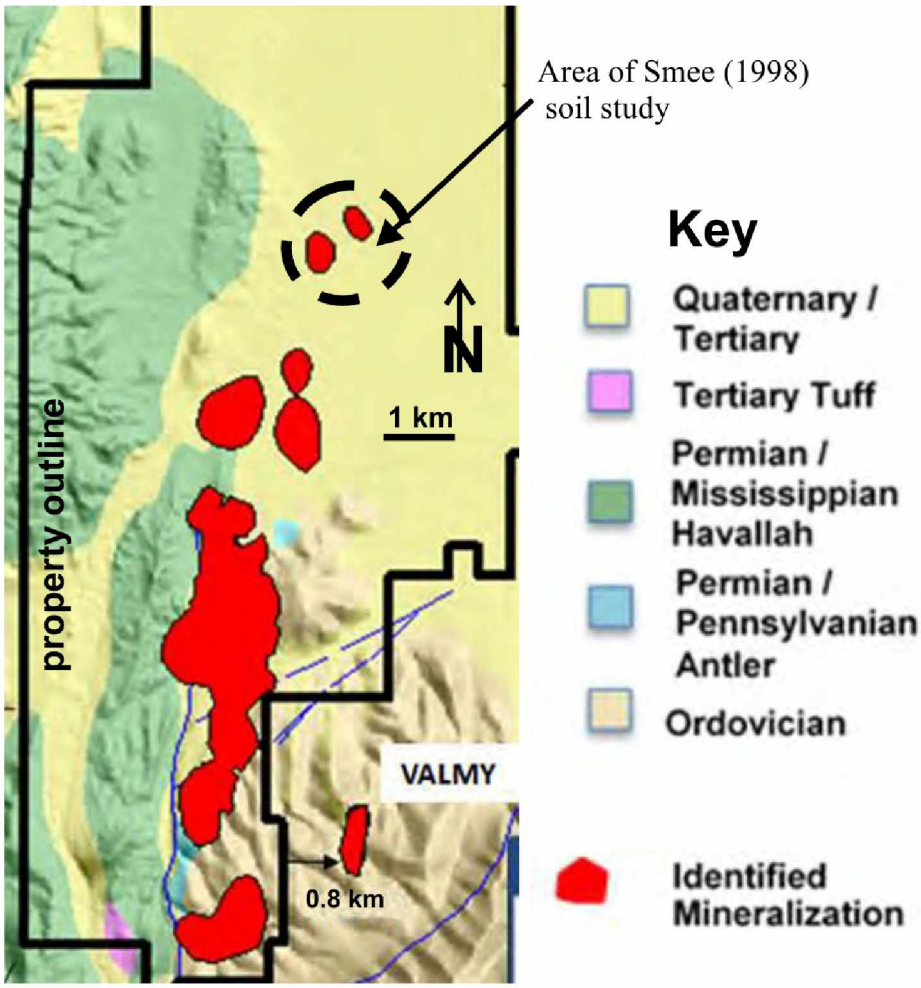

Figure 1.11: Simplified Geological Map of Marigold with Ore Bodies, showing locations of main open pits (current and planned). Property outline (solid black line) is the same as shown on figures 1.9-1.10. Modified from Carver et al. (2014).

The Marigold deposits as well as most others in the Battle Mountain Mining District are considered by many to be distal-disseminated Au systems (e.g., Theodore, 1998; Johnston & Ressel, 2005). That is, they are distal to intrusive-related hydrothermal systems. Theodore (1998) argues that the Marigold ore is the upper portion of a larger porphyry system. Cline et al. (2005) also suggest an igneous-related origin. To the north, at the nearby Lone Tree deposit, Panhorst (1996), identified two phases of alteration, the first of which is potassic and porphyry related. Given that Tertiary volcanic rocks occur within 1.3 km of known ore, that granodiorite bodies occur within 1.3 km of ore (Theodore, 1991a; 1991b; figure 1.10), and that several thin dacite porphyry dikes occur in deep drill holes (DePangher, 2010), the deposits could be related to either Cretaceous plutonism or Tertiary volcanism. Unoxidized ore is Au-bearing arsenian pyrite that contains up to 3% As and 760 ppm Au, typically present as overgrowths on 'normal' pyrite (Fithian et al., 2014).

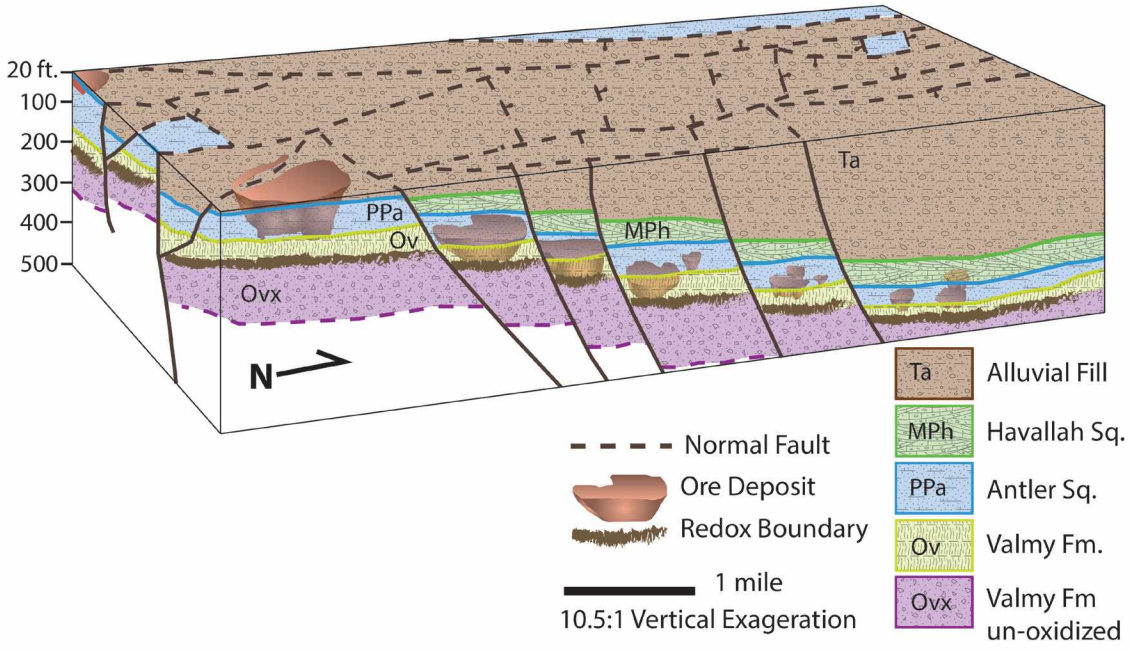

Figure 1.12: Simplified Marigold Deposit Cartoon, illustrating the displacement of ore bodies by post-ore faulting and the subsequent differences in the thickness of alluvial fill above deposits. Compiled from unpublished Marigold drilling sections. Note extreme vertical exaggeration.

The Marigold ore is deeply oxidized (to 700-1200 feet below the surface) and controlled by a combination of structural and stratigraphic elements (figure 1.12). Key features include north and northwest striking extensional faults that acted as conduits for ore fluids and favorable host rocks. Favorable hosts include the highly fractured Valmy quartzite, and in the Antler Sequence a pebble conglomerate and several sandstone units (Graney & McGibbon, 1991). Oxidation plays a key role in the economic viability of the deposit, as Au in solid solution in arsenian pyrite cannot be extracted by conventional cyanide treatment (Marsden & House, 2006; Mahlanga, et al., 2009). Oxidation of the Au-bearing pyrite caused Au to be re-precipitated as fine particles associated with the iron oxide from former pyrite. That an appreciable fraction of the Au has not been so oxidized is indicated by the average Au recovery of 71.6% (Carver et al., 2014). Extensive As-pyrite oxidation presumably released 'mobile' Au into solution.

The deposits at Marigold have been displaced by post-ore faults (figure 1.12), so that they now occur at variable depths, with varying thicknesses of alluvial cover. In general, the depth to the ore increases from south to north (figure 1.12). Isolated, tabular, partly oxidized bodies appear to be typical.

Two aquifers exist on the property, an alluvial aquifer and an underlying bedrock aquifer. The two are in communication with each other, elevations below the surface for the alluvial aquifer are between 35 and 150 meters. Before neighboring dewatering activities throughout the 1990's, maximum depth to the aquifer was ~100 meters (Hoffman, 2010).

Smee (1998) tested the effectiveness of conventional soil geochemistry for identifying two small deposits (figure 1.13; location shown on figure 1.11) that were

known to be buried under 30-100 m of alluvium. Lines 1 and 2, with approximately 30 m of alluvial cover over a hundred m of bedrock above mineralization each yielded one Au-in-soil anomaly. Lines 3 and 4, with 100 m of alluvium over mineralization, yielded no significant Au-in-soil anomalies over mineralized rocks (figure 1.13). Line 3 did yield two false anomalies, each located 100-130 meters away from the deposit at depth. Lack of success in targeting buried mineralization using conventional soil sampling (figure 1.13) prompted the use of MMI surveys in the Marigold area.

Key reasons for choosing the Marigold property as a site for investigation include an abundance of legacy data including significant subsurface data obtained through drilling. Detailed documentation of the variable alluvial thickness (Forbush, 2010; Carver et al., 2014) makes investigations of MMI's effectiveness over different thicknesses possible, and active development of prospects which were sampled by MMI allow for the most real comparisons of MMI Au vs. subsurface Au available.

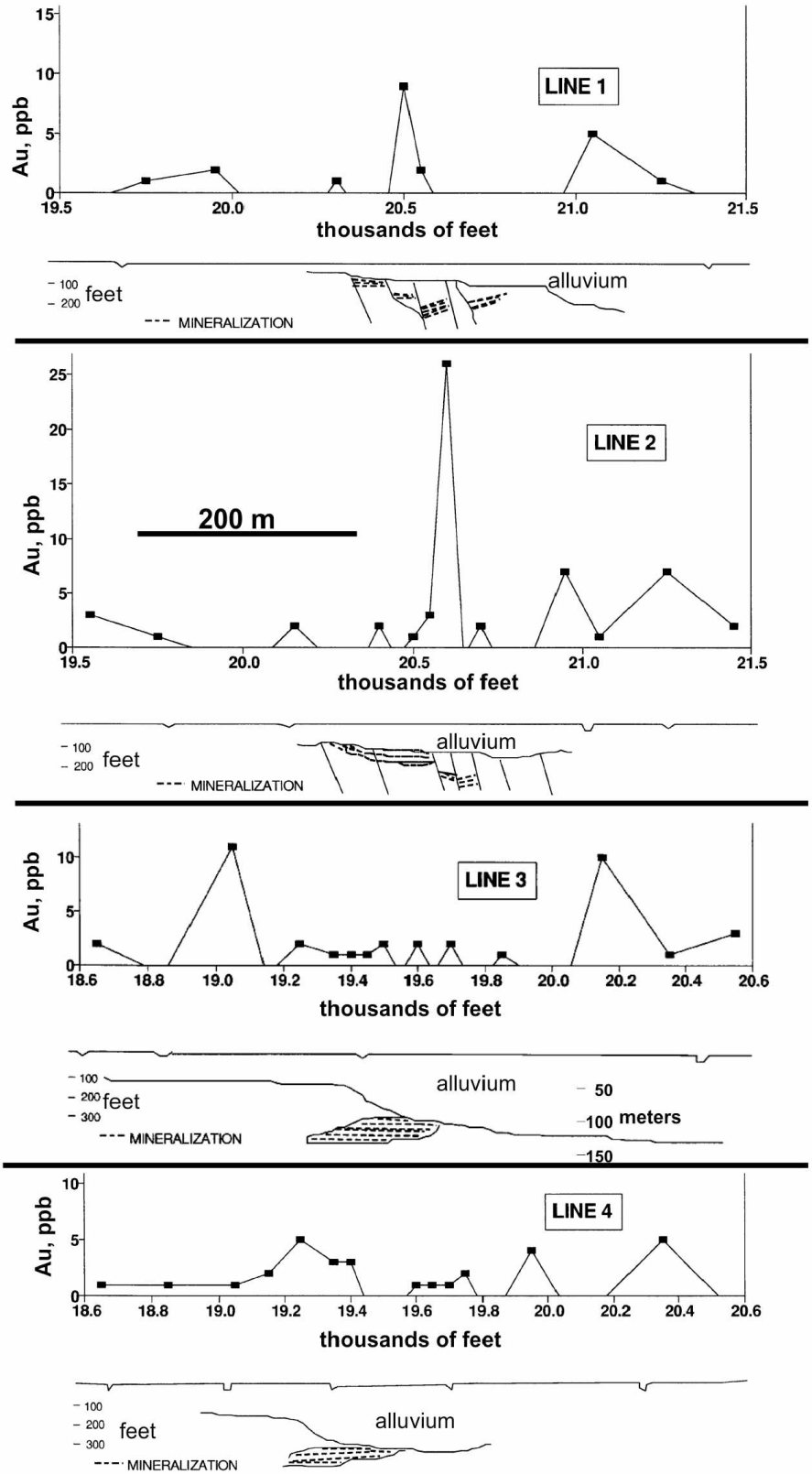

Figure 1.13: Marigold Conventional Soil results for Au. Gold concentrations from conventional soil lines taken over small deposits at North Marigold (Figure 1.11). Vertical exaggeration 0.6:1. Modified from Smee (1998).

1.7 Geologic summary of the Gil prospect, interior Alaska

The Gil Deposit is located 32 kilometers northeast of Fairbanks, Alaska and 10 kilometers northeast of the Fort Knox Mine (figure 1.14) and contains a resource of 0.5 million oz Au contained in 30 Mt at a grade of 0.56 g/t Au (Sims, 2015). The host rocks are lower to mid Paleozoic metavolcanic and metasedimentary rocks ("Fairbanks schist", Robinson, 2010). Gold mineralization at Gil is primarily as quartz-sulfide and quartz-carbonate veins, clay-filled shear zones, and limonite-stained fractures. Gold mineralization is widespread, but higher grade zones are associated with faults, fractures, and preferential carbonate-rich host rocks (Sims, 2015). Gold is associated with Bi and to a lesser degree Te and As (Robinson, 2010).

Figure 1.14: Geology of the area between Gil and Fort Knox, modified from Newberry et al. (1996). Black box encloses the Gil claims area. Rock units include amphibolite-bearing schist (green) and 'Fairbanks schist' (brown), consisting of quartzite and schist. Plutonic rocks in the general vicinity include granite (red) and granodiorite (purple). Tertiary Basalt ('Bs') occurs 1.5 km north of the prospect.

Several small, highly-altered, but un-mineralized quartz diorite dikes predate mineralization. Broadly similar dikes in the district yield Ar^{40}/Ar^{39} and K-Ar ages of 85-95 Ma (McCoy et al., 1995; McCoy et al., 1997). The metamorphic rocks contain contact metamorphic minerals including clinopyroxene and extensive retrograde alteration, suggesting that the deposit is broadly intrusion-related. Alteration in the Main Gil zone is represented by retrograde conversion of higher temperature minerals (e.g., pyroxene, plagioclase) to lower-temperature assemblages.

Legacy studies at the Gil which include conventional soil data, channel samples from exploration trenches, and some drilling provide opportunity for comparisons to MMI. This in combination with the Gil's sub arctic location, accessibility, and previous mineralization studies (Robinson, 2010; Sims, 2015), make the Gil and excellent site for MMI investigations in extremely northern climates. The two site areas will provide complimentary studies; Marigold focusing on reproducibility tests of the MMI technique and comparisons to subsurface ore, while at Gil comparisons to conventional sampling methods and detailed soil profile examinations are made. My hypothesis, tests, and experiments are outlined in detail in the next section.

1.8 Hypotheses to be tested in this thesis

Through this study of MMI I will be testing several different hypotheses. These have bearing on the nature of MMI and the anomalies that are produced. The overall goal is to facilitate explorationists by increasing their understanding of how these anomalies form, what they represent, the degree with which they can be replicated, the effect of various environmental factors, success rates, and comparisons to conventional methods to determine if or when the utility of MMI exceeds existing methods. I do so

through the acquisition of data and subsequent results concerning relevant questions presently unaddressed in literature, and in regards primarily for Au exploration. My hypotheses, tests, and experiments are as follows:

Hypothesis 1: MMI produces elemental correlations similar to mineralized rocks

Given the differences in chemistry of the various ore-related elements and their variable degree of adsorption and extraction into the MMI solution, it is unclear to what extent ore-associated elements (in bedrock) are associated with MMI Au. So-called 'pathfinder elements' are commonly used with or instead of Au, due to the limited chemical mobility of Au and the comparatively low concentrations of Au to other elements. My first hypothesis is that MMI does produce elemental anomalies that mimic rock associations.

I have a limited dataset for metals present with ore at the Marigold deposit. These include 7 composite samples with data for Au, As, Sb, and Hg (Graney & McGibbon, 1991) and another dozen composite and individual samples. The Graney and McGibbon (1991) dataset (Table 1.3) indicates strong Au-As and Au-Sb correlations. I combine these data sets and then determine correlation coefficients for As, Sb, Hg, and others with Au. I also determine correlation coefficients for elements with Au from the MMI surveys and then compare the two.

Table 1.3: Gold correlation coefficients for Marigold mineralization data.

Element	As	Sb	Hg
Au correlation coefficient	0.86	0.97	0.28

The Gil deposit, in the vicinity of the world-class Fort Knox Au deposit, possess a strong Au-Bi relationship (Robinson, 2010). I test for correlations between elements in MMI soil analyses.

In the case of Marigold, I expect to see strong positive correlations in the MMI data between Au, As, and Sb (+ other elements). For the Gil MMI data I expected to see strong positive correlations between Au and Bi (+ other elements). If I do not see such correlations in the MMI data I will know that the various Au-associated elements are concentrating in a manner different from Au.

Hypothesis 2: MMI anomalies are reproducible.

I test the reproducibility of MMI anomalies by comparing results from Marigold MMI samples taken 1.5, 3, 6, and 30 m from each other. I expect closer spaced samples to yield compositions similar to each other and that compositions will become increasingly dissimilar with increasing distance. I also test the reproducibility of results for duplicates taken from splits of the same material. The original Marigold MMI survey contains approximately 750 duplicate samples; these are compared to the original sample to determine the variability. I expect that duplicates will in general agree within 10% of the amount present, but the degree of disagreement will increase with smaller concentrations.

Hypothesis 3: MMI Au anomalies can be correlated with Au concentrations in the sub-surface

I will test this hypothesis using several cross-sections from Marigold and one from the Gil deposit. I use the cross-sections based on drilling to estimate zones of

higher grade in the shallow subsurface and compare the Au drilling values to the MMI soil Au values. I anticipate that MMI will identify Au-enriched zones in the subsurface.

Hypothesis 4: MMI yields well-defined anomalies even in the permafrost-rich soils of Interior Alaska.

For this purpose I employ data for soil cores from the Gil prospect near the Fort Knox mine, Alaska. The core samples are ~30 cm long. I collected 2 cm thick samples along the length of each of these cores. The samples were then analyzed using the MMI extraction and subsequent ICP-MS analysis. Additionally solid phase total organic carbon (TOC) data was collected for each of the analyzed samples. I then compare the MMI results to TOC concentration along the length of the cores. I anticipate that the elemental patterns present will be such that the majority of elements display higher MMI concentrations in the upper portion of the B horizon and thus be consistent with previous studies (Mann et al., 2005; Gray et al., 1999).

Hypothesis 5: MMI yields results that are different from conventional soil surveys but which better reflect the nearby/underlying metal anomalies.

Over the last decade exploration activities involving the Gil deposit have generated MMI and conventional soil data, as well as data from trenches in the same area. I test this hypothesis by comparing values from MMI and conventional soils, with values measured from rocks in nearby trenches.

Chapter 2: Geochemistry of the Marigold Deposit Mineralization

2.1 Marigold ore datasets

To some extent, the effectiveness of Mobile Metal Ionization (MMI) or any other soil geochemical method depends on how well many elemental compositions (and not just the ore element) obtained reflect the metal concentrations in the deposit (Hoffman, 1986a); it can be argued: for a Au deposit, all one cares about are Au concentrations. However, if that's the case, why bother getting any additional compositional data? To compare MMI data I first need to establish what the typical metal concentrations and ratios are at Marigold. Unfortunately, such data is sparse for Marigold. To this end I have attempted several small geochemical projects to describe the mineralized rock compositions. The purpose of this chapter is to present those results.

The data sets (including analytical techniques) are summarized as follows:

- 8 Ore and host samples (variably sub-sampled): X-ray Fluorescence (XRF)
  Analyzed at: Advanced Instrumentation Laboratory- University of Alaska-Fairbanks
- 7 Ore and host samples: 2 acid inductively coupled plasma-mass spectrometry (ICP-MS)
  Analyzed by: SGS Minerals, Vancouver, B.C.
- 21 Drill hole sample composites: 2 acid ICP-MS
  Analyzed by: American Assay Laboratories Inc., Sparks, Nevada
- 16,000 property wide 5 foot drill interval samples: 2 acid ICP-MS
  Analyzed by: American Assay Laboratories Inc.& Inspectorate America Corp., Sparks, Nevada

2.2 Compositions of ore and host samples

Eight ore samples were collected from exposed ore bodies during mining. Their locations (near the south end of the property) are shown on figure 2.1. Ore hand samples 176-179 are from the Antler Sequence and hand samples 180-182 are from within the Valmy Formation. Of the samples, two are heavily oxidized fault gouge, the others are sandstone, quartzite, and shale. Figure 2.2 contains photographs and brief descriptions. Sample preparation details are

in Table 2.1. For samples with obvious fractures, sub-samples ('Fr', Table 2.1) were prepared by concentrating fracture surfaces using a rock saw. Gouge samples were sized using 0.5 mm and 0.05 mm sieves; then each of the three size fractions were separately analyzed (Table 2.1). Following preparation, all samples were pulverized using a SPEX SamplePrep mixer/mill and subsequently formed into 37 mm pressed pellets.

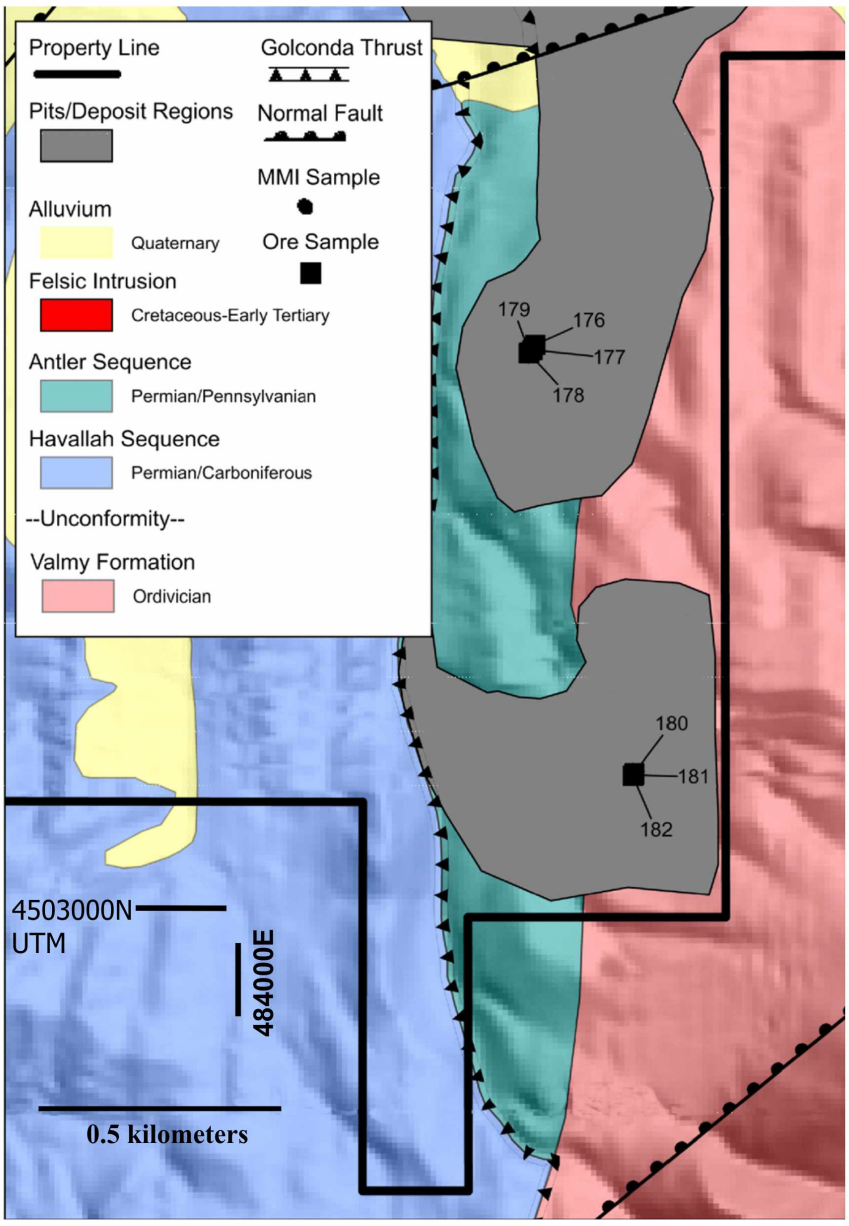

Figure 2.1: Location Map of Marigold Ore Samples, coordinates are WGS84 UTMs in meters. Modified from unpublished Marigold data.

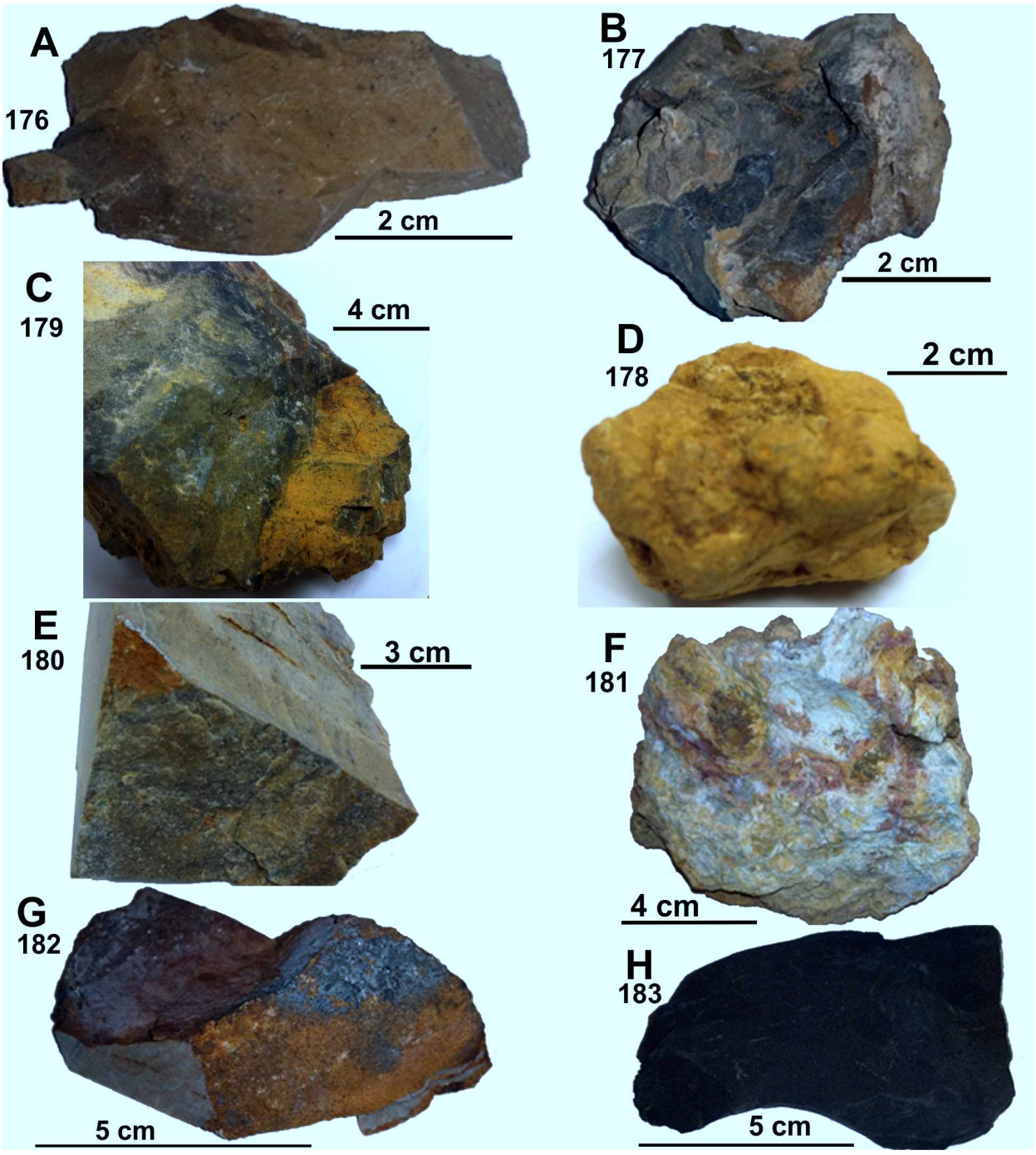

Figure 2.2: Marigold Ore Samples, A=176= Tan, very fined grained, quartz rich sandstone. B= 177 = Fine to medium grained sandstone, black to olive green, ~90% quartz, 10% lithics. Fractures coated with Fe-oxides and calcite. C= 179= Dark, fractured chert, with orange oxide coating on fracture. D= 178 = Yellow-orange gouge, oxidized vein, and fine grained pieces of quartzite. E= 180= Fractured sandstone, light grey, fine to medium grained. Orange oxides in pore spaces and fractures. F= 181= Multi-colored gouge. Original rock may have been a grey siltstone. G= 182 = Fractured quartz sandstone, grains are sub angular to angular with oxides on fracture surfaces. H = 183 = Black, medium to coarse grained calcareous shale, with calcite on fracture surfaces.

XRF results are presented in Tables 2.2 and 2.3.The advantage of XRF is that it yields total elemental abundance and is not affected by incomplete dissolution or post digestion precipitation issues that can be significant challenges for other methods. The limitation, however, is that lower limits of detection(LLD) are much higher (typically 10-1ppm) compared to ICP (typically 1 to<1ppb; Tyler, 2011) and inter-element interferences need to be taken into account; e.g. As $K\alpha$ and Pb $L\alpha$ (Goldstein et al., 2007). In a few cases where Au was below detection by XRF, the Au values from ICP-MS analyses are given.

The samples with higher Au concentrations also contained anomalous concentrations of As and Sb (consistent with results in Graney & McGibbon,1991), Fe , Ni, V, Zn and in some samples Hg and Ba (Tables 2.2, 2.3). For the five samples with whole rock and 'fracture concentrate' subsamples, the fracture 'concentrate' contained significantly higher (2.7 times) concentrations than the whole rock (figure 2.10A). The two gouge samples returned significantly higher gold concentrations than the rock samples (Tables 2.2, 2.3); however, the coarsest fraction of the gouge (>0.5 mm) contained higher gold concentrations than the finer fractions (figure 2.3B).

Because Au and other ore metals were below XRF detection limits for several of the samples, many of the specimens were re-analyzed using ICP-MS techniques. Table 2.1 describes the analytical methods used for each. The ICP-MS samples were treated with a two acid (HCl-HNO_3) digest, which is sufficient to dissolve elements present as sulfides, native metals, or elements adsorbed onto clay or iron oxide surfaces including: Au, Ag, As, Cu, Hg, Pb, and Sb. However, this digest does not appreciably dissolve Al or Ti oxides or elements bound in silicate minerals. Because of this, even though these latter elements (Al/Ti oxides & those bound in silicates) are reported by the lab, I have left them out of Table 2.4.

Table 2.1: Ore Sample Preparation Summary.

Sample #	sub-sample	preparation	analysis
176	176WR	Representative rock including occasional fracture	XRF + ICP-MS
	176Fr	Concentrated 10 gm of fracture-rich material	XRF
177	177WR	Representative rock including occasional fracture	XRF + ICP-MS
	177Fr	Concentrated 10 gm of fracture-rich material	XRF
178	178WR	Gouge, all grain size fractions of material included	ICP-MS
	178vfg	Gouge particles <0.050 mm	XRF
	178B	Gouge fragments >0.5 mm	XRF
	178C	Gouge particles 0.5 mm to.05 mm	XRF
179	179WR	Representative rock including occasional fracture	XRF + ICP-MS
	179Fr	Concentrated 10 gm of fracture-rich material	XRF
180	180WR	Representative rock including occasional fracture	XRF + ICP-MS
	180Fr	Concentrated 10 gm of fracture-rich material	XRF
181	181WR	Gouge, all grain size fractions included	ICP-MS
	181vfg	Gouge particles <0.05 mm	XRF
	181B	Gouge fragments >0.5 mm	XRF
	181C	Gouge particles 0.5 to 0.05 mm	XRF
182	182WR	Representative rock including occasional fracture	XRF + ICP-MS
	182Fr	Concentrated 10 gm of fracture-rich material	XRF
183	183WR	Representative rock including occasional fracture	XRF
	183Fr	Concentrated 10 gm of fracture-rich material	XRF

*Abbreviations: Fr=Fracture, WR=Whole Rock, vfg= <0.05 mm, 0.05 mm<B<0.5 mm, C= >0.5 mm

Table 2.2: XRF Analyses of Marigold Ore Samples- Part 1

Sample ID*	176 Fr	176 WR	177 Fr	177 WR	178_B	178_C	178 vfg	179 Fr	179 WR
Rock Type	Sandstone	Sandstone	Quartz Sandstone	Quartz Sandstone	Orange Gouge	Orange Gouge	Orange Gouge	Chert	Chert
Wt%									
SiO_2 %	92.0	93.9	92.5	93.0	73.7	75.1	70.1	97.0	99.3
Al_2O_3 %	2.8	2.1	1.6	3.3	**7.8**	**5.7**	**10.8**	0.5	0.1
BaO %	0.03	0.03	0.03	0.03	0.07	0.06	0.08	0.14	**0.19**
CaO %	0.65	0.65	0.61	0.52	1.16	0.88	1.07	0.33	0.06
Fe_2O_3 %	2.7	1.7	4.2	0.80	**12.7**	**8.5**	**12.4**	1.64	0.22
K_2O %	0.75	0.59	0.40	1.00	1.73	1.60	2.15	0.09	0.01
MgO %	0.27	0.20	0.15	0.44	0.72	0.51	0.92	0.03	0.05
MnO %	0.05	0.03	0.09	0.01	0.06	0.03	0.13	0.02	0.01
Na_2O %	0.06	0.06	0.04	0.25	0.09	0.07	0.14	0.02	0.03
P_2O_5 %	0.47	0.42	0.09	0.31	**0.85**	**0.63**	**0.73**	0.08	0.01
TiO_2 %	0.15	0.13	0.08	0.22	**0.44**	**0.34**	**0.63**	0.03	0.01
F %		0.01		0.01		0.19			
ppm									
As	341	327	312	9	**2401**	**1811**	**3060**	146	20
Ag	0.5	0.3	0.5	0.8	0.5	1.0	2.0	0.5	0.5
Au[#]	**0.6**	**0.3**[#]	**0.4**	0.1[#]	**1.6**	**5.6**	**2.0**	**0.5**	**0.1**[#]
Co	6	5	5	2	11	7	4	4	3
Cr	64	53	108	88	268	203	270	76	1
Cu	12	20	42	18	**122**	**88**	**139**	9	1
Hg	3	1.3	5	3	3	5	3	3	0.5
Mo	7	11	16	18	3	3	2	14	4
Ni	38	45	61	21	131	101	174	11	1
Pb	15	27	13	28	44	32	34	10	7
Rb	34	31	20	44	71	56	100	11	5
S	167	128	88	567	202	284	893	681	412
Sb	16	13	15	14	**185**	**124**	**195**	17	**4**
Se									
Sr	24	23	19	29	74	54	83	39	34
V	129	124	78	72	**754**	**596**	**900**	78	**21**
W	3	1	6	1	38	26	46	4	1
Y	11	10	5	7	34	1	47	3	3
Zn	100	78	127	73	**704**	**404**	**710**	49	**17**
Zr	20	45	16	124	237	187	820	16	9

*Abbreviations: Fr=Fracture, WR=Whole Rock, vfg= <0.05 mm, 0.05 mm<B<0.5 mm, C= >0.5 mm;
[#]gold analysis by ICP-MS.**Bold=high concentration, Bold= extremely high concentration.**

Table 2.3 XRF Analyses of Marigold Ore Samples- Part 2

Sample ID*	180 Fr	180 WR	181_B	181_C	181 vfg	182 Fr	182 WR	183 Fr	183 WR
Rock Type	Quartzite	Quartzite	Yellow Gouge	Yellow Gouge	Yellow Gouge	Quartz Sandstone	Quartz Sandstone	Calc-Shale	Calc-Shale
Wt%									
SiO_2 %	94.8	98.2	56.2	59.0	59.0	95.5	98.8	72.8	74.8
Al_2O_3 %	2.7	0.9	**26.5**	**23.0**	**23.4**	1.6	0.6	**11.4**	**10.4**
BaO %	0.04	0.02	**0.23**	**0.19**	**0.23**	0.11	0.03	0.07	0.09
CaO %	0.06	0.06	0.22	0.20	0.32	0.06	0.04	5.8	5.9
Fe_2O_3 %	1.4	0.20	**6.5**	**5.5**	**7.8**	1.98	0.18	3.9	2.9
K_2O %	0.54	0.23	6.7	5.4	5.5	0.32	0.12	2.4	2.5
MgO %	0.24	0.09	1.8	1.6	1.5	0.11	0.10	0.81	0.72
MnO %	0.01	0.01	0.01	0.004	0.02	0.03	0.01	0.01	0.02
Na_2O %	0.03	0.04	0.08	0.08	0.10	0.03	0.02	0.19	0.16
P_2O_5 %	0.05	0.05	**0.31**	0.26	**0.66**	0.07	0.03	1.3	**1.6**
TiO_2 %	0.08	0.05	**1.0**	0.82	**0.89**	0.06	0.03	0.57	**0.58**
F %		0.01	0.01	0.27	0.03				0.01
ppm									
As	109	60	**917**	**840**	**1490**	198	32	11	33
Ag	0.5	0.1	0.5	1.0	5.0	0.5	0.5	0.5	
Au[#]	**0.6**	0.1[#]	**4.0**	**6.6**	**5.6**	**4.9**	**1.8**	**0.3**	
Co	4	2	15	10	13	5	2	7	12
Cr	80	98	166	121	182	48	1	812	780
Cu	2	9	27	20	51	10	2	17	32
Hg	4	1	12	20	9	8	0.5	0.5	
Mo	6	2	**22**	**20**	**24**	8	**1**	5	3
Nb		3		34	44		3		9
Ni	6	50	33	42	46	9	20	47	76
Pb	7	93	39	36	**84**	14	5	8	47
Rb	18	14	189	159	170	13	11	127	145
S	252	206	230	219	1050	462	112	303	350
Sb	24	5	**81**	**72**	**127**	24	**4**	18	1
Se				9	26			24	15
Sr	13	25	418	363	856	39	15	158	178
V	39	6	**260**	**221**	**195**	27	**6**	181	232
W	2	2	8	12	63	2	1	4	4
Y	2	7	28	26	32	1	7	50	66
Zn	24	29	**141**	**121**	**243**	33	11	113	113
Zr	71	76	231	211	266	71	78	112	91

*Abbreviations: Fr=Fracture, Wr=Whole Rock, vfg= < 0.05 mm, 0.05 mm<B<0.5 mm, C= >0.5 mm;
[#]gold analysis by ICP-MS.**Bold=high concentration, Bold= extremely high concentration.**

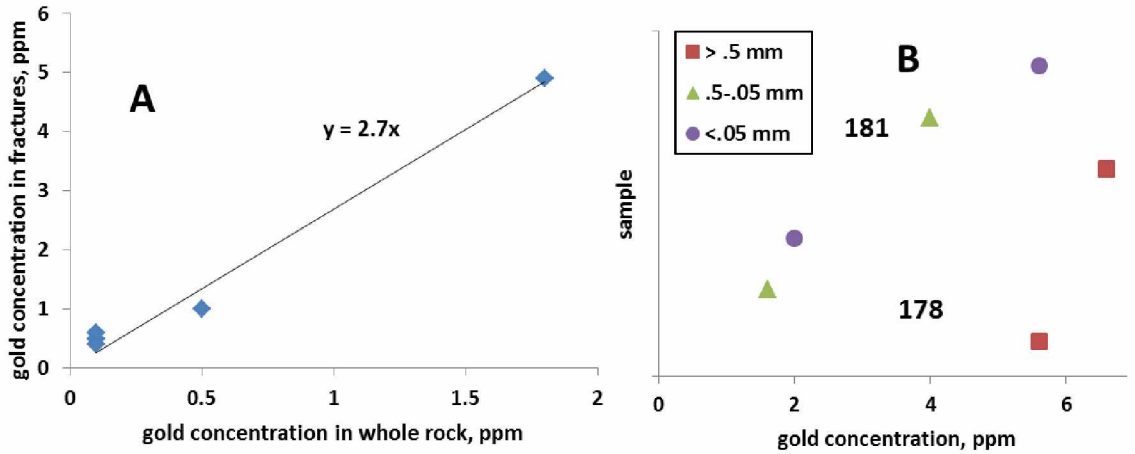

Figure 2.3: Gold concentrations in Mineralized Rock Sub-samples, A = gold in whole rock vs. Au in fracture concentrate. B = gold concentration of different size fractions. Data in tables 2.2 and 2.3.

Table 2.4: ICP-MS analyses for Marigold whole rock samples, excluding elements partially digested*

sample	Au	Ag	Cu	%Fe	As	Mn	Ni	V	Zn	Bi	Cd	Co	Hg	Mo	Pb	Sb	Tl	U
176	0.48	0.25	67	2.05	357	481	45	102	117	0.05	1.52	4.7	1.3	11	13	13	2	3
177	0.05	0.79	53	2.84	346	607	74.6	110	157	0.06	2.02	2.2	3.3	18	9.3	14	1	1.7
178	0.12	0.59	130	7.72	2680	454	137	579	593	0.08	7.69	7.3	3.3	4.9	11	133	1.9	16
179	0.06	0.53	26	1.11	68	149	9.2	14	25	0.01	0.22	2.1	0.5	6	3	4.3	0.1	5.3
180	0.06	0.07	15	0.64	60	56	6.5	3	12	0.01	0.07	1.6	0.8	1.9	1.6	4.9	0.2	0.4
181	4.13	0.12	39	4.0	1100	99	31.8	24	163	0.16	0.67	17	5.7	23	20	60	1.1	4.9
182	2.66	0.19	29	1.74	123	184	15.4	8	20	0.08	0.17	4.5	4.4	6	6.4	11	1.6	0.7

*All concentrations in ppm except Fe in wt%.

Table 2.5 summarizes the inter-elemental correlations for ore elements for as analyzed by XRF (plus some Au ICP values). This table excludes elements that 1) are below the detection limit in more than 1/3 of the samples and 2) where correlations are below the critical r value (0.51, n=14). Particularly high correlations appear in bold text. Notable correlations include Au-Hg (r = 0.79); As-Sb-Cu-Ni-Zn-V-Fe (r = 0.92-0.98); and W-Pb-Sb-Ag (r = 0.83-0.88). The second group consists of elements that are likely to be sorbed onto iron oxide surfaces. These same elements are most concentrated in the finest-grained (<0.05 mm) fractions of the gouge samples (Tables 2.2 and 2.3). Interestingly, gold does not correlate

appreciably with elements of this group and is in higher concentrations in the coarser-grained fractions of the gouge (figure 2.3 B).

Table 2.5: Significant* r values for 14 rock samples analyzed by XRF (+ some ICP Au values)

	Ba	*Fe*	*Mn*	*As*	*Ag*	*Au*	*Bi*	*Cu*	*Hg*	*Ni*	*Pb*	*V*	*Zn*	*Sb*
As		**0.96**	0.59											
Bi		0.57		0.69										
Cu		**0.94**	0.71	**0.96**			0.58							
Hg	0.59					**0.79**								
Ni		**0.91**	0.76	**0.92**			0.59	**0.97**						
Pb	0.54	0.69		0.65	**0.83**	0.63		0.51						
S					**0.78**		0.56				0.54			
V		**0.93**	0.6	**0.95**			0.63	**0.96**		**0.96**				
Zn		**0.95**	0.65	**0.96**			0.55	**0.99**		**0.96**		**0.98**		
Sb		**0.97**		**0.98**			0.64	**0.93**		**0.87**	0.73	**0.93**	**0.94**	
W		0.81		0.84	**0.83**		0.56	0.76		0.7	**0.88**	0.68	0.75	**0.87**
Mo	0.71					0.50			0.74		0.54			

*critical r (95% prob) for 14 samples = .514, **bold=high correlation**.

Table 2.6 gives significant correlation coefficients for the 7 samples analyzed by ICP-MS, excluding elements partially digested in the 2-acid mix. The significantly correlated elements include Au-Bi-Hg (r =.81-.84); Fe-Cu-As-Ni-V-Zn-Cd-Sb-U (r = .89-1.0); and Bi-Co-Hg-Pb (r = .88-.94). The Fe-associated group is essentially the same as that identified by XRF, with additional elements present below detection by XRF. The addition of Bi as a gold-associate might be spurious, as all the values are very low (<0.2 ppm; Table 2.4).

Table 2.6: Significant* correlation coefficients for 7 hand specimens, analyzed via ICP-MS techniques

	Au	*Cu*	*Fe*	*As*	*Ni*	*V*	*Zn*	*Bi*	*Cd*	*Co*	*Mo*	*Sb*
Fe		**0.90**										
As		**0.88**	**0.98**									
Ni		**0.96**	**0.91**	0.86								
V		**0.96**	**0.9**	**0.92**	**0.94**							
Zn		**0.95**	**0.97**	**0.97**	**0.95**	**0.97**						
Bi	0.84											
Cd		**0.97**	**0.92**	**0.92**	**0.96**		**0.98**					
Co	0.81							**0.93**				
Hg	0.81							**0.94**				
Pb								**0.89**		**0.88**	0.79	
Sb		0.85	**0.98**	**1.00**	0.83	**0.89**	**0.95**		**0.89**			
U		0.86	**0.89**	**0.93**	0.80	**0.91**	**0.92**		**0.9**			**0.92**

*critical r for n =7 is 0.755; **bold=high correlation**

2.3 Metal correlations in Marigold composite samples

A second attempt at characterizing the Marigold ore's geochemistry involved the investigation of 21 legacy composite samples. The samples were originally made by combining equal amounts of 8-10 pulverized samples, each representing 1.5 m of drilling from a single drill hole. A total of 21 composites were made from 8 different drill holes. The degree to which the various sub-samples represent the original samples, the degree to which sub-samples were of equal weights, and the degree to which the various sub-samples were homogenized before analysis is not known.

The composites provide a broader or less localized view than the ore hand samples. Concentrations (Table 2.7) are lower by an order of magnitude than the 8 ore samples (Tables 2.2-2.5), e.g. 4-13 ppm Sb (Table 2.7) compared to 1-195 ppm Sb (Tables 2.2-2.5), but generally the same elements (i.e. Au, As, Sb, and Fe with which many elements have co-precipitated) yield significant concentrations.

Table 2.7: Analyses* of drill hole composite samples, in ppm unless indicated otherwise

smpl	Au-F	Au-I	As	Co	Cu	%Fe	Hg	Mn	Mo	Ni	Pb	Sb	Tl	U	W	Zn	%S
C1	0.96	0.24	84	2.6	33.1	2.24	0.1	186	3.2	29	3	13	0.1	0.2	2.1	11	0.03
C2	0.79	0.18	115	3.5	26.4	2.32	0.4	270	2.7	36	3.3	5.7	0.6	1.2	2.3	11	0.37
C3	0.51	0.43	217	4.8	32.4	2.43	0.6	484	3.2	64	3.4	12	0.8	0.8	8	21	0.11
C4	0.93	0.14	308	4.2	7.9	1.68	0.3	59	4.8	28	2.5	5.8	0.5	0.7	1.8	15	1.02
C5	0.45	0.19	77	1.9	9.5	0.6	0.3	127	7.4	28	1.2	5.2	0.4	0.2	3.3	7	0.03
C6	0.34	0.17	163	3.5	32.1	1.14	0.5	56	7.5	45	4.2	6.7	0.2	0.3	7.9	25	0.5
C7	0.38	0.16	254	3.5	15.3	1.75	0.5	125	7.3	41	2.6	8.9	0.4	0.5	3.9	12	0.48
C8	0.07	0.02	78	2.75	27.4	1.59	0.8	59	4.2	31	3.9	3.8	0.3	0.6	1.2	23	0.03
C9	0.1	0.05	43	1.3	4.5	0.38	0.1	44	8.2	29	0.7	2.3	0.1	0.1	6.2	4	0.03
C10	0.48	0.4	305	2.8	17.2	1.06	0.2	61	6.3	26	3.8	19	0.1	0.5	2.8	26	0.2
C11	0.41	0.25	272	5.8	24.8	1.2	0.2	80	7	31	4.1	6.6	0.3	0.5	16	31	0.11
C12	1.85	0.72	89	1.1	19.2	0.4	0.2	284	4.1	18	1.4	9.3	0.7	0.1	2.3	13	0.03
C13	0.72	0.33	206	2.5	8.5	1.14	0.7	87	6.4	30	2.3	17	0.4	0.3	1.4	14	0.03
C14	0.24	0.11	202	2.9	20.6	1.03	0.5	90	6.6	30	6.3	8	0.4	0.4	2.2	24	0.03
C15	0.31	0.12	118	3.3	12.1	1.27	0.6	100	2.4	16	3.4	6.2	0.4	0.6	3.3	27	0.32
C16	0.19	0.05	79	3.2	23.8	0.9	0.3	53	2.6	12	2.9	4	0.1	0.3	11	27	0.01
C17	1.47	0.73	97	2	20.1	0.53	0.6	122	4.8	24	2.1	7.2	0.3	0.2	2	13	0.03
C18	0.34	0.15	276	3.7	19.2	1.55	0.8	79	6.7	31	4.8	18	0.3	0.7	1.2	26	0.06
C19	0.75	0.27	64	1.3	7.9	0.54	0.3	123	5.1	23	1	3	0.1	0.2	2	6	0.03
C20	0.27	0.12	277	2.5	10.6	1.18	0.5	52	4	20	2.5	13	0.1	0.3	6.8	14	0.03
C21	0.41	0.15	231	6.7	18.8	1.17	0.4	113	6	26	4.1	16	0.1	0.4	32	17	0.03

*All except 'Au-F' (gold by fire assay) by ICP-MS following a 2-acid digest; analysis by American Assay Laboratories Inc.

Correlation coefficients (Table 2.8) for the drill hole composite samples are much lower than those of the 'ore samples', with a maximum r of 0.8 compared to maximum r = 1.0 for the ore samples (Tables 2.4, 2.6). The best correlation is between Au by fire assay (FA) vs. Au by ICP-MS, but the concentrations as given by the two techniques are quite different and for each sample, Au concentration by FA is always higher than Au by AR digest-ICP-MS (Table 2.7). Hoffman et al. (1998), noted this as a common problem and suggested that encapsulation of Au in a silicate mineral could be responsible for partial extraction by aqua regia. Despite this problem, the Au as measured by both techniques yields near-identical correlation coefficients for Mn (.46-.52) and Tl (.5-.48).

For this data set the most significant correlations include: As-Sb (r =0.69); Co-W (r=0.69); Fe-U (r =0.76); Pb-Zn (r=0.8); and Mn-Tl (r=0.73). A strong As-Sb correlation is in agreement with the ore hand sample data set as well as with data provided by Graney & McGibbon (1991). Notably none of the elements in this dataset correlate particularly well with Au (maximum r = 0.52), Hg (maximum r = 0.49), or Tl (maximum r <0.52), meaning that the potential use of other elements as pathfinders for Au (as indicated by this data set) is not promising. Silver and Bi were not included in the correlation calculations because more than half of the values were below the detection limits. Due to the various analytical and sampling problems associated with this data set, it should be employed with limited confidence.

Table 2.8: Significant* correlation coefficients for 21 drill hole composite samples

	Au-F	*Au-I*	*As*	*Co*	*Cu*	*Fe*	*Hg*	*Mn*	*Ni*	*Pb*	*Tl*
Au-I	**0.84**										
Co			0.63								
Cu				0.45							
Fe			0.45	0.57	0.63						
Mn	0.46	0.52			0.48	0.5					
Mo											
Ni					0.52	0.63		0.58			
Pb			0.53	0.63	0.60	0.49	0.49				
Sb			**0.69**	0.4	0.27						
Tl	0.50	0.48						**0.73**	0.50		
U				0.54		**0.76**			0.47	0.49	0.52
W				**0.69**							
Zn			0.48	0.59	0.54		0.44			**0.80**	

*critical r (95%) for n=21is0.43; Au-F = Au by Fire Assay; Au-I = Au by ICP-MS;
Bold=high correlation.

2.4 Sulfide and oxide ores at Marigold

A final data set is for several thousand 1.5 m interval drill hole cuttings. These are problematic, as they have been analyzed by different laboratories at different times, with different detection limits. They also are derived from a variety of sites around the property and represent a variety of different host rocks. Finally, they represent a variety of depths. Most are strongly oxidized (similar to the samples analyzed by XRF) but a significant number (from deep intercepts) contain fresh sulfide, as indicated by high (up to 3%) concentrations of sulfur. High-sulfur intercepts are restricted to drill hole depths greater than 600 feet (182 m; figure 2.4) indicating that pervasively oxidized rocks are present to at least 180 m below the surface. Low sulfur concentrations in deeper samples suggest that partial oxidation is still present at considerable depths.

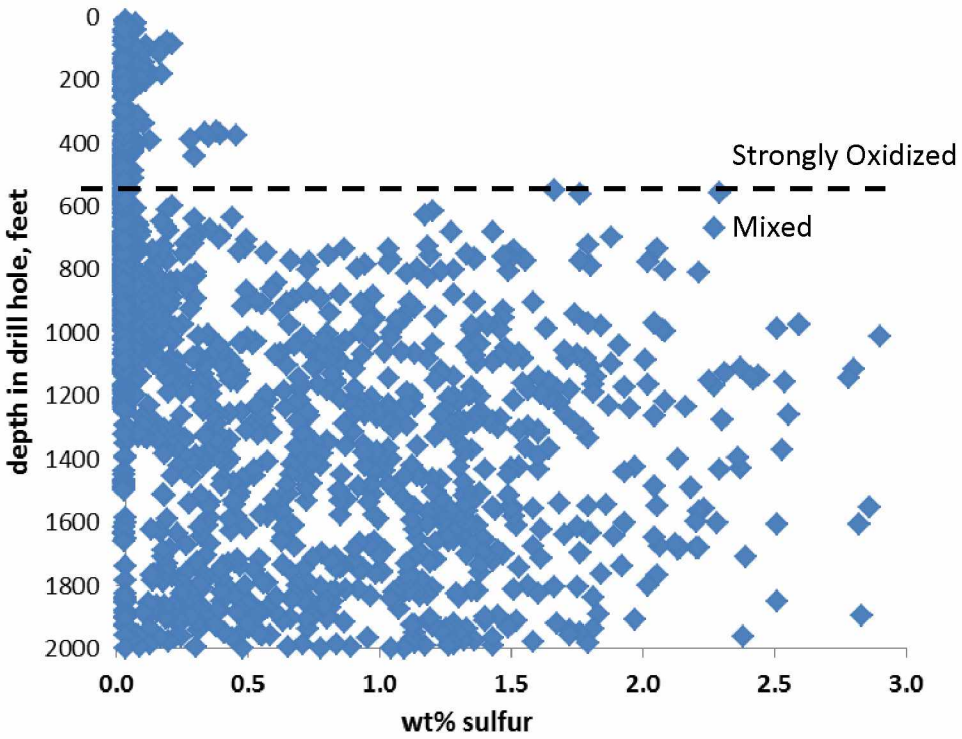

Figure 2.4: Weight % S vs. Drill Depth, for several thousand samples from Marigold drilling. Data from unpublished Marigold sources.

Table 2.9: Average elemental concentrations* in high-Bi intercepts, Marigold Mine

Au	Ag	As	Bi	Co	Cu	%Fe	Mn	Mo	Ni	Pb	%S	Sb	Se	Tl	Zn
0.05	0.1	35	874	6	2135	3.10	394	551	89	2121	1.05	4	4	0.4	352

*concentrations in ppm unless indicated otherwise

One odd ore type present in only one drill hole (but multiple deep intercepts in that hole) is rich in Bi, Pb, Mo, and Cu (Table 2.9). This ore type is of unknown origins. Intercepts with the Bi-rich assemblage grossly skew the elemental correlations if left in the data set. Consequently, they were not included in further investigations.

That sulfide-rich (unoxidized) and sulfide-poor (oxidized) ores have different metal associations is illustrated by the variation between tables 2.10 and 2.11, correlation coefficients for samples with >1.5% S and <1% S, respectively. These correlations suggest changes in the mineralization before and after surficial oxidation. Oxidized ore is both expected to produce more mobile ions and is also closer to the surface; therefore, MMI samples are expected to more closely reflect oxidized metal associations.

The higher-sulfur samples (Table 2.10) display a strong Au-As correlation (r= 0.77), consistent with results reported by Fithian et al. (2014) and modest Fe-Co-S correlations (r=0.58), consistent with the presence of Co-bearing pyrite and an association between Au and arsenian pyrite. The very strong Cd-Zn correlation (r =0.92) is consistent with Cd in solid solution in sphalerite and the strong Se-Ag correlation (r=0.91) suggests the presence of an Ag-Se phase in the unoxidized material. The weaker Ni-Mo-U association is of unknown origins.

In contrast, the lower-sulfur samples (Table 2.4) display a modest As-Hg-Tl association (r = 0.41-0.51) and a weak correlation with Au (r = 0.31-0.32). Arsenic displays a weak

negative correlation with S, indicating that these rocks are truly oxidized and contain little sulfide. Both the Cd-Zn and Ag-Se correlations are still present, but are much smaller (r = 0.48-0.63) indicating these elements were partly re-distributed during oxidation. In these rocks Ni correlates with Cu (r =0.7), and a modest Fe-Mn-Ni-(Cu-Co) association is present.

In sum, the correlations for sulfur-rich rocks make sense given the presence of reasonable sulfide ore minerals (Hoffman, 1986a). The oxidized ore correlations are more difficult to interpret because they still in part reflect the original pre-oxidation mineralogy, but also give evidence for a partial redistribution of elements and metal associations developed during oxidation.

Table 2.10: Significant* correlation coefficients for samples with S>1.5%

	Au	*Ag*	*As*	*Cd*	*Co*	*Cu*	*%Fe*	*Hg*	*Mo*	*Ni*	*Se*	*Th*	*U*
As	**0.77**												
Cd		**0.78**											
Co													
Cu		0.32											
%Fe					**0.58**								
Hg	0.26	0.31	0.35	0.39									
Mo		**0.67**		**0.65**		0.21		0.40					
Ni		**0.69**		**0.63**		0.22		0.31	0.58				
Pb									0.21				
%S					0.27		**0.58**						
Sb			0.32										
Se		**0.91**		**0.77**		0.36		0.32	**0.65**	**0.67**			
Th					0.27	**0.52**	0.22						
Tl	0.35		0.55					0.42					
U		**0.69**				0.44		0.27	**0.65**	**0.56**	**0.70**	0.31	
Zn		**0.70**		**0.92**		0.23		0.37	0.55	**0.59**	**0.67**		**0.61**

*r critical for n = 373 is 0.11;**bold=high correlation, bold=extremely high correlation.**

Correlation coefficients for 161 Au-rich (>1 ppm Au) intercepts indicate a modest Au-Ag-Sb (As) association with r=0.4-0.57 (Table 2.12). The relatively strong Cu-Fe-Ni and the low S concentrations of these samples indicate that they are predominantly oxidized rocks.

Table 2.11: Significant correlation coefficients for 1809 samples with <1% S

	Au	*Ag*	*As*	*Bi*	*Cd*	*Co*	*Cu*	*%Fe*	*Hg*	*Mn*	*Mo*	*Pb*	*%S*	*Se*	*Th*	*Tl*
As	0.31															
Bi			0.28													
Cd		0.26														
Cu		0.25														
%Fe						0.31	0.23									
Hg			**0.47**		0.37											
Mn								**0.47**								
Mo		0.29			**0.46**											
Ni							**0.70**	**0.54**		0.30						
Pb		0.22	0.23													
%S			-0.29													
Se		**0.48**			0.29						0.30					
Th												0.30	0.29			
Tl	0.32		**0.51**	0.33					**0.41**			0.22	-0.28			
U			0.44	0.37	0.41						0.23	0.26		0.23		**0.7**
Zn		0.32			**0.63**				0.32		0.38		0.32		0.29	

bold=high correlation

Table 2.12: Significant* correlation coefficients for samples with >1 ppm Au

	Au	*Ag*	*As*	*Bi*	*Cd*	*Cu*	*%Fe*	*Hg*	*Mn*	*Mo*	*Ni*	*%S*	*Sb*	*Se*	*Th*	*Tl*
Ag	**0.41**															
As	0.21															
Cd			0.35													
%Fe			0.34			0.24										
Hg			0.26		**0.89**											
Mn	0.23		0.39		0.25		0.23									
Ni			0.43			**0.67**	**0.51**		0.31	0.24						
%S			0.34			0.22		0.31		0.28						
Sb	**0.40**	0.27	**0.57**				0.29		0.27		**0.51**	0.28				
Se			0.33		**0.52**	0.24		**0.78**				0.37				
Th			0.27	0.51			0.23				0.25		0.2			
Tl				0.23		0.40	0.21	0.31			0.41	0.31	0.3	0.24	0.50	
U				**0.73**				**0.74**							**0.69**	0.44
Zn			0.37		**0.80**		0.23	**0.90**			0.24		0.3	0.39		

*r critical (95% confidence) for 161 samples = .155; **bold=high correlation, bold=extremely high correlation.**

2.5 Summary of Marigold metal correlations

In sum, analysis of a wide variety of ore types and materials by a variety of techniques broadly confirms earlier suggestions (Graney & McGibbon, 1991) of an Au-As-Sb elemental association in the ores. However, this association depends on the degree to which the ores are oxidized, a process which tends to cause As and Sb to be associated with iron oxide (Cheng et al., 2009; Asta et al., 2012) and not as strongly associated with Au (e.g., Tables 2.5, 2.8, 2.12). The most consistent elemental association is between Zn and Cd, a reflection of the similar characteristics of these two elements.

Soil surveys in the general vicinity of Marigold ought to reflect metal associations similar to those just mentioned, the key association being Au-Sb-As. Considering MMI specifically, the method samples "mobile" ions, essentially requiring the deposit(s) to be sufficiently oxidized to liberateions to travel up through the subsurface which are subsequently concentrated in the upper B horizon soils. That such is the case is indicated by the considerable depth required for significant sulfur to be present in drill hole samples (e.g., figure 2.4). If the various elements present in the Marigold ores behave similarly to each other with regards to low temperature metal transport, and adsorption onto (and release from) fine-grained materials, then one would expect the same sorts of metal associations present in the oxidized ore to be seen in the MMI data.

Chapter 3: Mobile Metal Ion Investigations of the Marigold Deposit

3.1 Introduction to Marigold MMI studies

Presented in this chapter are several investigations regarding Mobile Metal Ionization (MMI) relative to the Marigold deposit, a low grade Au deposit in a fringe arid/semi-arid (Köppen scale) climate (Peel et al., 2007). Together these are aimed at testing the overall utility of the method for Au exploration in such a climate. I investigate reproducibility both analytically and geologically, make comparisons to conventional soil data, and compare anomalies with ore identified through exploration drilling. These studies test 1) geologic reproducibility of MMI, 2) reproducibility of MMI with respect to time, 3) comparisons to conventional soil sampling techniques, 4) comparisons to subsurface drilling, and 5) overall effectiveness of deposit identification. These studies employ multiple cross-sections, with locations shown on figure 3.1.

3.2 Marigold soil properties

The soils at Marigold have been described as aridisols; they are generally tan to gray in color and have a texture that ranges from silt to sand, and in several areas have a trace of pedogenic carbonate (Smee, 1998). Little horizon development is observed, the amount of alluvial fill between the bedrock and the soil ranges from more than 100 m in the basins on the northern portions of the property to cm in the mountainous southern region. Three soils from various un-mineralized locations on the property collected at the 10-20 cm depth (B horizon), yielded a relatively basic pH between 8.1 and 8.5. Smee (1998) recorded pH measurements in the C horizon of 7.7 - 9.6.

3.3 Methods

For the initial MMI orientation survey in 2007, samples were collected at 15 cm and at 76 cm depth. The shallower samples returned higher concentrations. A standardized collection procedure developed that involved digging a collection pit with either a pick axe or chisel-ended rock hammer followed by the identification of the maximum depth of root hairs (trichomes), usually 8-16 cm below the surface; root hair maximum depth was the best indicator in the field of the A/B horizon contact throughout the property. Samples consisted of 200-400 grams of material collected along a vertical profile beginning at the base of the root hairs to a maximum depth of 25 cm. A vinyl trowel was used to reduce risk of contamination as well as strict procedures forbidding the wearing of jewelry. Generally samples were collected at 30 m intervals along lines spaced 150 m apart. Coordinates were preloaded into handheld GPS units which were used to navigate to sample locations. Areas of soil disturbance were avoided. In some cases sample depths were less than 10 cm due to thin soils over bedrock, although these comprise less than 1% of the dataset. Samples were split and digested for 24 hours in the proprietary MMI solution. The decanted solution was then analyzed by ICP-MS. Duplicates were analyzed every 12-20 samples. The complete survey included approximately 11,500 sample locations (Forbush, 2010). In 2012 lines over known ore bodies were re-sampled using the above techniques but spaced at 1.5, 3, and 6 m, and were analyzed for the complete 48 element suite offered with the MMI-M package .

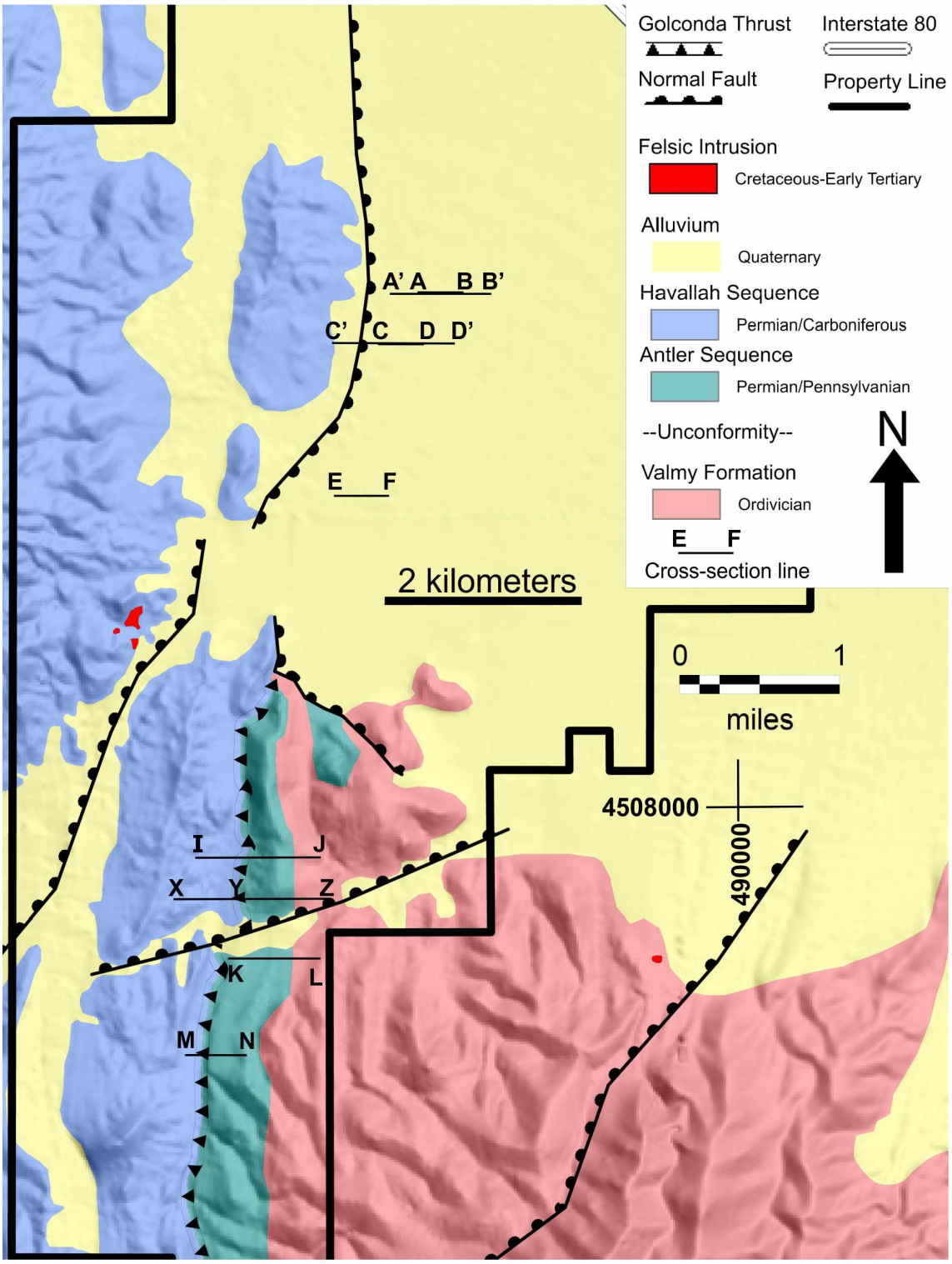

Figure 3.1: Locations of Geologic & Geochemical Cross-sections. Letter designators are explained in the individual cross-sections. Cross-section locations from Carver et al. (2014). Coordinates are NAD27 UTMs in meters.

3.4 Examination of duplicate samples

The Marigold MMI dataset contains 768 duplicates resulting from the laboratory's quality control measures. Of these only Au, Ag, As, Ba, Cd, Cu, Pb, and Zn were always analyzed as Marigold varied its suite of elements of interest slightly from year to year (Forbush, 2010). However, these duplicate analyses can be viewed in several different ways.

One measure of the extent to which a duplicate analysis matches the original analysis can be gleaned by examining the correlation between original and duplicate. If the original and duplicate are exactly the same, then plotting one versus the other will yield a line with a slope of exactly 1.0, an intercept of exactly 0.0, and an R^2 value of exactly 1.0. The greater the deviation between original and duplicate, the more the values will deviate from the above.

Values of R^2, slope, and intercept for many of the elements yield values close to 'perfect' for many (Table 3.1). The data for the elements Pb and Sb show the largest divergence from ideal behavior (R^2 values <0.9, slopes <1); the data for Au is closest to ideal.

Table 3.1: MMI correlation statistics for original vs. duplicate analyses, Marigold data set

Element	Ag	As	Au	Ba	Cd	Co	Cu	Pb	Sb	Zn
DL* (ppb)	1	10	0.1	10	1	5	10	10	1	20
R^2	0.97	0.91	0.97	0.98	0.96	0.91	0.95	0.85	0.87	0.94
slope	0.95	0.93	1.00	0.98	0.97	0.91	0.96	0.91	0.87	0.97
intercept	1.16	0.79	-0.03	55	0.46	3.5	26	1.9	0.08	0.50

*DL = detection limit

A different measure of reproducibility of analysis is from the deviation between the original and duplicate. Because the differences will necessarily be smaller for smaller values, there is merit in normalizing the difference to the concentration of the original. Such data is shown for Au and Ag (figure 3.2). These figures show relatively high % deviations between original and duplicate analyses, even for values more than 50 times the detection limits (Table 3.2). In particular, duplicate values are commonly ± 20-30% of the original values.

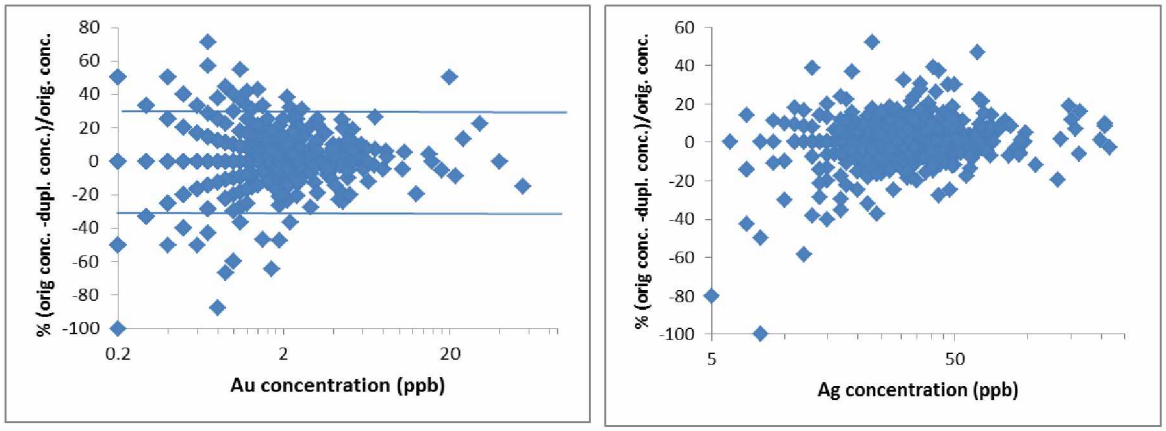

Figure 3.2: Relative % Difference vs. Concentration, for Au (left) and Ag (right) MMI analyses

A related measure of analytical reproducibility is the mean of the absolute value of the % deviation (the mean of the raw values will necessarily be close to zero). Such data (Table 3.2) show that the mean % deviation for the duplicate analyses is 6 to 20% of the original analysis. For Au, the mean deviation is 15%. That is, on average an original value of 5 ppb would have a duplicate value that was 15% higher (5.8 ppb) or lower (4.3 ppb). Such a degree of reproducibility ought to be adequate for distinguishing anomalous (>5 ppb) from background (<2 ppb) concentrations.

Table 3.2: Mean values for absolute value of % deviation, between original and duplicate analysis

element	Ag	As	Au	Ba	Cd	Co	Cu	Pb	Sb	Zn
mean % deviation	7	12	15	8	7	14	6	20	17	13
standard deviation	13	29	22	11	8	12	7	77	29	26

3.5 Interval studies and geologic reproducibility of MMI values

Two major investigations were undertaken to determine the extent to which MMI values are geologically reproducible, that is, the degree to which two closely spaced samples yield the same MMI values. One involved taking samples every hundred feet along two lines (X-Y-Z and E-F, figure 3.1) both in 2008 and 2012. Sixty-three sites were sampled at 30 m intervals. A second involved taking additional samples in 2012 at distances of 1.5, 3, and 6 m from the 30 m base samples (figure 3.3). Due to potential problems involved with the 2008-2012 comparison, the detailed interval study is presented first. In both cases most MMI samples were collected between 10 and 15 cm below the surface, that is, in the upper part of the 10-25 cm range recommended by SGS.

Given the broad zones of mineralization present at Marigold (Chapter 2), one would expect that elemental concentrations in soils above mineralized zones would be relatively high over the mineralized zones and low over non-mineralized zones. Given that the bedrock elemental concentrations are relatively uniform over short (e.g., 1.5 m) distances, one would expect that elemental concentrations in soils would also be relatively uniform over short (e.g., 1.5 m) distances. Consequently, one would expect that samples collected 1.5 m apart from each other would yield similar MMI concentrations for the various elements and that the greater the spacing between samples, the greater the divergence in concentrations. Ideally, then,

samples collected 1.5 m from the base sites would yield concentrations similar to those at the base sites and samples 3 m from the base sites would yield concentrations similar to those at 1.5 m and less similar to those at 3 m. In sum, the degree to which MMI concentrations in soils can be correlated with each other ought to vary with sample spacing.

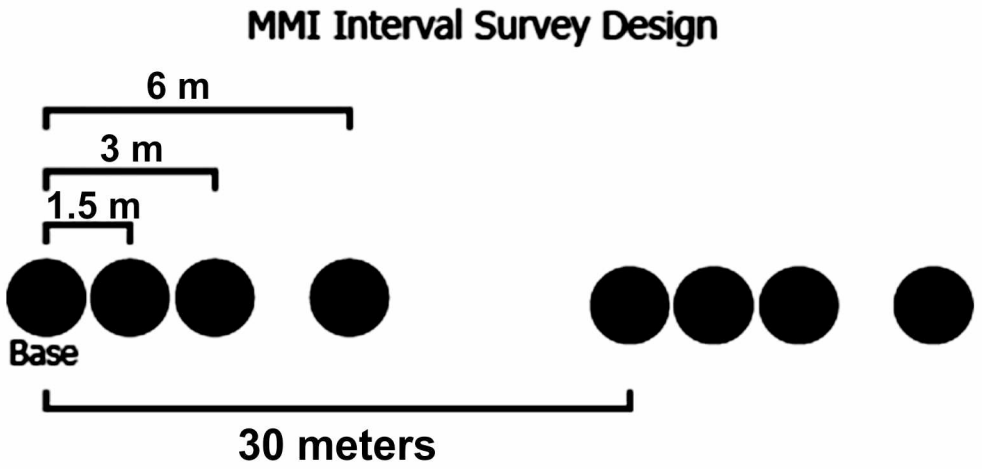

Figure 3.3: MMI Interval Survey Design, black circles are sample locations. The survey extended with this sampling pattern along lines E-F and X-Y-Z (figure 3.1) 400 m and 1300 m respectively.

Recognizing from the analytical reproducibility study that correlation coefficients provide a reasonably robust means of assessing such similarities, Table 3.3 gives values for correlation coefficients for different elements and different sample spacings. The elements Sb and Cd behave closest to the 'ideal': r values for 1.5-0 m and 1.5-3 m (both spaced 1.5 m apart) are nearly the same and are progressively higher than those with larger sample spacing. The elements As, Cs, Ag, U, Cu, and Fe display less ideal behavior, but r values for the two 1.5 m spaced intervals are broadly similar and these are broadly higher than r values for more distant spacings. The elements Mo, Pb, and Zn yield very low (below significance for n = 63) correlation coefficients for at least one of the 1.5 m spacing pairs. Gold and Hg display the

least ideal behavior: correlation coefficients are lowest for the closest-spaced samples (and not statistically significant for the 1.5-3 m samples), and generally low r values overall.

Detailed examination of the Au data shows that the low correlations are mostly due to two anomalous samples (Table 3.4): the highest Au concentrations for the samples at 1.5 m and 3 m from the base are an order of magnitude larger than the concentrations from the other nearby samples. A plot of Au concentrations for the base, 1.5 m, and 3 m samples (figure 3.4) shows that eliminating the two anomalous values raises the correlation coefficients to 0.86-0.95. That is (ignoring the highest Au concentrations) over a wide range of Au concentrations (0.4-40 ppb) Au concentrations in samples taken 1.5 m apart from each other are strongly correlated.

Table 3.3: R-values for MMI elemental concentrations, measured at different intervals from a base sample.

Element	**Interval**				
r value r critical (n63)=0.25	**1.5-0 m**	**1.5-3 m**	**0-3 m**	**0-6 m**	**0-30 m**
Sb	**0.80**	**0.85**	**0.75**	**0.43**	**0.29**
Cd	**0.64**	**0.80**	**0.80**	**0.55**	**0.63**
As	**0.52**	**0.56**	**0.44**		
Cs	**0.68**	**0.52**	**0.29**	**0.25**	
Ag	**0.75**	**0.47**	**0.47**		
Cu	**0.43**	**0.74**	**0.58**		
U	**0.72**	**0.34**	**0.33**	**0.41**	**0.41**
Fe	**0.66**	**0.42**		**0.57**	**0.58**
Mo	**0.30**	**0.39**	**0.47**		
Pb		**0.67**	**0.81**		
Zn		**0.72**	**0.73**	**0.44**	
Hg	**0.44**				
Au	**0.39**		**0.59**	**0.46**	**0.34**

Note: only statistically significant values are displayed

Table 3.4 MMI Au concentrations (ppb) for those samples with the highest Au concentrations

	Distance from Base Sample			
Base #	0	1.5m	3m	6m
MMI 41-6	34	37	35	20
MMI 41-7	24	31	24	23
MMI 41-19	29	27	27	28
MMI 41-20	12	10	10	27
MMI 41-13	8	3	2.3	39
MMI 41-21	25	20	18	49
MMI 41-22	13	12	13	99
MMI 52-13	43	29	**590**	13
MMI 52-14	4	**135**	9	2

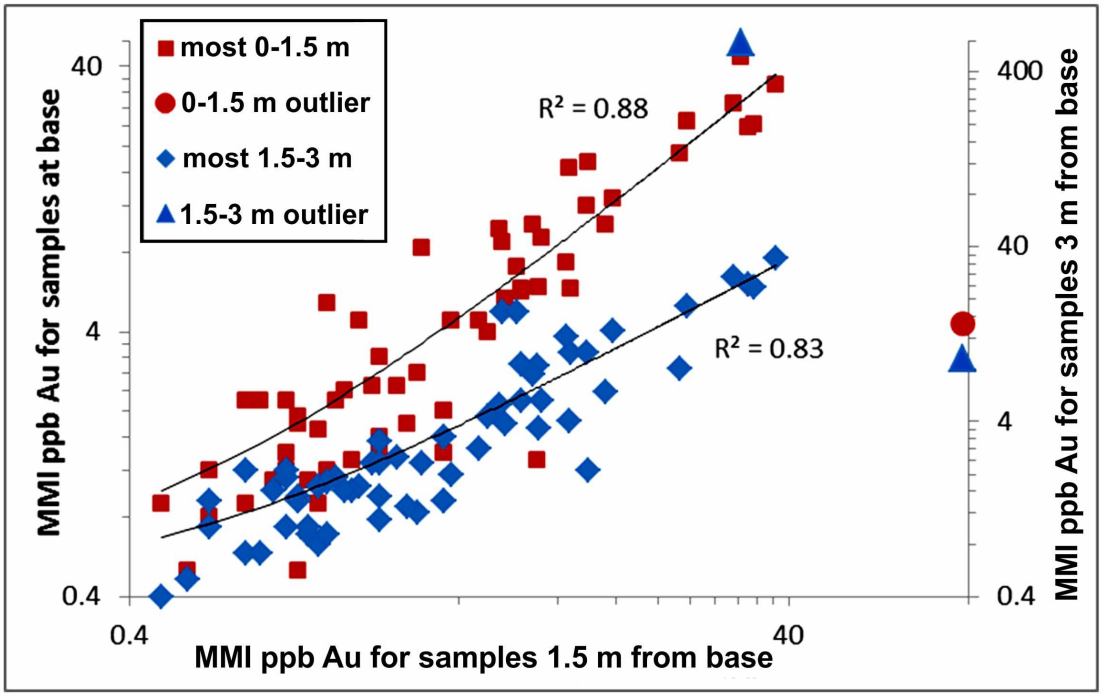

Figure 3.4: MMI Au concentrations (ppb) for samples taken 1.5 m apart. The vast bulk of the data show good agreement in concentrations for closely-spaced samples.

This problem of non-reproducibility of highest elemental concentrations is not restricted to Au. Metal concentrations for the set of 4 (0, 1.5, 3, and 6 m) that contain the 1-5 highest concentrations of a given metal are given in Tables 3.5 and 3.6. For most of these, the highest concentration of an element is more than 10 times the concentration of that same element in the nearby samples. In other words, the highest concentrations of a given element are not reproducible. In about 3/4 of the cases, a sample with very high concentration is highly anomalous in only one element. For the other 1/4, a single sample contains the very high concentrations for 2 or more elements.

The elemental associations for samples with first and second highest concentrations (Table 3.7) in some cases make geochemical sense, and in other cases they don't. For example, Au and Hg possess similar chemical properties, so their joint occurrence as highest concentrations in sample 52-13-10 (Appendix 1.3) seems reasonable. On the other hand, Pb and Zn possess similar chemical properties, but their occurrence with Au in sample 52-14-5 (Appendix 1.3) is not easily explained. Other odd associations noted include: Ag and Li, Mo and As, Cs and Tl, Ca and Fe and Sb with Cu and Ni.

A single sample (41-19-10, Appendix 1.5) contains the highest concentrations of Al, Fe, Zr, Ti, U, Th, Y, and Dy: most of these elements are extremely insoluble at high oxidation state, but U is relatively soluble under such conditions. This sample contains 5 times as much Fe, 3 times as much Al, 10 times as much Zr, 35 times as much Ti, 7 times as much U, 12 times as much Th, 3 times as much Y, and 7 times as much Dy as the nearby samples. Most of these elements are only solubilized by extremely low pH solutions (Brookins, 1988) —which are neither realistic for the soil pH present at Marigold, nor for the weak organic extracting agent employed.

Table 3.5: MMI concentrations (ppb) for sample sets containing highest metal concentration part-1

0	1.5	3 m	6 m	0	1.5	3 m	6 m	0	1.5 m	3 m	6 m	0	1.5	3 m	6 m	0	1.5	3 m	6 m	0	1.5	3 m	6 m
Mo				**Hg**				**As**				**Tl**				**U**				**W**			
60	46	20	**179**	5	3	**110**	2	50	60	30	**3220**	1	1	**11**	2	21	35	16	**219**	**194**	12	4	10
140	15	2	4	0.5	1	**94**	1	10	20	**540**	20	1	3	**8.1**	1	45	15	**203**	30	14	11	**112**	22
112	22	17	8	1	**45**	23	1	110	190	**400**	160	0	1	**7.7**	1	17	32	**196**	7	11	32	**109**	22
9	7	5	**73**	1	2	2	**40**	80	60	**380**	70					35	57	60	**142**	5	74	14	5
								20	40	**370**	10					26	31	**116**	13				
0	1.5	3 m	6 m	0	1.5	3 m	6 m	0	1.5 m	3 m	6 m	0	1.5	3 m	6 m	0	1.5	3 m	6 m	0	1.5	3 m	6 m
Ti				**Cs**				**Pb**				**Th**				**Zr**				**Sb**			
14	9	**350**	10	2	11	**80**	3	**9990**	1890	1770	70	15	7	**118**	9	24	21	**225**	18	8	14	6	**50**
20	11	**47**	12	1.6	1	**56**	2	240	**10700**	1230	70	1	1	2.7	**17**					1	1	2	**14**

Notes: (1) highly anomalous values, generally those an order of magnitude greater than surrounding samples, are in bold; (2) for each element a single row represents one set of samples located 0, 1.5, 3, and 6 m from the base; (3) the rows for different elements usually represent different sites; (4) no single sample contains the highest concentrations of more than 3 different elements.

Table 3.6: MMI concentrations (ppm) for sample sets containing highest metal concentration part-2

0	1.5	3 m	6 m	0	1.5	3 m	6 m	0	1.5	3 m	6 m	0	1.5	3 m	6 m	0	1.5	3 m	6 m	0	1.5	3 m	6 m
Fe				**Al**				**Cu**				**Mn**				**Ni**				**P**			
3	3	**15**	3	12	12	**43**	9	0.8	2.2	1.5	**5.8**	4	**22**	2	5	0.2	0.3	0.5	**1.9**	0.4	1	**3.7**	0.4
4	4	**9**	4	26	**33**	23	12	**4.9**	1.5	1.9	2	4	2	**20**	7					1.1	**3**	0.9	0.3
				22	**28**	23	17	1.4	**4.2**	2.6	1.4	2	4	**19**	14					**1.6**	0.2	0.2	0.4
				12	18	13	**25**	**3.6**	1.8	1.2	1.2									**1.4**	0.3	0.7	0.7

Notes: (1) highly anomalous values are in bold; (2) for each element a single row represents one set of samples located 0, 1.5, 3, and 6 m from the base; (3) the rows for different elements usually represent different sites; (4) no single sample contains the highest concentrations of more than 3 different elements.

Table 3.7: Samples containing the two highest concentrations of 2 or more elements

sample #	highest conc. elements*
41-19-0	Ag, Li
41-19-5	Ag, Li
41-19-10	Fe, Al, Th, Ti, U, Y, Dy, Zr
41-21-10	Fe, Ca
41-21-20	Cu, Ni, Sb
41-22-20	Mo, As
41-47-20	Th, Y
41-48-0	Cu, Ni, Mn
41-49-0	Ca, Ba
52-13-0	Pb, Zn
52-13-10	Au, Hg, Tl
52-14-5	Au, Pb, Zn
52-14-10	Cs, Tl
52-21-10	Hg, Cs

*Data in Appendix 1.3 & 1.5.

The problem of anomalous highest elemental concentrations is illustrated for the metals Au, Hg, Pb, and Zn along a 90 m traverse line (figure 3.5). The sample at 19495 yielded the highest Pb and Zn MMI concentrations and the second-highest Au and Hg concentrations. The MMI concentrations for the samples 1.5 m on either side are much less than at the spike, and typically 1/10th as high. A single isolated Au-Hg anomaly at 19590 contains the highest Au and Hg MMI concentrations among the 252 interval samples; Hg and Au on either side are barely anomalous, if at all. This same sample contains elevated Zn and Pb, but the second-highest concentration of each is in the sample taken 3 m away (19600) from the highest Au-Hg sample. Because Pb and Zn do not occur with Au in bedrock, these two isolated spikes cannot reflect bedrock-elemental covariations. Why the highest and second highest concentrations should occur as two isolated anomalies separated by 30 m of low concentration samples admits no ready explanation.

The easiest conclusion based on these non-repeatable anomalies is that very-high concentration MMI values happen for unknown reasons at a rate of 1-5 for each element per approximately 250 samples. Whether these represent some extremely localized 'best case metal adsorption' phenomena or represent some analytical problem is unknown. Ironically, then it would appear that the highest MMI values for a given element should probably be ignored.

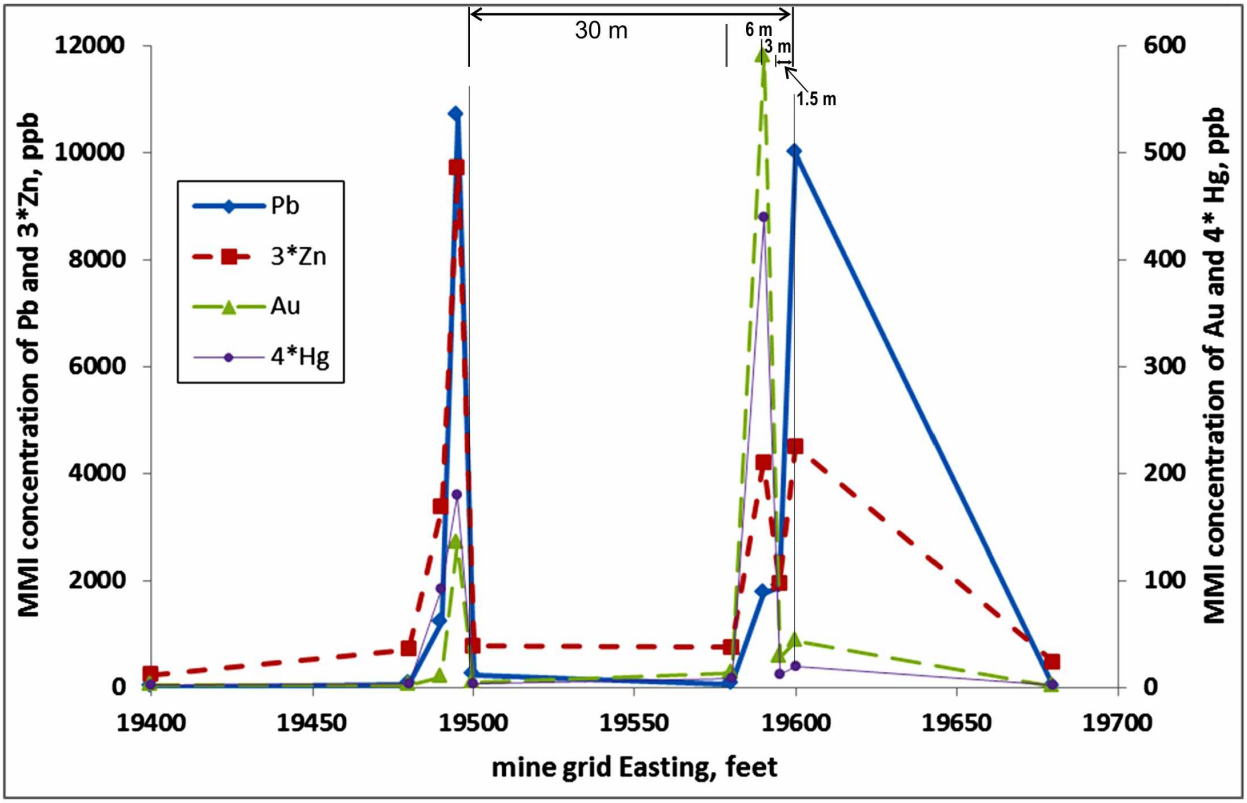

Figure 3.5: MMI Concentrations of Pb, Zn, Au, and Hg, on a portion of line 52, Marigold mine. Note the enormous changes in concentration for samples as little as 1.5 m apart from each other.

Putting aside the problem of non-reproducible highest values, another measure of the degree of sample reproducibility is the normalized % difference between two samples, as used in the analytical reproducibility tests. Such data for MMI Au using the two sets of samples

spaced 1.5 m apart show larger % deviations (figure 3.6) than was seen for analytical reproducibility (figure 3.2), but the bulk of normalized deviations are $\pm$ 50% of the concentration in the 1.5 m sample. The mean of the absolute values of % normalized deviations are 36-41%. (This mean includes % deviation for the two anomalous samples; their contributions to the mean are drowned out by the other values.) These mean % deviations are about twice as high as the % deviations indicated for analytical variability. They indicate that (ignoring the very high concentrations) different soil samples taken from nearly the same location are likely to possess concentrations 35-40% different from each other. That is, on average, a sample yielding 10 ppb Au is likely to be 'replicated' as 14 ppb (40% larger) or 6 ppb (40% smaller).

The normalized % deviation for all the elements and all the different sites yields an unwieldy number of diagrams. To simplify, I have considered only the two sets 1.5 m apart (the 0-1.5 m and 1.5-3 m sets) and determined the absolute value of normalized % deviation between values in the two sets for each element. I then determined the average normalized % deviation and averaged the value for the 0-1.5 m and 1.5 m-3 m sets. This data (Table 3.5) shows that the typical mean % deviation is about 50%, with lower values of about 20% for major elements (e.g., Ca, Fe, Mg) and higher values for rarer elements (Cs, Hg, W, U). The second highest average % deviation, however, is for As (111%), despite being a relatively abundant element. The bulk of these average relative % deviations are similar to the values for Au.

In sum, the interval studies indicate that in general closely-spaced (1.5 m) samples yield broadly reproducible MMI concentrations ($\pm$ 20-60%) at low to moderately high concentrations. The highest 2-5 concentrations for each element, however, are not reproducible.

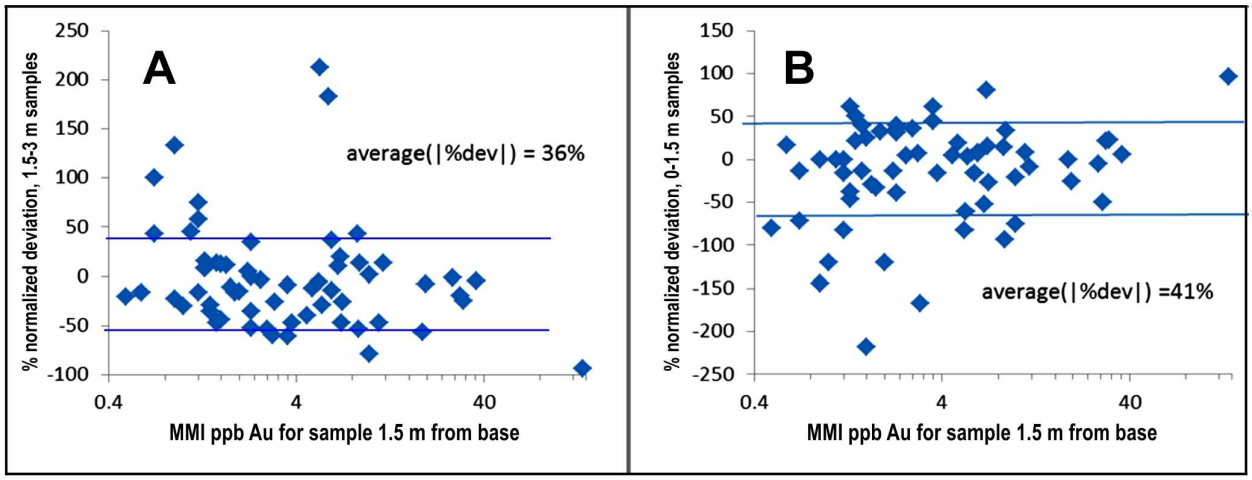

Figure 3.6: Percent (%) normalized deviations for samples spaced 1.5 m apart. A = deviations for samples 1.5 m and 3 m from the base; B = deviations for samples 0 and 1.5 m from the base. Deviations for the two highest Au concentrations have been omitted on these figures.

Table 3.8: Mean normalized % deviation for 1.5 m interval MMI samples, the 0-1.5 m and 1.5-3 m intervals are investigated, Marigold mine

	Ag	Al	As	Ba	Ca	Cd	Co	Cs	Cu	Fe	Hg	K	Li	Mg	Mn
Av % dev*	25	30	**111**	47	19	37	61	**84**	22	21	**133**	40	28	23	60
	Mo	Ni	P	Pb	Rb	Sb	Sr	Th	Ti	Tl	U	W	Y	Zn	Zr
Av % dev*	69	30	75	43	36	60	20	47	40	65	70	**79**	55	56	48

% dev = 100(conc. 0 – conc. 1.5 m)/conc.1.5 m; Av = average of the absolute values of % dev, averaged for the 0-1.5 m and 1.5-3 m sets; bold = especially high; underlined = especially low

A completely different test for geologic reproducibility is given by comparing MMI values at the 63 base sites as sampled in 2008 and again in 2012. Re-occupation of the sites in 2012 was based on using GPS coordinates taken in 2008, however, sites were 'tagged' in 2008 and in many cases these tags were relocated in 2012 allowing for sample relocations 0-1.5 m from the 2008 survey. In addition, the interval studies conducted in 2012 indicate that similar concentrations should be expected even if the sites were not exactly relocated.

A comparison of MMI concentrations for samples taken at the 'same' sites (Table 3.9) yields discouraging results. Correlation coefficients are low and are typically below significance levels. That is, MMI concentrations for samples taken in 2008 bear little or no relation to concentrations in samples taken at the same sites 4 years later. In other words, the data could not be reproduced.

Examination of the Au data shows that the problem is not simply 1 or 2 non-reproducible values (figure 3.7): with two exceptions, the higher Au samples from 2008 were not high in 2012 and the higher Au samples in 2012 were not high in 2008. Of the 12 samples taken in 2008 and 2012 with more than 15 ppb Au, for only 2 did the 'replicate' samples contain more than 15 ppb Au.

Table 3.9: R* values for MMI concentrations in samples taken in 2008 and 2012

Ag	As	Au	Ba	Cd	Co	Cu	Pb	Y	Zn	Zr
		0.35	**0.37**	**0.53**		**0.46**				

*critical r for n =63 is 0.25; only statistically significant values are given

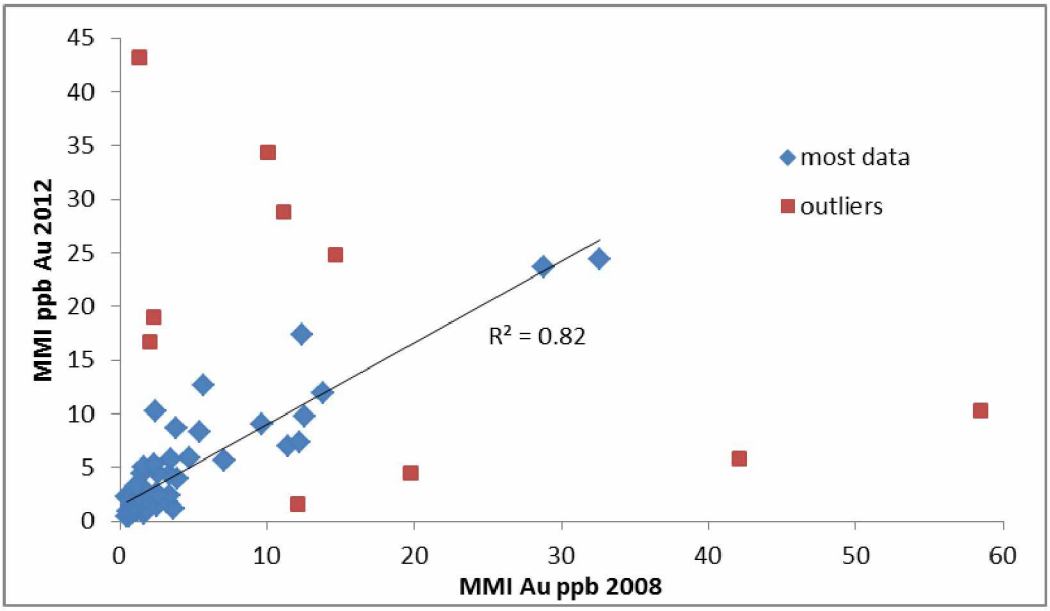

Figure 3.7: MMI Au Concentrations for Re-occupied Sites, samples taken in 2008 and at approximately the same sites in 2012.

This problem of non-matching high values is not restricted to Au. MMI Cu concentrations for the same sites in 2008 and 2012 (figure 3.8) show a modest degree of correlation once the top 4 concentrations of 2012 are removed. However, the problem is not simply a few high concentrations: Table 3.10 shows that the mean values for each of the elements from the same sites are higher for 2012 than for 2008. This is true despite the fact that for several elements (e.g., Au, Pb, Y, Zr) the maximum concentration among the 63 samples was higher for the 2008 set than for the 2012 set. In other words, the non-reproducibility of MMI values for samples taken at the same sites in 2008 and in 2012 is almost certainly an analytical problem superimposed on a geologic problem. It would appear that the metals were extracted by the organic reagent more strongly in 2012 than in 2008. If this was the only problem, however, the 2008 concentrations would strongly correlate with the 2012 concentrations—which is not the case.

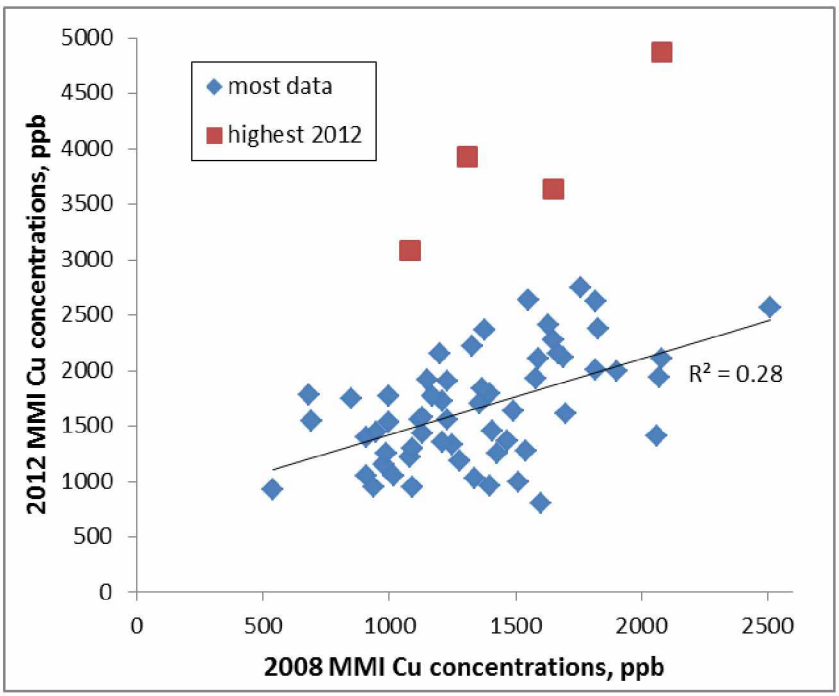

Figure 3.8: MMI Cu Concentrations for Re-occupied Sites, samples taken in 2008 and at approximately the same sites in 2012.

Table 3.10: Mean and maximum values for 63 MMI samples, taken at the same locations in 2008 and in 2012, Marigold mine

	'08	'12	'08	'12	'08	'12	'08	'12	'08	'12	'08	'12	'08	'12	'08	'12	'08	'12	'08	'12	'08	'12
	Ag		**Au**		**As**		**Ba**		**Cd**		**Co**		**Cu**		**Pb**		**Y**		**Zn**		**Zr**	
mean	35	**43**	6	**7**	21	**25**	3	**11**	23	**34**	41	**173**	1.4	**1.8**	24	**56**	22	**47**	74	**137**	9	**13**
max	85	**104**	**59**	43	90	**180**	9	**45**	56	**107**	192	**1030**	2.5	**4.9**	**280**	240	**412**	168	400	**1500**	**76**	30

Concentrations are in ppb except for Ba and Cu in ppm. Bold values are the higher of the 2012 and 2008 set.

In sum, tests for analytical and geologic reproducibility of MMI concentrations using Marigold data yields somewhat unsatisfactory results. For 2 splits of the same sample from a single year, the analytical reproducibility is approximately 6-20% of the amount present, and is higher for some elements than others. Comparisons for samples taken from the same sites in different years indicate systematic differences that make combining datasets from multiple years at least problematic. Finally, the geologic reproducibility is complicated by the fact that among the 252 'interval' samples every element is present at very high concentration (typically >10 times concentrations neighboring samples) in 1-5 samples. These very high concentrations are simply not reproducible. The mean normalized % deviations for samples taken 1.5 m apart are mostly 20-70%, that is the elemental concentrations in two adjacent samples are, on average, different by $\pm$ 20-70 relative %.

3.6 MMI Au response compared to drill hole based sub-surface grade and geology

Having examined problems with analytical and geological reproducibility, in this section I compare MMI Au concentrations in soils along several soil lines for which published geologic and generalized grade cross-sections are available (Carver et al., 2014). Comparing other elements besides Au to these cross-sections is beyond the scope of this study, especially as I lack reliable data for other elements besides Au in the sub-surface. Cross-sections are located in figure 3.1, and are mostly presented from the north to the south end of the property. With one exception, all the MMI Au data was acquired in 2007 and 2008 and based on a sample spacing of 30 m.

Figure 3.9 shows the geologic cross-section A-B and the accompanying MMI soil survey A'-B', which extends well beyond the area of drill information. The mineralized zone is about 150 m wide and is under 3 –50 m of alluvium and 6-20 m of rock. None of the six samples over the orebody produced a significant MMI Au concentration (1.5-0.5 ppb, Appendix 1.1) and the highest values (3.0 and 3.7 ppb, Appendix 1.1) are above barren rock (figure 3.9). The implication is that because MMI Au concentrations of 3.7 ppb (and possibly higher) occur outside the ore zone, values at and below these concentrations should be considered background. The threshold for the minimum anomalous value will be the lowest value that accurately locates subsurface mineralization. In the case of figure 3.9 this threshold was not reached; it was however identified along line C'-D' (figure 3.10). In the absence of subsurface data mathematical methods can be used to calculate anomaly thresholds for the various elements. One such method is explained in more detail for As, Hg, and Sb in section 3.7.

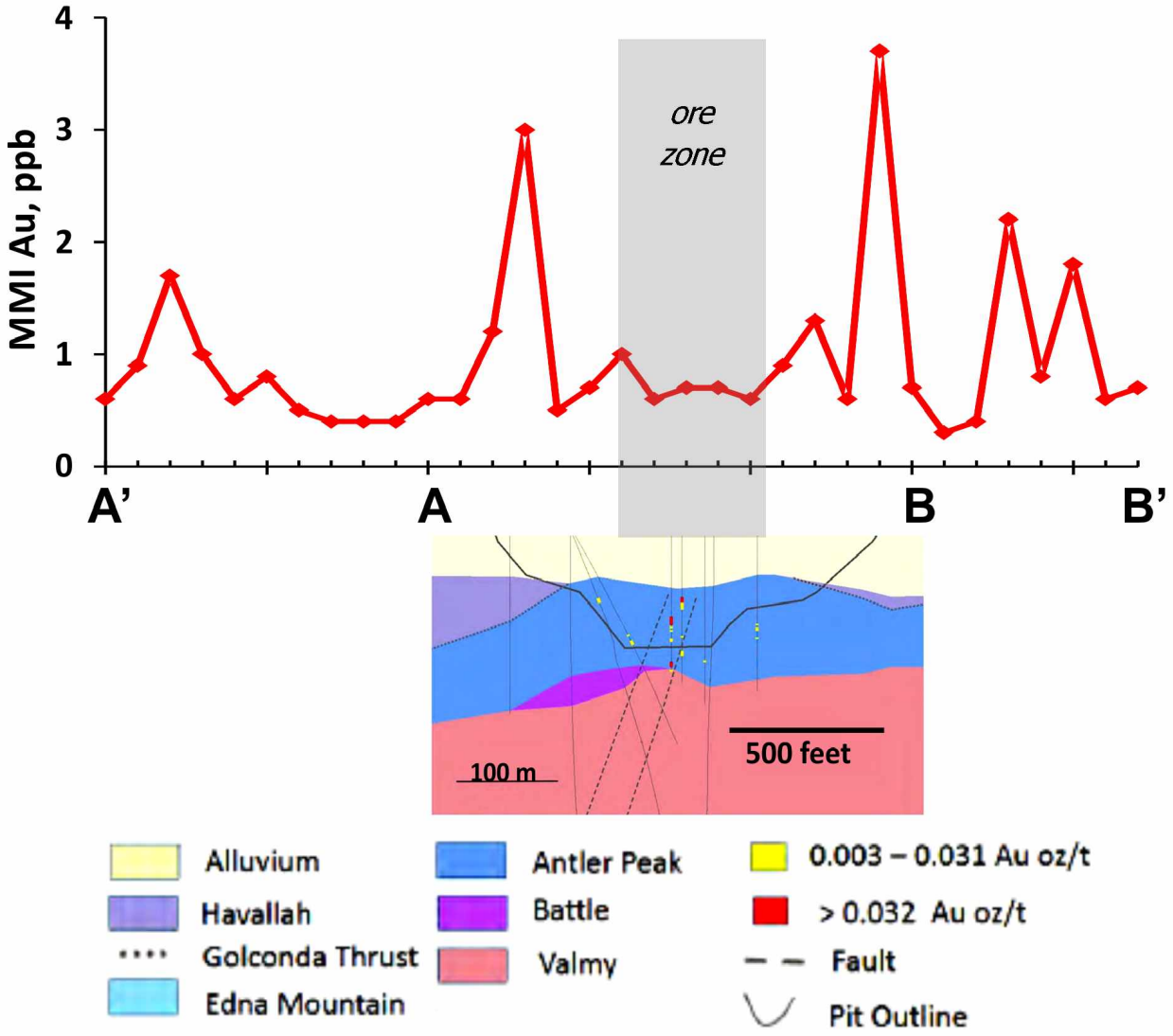

Figure 3.9: Geologic & Au Grade Cross-section A-B, with accompanying MMI Au concentrations. Note lack of any MMI response over the ore body. Geology from Carver et al. (2014). Complete MMI analyses in appendix 1.1.

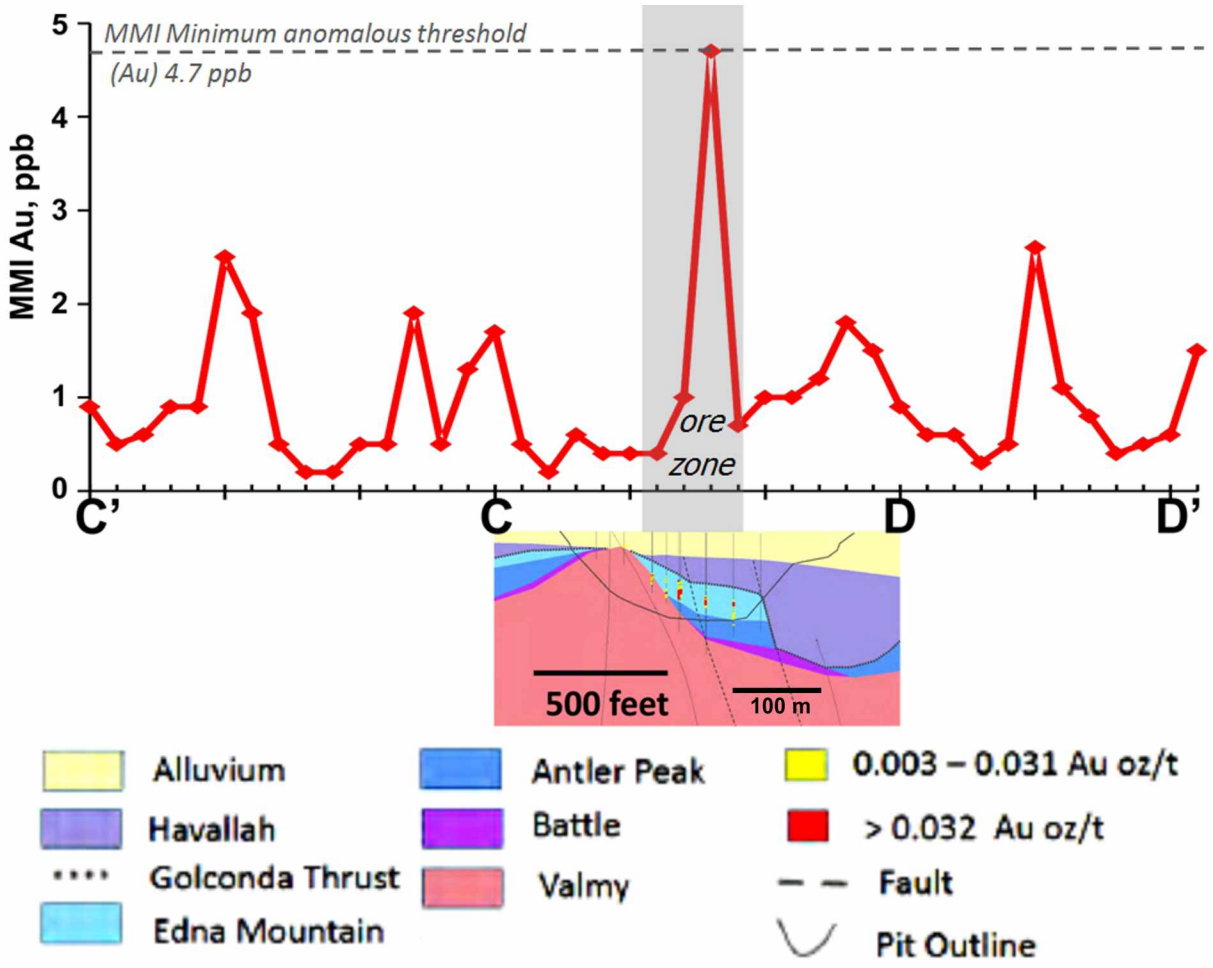

Figure 3.10: Geologic & Au Grade Cross-section C-D, comparison of MMI Au concentrations along line C'-D' to geologic cross-section C-D (after Carver et al., 2014). Complete MMI analyses in appendix 1.2.

Figure 3.10 shows the MMI soil survey and accompanying geology for cross-section C-D. Here the zone of mineralization is 120 m wide and buried by 30 m of alluvium and 30-45 m of bedrock. Of 4 sites directly above mineralized rock, one sample yielded 4.7 ppb Au; all other values were 'background' of 0.2-2.5 ppb (Appendix 1.2). If this line is representative, than a concentration of 4.7 ppb is adequate for discriminating underlying Au mineralization at Marigold. I have assumed it is representative, and employ 4.7 ppb Au as the minimum anomaly threshold throughout the remainder of the study at Marigold.

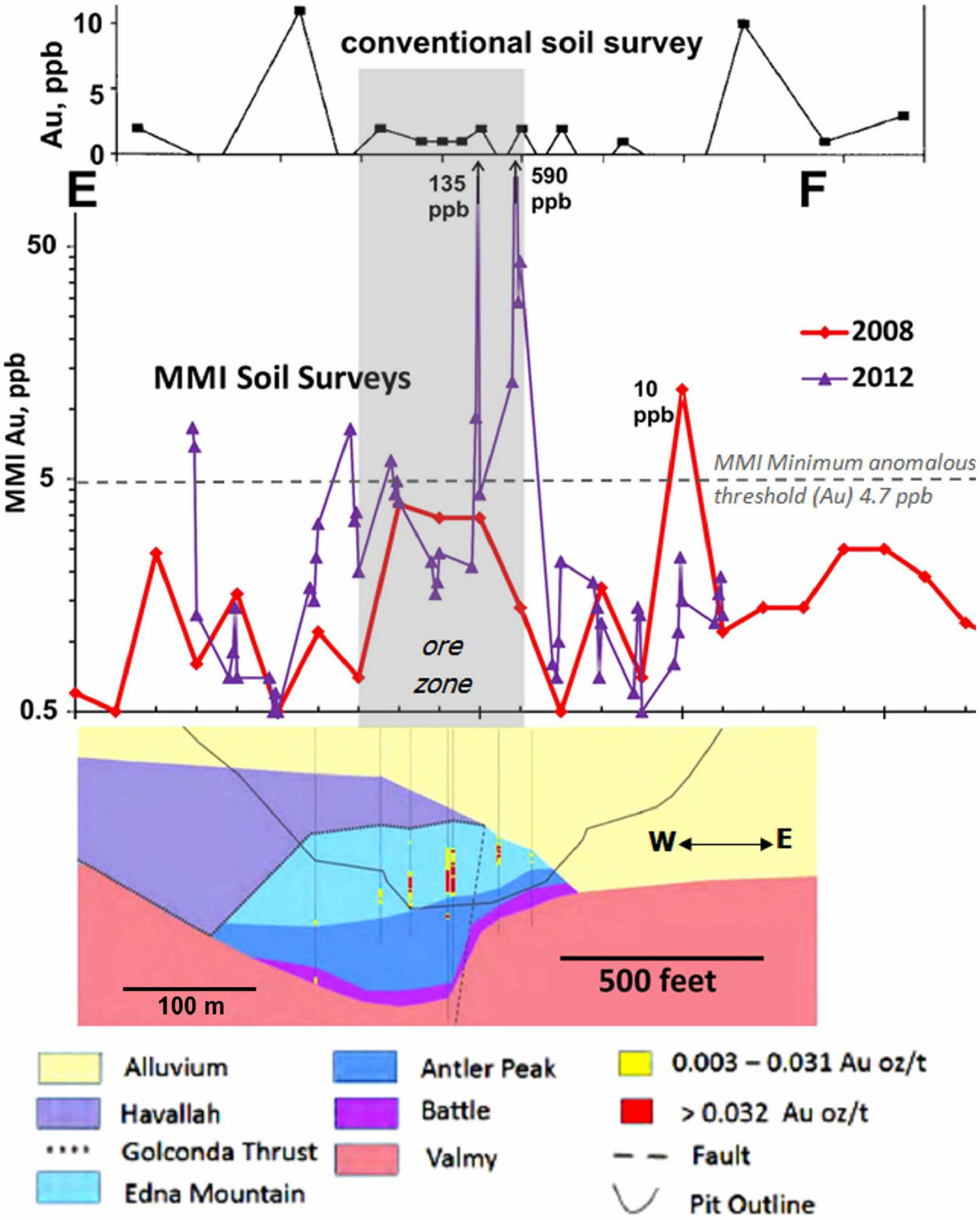

Figure 3.11: Cross-section E-F Geology, Drilling, & Soil Chemistry, drilling results (Carver et al., 2014) compared to a conventional geochemical survey (Smee 1998), and two MMI surveys conducted in 2008 and 2012. Complete MMI analyses in appendix 1.3.

Soil geochemical data accompanying geologic cross-section E-F (figure 3.11) is complicated because it includes three different surveys: conventional (Smee, 1998), MMI in 2008, and MMI in 2012. The mineralized zone is 180 m wide and is buried by 35-90 m of alluvium and 3-110 m of bedrock. Conventional soil sampling failed to produce an Au anomaly in soil above the deposit; instead, it yielded two 10 ppb false anomalies well outside of the orebody. The 2008 MMI survey produced seven Au values less than the suggested cutoff of 4.7 ppb over the orebody and one 10 ppb anomaly 120 m east of the orebody. Of 28 samples (2012) taken over the orebody, 7 yielded Au concentrations above the 4.7 ppb background value. Of 25 samples taken from outside of the ore body, two were 'false anomalies' above 4.7 ppb. The correlation between 2012 MMI Au concentrations and underlying ore grade is not straightforward: samples immediately above the thickest, highest-grade zone were all below 4.7 ppb and the highest MMI Au grade (590 ppb) is above the eastern, barely-mineralized edge (figure 3.11). Of the 3 samples in the immediate vicinity of the second-highest MMI Au anomaly (135 ppb) only 1 is above the 4.7 ppb background value. In other words, the 2012 MMI Au anomalies are above the lower-grade west and east edges of the orebody, and not above the higher-grade center.

Collecting soil samples along cross-section I-J was hindered by removal of overburden prior to the survey, so samples could only be collected above the deeply buried western half of the deposit (figure 3.12). The thickness of alluvium was essentially zero and the mineralization is overlain by approximately 300 m of bedrock. This deeply buried mineralized zone is approximately 520 m wide. Of the 17 MMI samples collected above ore, four yielded Au concentrations above 4.7 ppb. The strongest anomaly (10.3 ppb) is offset 30 m east of the thickest and highest grade mineralization. It is unclear whether the 7 ppb anomaly at the far western end of the soil line overlies mineralization.

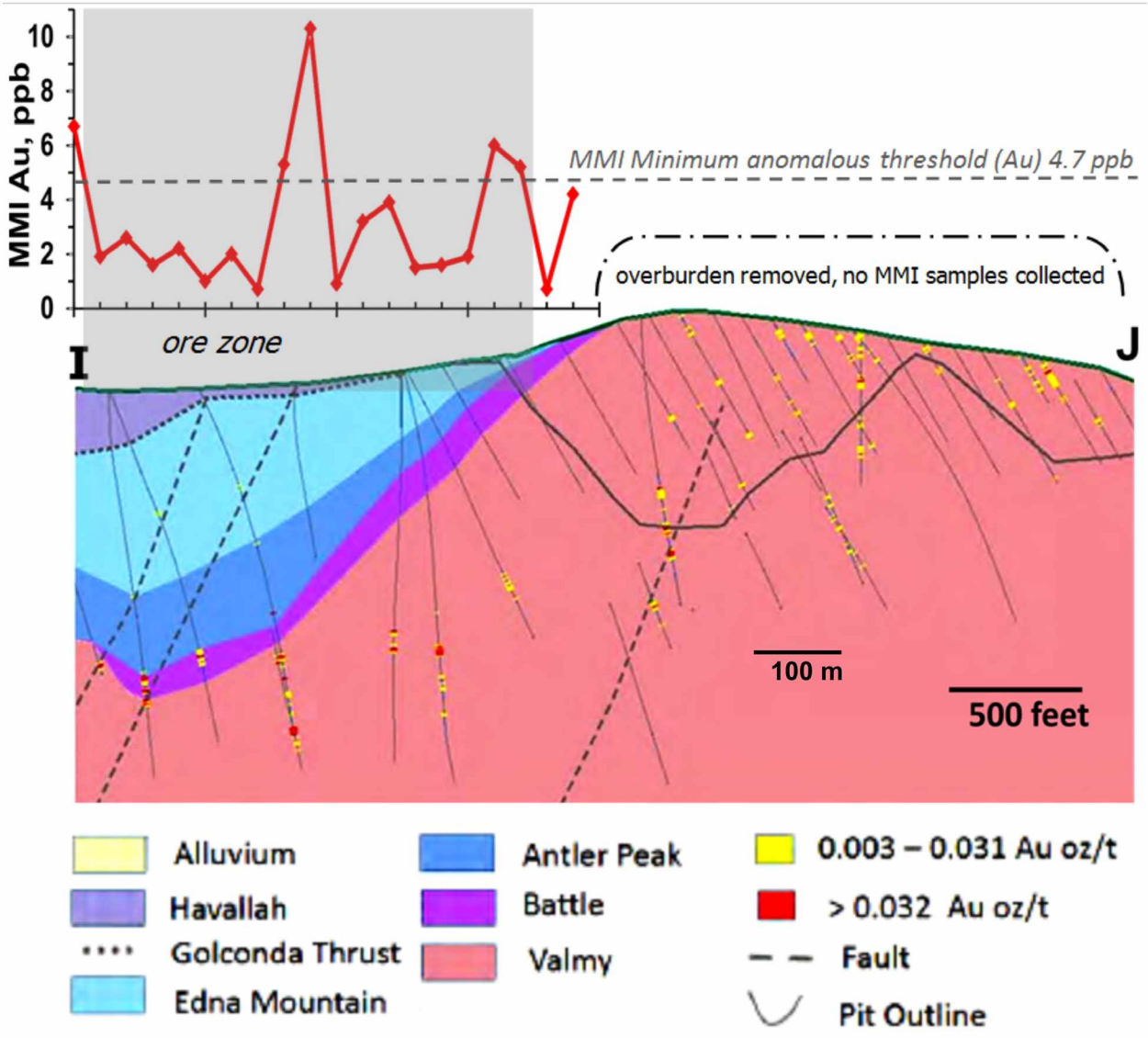

Figure 3.12: MMI Au Concentrations & Geologic Cross-section I-J, (after Carver et al., 2014). Complete MMI analyses in appendix 1.4.

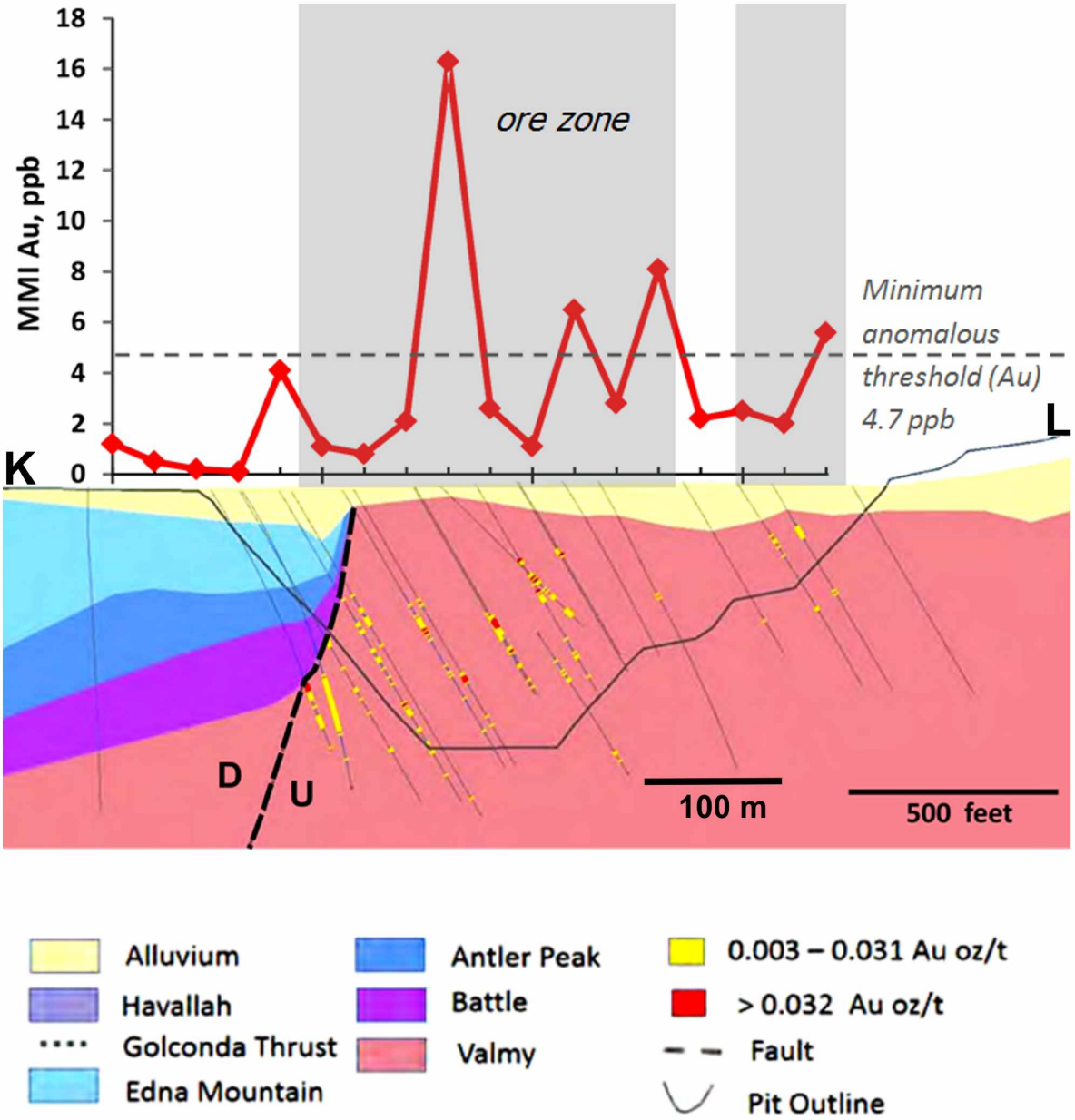

Figure 3.13: MMI Au Concentrations & Cross-section K-L, (after Carver et al., 2014). Complete MMI analyses in appendix 1.6.

MMI soil anomalies and associated geologic section K-L are shown in figure 3.13. Here the mineralized zone is 400 m wide and overlain by 9-30 m of alluvium and 30-90 m of bedrock. Of the 14 samples take above mineralization, 4 yielded Au values above background, and 3 of the 4 are above the eastern, low-grade portion. Of the six samples directly above the higher-grade and thickest western part, only one returned a value above background.

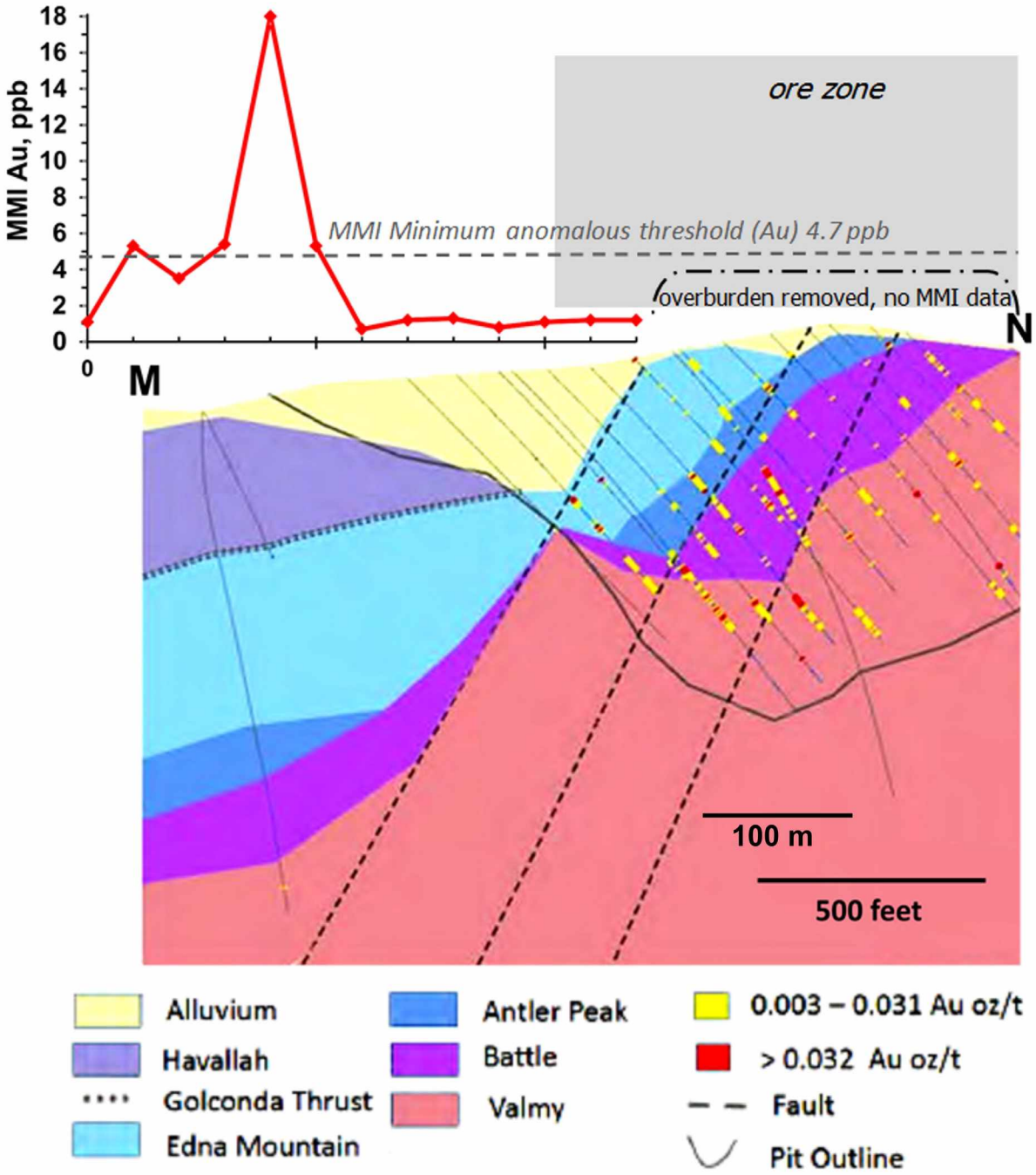

Figure 3.14: MMI Au Concentrations & Cross-section M-N, (after Carver et al., 2014). Complete MMI analyses in appendix 1.7.

Soil samples could only be collected above the western half of geologic cross-section M-N (figure 3.14) and only the easternmost 3 samples could be considered above mineralization. That part of the deposit is buried under 6-90 m of alluvium and 6-130 m of bedrock. None of the 3 samples above mineralization yielded an MMI Au anomaly. However, of 8 samples

overlying barren rock at the western end of the section, 4 yielded Au concentrations above 4.7 ppb and include a value of 18 ppb (Appendix 1.8), the highest 2007-2008 concentration recorded in any of the six geologic sections with drill hole data. Its location directly above an isolated interval of low grade mineralization more than 300 m below the surface is curious.

Drill holes at Marigold are rarely spaced closer than 30 m and the MMI lines are typically not directly above drill holes. In an attempt to most accurately compare the MMI to underlying subsurface mineralization I was able to secure from Marigold mine a portion of the drill hole-based block model through cross-section X-Y-Z (figure 3.1), which corresponds to a long 2008 MMI line and a detailed (sampling interval) 2012 MMI line. A block model is the calculated locations, grades, and quantities of ore. The block model is constructed by incorporating drilling results with geologic interpretations. The process uses Kriging, a statistical technique; the end result is the model that is used in mine planning and design.

Figure 3.15 shows the combined block model data (as points with a grade range) and the two MMI surveys. This section represents a 'best case' scenario for soil sampling, as both the thickness of alluvium (0-30 m) and of bedrock overlying mineralization (0-60 m) is small. To the extent that virtually every spot on the surface between mine eastings of 14500 and 18300 is underlain by rock containing at least 0.1 ppm Au (and usually at least 0.2-0.3 ppm Au) the entire line from 14500 to 18300 is above ore grade (figure 3.15). For the 2008 survey, of 37 sites above ore, 18 samples (49%) returned MMI values above 4.7 ppb Au and all of the 12 samples west of the edge of ore were below 4.7 ppb Au. For the 2012 survey, of the 183 sites above ore, 80 samples (44%) returned MMI values above 4.7 ppb. Of the 48 samples taken west of the edge of ore (not all shown on figure 3.15), only three returned Au concentrations greater than 4.7 ppb. These success rates are much higher than for the other cross-sections and are most likely a reflection of the shallower cover.

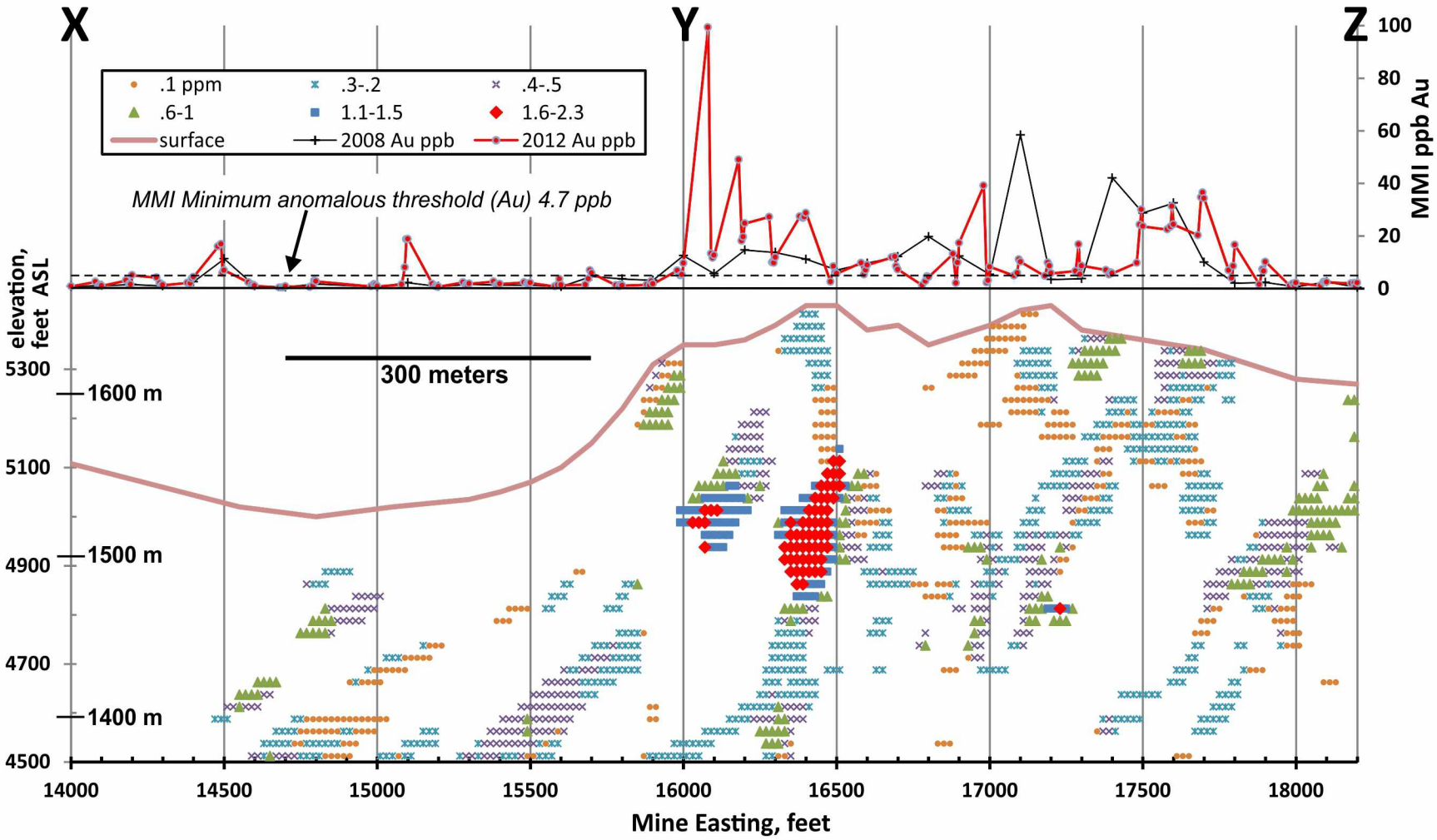

Figure 3.15: Comparison of MMI Anomalies to Sub-surface Block Model, the 2008 and 2012 MMI Au anomalies are compared to the Marigold block model along cross-section X-Y-Z (figure 3.1). Complete MMI analyses in appendix 1.5. Block model data provided by the Marigold Mine Engineering Department.

That said, the lack of direct correlation between the 2008 survey and the 2012 survey even in terms of 'high' and 'low' values is striking (figure 3.15). Only in the vicinity of eastings 17500-15600 did both MMI surveys report high (22-33 ppb) Au concentrations. This general lack of correspondence for higher Au values (figure 3.7) is characteristic of the 2008 vs. 2012 MMI surveys. Further, the 2012 survey showed extreme variation in Au concentrations over very short distances. For example, the highest Au concentration (99 ppb) at 16080 Easting, is surrounded by MMI Au concentrations of 5-13 ppb, 10-20 times lower.

Trying to turn MMI Au concentrations into some meaningful measure of the underlying grade is problematic. Figure 3.16 shows (for the 2012 data set) MMI Au concentration vs. maximum Au grade within 75 m and within 150 m of the surface. The vertical line in each is at 4.7 ppb, separating 'background' from 'anomalous' values. No relationship is apparent for grade within 75 m of the surface (figure 3.16 left). An interesting observation however, is--with one exception--in all cases where Au grade within 150 m of the surface is 1 ppm or greater, MMI Au concentrations above them are >4.7 ppb (figure 3.16, right). That is, there may be a relationship between the MMI Au categories (background versus anomalous) and underlying Au grades rather than between the absolute values of either.

In a similar manner, the 2008 and 2012 data sets display more consistency when viewed as categories, rather than values. Figure 3.17 shows the MMI data set of cross-section X-Y-Z (figure 3.15) presented as categories. The 2008 Au MMI data are categorized as: <4.7 ppb Au = 0, 4.7-10 ppb Au = 1, 10-12 ppb Au = 2, 12-20 ppb Au = 3, and >25 ppb Au =4. The 2012 data include 4-closely spaced sites every 30 m: at 0, 1.5, 3, and 6 m from the 2008 sites. This MMI data is presented as the number of stations from which a Au concentration of 4.7 ppb or higher was obtained. What is striking about the latter is that 40 out of the 49 sites yielded either zero or all 4 samples above 4.7 ppb Au. That is, although the absolute Au

concentrations were not reproducible (e.g., Table 3.3, figure 3.6) the presence or absence of an anomaly (as defined by the cutoff of 4.7 ppb) is commonly reproducible.

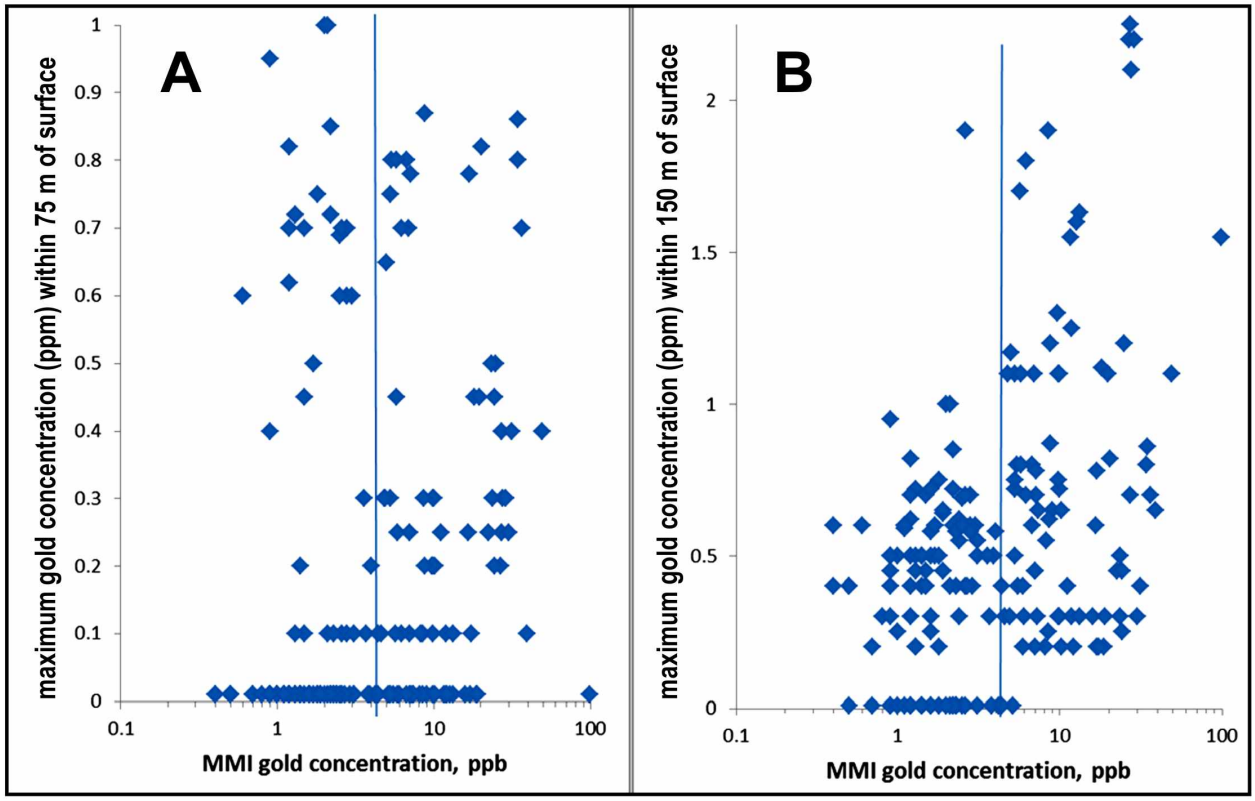

Figure 3.16: MMI Au Concentration vs. Maximum Au Concentration In Rock, within 75 m of the surface (left) and within 150 m of the surface (right). Vertical line is at 4.7 ppm and separates 'background' values from 'anomalous' values.

As indicated in figure 3.17, all but one (out of 18) of the sites which yielded an MMI Au anomaly in 2008 also yielded at least 2 (of 4) anomalies from the closely spaced sites in 2012. The lone exception is at easting 15100 (figure 3.17). Further, 13 of the 18 sites with anomalous Au in 2008 returned anomalous Au concentrations in ALL of the closely-spaced samples. Six additional anomalous sites were identified in 2012 (based on at least one of the 4 closely-spaced samples yielding at least 4.7 ppb Au), two of which, west of 14300 (figure 3.15) are likely false anomalies.

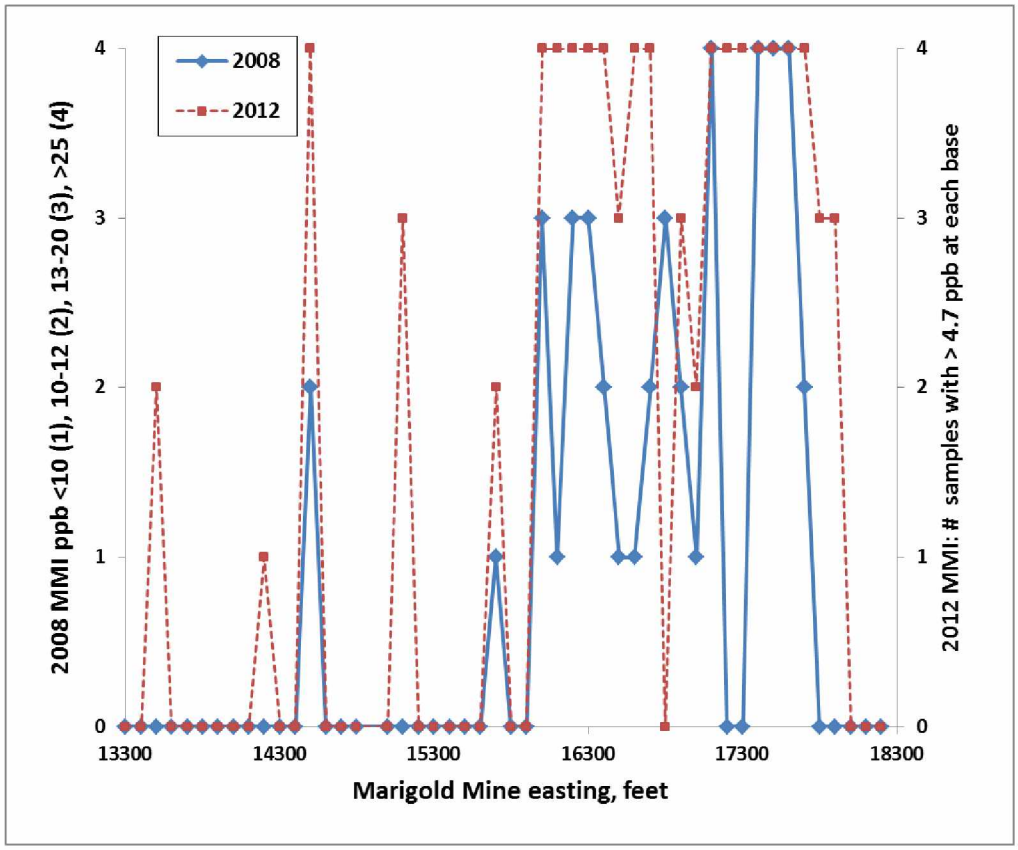

Figure 3.17: Results of the 2008 & 2012 Au MMI Surveys, along line X-Y-Z (Figure 3.1) presented as categories vs. Mine easting. For the 2008 data, <4.7 ppb =0, 4.7-10 ppb = 1, 10-12 ppb =2, 13=20 ppb = 3, and >25 ppb Au =4. For the 2012 survey, the number of closely spaced samples (out of 4) with >4.7 ppb Au are plotted. In most cases, an Au anomaly in 2008 is replicated as an anomaly in 2012.

Table 3.11 summarizes the results from the seven different cross-sections and associated Au MMI concentrations. The most obvious feature is that the success rate (MMI Au concentration is above background when the sample is above Au ore) is highest in the case of cross-section X-Y-Z. Here the ore is buried by less than 30 m of alluvium and rock, and much is very close to the surface (figure 3.15). In this case the success rate for both the 2008 and the 2012 surveys is approximately 50%, as compared to 0-29% for the cases with greater deposit burial (Table 3.7). The success rate could be increased by lowering the 'threshold' value for a MMI anomaly, but doing so would also increase the rate of false positive values, that is, anomalies present without ore below. Interestingly, the success rate employing the 4 samples

per site strategy of 2012 increases the success rate to nearly 60% if a success is counted for any of the 4 samples yielding Au concentration above the background value. This seems quite logical: given the relatively poor geologic sample reproducibility (e.g., Table 3.5) with 4 samples at nearly at the same location the likelihood of a sample yielding a value above background is greater than with only one sample.

Table 3.11: Summary of Au MMI and cross-section grade comparisons

X-section	year	burial depth (m)		# samples	# with	%	highest	# false	highest
		alluvium	rock	above min'z'n*	Au	'hits'	Au	positive	false Au
A-B	2008	35 - 50	6 - 20	6	0	**0**			
C-D	2008	30	30 - 45	4	1	**25**	4.7 ppb		
E-F	2008	35 - 90	3 - 100	7	0	**0**		1	10 ppb
E-F	2012	35 - 90	3 - 100	28	7	**25**	590 ppb	2	8.3 ppb
I-J	2007	0	350	17	4	**24**	10 ppb		
K-L	2008	9 - 30	30 - 90	14	4	**29**	16 ppb		
M-N	2007	6 - 90	130 - 6	3	0	**0**		4	18 ppb
X-Y-Z	2008	0 - 30	0 - 30	37	18	**49**	59 ppb		
X-Y-Z(1)	2012	0 - 30	0 - 30	148	79	**53**	99 ppb	3	5.5 ppb
X-Y-Z(2)	2012	0 - 30	0 - 30	37	22	**59**		2	
*min'z'n = mineralization 1= expressed as individual values; 2 = expressed as 4- sample sites									

It is difficult to tease out the relative importance of burial by alluvium versus bedrock in diminishing the MMI Au response, as both vary in most of the cross-sections. However, in two of the three cases (A-B and E-F, Table 3.11) with no measured anomalies the alluvial thickness was at least 35 m and the depth to bedrock as little as 6 m. Conversely, section I-J with essentially no alluvial cover at mineralization overlain by 300 m of bedrock yielded four samples with measurable MMI Au anomalies (Table 3.11). The other case with no measurable anomaly (M-N, Table 3.11) is characterized by inversely related thickness of alluvium and of bedrock.

Where the alluvium is 6 m thick, the ore is below 130 m of rock and where the alluvium is 90 m thick there is almost no rock cover. However, the largest MMI anomalies for the entire Marigold area (E-F, figure 3.10) are 135 ppb Au and 590 ppb Au, above 65 and 90 m of alluvium, respectively. (Notable, however, is the fact that these enormous anomalies could not be reproduced in samples 1.5 m away.)

Absolute values of Au concentrations by MMI appear to make no simple pattern with regards to depth to ore or Au concentration in the subsurface. The various factors that ultimately cause a given Au concentration to be extracted from the soil appear to be so complex as to make absolute values fairly meaningless. That is, a 30 ppb anomaly (or for that matter, a 590 ppb anomaly) does not appear to reflect 'better' sub-surface mineralization than a 20 ppb anomaly.

In sum, MMI in arid Nevada appears to detect anomalous Au values where ore is near the surface with a success rate of about 50%. The success rate could be increased by: 1) lowering the anomaly threshold, but at the expense of drastically increasing false positive values or 2) increasing the number of samples at or near each site to mitigate the low reproducibility issues addressed earlier, which would increase primarily analytical costs. Of the two options for increasing the success rate the second is recommended over the first, as subsequent drilling of even a few false positives would completely negate any analytical or labor savings. With burial by 35 m of alluvium the success rate drops to 0-25%, but the relation between success rate and depth of burial is not straightforward. MMI gold anomalies can be produced, however, even if the ore is 300 m below the surface (approximately 25% success rate) if there is little overlying alluvium.

3.7 MMI inter-elemental correlations

One final topic of concern with regards to MMI at Marigold is the question of associated elements. The MMI procedure as of 2015 generates data for some 35 elements; an obvious question is whether the 34 outside of Au have much value. One test of this is to look for inter-element correlations. This can be done with the entire data set or with a subset of the data. The entire dataset (>11,500 samples) is cumbersome, includes data from multiple years (2007-2012), is dominated by samples with low Au concentrations, and generally lacks data for Sb and Hg (only included in 2012). In order to best look for elemental correlations involving Au, Hg, and Sb I restricted the data set to the 2012 data with Au concentrations of 10 ppb and higher. This left only 44 analyses, but ones that clearly contain elevated Au. The data are given in Table 3.12, grouped into Au-, Ag-, and REE-associations.

The most important for this study is the strong correlation in the MMI between Au and Hg, which is an association that had been observed to varying degrees in both the rock sample and ore data sets and in data from Graney and McGibbon (1991). However, this strong correlation is almost exclusively the result of including the three samples with the highest (not reproducible) gold contents (590, 135, 99 ppb Au). These three samples also contain the 3 highest Hg concentrations and the 3 highest Tl concentrations. Progressively removing these samples from the correlation (Table 3.13) causes a progressive drop in correlation between these elements and Au, while raising the r-values for other elements. Exactly how this data should be employed is not clear; particularly as the highest MMI concentrations are extremely non-reproducible. Further, all of the highest Au samples are from cross-section E-F; none of the high Au samples from line X-Y-Z contain much Hg.

Table 3.12: R-values (above critical) between elements for MMI samples with >10 ppb Au*, collected at the Marigold property.

	Au	Hg	As	Pb	Ag	Co	Cu	Fe	Ce	Dy	Er	Eu	Gd	Nd	Sc
Hg	**0.93**		0.41												
Mo	0.31	0.50	**0.79**												
Tl	**0.92**	**0.80**		0.37											
Zn	0.48	0.55		**0.91**			0.32								
Co					**0.79**										
Ni					**0.81**	0.87	0.67								
Sb					0.57	0.63	0.47								
Cu					0.65	0.70			0.31						
Fe									0.75	0.71	0.69	0.78			
P			0.39						0.43	0.41	0.39	0.42	0.43	0.46	
Th							0.32	0.76	**0.95**	**0.96**	**0.93**	**0.95**	**0.98**	**1.00**	0.80
Sm							0.32	0.76	**0.95**	**0.97**	**0.95**	**0.96**	**0.99**	**1.00**	0.82
Dy							0.34		**0.95**						
Er							0.35		**0.93**	**0.99**					
Eu							0.31		**0.90**	**0.94**	0.92				
Gd							0.32	0.74	**0.95**	**0.99**	**0.98**	0.96			
Nd								0.76	**0.93**	**0.95**	**0.92**	**0.95**	**0.98**		
Sc								0.72	**0.81**	**0.81**	**0.79**	**0.80**	**0.82**	**0.81**	

*Excludes 3 samples not analyzed for Sb or Hg, n=44, r critical= 0.30. High values are in bold font.

Removing these, a weaker correlation between As and Hg was observed, however As-Sb ± Au correlations were not identified. Such correlations would be expected considering the ore compositions (Tables 2.5, 2.6, 2.12, and 3.14). Other notable correlations were between several of the rare earth elements (REEs), and also between REEs and Fe. These associations suggest the REEs co-precipitate with or are sorbed onto Fe-(oxy)hydroxides. Finally, a very strong correlation between Pb and Zn was also present. This correlation is entirely due to four high

Zn-Pb samples, all on line 52 (figure 3.5) and all located within 30 m of each other (Table 2.10). What caused these four samples to yield exceptionally high MMI Zn-Pb concentrations is unknown, but was apparently unique to them.

Table 3.13: Correlation coefficients between selected elements and Au, with the data modified by progressively removing highest-Au concentration samples.

Samples used	**element**						
	Hg	**Tl**	**As**	**Sb**	**Pb**	**Zn**	**Cu**
all 44	**0.93**	**0.94**	0.21	-0.03	0.24	0.48	-0.04
-top Au	0.78	0.74	0.56	0.21	**0.63**	**0.71**	0.31
-2 top Au	0.61	-0.1	**0.75**	0.38	0.2	0.13	0.11
-top 3 Au	0.14	-0.1	0	**0.49**	0.37	0.29	0.45

For comparison to tables 3.12 and 3.13, table 3.14 provides inter-elemental correlations for the Marigold composite results published by Graney and McGibbon (1991). Noticeably the same correlations that exist in the ore between Au-As-Sb-Hg are not reflected in the MMI, though other isolated associations can be found. The data suggests that elements are concentrated and (or) extracted with the MMI digest in a manner that does not preserve metal ratios consistent with the actual ore mineralogy. This is discouraging for those who would wish to use As, Sb, or even Hg as pathfinders at Marigold. Arsenic in particular would make a seemingly excellent pathfinder element given it association with Au in the original sulfide (Fithian et al., 2014) and its higher concentrations than Au (Tables 2.2 and 2.3), but the processes of oxidation and sorption with Fe-(oxy)hydroxides (Cheng et al., 2009; Asta et al., 2012) have likely redistributed As enough to potentially jeopardize its effectiveness as a pathfinder element.

Table 3.14: Correlation coefficients for 7 Marigold ore composite samples, between Au and As, Sb, Hg. Calculated from Graney & McGibbon (1991).

	Au	As	Sb
As	0.93		
Sb	0.98	0.94	
Hg	0.53	0.46	0.42

n=7, 95% r critical=0.75, significant values underlined.

Acknowledging that the elemental correlations for rocks and MMI do not agree, the potential causes are myriad. The complex oxidation history at Marigold (Theodore, 1998), and other geochemical complexities involving the mobility, redistribution, sorption, and changes in elemental oxidation state in systems with As-Sb-Fe (Asta et al., 2012; Cheng et al. 2009) are potential explanations for the disagreement between correlation statistics for the two different media (MMI soils and rocks).

Even though the MMI correlations did not agree with correlations from ore rocks, it seems prudent to test the potential usefulness of pathfinder elements from existing data. From the results of the previous investigations (Graney & McGibbon, 1991) and those presented in chapter 2, As, Sb, and to a lesser extent Hg have the highest probability of being useful as pathfinders for Au at Marigold. Unlike Au, however, I have no data for concentrations of these elements in the subsurface. I calculated an anomalous threshold value for each by averaging the lower half of the responses for samples collected along line X-Y-Z and rounding to the nearest whole number. This produced a minimum anomalous value of 2 ppb for both Hg and Sb and 8.2 for As. However, because I wanted the threshold value significantly above the detection

limit (5 ppb for As) I instead used 20 ppb as the minimum value for As. I then compared the presence or absence of values above the anomaly threshold to the subsurface block model (figure 3.13) to estimate the frequency that an anomalous MMI value for As, Sb, or Hg is associated with significant Au in the sub-surface. For the 128 sites comprising the western or mineralized portion of X-Y-Z, Sb had the highest success rate: 68%. Results for all elements are summarized in table 3.15. Also if successful identification is defined as an anomalous value of the primary element (Au) or any of the pathfinder elements (As, Hg, Sb), than for these 128 sites MMI has a success rate of 93%. However, many MMI anomalies are also present (Table 3.15) in the area east of 15800 (figure 3.13), that is, not above known ore. The proportion of samples with MMI Hg anomalies above 'no known ore' is only ½ of those than above 'known ore'. Further, all but 5 of the sites with anomalous Au also had anomalous Hg. None of these 5 are located above known ore. Raising the minimum anomalous concentration would reduce the large number of false anomalies, but would also reduce the identification of true anomalies. The same considerations are true from Sb and As: MMI anomalies occur both above 'known ore' and above 'no known ore'.

Line X-Y-Z is an ideal location for MMI, with relatively shallow burial depths and minimal alluvial cover. In this 'ideal' case, it's clear that As, Sb and Hg anomalies are present, but they are by no means restricted to zones above known ore. Employing pathfinder elements increases the number of anomalies, both 'true' and 'false'. More work is needed to determine if the approach of using pathfinder elements (with MMI) is fruitful.

Table 3.15: Effectiveness of pathfinder elements at producing MMI anomalies, directly above known ore at 128 sites and above non-ore sites along line X-Y-Z

	element			
	As	**Hg**	**Sb**	**Au**
Detection limit (ppb)	5	0.5	0.5	0.1
Anomalous Min. (ppb)	20	2	2	4.7
Effectiveness %	62	25	68	57
Comb. Effectiveness%				**93**
% anomalous, no ore	48	10	31	

3.8 Discussion of the Marigold studies

Some specific questions in regards to MMI require discussion in light of the Marigold studies, the first of which is reproducibility. The Marigold duplicate data set demonstrates the analytical reproducibility (splits of the same sample re-analyzed) of the MMI method is 6-20% mean deviation between the original sample and the duplicate. For Au specifically, the mean deviation is 15%, which is generally acceptable for distinguishing anomalies in soils given concentrations greater than 4 ppb and with lower limit of detection (LLD) of 0.1 ppb. Interpretation of geochemical data, however, requires determining background and anomalous concentration cut-offs. These will vary by element and likely by location. There are many statistical methods that can be employed to determine the absolute minimum value of an anomaly. However, the lower the minimum value, the greater number of total anomalies, both true anomalies and false positives. Alternatively, a higher cut-off value results in fewer false positives, but also fewer 'true' anomalies. That is, the chance of not identifying a site as likely above ore increases. At Marigold I benefitted by having geologic data from the subsurface, and chose a minimum anomaly value of 4.7 ppb for Au as yielding the highest number of true

anomalies and the smallest number of false ones. Without subsurface data one would need to start by employing mathematical operations similar to those used in section 3.7 with the pathfinder elements at Marigold, and refine background and minimum anomalous values as more data becomes available. Conducting geochemical studies similar to those presented in chapter 2 prior to soil investigations would aid in the MMI (or any geochemical soil method for that matter) survey design as it would help the explorationist know "what to look for".

The geologic reproducibility at Marigold is more complicated, ironically due to samples yielding the highest MMI Au concentrations. As noted earlier, MMI commonly yields single point anomalies that can be two orders of magnitude greater in concentration than the surrounding samples, and at least in the case of the high density sample lines (2012), closely spaced samples do not reproduce the high values. These samples may represent a best case scenario of several combined variables including everything from sub-surface oxidation rates and metal availability, to ion transport within the soil, concentration via absorption onto soil organics/clays, and finally extraction by the MMI digest at. There is always the possibility that these high absolute value samples could be a result of analytical error, but both the 135 and 590 ppb Au samples occurred above an ore zone. Even at 1.5 m away neither sample was reproducible in terms of absolute value, but both were near samples that were "anomalous" (above 4.7 ppb). These high absolute value samples were also problematic when constructing the various correlations. For example, their removal allowed the interval data to better show more compositional similarities in closer-spaced samples. If they are included in the analysis then no patterns are apparent; but when removed, samples spaced 1.5 m apart had a reproducibility of 20-60 relative %. Also, removing the one sample with the largest values of Fe and the REEs removed essentially any significant relationships between those metals in the dataset, and (Table 3.13) simply adding or removing one or two high value samples results in wide variations

in correlation coefficients among Au-As-Sb-Hg. In mineral exploration it is common practice to focus on the unusually high value samples, as they typically provide some of the best data about the ore; however, in this dataset especially, correlations are typically driven by less than 5% of the samples. Also the absolute value of an MMI anomaly appears to have no significance in terms of ore grade or depth to ore. The same Au concentrations buried by the same amount of rock and alluvium can produce either a 20 or 590 ppb anomaly (figure 3.13)--presumably a result of poorly understood variables involving the MMI process. In sum, MMI anomalies are commonly not reproducible in terms of absolute magnitude, especially in the case of the very high concentrations, but are more reproducible for generating a value above the minimum anomaly threshold.

This observation allows for an interesting approach to the way in which samples may be collected. That is, instead of collecting a single sample at a point, collecting samples in groups, allows for better likelihood of anomaly identification. This is because the combined effects of analytical reproducibility (6-20%) and geologic reproducibility (20-110%) cause enormous concentration variations. Even above an ore zone with ideal conditions, not all samples will return anomalous values, but the probability of 1 in 4 samples doing so is higher. This approach along cross-section X-Y-Z allowed MMI to achieve a success rate of 59% for Au (Table 3.11).

A thought while considering alluvium and bedrock above ore is total burial depth. If the ore is deep enough to be below the redox boundary it will not be producing any ions that can migrate. Many deep intercepts (>200 m, Table 2.11) at Marigold contain considerable sulfide (figure 2.11). This may potentially apply to some of the deposits on the northern portions of the Marigold property, and deeper portions of existing deposits. The degree of oxidation of the mineralization is important, as the cyanide leaching process employed by the mine is only effective for strongly oxidized rocks containing no sulfide minerals (Carver et al., 2014). In

other words, MMI should not be able to detect Au anomalies above un-oxidized rocks, but such rocks really wouldn't constitute 'ore' even with high Au concentrations, since it wouldn't be extractible with Marigold's current process and infrastructure.

Another question is the effect of bedrock and alluvium thickness on the ion migration process. Table 3.11 best summarizes my observations in this regard, though the question is difficult to quantify as both variables (bedrock and alluvial depth) change between the sample locations. In general however the data suggests that a meter of alluvial cover has a greater effect on inhibiting ion migration that a meter of bedrock. For example, data along cross-section I-J generated an anomaly through 300 meters of bedrock (figure 3.12), and no true anomaly was observed through more than 100 meters of alluvium (e.g., figure 3.9). Similarly poor results through thick packages of sediment cover were found by Fabris et al. (2009b) in southern Australia. They attributed the lack of success to thick cover (>100 m, similar to portions of Marigold) and the presence of a known subsurface aquitard beneath a portion of the study area. At Marigold the alluvial fill almost certainly has a greater cation exchange capacity (CEC) than the bedrock. This is due to the higher porosity and greater abundance of clay, Fe-Mn oxides, and organic matter in the alluvium than in bedrock (Thurman, 1985). (However, these would change depending on the degree of oxidation of the bedrock). If the alluvium was a uniform thickness one would not worry about the migrating ions it was capturing because all areas would be effected more or less equally. However, at Marigold, alluvium is centimeters to hundreds of meters thick, and consequently exerts a variable influence on MMI. At Marigold MMI responses were invariably higher in areas of thinner alluvium, resulting in more effective surveys (Table 3.11). The exception is cross-section E-F (figure 3.11, Appendix 1.3) which returned the highest MMI Au concentrations (135 and 590 Au ppb) in 2012 despite 75 m of overlying alluvium. These concentrations were not reproduced in samples taken 1.5 meters

away, nor were they seen in the 2008 survey at the same locations. Explaining how such enormous anomalies can arise in this setting is beyond the scope of this study.

The use of As, Hg, and Sb, as pathfinders proved effective in identifying Au in the subsurface along line X-Y-Z despite redistribution effects of oxidation. Arsenic and Sb proved more effective, around 60%, compared to Hg at 25% (Table 3.15). However, numerous false anomalies were also generated by this approach, a proportion equal to or greater than the true anomalies. These percentages would be expected to diminish moving into less ideal sampling areas. The broad nature of this particular deposit (figure 3.15) is also partly responsible for these results; a smaller, more isolated deposit might yield a more focused response. Inarguably the use of pathfinders would be most effective after acquiring a sound geochemical understanding of the target ore. Results from studies similar to those preformed in chapter 2 would prove invaluable for the initial design of an MMI survey.

3.9 Conclusions after the Marigold studies

1. MMI produces anomalies in the same elements as mineralized rocks, however elemental correlations generally do not closely resemble those of mineralized rocks.

2. MMI anomalies are analytically reproducible, but are only site reproducible as indicating an anomaly for a given year. MMI highest concentrations cannot be found in samples 1.5 m apart and cannot be reproduced by surveys in different years.

3. In areas of thin (<10 m) alluvial cover MMI Au anomalies can be correlated with Au concentrations in oxidized sub-surface rocks with success rates of nearly 60% and some

false anomalies. Success rates fall drastically, and false anomalies increase, with increasing alluvial cover.

4. The use of MMI anomalies of pathfinder elements is variable especially as MMI pathfinder element concentrations do not strongly correlate with Au. Under ideal conditions (<10 m cover) Sb and As yielded success rates as high as 68%. However, pathfinder elements also generate a significant number of false anomalies.

Geochemical Investigations of the Gil Prospect, Alaska

4.1 Introduction to the Gil Studies

The Gil Prospect, near Fairbanks, Alaska (figure. 4.1) has Au grades similar to those of the Marigold deposit, but is hosted in complexly-deformed metamorphic rocks, and has a different geomorphic and climatic setting. It is overlain by a thick moss and organic soil horizon, under which variably thick deposits of loess (wind-deposited silt) are present, as well as decomposed bedrock. Depth to bedrock is much shallower (<3 meters) when compared to Marigold. Also, the deposit is in the discontinuous permafrost region and permafrost is variably present, factors that make the use of MMI potentially questionable, at least compared to the desert environment of Marigold. The purpose of this chapter is to investigate the effectiveness of MMI in locating bedrock Au sources at depth, and to better understand the distribution of mobile metals in sub-arctic soils. The dataset for the Gil prospect includes:

2 soil cores
- -total organic carbon 2 cm intervals
  - *U.S. Army Fort Wainwright soil testing laboratory*
- -MMI 2 cm interval
  - *SGS Minerals Toronto, Canada*

30 MMI soil samples
- *SGS Minerals Toronto, Canada*

49 multi-element, 2 acid digest soil samples
- *ALS-Chemex Fairbanks, AK*

342 Au-fire assays of trench channel samples
- *ALS-Chemex Fairbanks, AK*

Survey and individual sample locations are provided in figure 4.2. After addressing relevant background information, I start with an examination of metals and carbon in soil cores and then show results of a MMI soil survey compared to Au concentrations seen in nearby soil samples and the nearby trench.

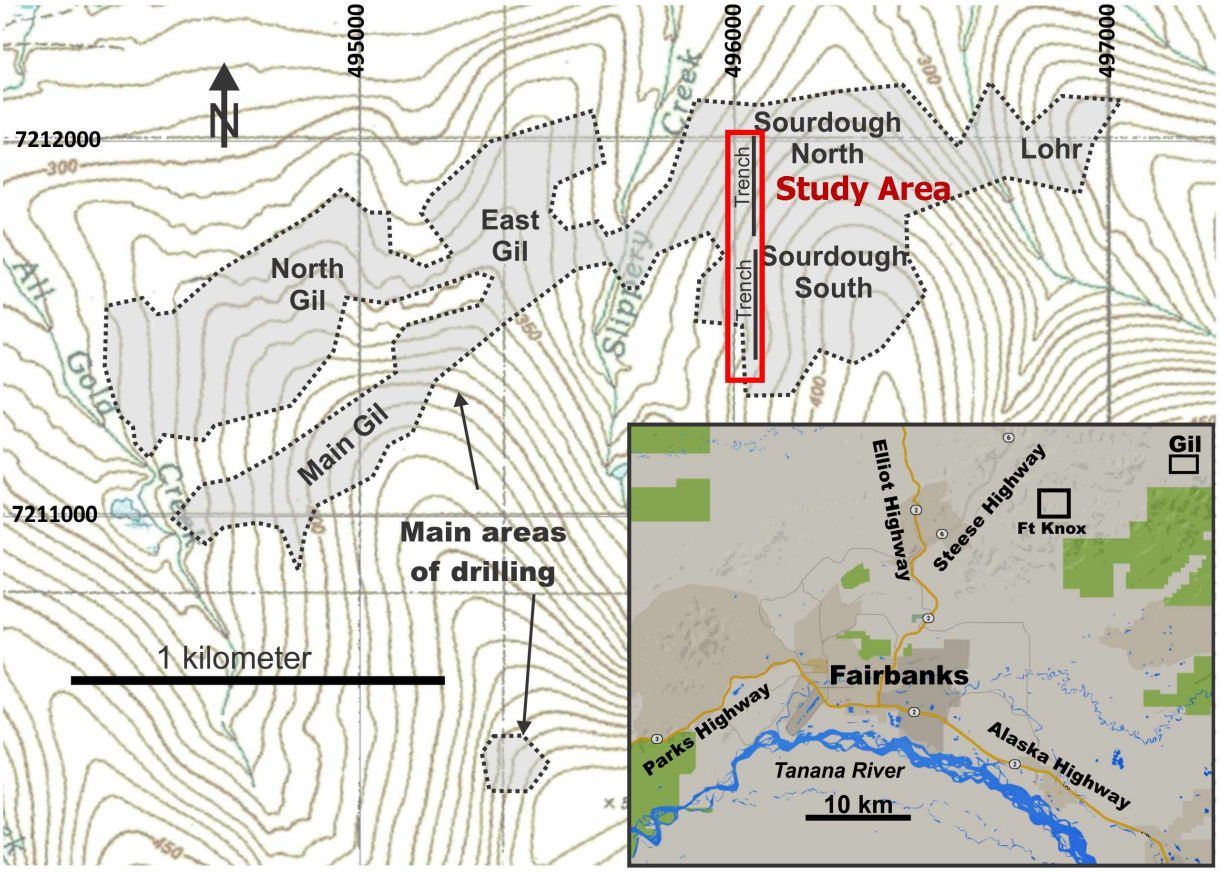

Figure 4.1: Location map of the Gil Prospect, showing the primary exploration areas.

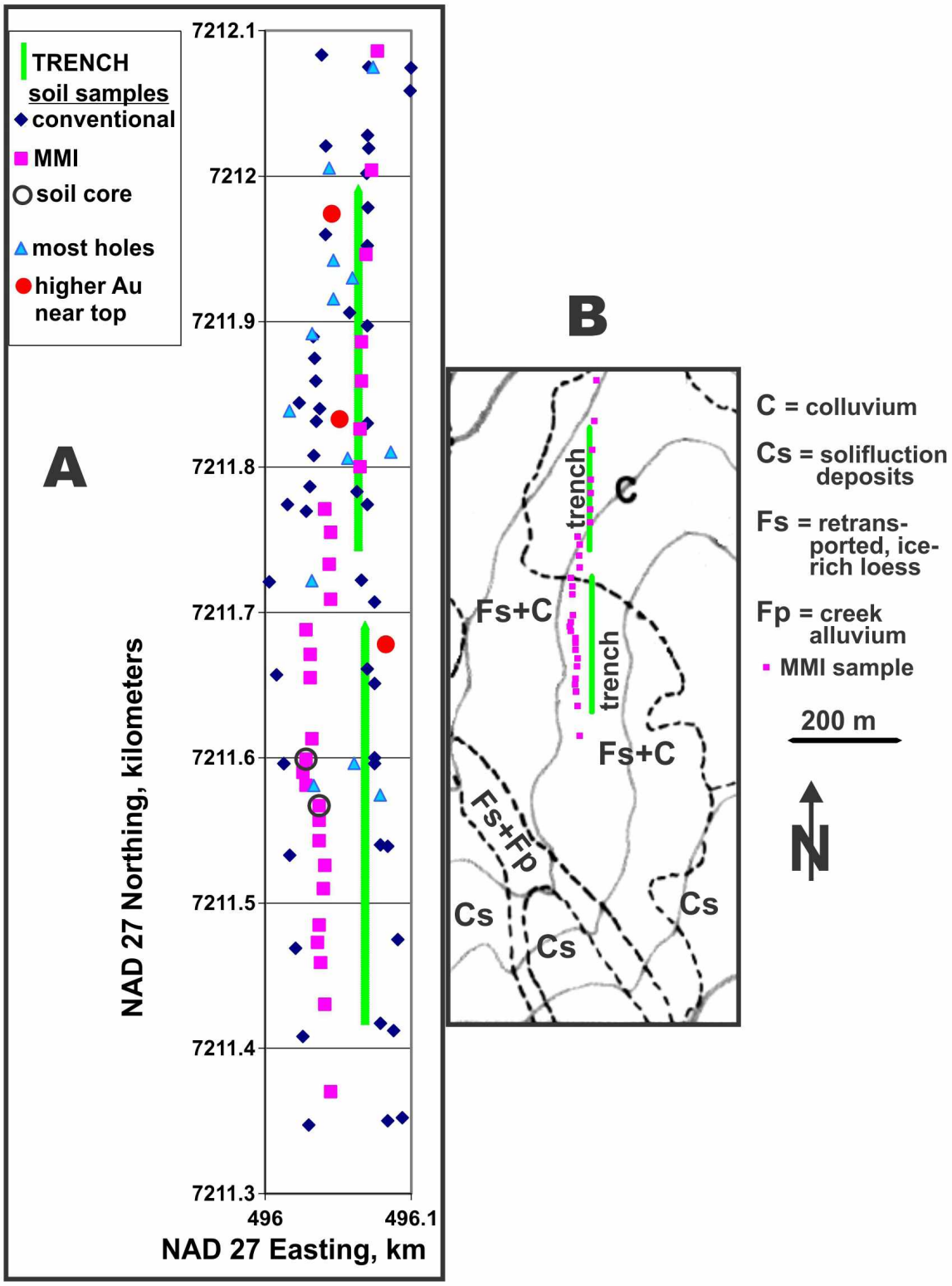

Figure 4.2. Geochemical sample locations, Gil prospect, Alaska. A = detailed map on a NAD 27 UTM grid. B = Trench and MMI samples superimposed on a surficial geologic map (modified from Lee, 1982). The study are and trench locations are shown boxed in red on figure 4.1. Complete soil core analyses in Appendix 2, MMI soil analyses in Appendix 3.

4.2 Geologic setting

Gold is associated with Bi and to a lesser degree Te and As at Gil (Robinson, 2010.) At South Sourdough (figure 4.1), Au mineralization largely appears strata bound within calc-silicate units; however, Au is predominately localized on veins and joints (Sims, 2015). Veins are up to 30 cm wide of white quartz, and later, thinner, quartz-calcite (± amphibole). Both sets of veins are steeply dipping and cut foliation. At North Sourdough (figure 4.1) Au is almost exclusively associated with quartz veins. Here the quartz veins are less than 5 cm wide and consist of milky-white quartz-arsenopyrite, quartz-calcite, and (or) quartz-albite (Sims, 2015). Pyrite and arsenopyrite are the most common accessory minerals observed in the veins, typically in concentrations of <1%.

The surficial environment at Gil is boreal forest. Soils are covered with a 10-40 cm mat of moss; the upper-most O horizon varies between 2-4 cm of partially decomposed organic material, it grades downward into the A horizon comprising 2-6 cm of fine grained organic particles, organic rich clay, and silt (figure 4.3). At Gil the A horizon though still somewhat loose and porous is more consolidated than the O horizon, so that the O horizon is easily brushed off of the A horizon at the A's upper contact. The A horizon's lower contact grades over a space of 5-6 cm to a loamy silt matrix including 0.5-1.5 cm clasts of partly decomposed schist comprising the B Horizon; observed thicknesses were between 25-40 cm. The lower contact of the B Horizon is also gradational moving into the C horizon which is characterized by a silt/sand matrix around progressively larger (>10 cm) clasts of green schist, and noticeably less clay. The hillside sampling area for this study had C Horizons ranging in thickness from 0.5 to <3 meters, though property wide thicknesses as great as 20 meters have been encountered (Jenks, 2002). Surficial geology in the vicinity of the MMI samples (figure 4.2 right) is colluvium and retransported ice-rich loess, however solifluction deposits are common in the vicinity. In most

cases depth to bedrock is less than 3 meters. The area was cleared for drill roads and trenches starting in the 1990s; stripping vegetation removed the insulating layer, exposed ice lenses and permafrost (Robinson, 2010) which have melted in the subsequent decades. Although permafrost was common in the 1990s, I encountered no ice while sampling in early September. The soils in three locations were tested at ~20 cm depth for pH and yielded 4.1-5.7, or acidic.

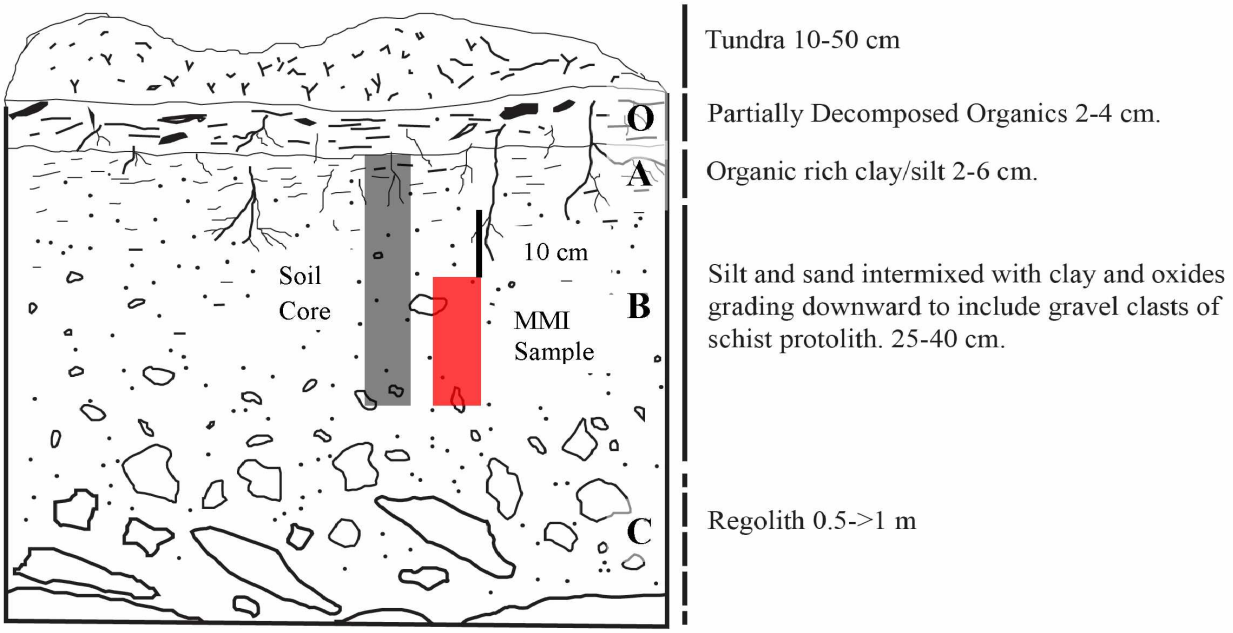

Figure 4.3: Idealized soil profile of the Gil Prospect, Alaska. Note the soil horizons and depth, also the MMI sample (in red) collection began 10cm below the base of the organic-rich zone, and continued for 15cm.

4.3 Methods

Two sets of soil cores were collected at the locations identified on figure 4.2 using 30 cm long sections of Acrylonitrile-Butadiene-Styrene (ABS) pipe with inner diameter of 10 cm. Each set consisted of three, immediately adjacent, essentially identical, tubes. Cores where allowed to desiccate for several weeks before removal from tubes. Cores were removed from the tubes by cutting the pipe on opposite sides. Cores were then cut into 2 cm thick discs with a vinyl

putty knife; the three discs (one for each core) for each 2 cm interval were then roughly homogenized in a plastic sample bag. Sample weights were 110 - 225 g. After homogenization, 5-25 g of material was removed for total organic carbon (TOC) analysis.

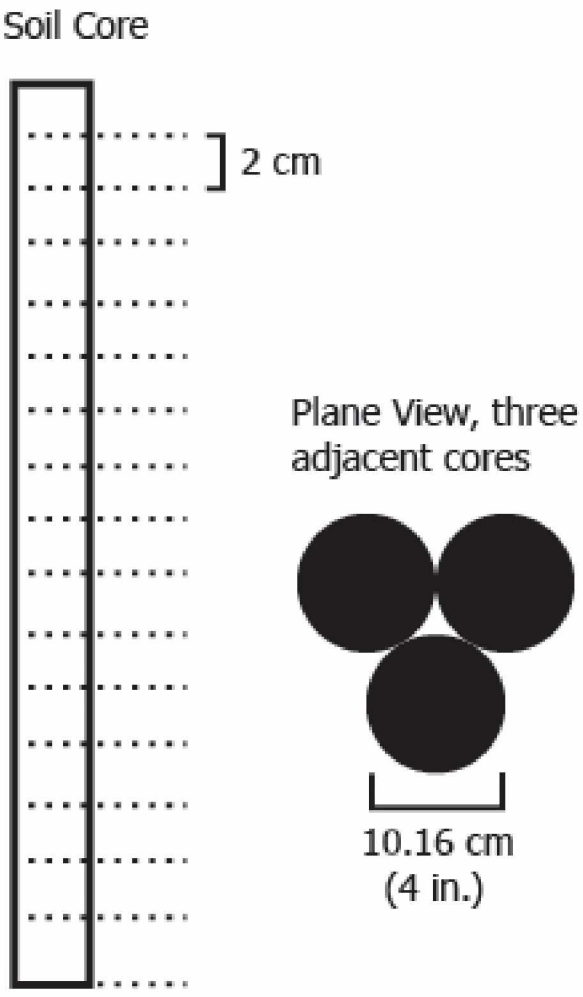

Figure 4.4: Soil Core Experiment, each soil core sampled 30-32 centimeters of material from the A and B horizons (figure 4.3). In order to collect sufficient sample masses (100g minimum) for the fine scale (2cm,) interval desired, it was required to collect three immediately adjacent cores in the arrangement shown above (right); this was done in both locations sample locations (figure 4.2). Each of the three cores were then subdivided (left) and MMI and TOC analysis preformed on each interval.

Material for TOC analysis was dried at 50° C (122° F), then pulverized and homogenized using a SPEX SamplePrep miniature ball mill. TOC analysis were performed utilizing a Shimadzu TOC-L total organic carbon analyzer. Calibration curves were generated by analyzing 0, 5, 10, 20, and 30 mg of carbon, with dextrose as the standard. Calibration curves yielded r^2 of 0.996. Triplicate analyses were performed and reported values are the average. I used approximately 50 mg of carbon-rich soil and approximately 1 g of mineral-dominated soil to keep TOC quantities within the calibration curve.

MMI soil samples were collected using a procedure previously employed by Fairbanks Gold Mining Inc. (FGMI) to make results compatible with earlier MMI surveys in the area. I first removed the tundra organic mat and then dug through the organic-bearing soil to the underlying material. I measured 10 cm below the base of visible organic matter (A horizon lower contact) and removed material from that point (A/B horizon contact -10 cm) to 15 cm below that point (A/B horizon contact -25cm) (figure 4.3). In comparison to Marigold, the Gil samples were collected deeper, as the A horizon is much more developed at Gil than Marigold.

4.4 Investigations of Gil soil cores

The objective of the cores was to observe how trace metal and organic matter concentrations vary with depth, with the goal of determining the ideal MMI sampling depth or interval within a soil horizon. Total organic carbon analysis would also chemically define the contact between the A and B horizons, and because organics are known to sorb metal ions (Sipos et al., 2008) this could be potentially beneficial in identifying/defining this ideal sampling interval. Complete data are given in Appendix 2.

From published works the pattern I expected to see for TOC content in the Gil soils is high concentrations in the A horizon with a drastic decrease in concentration moving into the B horizon, similar to the model presented by Foth (1984; figure 4.5 right). The gradational contact between the A and B horizon was observed to be 5-6 cm wide so I expect the decrease in concentration to be relatively abrupt.

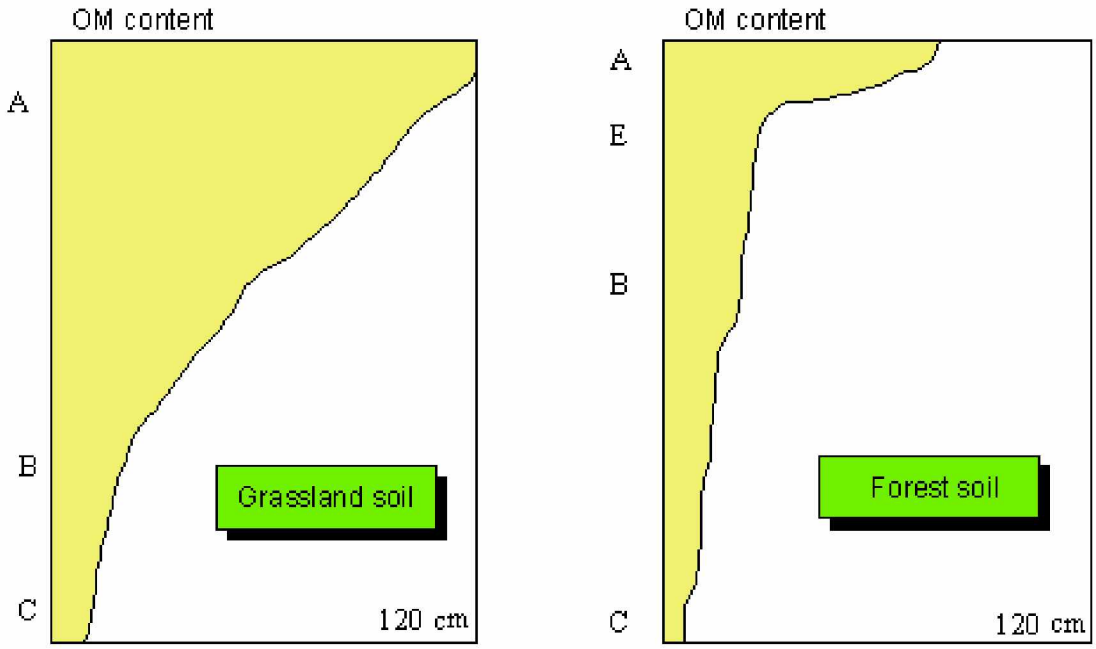

Figure 4.5: Organic Matter Content in Soils, comparison between a grass land and forest, modified from (Foth, 1984). TOC patterns collected at the Gil are expected to have a pattern similar to that presented for a forest soil, specifically a drastic decrease in TOC content moving out of the A horizon and into the B.

As for concentrations of the various metals I expected to see the highest MMI concentrations constrained to the upper portions of the B horizon (figure 4.6). Such results would be consistent with previously successful MMI studies such as Mann et al. (2005) and Gray et al. (1999).

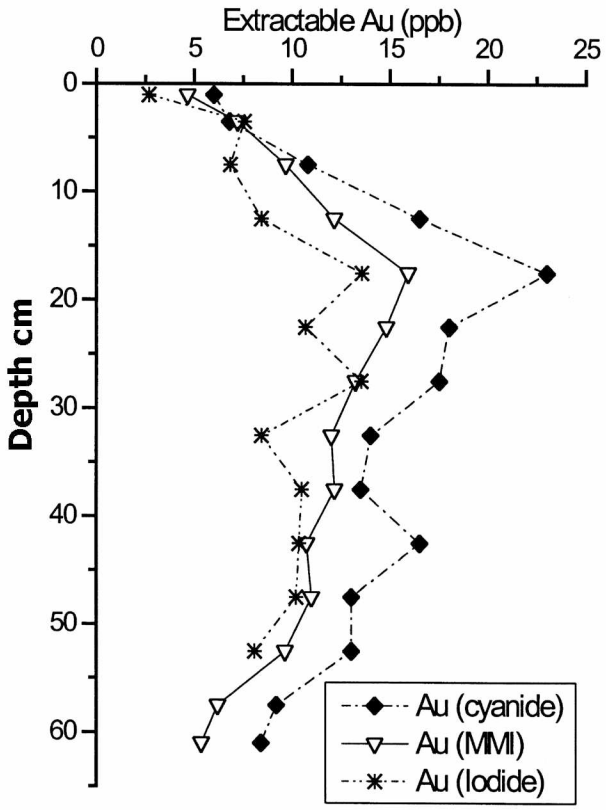

Figure 4.6, Extractable Au in Calcareous Soil, modified Gray et al. (1999). In this sampled soil profile multiple extractants (including MMI) solubilized the maximum concentration from the upper B horizon. A similar pattern is expected for MMI analysis of the Gil soil cores.

Results of analysis of the Gil cores yielded both expected and unexpected results. As an example, figure 4.7 shows MMI Au and Bi concentrations and %TOC (total organic carbon) from the bottom of the decomposing organic layer (the start of the A horizon) to the bottom of the core at ~30cm. Bismuth was chosen to accompany Au on the chart as the two are known to have a mineralogical relationship at Gil (Robinson, 2010; Sims, 2015). The uppermost soils contain the highest TOC, which drops drastically at 6-8 cm from the surface and stays at 1-2%

through the remainder. The break between organic-rich and organic poor in the soil is the A/B horizon contact. This is consistent with the model provided by Foth (1984, figure 4.5).

Unlike %TOC , which displays a simple and regular pattern, MMI Au and Bi concentrations show contrasting and complex patterns. The highest Au concentration in core 9829 and second-highest in core 9825 was at 17 cm; the highest Au in the latter core was at 29 cm (figure 4.7, Appendix 2). In both cores the highest Au concentrations were in the B-horizon, although a Au spike is present at the bottom of the A horizon in core 9825 (figure 4.7). In contrast, the highest Bi concentrations in both cores were in the A horizon, although core 9829 contains a secondary Bi spike at 11 cm, well into the upper B horizon. The most striking feature is how much the two cores—taken only 35 m apart—differ from each other in their metal profiles.

The vertical distribution of other MMI concentrations (Ag, As, Cu, Ni, Zn, and Zr) for the two cores (figure 4.8) also display complex patterns. MMI concentrations of Zn and As are highest in the A horizon, although secondary peaks for As occur in the upper B horizon. Silver concentrations, in contrast, peak in the lower part of the lower B horizon (figure 4.8). For the others (Zr, Cu, Ni) concentrations are always higher in the B than the A horizon, but with variable maxima in the upper or lower B horizon, depending on the core. Zirconium's concentration in the lower B horizon in core 9825 makes sense as Zr is considered immobile, and therefore having concentration increase with the mineral fraction of the soil is logical, the same pattern is not observed however in core 9829. Both cores do show elevated concentrations of Zr in the upper B horizon (consistent with MMI theory).

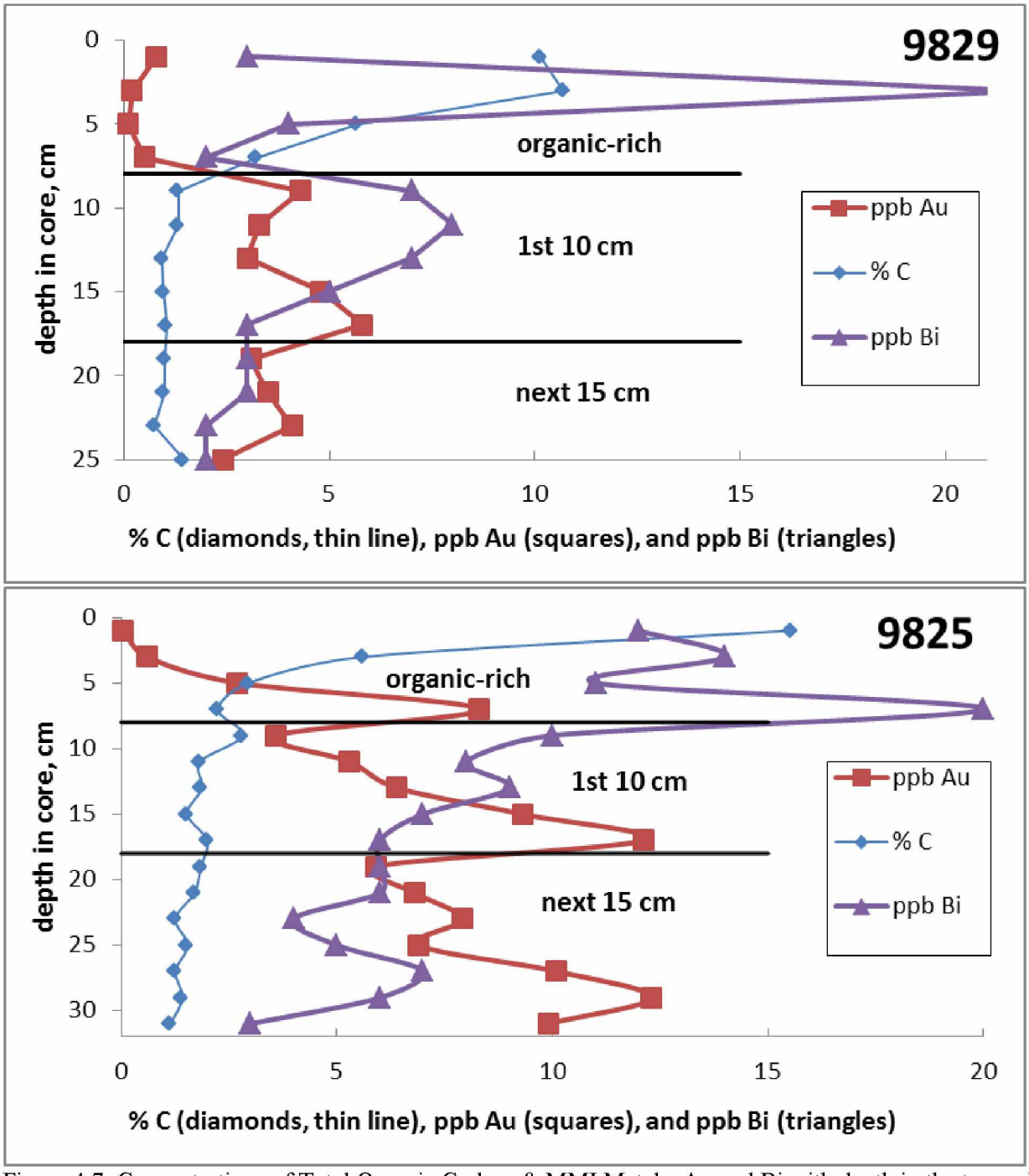

Figure 4.7: Concentrations of Total Organic Carbon & MMI Metals, Au and Bi with depth in the two soil cores. Black lines separate different soil zones: uppermost = A horizon, middle = upper B, lower is lower B. The lower B corresponds to the interval for which MMI samples were taken. (Appendix 2)

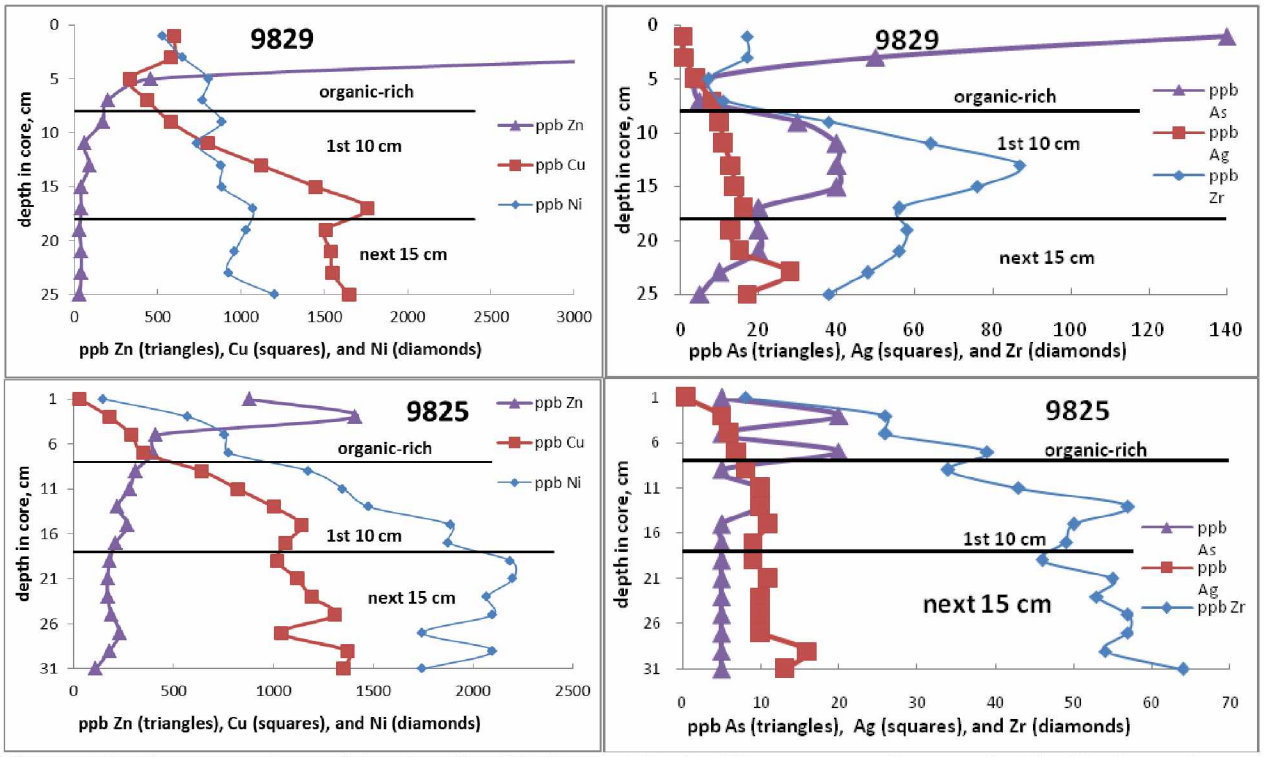

Figure 4.8: Concentrations of As, Ag, Cu, Ni, Zn, and Zr, in Gil prospect soil cores (ppb). Horizontal lines mark soil zones, as described for figure 4.4. Different metals tend to concentrate in different horizons, some in the organic-rich zone (e.g., Zn, As), others at various depths in the B-horizon. (Appendix 2)

MMI concentration distributions for many elements (figure 4.9 and Table 4.1) show both consistent and inconsistent patterns, as summarized in Table 4.2. Of the 33 elements (treating the 15 rare earth elements as 1 element) with MMI concentrations routinely above detection for the two soil cores, the largest single group consists of those with highest concentrations in the 'A' horizon (Table 4.2) This group includes the two elements (Bi and As) most commonly associated with Au at Gil (Robinson, 2010). The second largest group (6 elements) consists of those with highest concentrations in the lower 'B' horizon. The smallest group (3 elements) contains those with highest concentrations in the upper 'B' horizon. Strikingly, 14 elements (nearly half) concentrate differently in two soil cores, some with radically different concentration patterns. For example, MMI concentrations of Ca, Sr, and Mg are highest in the A horizon in

core 9829 but highest in the lower B horizon of 9825 (Table 4.2). Conversely, MMI concentrations of Ti, Al, Ga, and Nb are highest in the A horizon of soil core 9825 and highest in the upper B horizon of core 9828.

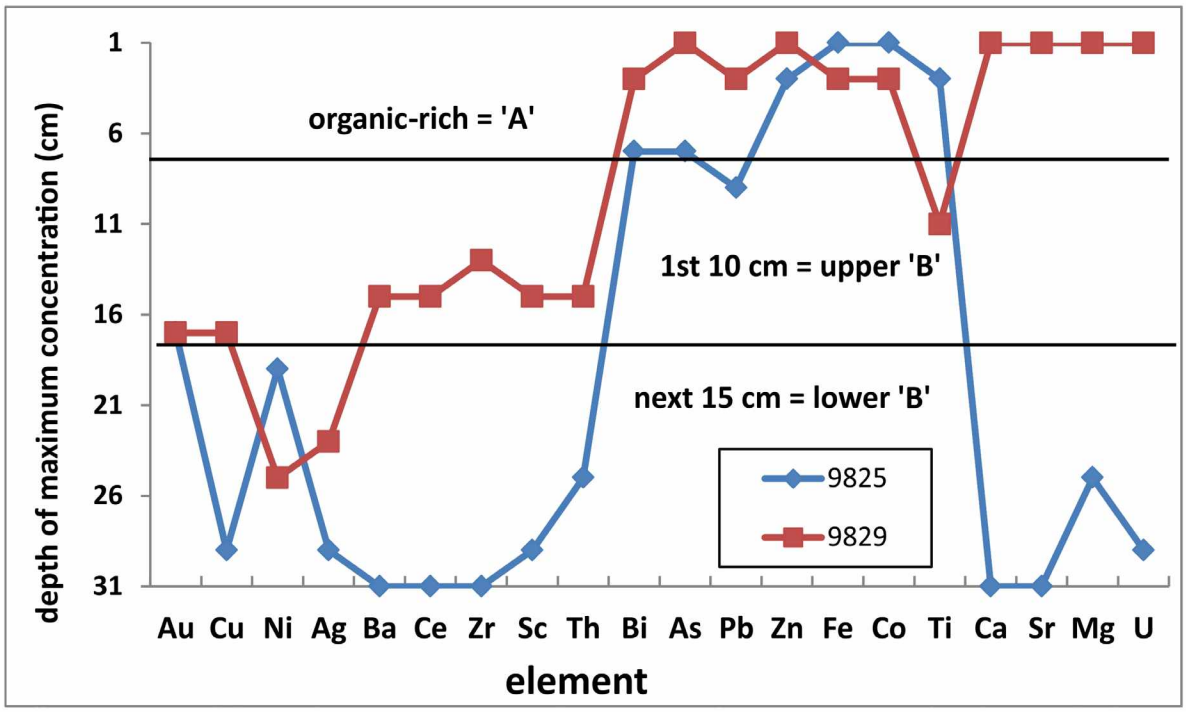

Figure 4.9: Depth of Maximum Concentration, for selected elements in the two soil cores. (Appendix 2)

Table 4.1 Average MMI elemental concentration for many elements in three major soil zones, for each soil core . (Appendi

core 9825	**Au**	**Cu**	**Ag**	**Ni**	**Bi**	**As**	**Zn**	**Pb**	**Rb**	**U**	**Zr**	**Ti**	**Ba**	**Ca**	**Fe**	**Mn**	**Al**
avg concentration (ppb unless indicated otherwise)													ppm	ppm	ppm	ppm	ppm
A: organic-rich	3	213	5	566	**14**	**13**	**775**	195	45	17	25	**307**	3.9	155	**167**	**12**	**208**
B: 1st 10 cm	7	932	10	1556	8	7	258	**242**	**141**	49	47	159	**8.1**	210	109	3	188
B: next 15 cm	**9**	**1200**	**11**	**2023**	5	5	176	196	128	**68**	**55**	75	7.2	**286**	78	3	137
core 9829																	
avg concentration	**Au**	**Cu**	**Ag**	**Ni**	**Bi**	**As**	**Zn**	**Pb**	**Rb**	**U**	**Zr**	**Ti**	**Ba**	**Ca**	**Fe**	**Mn**	**Al**
A: organic-rich	0	488	3	688	**8**	**50**	**3213**	**370**	17	33	13	184	3.7	**258**	**159**	**15**	189
B: 1st 10 cm	**4**	1142	13	891	6	34	80	332	129	46	**64**	**923**	**5.3**	100	82	2	**206**
B: next 15 cm	3	**1563**	**18**	**1030**	3	14	35	295	**143**	**54**	50	395	5.1	138	59	1	161

Table 4.2: Summary of MMI concentration patterns for the 2 soil cores (Appendix 2).

Highest concentration zone	**elements**	**number***
Always in 'A' horizon	**Bi, As**, Zn, Fe, Co, Mn, K, P, Li, W	10
Always in upper 'B' horizon	Ba, Cs, Tl	3
Always in lower 'B' horizon	Cu, Ni, Ag, U, Th, Sc	6
'A' (usually 9825)or upper 'B' (9828)	Ti, Al, Ga, Nb; Pb, Cd	6
Upper (9829) or lower (9825) 'B'	**Au**, Rb, Zr, Y, Rare Earth Elements	5
'A' (9829) or lower 'B' (9825)	Ca, Sr, Mg	3

*Number of elements in each group, counting all rare earth elements as 1 element, **bolded** elements are associated with the Gil ore.

A final comparison between elemental concentrations in the two soil cores is shown from the Pearson correlation coefficients (r^2 values) for the various elements (Table 4.3). Correlations between elements in the soil cores is a measure of how similarly the elements concentrate, and not of concentrations in the underlying bedrock. For example, the elements Ca, Mg, and Sr display very high r^2 values (>0.9) despite the fact that in one core hole they are highest in the A horizon and in the other they are highest in the lower B (Table 4.2) because all three elements display very similar elemental concentration patterns. Other elemental groups that display similar concentration patterns (r^2 values $\geq$0.70) include Ba-Au, Cu-Ce-Y-Zr-Th (usually highest in the lower B horizon), As-Cd-Zn (always concentrated in the A horizon), and K-P-Li-Mn (always highest in the A).

Table 4.3: r^2 values for MMI elemental correlations in two soil cores, Gil prospect, AK (calculated from appendix 2)

	Y	*Ba*	*Au*	*Cu*	*Ag*	*Ce*	*Zr*	*Sc*	*Th*	*Bi*	*As*	*Zn*	*Fe*	*Co*	*Ca*	*Sr*	*Cs*	*Cd*	*K*	*P*	*Li*
Au		0.75																			
Cu	**0.80**																				
Ni			0.67																		
Ag				0.65																	
Ce	**0.87**	0.60		0.63																	
Zr	0.71					0.77															
Sc	**0.96**			**0.84**		**0.84**	0.73														
Th	0.74			0.70	0.62		**0.80**	0.79													
Zn											0.76										
Fe										0.64											
Co					0.65								0.66								
Sr															**0.96**						
Mg															**0.92**	**0.95**					
U	0.62			0.68		0.68		0.64													
Cs	0.64					0.65	0.62														
Rb	0.78			0.62		0.69	0.71	0.75	0.75								**0.87**				
Cd											0.69	**0.95**		0.61							
Ga																					
K												**0.80**		**0.86**				0.73			
P												0.74		0.75				0.77	**0.84**		
Li											0.72	**0.95**		0.68				**0.92**	**0.86**	**0.80**	
Mn											0.62	**0.85**						0.68	0.76		0.78

Note: only values $\geq$0.6 are displayed; values $\geq$0.8 shown in bold

4.5 Tests for reliability of MMI data

The most straightforward test of MMI reproducibility is derived from the fact that the MMI samples were taken centimeters from the soil cores. One would expect that the average concentrations for the lower part of the two cores (10-25 cm below the A horizon) would match the MMI concentrations in the adjacent samples. Representative elements display serious differences (0% to 200%) between core and adjacent normal sample; in contrast, agreement in MMI Au concentrations is better (5-27%; Table 4.4.) The average % difference between soil and core MMI concentrations is approximately 47% (Table 4.4). The % difference between soil core and adjacent soil MMI values generally decreases with increasing MMI concentration (figure 4.10), but even for high concentrations % differences are still $\pm$ 50%.

Table 4.4: MMI concentrations* in soil core vs. adjacent sample, for selected representative elements

						ppm							
Element	Ag	Au	As	Bi	Ba	Ca	Cu	Mn	Ni	Pb	Zn	Co	Avg#
9825-soil	10	6.2	5	8	5.0	150	820	2.5	1730	240	160	510	
9825-core	11	8.5	5	5	7	286	1200	2.7	2023	196	176	301	
% difference	-11	-27	0	51	-31	-48	-32	-7	-14	23	-9	70	43
9829-soil	16	3.1	40	5	4.6	100	1270	1.6	785	330	50	214	Avg#
9829-core	18	3.3	14	3	5	138	1563	0.7	1030	295	35	131	
% difference	-12	-5	191	100	-10	-27	-19	136	-24	12	43	63	50

*Concentrations in ppb unless indicated otherwise; #Average of absolute values of % differences for 33 elements

In sum, MMI concentrations in soil vs. those in the lower part of the adjacent soil cores display major discrepancies and suggest only modest geological reproducibility of MMI values. The only modest agreement between MMI concentrations in samples taken several centimeters apart is striking.

Table 4.5: Elemental correlations for broadly Au-Ag-As-related elements, in MMI soil samples, Gil prospect

	Ag	*As*	*Au*	*Ba*	*Ca*	*Mg*	*Pb*	*Fe*
Ba			**0.84**					
Ca			0.69	**0.89**				
Fe	-0.74		-0.64	-0.70	-0.63			
Mg				**0.81**	**0.87**			
Nb		0.68			-0.61	-0.68		
P		0.78			-0.61	-0.73		
Sb								0.66
Sc	0.62						0.61	-0.61
Sr	0.62		0.65	**0.88**	**0.96**	**0.94**		-0.62
U	**0.82**		0.61	0.74	0.71			-0.71
Y							0.60	-0.63
Zn							0.65	

r values <|0.6| are omitted; higher values are shown in bold and underlined

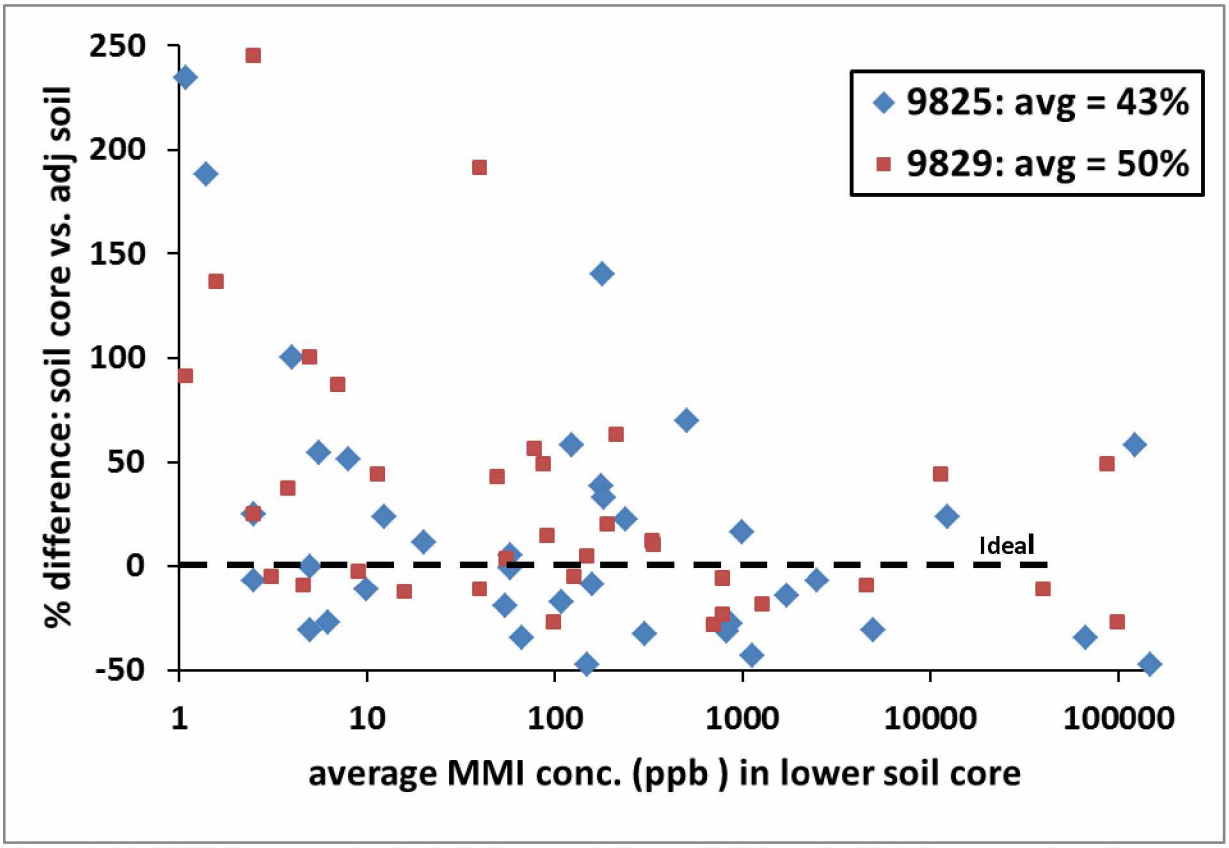

Figure 4.10: MMI Concentration in Soil Core vs. Adjacent Soil Sample, % difference and total concentration for all elements in soil cores and adjacent soil (MMI) samples. Elements with higher agreement are closer to 0% difference with their corresponding concentrations (ideal, plot along dashed line). Note that several element concentrations vary greatly even though sampled only centimeters apart. Higher MMI concentrations were typically reported for the lower part of the soil cores than the adjacent soil sample. (Appendix 2 & 3)

Correlations between MMI concentrations for different elements yield somewhat peculiar values (Tables 4.5, 4.6). The Au-As-Bi association, broadly seen in Gil rocks and soils (Robinson, 2010) is not displayed by the MMI data. Instead, MMI Au displays a strong correlation with Ba (r = 0.84, Table 4.5) for reasons that are unrelated to bedrock concentrations. However, many of the correlations (e.g., Ca-Mg-Sr, Table 4.4; Cs-Rb, Ce-Y, Table 4.5) seem perfectly reasonable based on typical elemental patterns (Brand et al., 1998; Aljarrah & Medrai, 2008) and their close association in the soil cores (figure 4.9).

Table 4.6: MMI elemental correlations for elements with no correlation to precious or base metals, Gil prospect

	Cs	*Ga*	*Mn*	*Nb*	*P*	*Sc*	*Sr*	*Th*	*U*	*Ce*
Fe										-0.68
Nb		0.60								
P				**0.90**						
Rb	**0.89**									
Sb			0.71	0.61						
Sc										**0.86**
Sr				-0.68	-0.69					
Th	0.60					0.79				0.78
Ti		0.73		**0.85**	0.60					
U						0.75	0.70			0.69
W	0.67	0.75								
Y						**0.90**		0.62	0.69	**0.90**
Zr				0.64				0.64		

r values <|0.6| are omitted; higher values are shown in bold and underlined

4.6 Gil Prospect comparison of MMI, conventional soils, and trench data

Correlation between conventional soil data and MMI data is hampered by the limited spatial overlap between the two (figure 4.2). Most conventional soil samples were taken at locations >30 meters from the closest MMI sample. However, 10 conventional – MMI pairs were collected at distances of 4-15 meters apart, with an average distance of 11 m. Correlation coefficients for MMI vs. conventional soil concentrations in the same elements show only Cu (figure. 4.11A) with an r value greater than the critical value for N = 10 (0.63). If the highest (highly anomalous) Au concentration for the conventional soil samples is ignored, correlation coefficients for Au are also barely higher than the critical value (figure 4.8B).

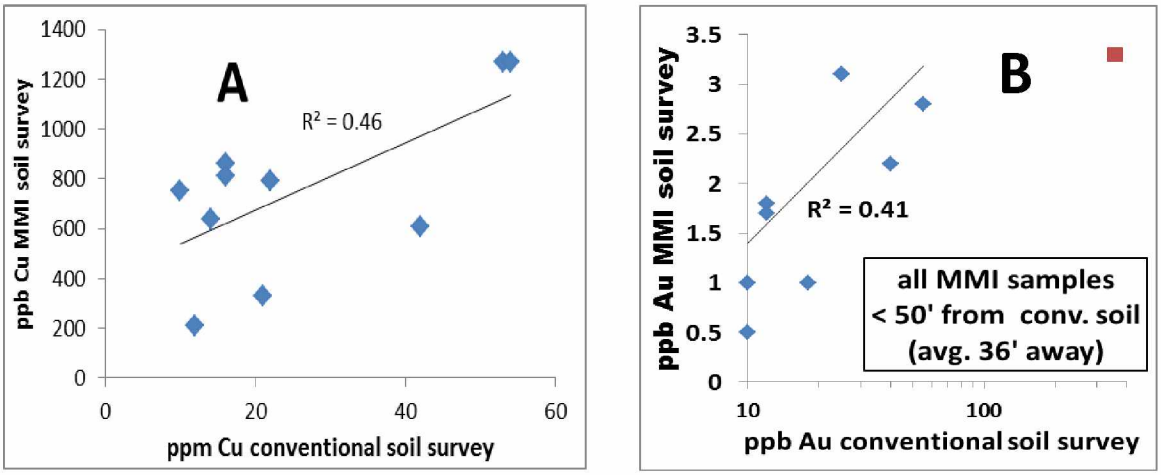

Figure 4.11: Correlations of Conventional & MMI Concentrations, of Cu (A) and Au (B) found in conventional soil surveys vs. MMI concentrations in nearby (<15 m away) MMI samples; r values are 0.68 and 0.64 for A and B, respectively.

Comparisons between MMI Au concentrations and those measured in 5 foot trench intervals are complicated by the fact that some MMI samples were taken nearly on top of the trench and others were much farther away (figure 4.2). A comparison between MMI Au concentrations and nearby (1-5 m away, average 2.7 m apart) trench rock samples shows no correlation whatsoever (figure 4.12).

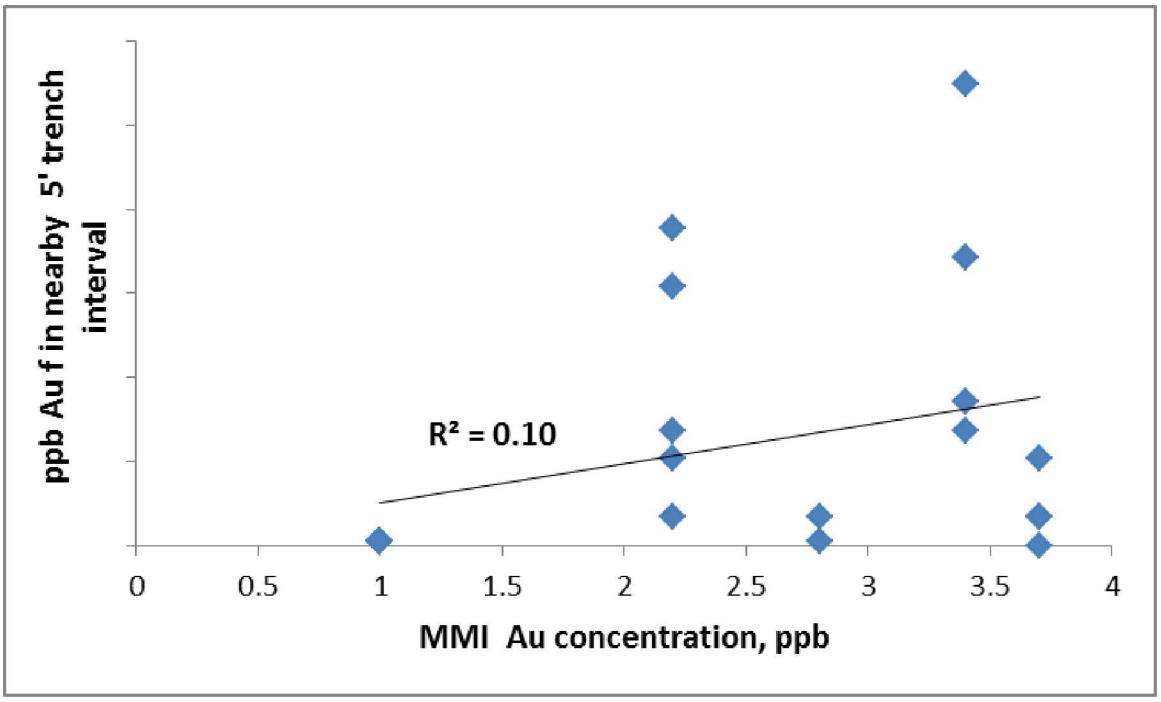

Figure 4.12: MMI Au Soil vs. Au Trench Fire Assay, MMI Au concentration in soil sample vs. Au concentration in nearby (1-5 m away) trench channel sample. The scale has been deliberately removed for trench Au concentrations but the lack of correlation between the two data sets is readily apparent.

As another comparison between trench, conventional soil, and MMI soil Au concentrations, figure 4.13 shows all three data sets plotted as a function of UTM northing. Samples at the same or nearly the same northing can be up to 50 meters apart (i.e., their eastings differ by up to 50 m, figure 4.2) and comparisons between the two are strictly valid only if Au concentrations exhibit E-W trends. Limited geologic mapping (Sims, 2015) suggests that geologic unit contacts do trend approximately E-W in this area, so such an assumption concerning Au grade patterns is possible. In terms of specific concentration variations vs. UTM northing, MMI Au values do not correlate particularly well with either trench or conventional soil concentrations. However, conventional soil concentrations do not appear to correlate with trench values either (figure 4.13). In more general terms however, they each highlight a zone with elevated Au roughly between northing 7211.5 and 7212.

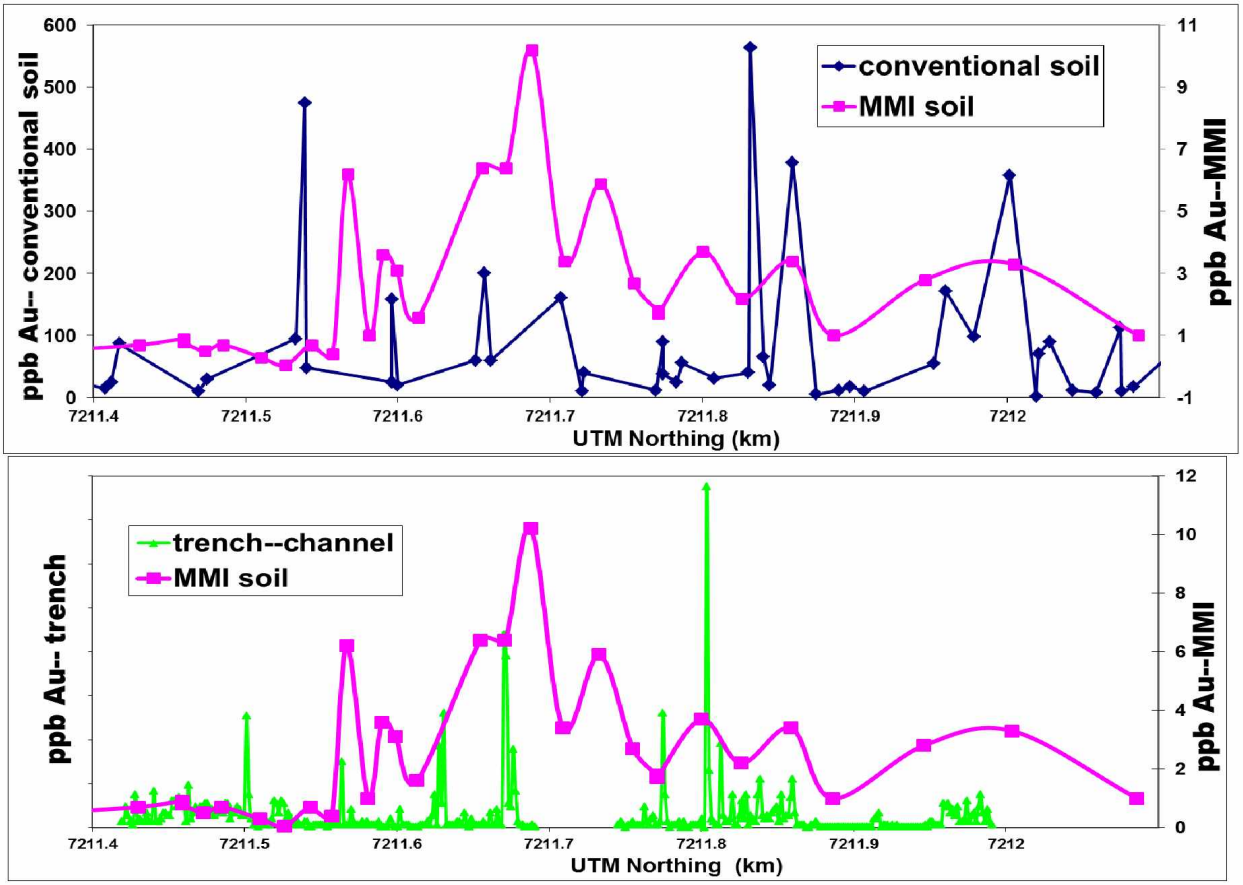

Figure 4.13: Comparison of Responses Between Geochemical Methods; conventional soils, MMI, and trench channel samples at the Gil Prospect, Alaska. Data are plotted vs. the NAD 27 UTM northing in kilometers; samples with the same northing are up to 50 m apart from each other. The upper diagram shows conventional soil Au and MMI soil Au concentrations; the lower shows trench (rock) Au and MMI Au values. Though there is a complete lack of agreement on a fine scale; each dataset limits mineralization to a zone roughly between UTM northing 7211.5 and 7212. The scale for conventional trench Au concentrations has deliberately been removed.

Another comparison (figure 4.14) is made from the spatial pattern of MMI, conventional soil, and trench results. Soil samples outline broadly E-W zones of higher Au concentrations; two of these correlate with the 4 highest Au concentrations seen in the trench samples. The highest MMI Au concentrations (all the values of 5-11 ppb, Appendix 3) define a narrow zone approximately 150 m long that correlates with two of the 6 highest Au concentrations in the nearby trenches. Additionally, two drill holes in areas of Au-rich soils yielded high Au

concentrations in the upper part of the drill holes. One drill hole near the location of the highest MMI Au value also contained high Au in the upper part.

Oddly, there is absolutely no correlation between the areas of highest Au in conventional soil samples and that of highest MMI Au. Instead, the two appear to be mutually exclusive: high MMI Au is present in an area where none of the conventional soil samples yielded significant Au and the areas of significant Au in conventional soil samples are outside of the area of anomalous Au in MMI samples.

Finally figure 4.15 compares both conventional soils and MMI soil samples to a drilling cross-section through the study area. Again we see the same pattern observable in figure 4.14, that each method identifies a portion of the mineralization only. Some additional points of interest are that the conventional soil anomaly CS1 and MMI1 (figure 4.15) might not be 'false'—there's no drilling in the area of those anomalies. Also MMI2 reflects high Au concentrations near the surface at DH1 (figure 4.15). There's no conventional soil anomaly at that point, but the closest soil samples are more than 20 meters away. Near-surface drill hole anomalies DH2 and DH3 are clearly reflected as conventional soil anomalies CS2 and CS4 (figure 4.15). CS3 is probably related to DH4, both of which are 70 m west of the line of cross-section. Also, MMI3 (figure 4.15) might be real, there's no drill data for the immediate vicinity.

In sum: there are 4 major zones of high Au concentration in the near surface. Of the 4, MMI identified 1 (25% success). Conventional soil identified 3, and arguably lack of nearby samples prevented identification of anomaly DH1, wide MMI sample spacing on the northern end of the line is likely partly responsible for the lack of success in that area.

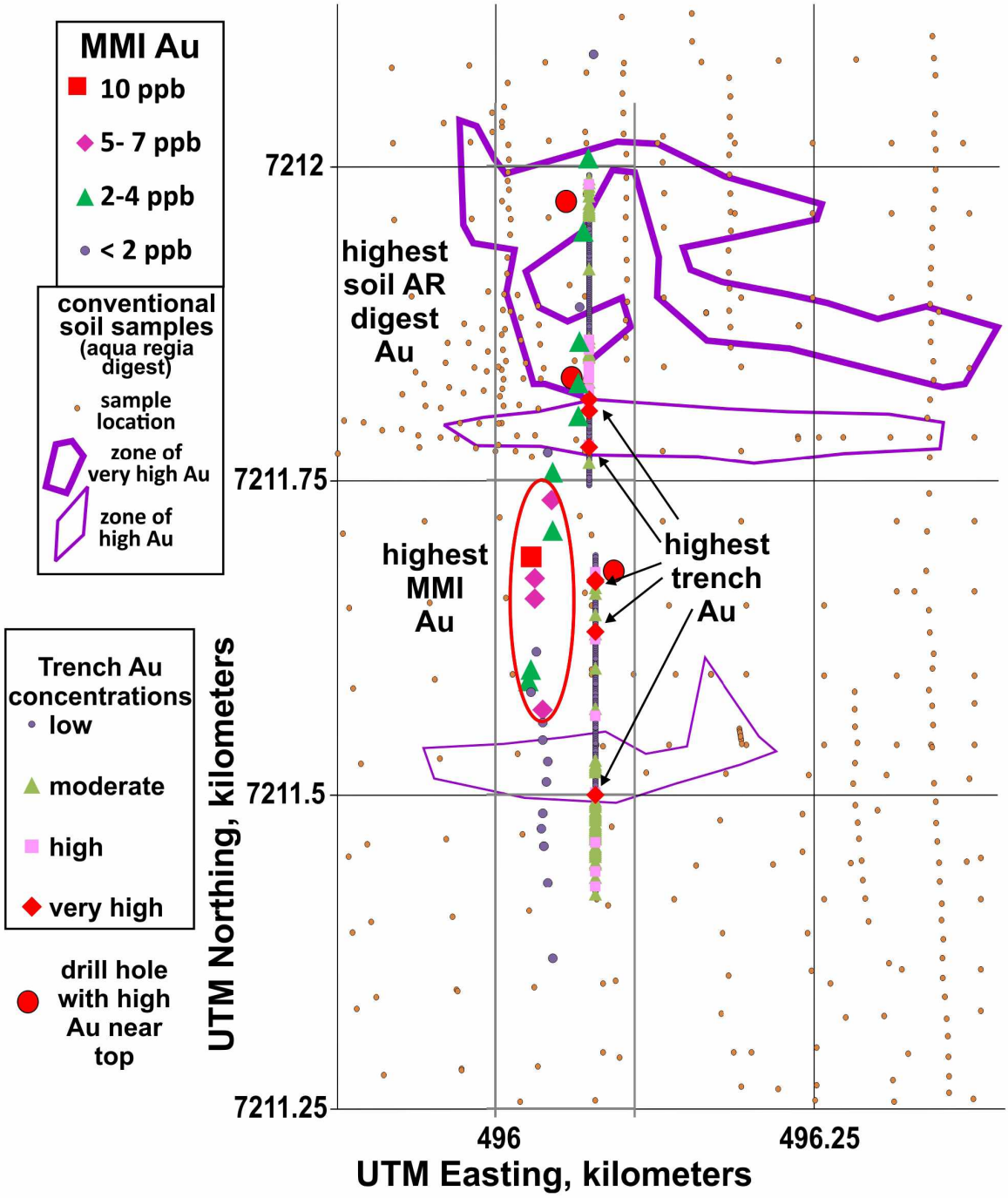

Figure 4.14: Geochemical Plan Map of a Part of the Gil Area, showing generalized regions on high Au in conventional soil samples (purple lines), MMI Au concentrations in 4 intervals, trench Au concentrations expressed qualitatively, and locations of drill holes with high Au concentrations in upper part of the hole. Data from FGI, Inc. and this study.

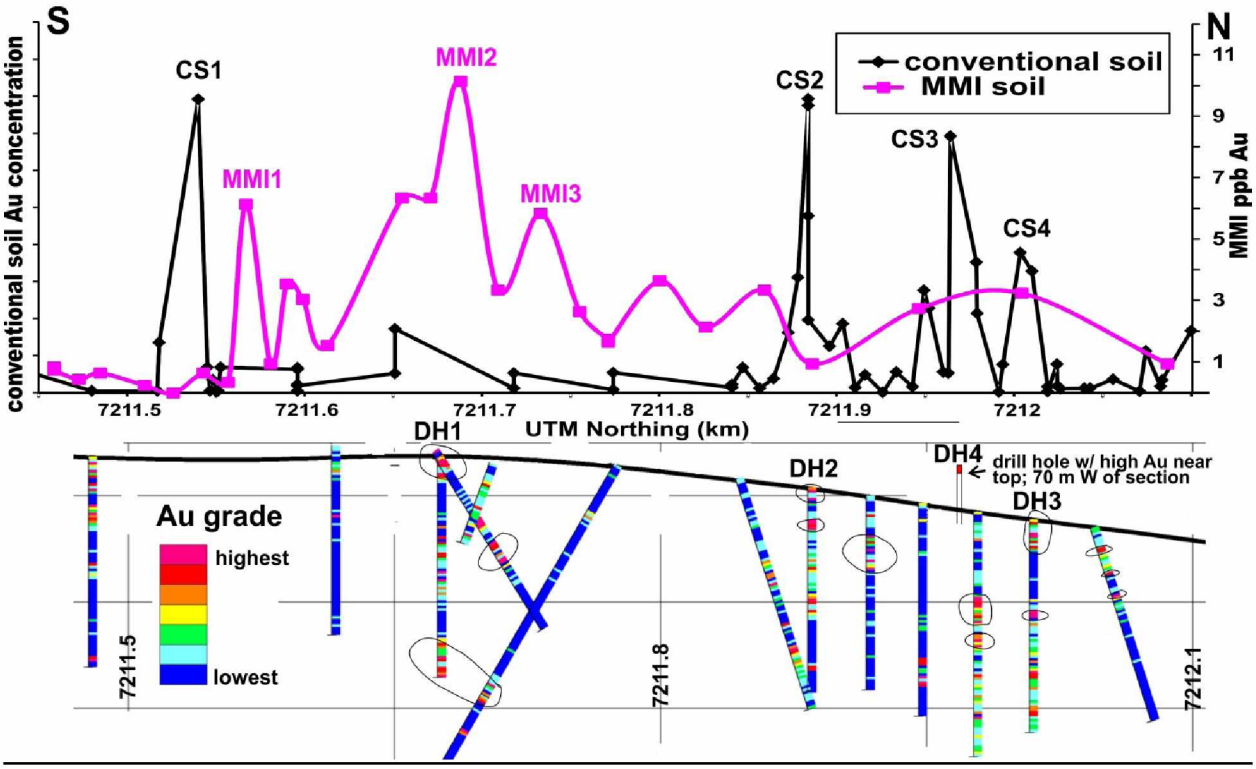

Figure 4.15: Drilling Cross-section & Geochemical Soil Traverse, through a portion of the Gil prospect near the MMI and conventional soil lines. The cross-section is constructed a little east of the trench and the conventional soil points include some that are closer to the line of section than those shown in figure 4.14. Most of the zones in drill core with anomalous Au are circled.

4.7 Discussion of the Gil Studies

The data from the Gil soil cores are both enlightening and intriguing. First many metals do concentrate in the uppermost portion of the B horizon, which is consistent with MMI theory (Mann et al., 1995; Cameron et al, 2004; Gray et al, 1999;). Secondly and in contrast to the generally accepted model of soil development/horizons (for which metals are depleted in the A horizon; Easterbrook, 1999), many metals appear to accumulate in the A horizon. MMI data collected near Assean Lake, Manitoba, Canada, showed similar results to those at the Gil in regards to Zn (Mann et al., 2005). Two major questions: (a) is this an artifact of MMI or are

many elements actually concentrated (as determined by other methods) in the A horizon? and (b) is the concentration of metals in the A horizon in the Gil soil cores a characteristic of sub-arctic soils that doesn't occur in soils of warmer climates? Antcibor et al. (2014) sampling arctic soils observed their highest Fe concentrations in the A horizon using a 2 acid extractant, and Gil produced similar results with MMI (Table 4.1). However broader and more detailed soil core compositional studies as functions of depth have not been performed, so I have no basis for further comparison. However, the variable concentration behavior of metals in the two cores, located only 35 meters from each other in a similar geomorphic setting (figure 4.2) suggests that variable degree of extraction by the MMI reagent might be part of the reasons for the observed elemental behavior.

Similarly, the lack of strong correlation between MMI concentration in the lower soil cores and the immediately adjacent soil sample is disappointing. These differences presumably reflect either actual variation in elemental abundance or variation in MMI extraction efficiency. I found significant total organic carbon in all of the soil cores examined (figure 4.7); it's possible that slight differences in TOC between adjacent samples could cause differential MMI extraction. This poor geologic reproducibility was also seen in closely spaced samples from the Marigold Mine (Chapter 3) and may represent a fundamental limitation of the technique.

The soil cores certainly highlight why it is essential to perform an orientation survey. The sampling protocols suggested by SGS minerals advise removal of the upper most 10 cm (A horizon) and then sampling of the next 15 cm (upper B horizon). Undoubtedly there will be variation in the depths and thicknesses of these horizons at different locations and environments throughout the world; a detailed orientation survey would allow scientists to design an appropriate sampling protocol specific to the site. For example an improved sampling protocol for the Gil may include the removal of the O horizon (moss and organic debris), then

removal of an additional 7 cm (A horizon) based on the TOC analyses (figure 4.7), and finally the sampling of the next 20-25 cm (upper B horizon) as the metals appear to be concentrating in a wider zone at the Gil.

The cores did explain (in part at least) why correlations could not be found between elements in the MMI survey or between the MMI, conventional soils, and trench data. This is because the metals are concentrating at different depths in the soil profile, and subsequently not all metals were effectively sampled. For example, Au and Bi correlate in the ore (Robinson, 2010); however, in the soil Bi concentrates in the A horizon (figure 4.7), whereas Au is concentrated in the upper B horizon (as expected) and was sampled. Consequently, the MMI data show no correlation between Bi and Au at Gil. The Au-Ba correlation (Table 4.5), in contrast, seemingly reflects a similar concentration of both in the B horizon (Tables 4.1, 4.2, 4.3) rather than any bedrock association. Just why the very different elements Ba and Au either do concentrate together or at least are extracted together by the MMI reagents is unknown. Such questions could be addressed once the proprietary secrets of the MMI reagents are released.

The ultimate question, of course is 'does MMI work for Au in sub-arctic soils?' If the results from my study combined with the existing conventional soil data, trench data, and drill hole data are representative, the answer is 'somewhat'. Conventional soil sampling revealed several Au-rich zones that correlate with higher Au concentrations in trench and drill holes (figures 4.14 & 4.15). However, conventional sampling missed an important zone that was detected by the MMI sampling (figures 4.14 & 4.15). The MMI sample spacing north of northing 7211.9 is wide (figure 4.15) and failed to identify the underlying ore zone, given the relatively poor reproducibility of MMI (sections 3.4-5) and relative success of the two interval lines at Marigold (figures 3.11 & 3.15, Table 3.11), an increased sample density from northing 7211.9

northward (figure 3.15) of the Gil survey could arguably produce an anomaly(s) over the mineralization in this area. In general however, the complete lack of overlap in Au anomalies between the conventional and MMI soil samples is striking. It seemingly indicates that some varieties of Au concentrations in bedrock are (at least at Gil) best found through conventional sampling and others through MMI.

4.8 Conclusions after the Gil Studies

1- Some metals extracted by the MMI digest concentrate in the uppermost portions of the B soil Horizon.

2- Some metals (As, Bi, Co, Fe, K, Li, Mn, P, W, and Zn) have a tendency to accumulate in the A Horizon and others (Ag, Au, Ba, Cs, Cu, Ni, Sc, Rare Earth Elements (REE's), Th, Tl, U, and Zr) in the B horizon and some metals (Ca, Sr, Mg) display different apparent concentration patterns in the two soil cores.

3- Both MMI and conventional soil sampling seem to identify bedrock Au concentrations, but they identify different bedrock anomalies.

4- An orientation survey is essential to properly design MMI sampling protocols for a specific site.

Chapter 5: Discussion and Conclusions

Several aspects of this study's results and their implications merit discussion. For continuity and relevance I will address these in relation to my five original hypotheses and then provide some general discussion on the employment and effectiveness of MMI.

5.1 Hypothesis 1- MMI produces elemental correlations similar to mineralized rocks.

To test this it was necessary to identify elemental correlations that existed in the ore, as it is logical that true metal anomalies in soil should bare chemical similarities to the rocks from which they are derived (Hoffman, 1986). At Gil this was straightforward as a Au-Bi correlation is known (Robinson, 2010). At Marigold a general correlation between Au-As-Sb and to a limited extent Hg was identified from published composites (Graney & McGibbon, 1991). This association is broadly confirmed by XRF and ICP-MS studies of ore samples and investigations of ICP-MS results from drill cuttings conducted as part of this study. However, elemental correlations at Marigold are complicated by a complex alteration (Panhorst, 1996) and oxidation (Theodore, 1998) history where original minerals have been disassembled and the majority of liberated metals co-precipitated (possibly multiple times) with Fe-(oxy)hydroxides (Tables 2.2, 2.3, and 2.5). As a result, the vast majority of elemental associations in rocks are with Fe. In the Marigold MMI there is a significant correlation between Fe and the REE's, but not with ore-related elements. A modest Hg-Au correlation is present, though not robust, as it is caused by the three highest Au-Hg samples. Removal of the two highest of these samples and the Au-Hg correlation diminishes while a significant As-Sb correlation appears. A significant Au-As-Sb correlation however was not identified, no matter which samples are included.

Similarly at Gil significant Au-Bi correlation in the MMI was not identified; however, a strong Au-Ba (not mineralogical) correlation appeared (Table, 4.5). The soil core examinations however clearly illustrate that MMI extractable Bi and Au concentrate in different horizons in the soil (i.e., Bi in the A horizon and Au in the upper B horizon, figures 4.4 & 4.6). As the A horizon is typically not sampled with MMI methodology (Mann et al., 1998; Cameron et al., 2004), it is, in hindsight, not surprising that an MMI Au-Bi correlation is not present in the Gil data. However, the highest MMI Ba concentrations were in the upper B horizon (figure 4.6, Table 4.1), hence the correlation with Au—one which apparently reflects similar behavior of Ba and Au in the soil environment that is unrelated to rock patterns. MMI analyses of the Gil soil cores showed that the highest extractable concentrations of not just Bi, but also As, Co, Fe, K, Li, Mn, P, W, and Zn in the A horizon. Mann et al. (2005) showed only a few elements, but also observed the greatest Zn MMI concentrations in the A horizon. If the Gil cores are representative of ion sorption patterns in soils, then the lack of an Au-As-Sb correlation in the Marigold MMI may be due to As and Sb enrichment in a different horizon from the Au.

5.2 Hypothesis 2- MMI anomalies are reproducible.

In this study I explored MMI's reproducibility analytically, geologically, and through time. I compared 768 duplicate MMI analyses (splits of the same soil samples separately analyzed) for select elements to test analytical reproducibility. These duplicates returned r^2 =0.85-0.97 (table 3.1); ideally all would yield r^2 = 1.0. Of the elements examined, Au yielded the highest r^2 and Pb the lowest. The % relative difference for duplicates (Au and Ag concentrations, figure 3.2) showed that disagreement generally increased as concentration approached the detection limit. However, relative deviations of ±20-30% are common even when concentrations are 50 times the detection limit. Further, none of the duplicates included a very high concentration sample; these seem non-reproducible in closely-spaced samples. Finally the mean of the %

deviation between original sample and duplicate (Table 3.2) is 6-20%, depending on the element. I hoped the values would to agree within 10 percent, as such is generally considered acceptable. MMI Cu yielded the lowest relative deviations and also the highest concentrations, Pb the greatest relative deviations, and Au yielded a mean relative deviation of ~15%. While not ideal, the analytical reproducibility of MMI is still adequate for effective use.

The geologic reproducibility was complicated by occasional high concentration samples that were not replicated in adjacent samples as little as 1.5 m away. I do not know what caused these, but for every element 1-3 samples yielded concentrations 100 times as high as the next highest. Excluding these outliers however, MMI Au concentrations in samples collected at 1.5 m intervals yielded an r^2 of 0.88, and correlations between Au concentrations for samples collected at greater intervals were lower, as would be expected. However, relative deviations for a variety of elements (for samples taken 1.5 m apart) averaged 20-60% (Table 3.8). That is, on average, the difference in concentration for a particular element in one sample relative to another sample taken 1.5 m away was 20-60% of the original concentration. This difference is far in excess of the differences seen for duplicate samples.

Concentrations of Au in Marigold samples collected at the same locations in 2008 and 2012 bore little relation to each other (Table 3.9). This lack of agreement is almost certainly an analytical problem superimposed on a geological problem. Based on higher overall MMI concentrations, the digest in 2012 appears to have extracted the elements more strongly (Table 3.10), but not in a consistent manner. Did the digest solution change or did the mobility of the ions change over this time period? I do not know.

The Gil soil cores may provide clues, as MMI metal abundance at different depths within the upper soil horizons (Table 4.1) varied between elements and between soil cores. If

collection depths were slightly different between the two years then perhaps the concentration differences could be explained. Another possibility worth consideration is that elements were redistributed by water variably moving through the soil (rain and snow melt) between 2008 and 2012. Would the loosely adsorbed ions go into solution when soils become saturated by rain only to later sorb as the soil moisture decreases due to evaporation, and could this have an effect at which depth the metals become concentrated, or redistribute them entirely? In partial answer, episodes of extreme precipitation (20+ cm rain) appear to have significant enough effects as to compromise a survey (SGS Minerals Services, 2009) in the short term (1-5 years). Nothing else has been published concerning changes in MMI responses to seasonal fluctuations in precipitation. In sum, excluding outliers, MMI under typical exploration sampling has an analytical reproducibility of 6-20% depending on the element (15% for Au, table 3.2), and a geologic reproducibility of 20-60% (36-41% Au) for closely-spaced (1.5 m) samples, and low geologic reproducibility through time (figure 3.11).

5.3 Hypothesis 3- MMI Au anomalies can be correlated with Au in the subsurface.

MMI anomalies at Marigold are intriguing, and more so on the northern portions of the property, where mobile ions need to migrate through thick alluvial sequences. The complex hydrology--which includes a bedrock and alluvial aquifer--and the past dewatering activities of the neighboring Lone Tree mine (Hoffman, 2010) are also worth consideration. The southern--more mountainous--portions of the property (figures 1.12 & 3.1) have soil thicknesses of 1-5 meters (Forbush, 2010) in which capillary rise (even if only on a seasonal basis) is viable. However, depth to aquifer is ~34 m to 140 m and is >60 m for many of the northern areas surveyed (Hoffman, 2010). This in most places is too great for capillary rise to be a viable migration mechanism (Cameron et al., 2004). Even before dewatering activities the aquifer was >30 m below the surface (Hoffman, 2010), meaning that MMI anomalies may actually be paleo

anomalies created during a wetter climate with higher aquifer elevations. The latest period plausible--considering regional climatic studies--is during the early Holocene (~10,000-8,000 ka) when the subsiding ancient Lake Lahonton experienced a period of partial re-expansion before its ultimate desiccation later in the Holocene (Adams et al., 1998; Harvey et al., 1999).

At Marigold the weakest positively identified anomaly over deeply buried ore (30 m alluvium + 45 m bedrock) was 4.7 ppb Au (figure 3.10). Comparison of an MMI line and cross-section of Marigold's block model show that MMI anomalies on the surface can be correlated with Au in the subsurface with a success rate as high as 57% in ideal conditions (no alluvial overburden; figure 3.15, Table 3.11).

In general alluvial cover is more of a hindrance to generating an MMI Au anomaly than bedrock overburden, and the success rate of MMI after exceeding 35 m of alluvial cover drops drastically (table 3.11). Also, there is no obvious connection between MMI concentration and Au concentration in the subsurface. An MMI concentration of 30 or even 590 ppb Au is not associated with higher grade, more extensive, or shallower Au in the subsurface (e.g., figures 3.11, 3.13). Rather, any value exceeding the anomaly threshold seems equally favorable for subsurface Au concentrations. MMI also seems to occasionally produce high magnitude concentrations that are not reproducible in samples as little as 1.5 m away. Some of these are false positives, and even though they are high concentrations, they should ironically be ignored unless in the vicinity of other lesser (but anomalous) samples. Hence a word of caution when employing mathematical operations sometimes applied to geochemical data to produce anomalies: the goal of such operations is to reduce background noise and extenuate anomalies. However, if data (like Marigold's MMI survey) has a few high magnitude false positives, then these will become even more pronounced and the lower magnitude true anomalies will be unnoticeable.

The high density lines that employed close sampling intervals at Marigold (figures 3.3, 3.11, 3.15) in many ways proved more effective at identifying mineralization. Collecting groups of samples near each other allows one to better asses if the results acquired are a true reflection of the subsurface. This makes sense given the relatively poor geologic reproducibility of MMI. The use of pathfinders can also be potentially useful, although their effectiveness at Marigold needs more investigation. The best case scenarios would allow for a multi element geochemical study on the target ore to establish which pathfinders are potentially the most useful. Also, detailed orientation surveys would identify where exactly in the soil profile each pathfinder element is concentrating, as it may be different from the primarily commodity. Such was the case with Bi and Au at Gil. Information from both studies would be invaluable when designing a more extensive survey.

5.4 Hypothesis 4- MMI yields well defined anomalies, even in permafrost rich soils of interior Alaska.

Investigations of MMI survey lines collected at Marigold show that in most cases MMI does produce a well defined anomaly that is easily distinguished from the background responses. Further comparison of these lines and their associated anomalies (figures 3.9-3.12, and 3.14) also reveals that these anomalies are usually located above ore. That is, the number of false positives are small (~0-9%) in ideal sampling conditions: thin alluvial cover, relatively near surface mineralization, and ore grades >1.5 ppm (table 3.11 & figure 3.14). However, the magnitude of an MMI anomaly is not useful for estimating the grades or quantities of ore in rocks; figures 3.11 and 3.14 illustrate that some of the largest anomalies are located over lower grade ores, and vice versa. Hence MMI (at least at Marigold) is only useful as an indicator of Au presence in the subsurface. That is to say, so long as an anomaly is greater than the determined threshold, above the background (regardless of the magnitude), the probability is

high that mineralization is present in the sub-surface (table 3.11). Although most of the MMI Au anomalies could be related to Au-bearing rocks in the subsurface, in the majority of cases an Au concentration in the subsurface did not produce an MMI soil anomaly. That is, the % of samples above Au mineralization that yielded an MMI response of >4.7 ppb Au was usually <50% (table 3.11). Only in the most-favorable case of nearly zero overlying alluvium in 2012 were >50% of the bedrock Au concentrations identified by MMI.

At Gil complications in the use of MMI include permafrost, soils subject to solifluction, and downward creep. Another complication is the variable depths at which different metals concentrate in the soil (figure 4.7-4.9), which at Gil is relatively broad, much greater than the recommended 15 cm vertical sampling interval (Mann et al., 2005). The degree to which permafrost and solifluction modify MMI concentrations at Gil was not explored. There is merit in further investigations concerning the degree to which MMI extractable metals concentrate at different depths in the soil, and to determine if there are any trends that can be identified for different environments. At Gil the maximum MMI Au anomaly is 10.2 ppb (Appendix 3). Though this is a well-defined anomaly, and it sits more-or-less directly above two drill holes with significant Au grades near the top of each hole (figure 4.16), MMI failed to identify two other similar places where significant Au is present near the tops of drill holes. That is, only 1/3 of the near-surface, Au-enriched zones below MMI samples were identified by MMI.

5.5 Hypothesis 5- MMI yields results that are different from conventional surveys, but which better reflect the nearby/underlying metal anomalies.

In this regard my results are similar to those of previous studies presented in the introduction: in some environments MMI is superior to other methods, and in other environments it is not. Gray et al. (1999) found MMI to be effective but not necessarily more so

than the conventional methods they employed. At Gil (figure 4.14) only 1/3 of the near-surface bedrock Au zones were identified by MMI. In contrast, conventional soil sampling identified 3 of 3 near-surface Au enriched zones (figure 4.14); the zone identified by MMI was not found with conventional soil samples because no soil samples were taken in that immediate area. In other words, based on this limited example, conventional soil sampling appears to locate near-surface bedrock Au concentrations at Gil better than MMI. This might be generally true in arctic and near-arctic soils.

At Marigold, MMI proved more effective at identifying deeply buried, low grade Au ore than the conventional methods employed by Smee (1998), in the one case where both conventional and MMI soil samples were collected (figure 3.11). However, MMI at Marigold was not effective over alluvial cover more than ~100 m thick (Table 3.11). Fabris et al. (2009b) came to similar conclusions with a test area in South Australia. Arguably, in many of thinly covered areas at Marigold where MMI proved most effective (Table 3.11), conventional methods might also have been successful.

5.6 - When to and when not to use MMI.

MMI is promoted as more effective for mineral exploration over conventional methods where soils are not derived from the underlying bedrock. That is, cases where soils are predominantly derived from materials transported by wind, water, creep or other means which overly bedrock. Alluvium, glacial till, and loess are examples of such materials. That is not to say that a target must be deeply buried for MMI to be effective, in fact, at Marigold MMI preformed best in thin soils with near-surface ore. Rather, conventional methods lose their effectiveness with burial depth as soil constituents no longer reflect the bedrock composition.

MMI relies on the migration of ions—regardless of what overlies mineralized rock--and is potentially still usable despite thick overburden.

However MMI's utility also seemingly decreases with increasing cover, as indicated by many examples at Marigold (e.g., figure 1.12, table 3.11). At Marigold alluvial fill had a negative effect on MMI responses. Though difficult to determine precisely (as depth to bedrock and additional variations were present), it appears that approximately 40 meters of alluvial fill is sufficient to diminish the success rate from 50% to 0-25%. Interestingly, thick sequences of bedrock do not appear to have the same level of negative impact.

The use of MMI for targeting deposits that are known to be completely unoxidized is discouraged. Ore minerals need to be oxidized in order to release ions that can go into aqueous solution and migrate upwards. It is plausible that for many deposits the climatic and hydrologic processes that are oxidizing the deposit are also responsible for the migration of the mobile ions.

MMI sampling should be avoided if any hydrologic event significantly 'flushes' the soils being sampled. These include heavy rains or flooding events (SGS Minerals Services, 2009). Also, areas with any ground disturbance which has disrupted the sampling horizon should be avoided. As the environment is usually not static, I recommend completing the sampling within the same year, or--if conducted over several years—sampling during periods of similar weather conditions, preferably dry. After conducting the Gil study I would caution against using MMI in soils undergoing solifluction, unless a detailed orientation survey provides data to adequately address local challenges.

From a logistical point of view MMI may in some cases be a better choice over conventional methods simply by the mode of sampling. In general an MMI analysis will cost

almost double that of a 2-acid digest ICP-MS analysis, but only requires 200-400 g of material, whereas larger samples (1-2 kg) are recommended for conventional soil methods. This larger sample is recommended due to the 'nugget effect' of a few tiny Au particles producing either large or low Au concentrations depending on how many 'nuggets' are in a sample (Thompson, 1986; Hoffman, 1986a). Of course, one could argue—given the non-reproducibility of the higher MMI concentrations that larger samples should also be employed for MMI surveys. The result is MMI surveys require less labor, especially if soils are thick enough that collection of the C horizon involves auguring through 2-3 meters of soil. In relatively flat open terrain a 2 person team can realistically collect 150-200 MMI samples a day, under the same conditions 40-50 conventional samples could be collected. In dense boreal forest with hilly terrain MMI and conventional sample collection rates could drop to 15-25 and 5-10 respectively. Considering that expenses increase with remoteness and time in the field, if both methods were equally effective at identifying the target, the saved labor costs of collecting MMI samples could potentially offset the higher analytical costs.

In sum, MMI appears to be the most effective geochemical technique for highly oxidized ores in terrains with thick (2-100 m) cover, performing best in semi-arid/arid environments. In soils thinner than 2 meters convention methods are capable of efficiently identifying near-surface mineralization (Cameron et al., 2004), and including this Marigold study, MMI has yet to be found effective for cover thicknesses exceeding 100 meters (Fabris et al., 2009b).

5.7 Future Work

This study has conducted and presented several tests regarding effective use of the proprietary MMI technique for metal exploration. Through this process several additional

questions and studies were identified that would significantly benefit the industry's understanding of MMI and exploration soil geochemistry in general. I present several below.

1- This study undertook several investigations to determine the reproducibility of MMI. It would be of great benefit to the industry if similar studies were conducted using conventional methods, and in several environments. Some of these could probably be performed using existing data sets, potentially supplemented with additional investigations similar to the MMI interval study presented in chapter 3.

2- There is value in better understanding the As-Sb-Fe system in regards to oxidation and mobility in ores and soils. Asta et al. (2012) provided foundational laboratory studies investigating this complex system, involving the simultaneous oxidation of these metals, comparing both abiotic and microbial variables. Arsenic and Sb both are commonly associated with Au ores (Hoffman, 1986a); understanding how these elements are affected by oxidation of sulfides and subsequent redistribution and behavior in soils would help explorationists know to what extent these elements can be used as pathfinders for Au in soil samples. In addition, an increased understanding of this system would benefit environmental efforts both in and out of the mining industry.

3- How do metals concentrate in soils, and is it the same in every environment? The generally accepted model for soils is that metal will be the most concentrated in the B horizon, or zone of accumulation (Easterbrook, 1999). However, 2 acid studies of arctic soils (Antcibor et al., 2014), the MMI investigation of this study, and Mann et al. (2005), show that many elements concentrate in the A horizon. A collection of several detailed soil cores in multiple environments, testing various reagents, could answer these questions, thus improving interpretations made by soil scientists in general.

4- Similar to study 3--but in consideration of MMI--the degree of concentration of As, Fe, Sb, Bi, Zn and other elements in the A horizon (Table 4.1) needs to be better addressed. Do these elements consistently concentrate in the A horizon? If so, this will potentially affect sampling protocols, as the A horizon is above the 10-25 cm sampling depth SGS minerals recommends. That is, if the results from Gil are generally the case, then many elements (some are important pathfinders and (or) commodities) are not effectively sampled with the current recommended procedures. Several detailed soil core analyses above known ore bodies from multiple environments around the world would address this question.

5- The composition of the MMI digest is proprietary, making the prediction of which elemental species are brought into solution by the reagent(s) difficult. Cameron et al. (2004) provided helpful information regarding the strength of the MMI digest compared to other commonly employed reagents. A further set of investigations testing the solubility of common ore and pathfinder elements in their various oxidation states at standard or near standard conditions replicating those of the soils being tested would significantly improve the designs and interpretation of future MMI surveys.

5.8 Conclusions

1- MMI elemental correlations reflect the degree to which two particular elements concentrate in—and are released from--the sampled soil interval. For yet-to-be identified reasons, metal ions of the different elements tend to behave differently, concentrating at different levels between the A and the lower B horizons. This phenomenon doesn't necessarily make MMI ineffective, but can limit the use of certain pathfinder elements and create metal associations that do not reflect the underlying ore mineralogy.

2- MMI occasionally produces outliers with concentrations an order of magnitude larger than those from adjacent samples and even occasionally between elements in duplicate samples. Excluding these, MMI has an analytical reproducibility of 6-20% depending on the element (15% for Au), and a geologic reproducibility of 20-60% (36-41% Au) for closely-spaced (1.5 m) samples.

3- MMI surveys produce Au anomalies that can be correlated with Au mineralization in the subsurface (perhaps to depths of 300 m), but the magnitude of the MMI anomaly bears no simple relation to size, grade, or depth of the underlying Au occurrence. Radical variations in MMI Au concentrations (>100 ppm to <6 ppb) occur over very short (1.5 m) distances even above relatively continuous Au ore.

4- In ideal environments (limited alluvial and bedrock cover), MMI does produce well-defined Au anomalies with an acceptably low percentage of false positives. However, this study suggests that--at best—about half of the time does bedrock with significant Au produce a significant MMI Au response. Thick sequences of alluvial fill and solifluction soils appear to negatively affect MMI's effectiveness. Overlying bedrock appears to have a significantly smaller effect on diminishing MMI responses than alluvial fill.

5- Based on one example at Marigold (where both conventional and MMI data were collected) MMI is more effective than conventional methods if employed over targets for which the soils are not derived from the underlying bedrock.

6- MMI is an effective exploration tool for Au in northern Nevada (better than conventional methods where cover is 5-100 m thick); it becomes less effective with increasing thickness of overlying alluvium, and is not effective in areas of >100 m overlying alluvium.

References:

Adams, K.D., & Wesnousky, S.G. (1998) Shoreline Processes and the Age of the Lake Lohontan highstand in the Jessup Embayment, Geological Society of America, bul. 110, pp. 1318-1332.

Aljarrah, M., & Medraj, M. (2008) Thermodynamic Modeling of the Mg-Ca, Mg-Sr, Ca-Sr, and Mg-Ca-Sr Systems Using the Modified Quasichemical Model, Computer Coupling of Phase Diagrams and Thermochemistry, vol. 32, pp. 240-251.

Antcibor, I., Eschenbach, A., Zubrzycki, S., Kutzbach, L., Bolshiyanov, D., & Pfeiffer, E.M. (2014) Trace metal distribution in pristine permafrost-affected soils of the Lena River delta and its hinterland, northern Siberia, Russia, Biogeosciences, vol. 11, p. 1-15.

Asta, M., Nordstrom, D.K., & McCleskey, R.B. (2012) Simultaneous Oxidation of Arsenic and Antimony at Low and Circumneutral pH with and without Microbial Catalysis, Applied Geochemistry, vol. 27, pp. 281-291.

Brand, U., Morrison, J., & Campbell, I.T. (1998) Strontium in Sedimentary Rocks, Encyclopedia of Earthscience: Geochemistry, Springer Netherlands, pp. 600-603.

Brookins, D. (1988) Eh-pH Diagrams for Geochemistry, 1st ed., Springer-Verlag, New York, 176 p.

Bodek, I.B., Lyman, W.J., & Reehl, W.F. (1988) Environmental Inorganic Chemistry; Properties, Processes, & Estimation Methods, Pergamon Press, SETAC spec. publ. ser., New York, 1280 p.

Bond, J.D. & Lipovsky, P.S. (2011) Surficial geology, soils and permafrost of the northern Dawson Range. In: Yukon Exploration and Geology 2010, K.E. MacFarlane, L.H. Weston and C. Relf (eds.), Yukon Geological Survey, p. 19-32.

Brady, N.C. (1974) The Nature and Properties of Soils 8th ed., Macmillian Publ. Co., New York, 639 p.

Cameron, E., Hamilton, S., Leybourne, M., Hall, G., & McClenaghan, M. (2004) Finding Deeply Buried Deposits Using Geochemistry, AAG/ Geological Society of London, Geochemistry: Exploration, Environment Analysis, Vol. 4, pp. 7–32.

Carmen, M., & McBride, M. (1998) Coprecipitates of Cd, Cu, Pb, and Zn in Iron Oxides: Solid Phase Transformation and Metal Solubility After Aging and Thermal Treatment, Clays and Clay Minerals, vol. 46, No. 5, pp. 537-545.

Carver, J., Rathnam, K., Rice, T., & Yeomans, T. (2014) NI 43-101 Technical Report on the Marigold Mine, Humboldt County, NV, Silver Standard Resources, 233 p.

Cheng, H., Hu, J., Luo, J., Xu, B., & Zhao, J. (2009) Geochemical Processes Controlling Fate and Transport of Arsenic in Acid Mine Drainage (AMD) and Natural Systems, Journal of Hazardous Materials, vol. 165, pp. 13-26.

Cline, J., Hofstra, A., Muntean, J., Tosdal, R., & Hickey, K. (2005) Carlin-Type Gold Deposits in Nevada: Critical Geologic Characteristics and Viable Models, SEG, Economic Geology 100th Anniversary vol., pp. 451-483.

DePangher, M. (2010) Marigold Mine Project: Petrographic Report, prepared for the Marigold Mining Company, Spectrum Resources, Vancouver, B.C., 29 p.

Dold, B. (2003) Speciation of the Most Soluble Phases in a Sequential Extraction Procedure Adapted for Geochemical Studies of Copper Sulfide Mine Waste, Journal of Geochemical Exploration, vol. 80, pp. 55-68.

Easterbrook, D.J. (1999) Surface Processes & Landforms, 2nd ed., Prentice-Hall, Inc., New Jersey, 546 p.

Fabris, A., Keeling, J., & Fidler, R. (2009a) Soil geochemistry as an exploration tool in areas of thick transported cover, Curnamona Province, MESA Journal, vol. 54, pp. 32-40.

Fabris, A., Keeling, J., & Fidler, R. (2009b) Surface Geochemical Expression of Bedrock Beneath Thick Sediment Cover, Curnamona Province, South Australia, Geochemistry: Exploration, Environment Analysis, vol. 9, pp. 237-246.

Fithian, M., Holley, E., & Kelly, N. (2014) Geochemical Characterization of Gold Mineralization and Alteration in Sedimentary Host Rocks and Porphyritic Intrusions, Marigold deposit, Nevada. Poster Presentation at SEG 2014, Keystone, Colorado, September 27-30.

Forbush, T. J. (2010) MMI Geochemical Survey: 2007-2010, Internal Exploration Report, Marigold Mining Company, 22 p.

Foth, H.D. (1984) Fundamentals of Soil Science, John Wiley & Sons, New York, 435 p.

Garrels, R.M & Christ, C.L. (1965) Solutions, Minerals, and Equilibria, Freeman, Cooper, and Co., San Francisco, 450 p.

Goldberg, I.S. (1998) Vertical Migration of Elements from Mineral Deposits, Journal of Exploration Geochemistry, vol. 61, pp. 191-202.

Goldstein, J., Newbury, D., Joy, D., Lyman, C., Echlin, P., Lifshin, E., Sawyer, L., & Michael, J. (2007) Scanning Electron Microscopy and X-Ray Microanalysis, 3rd ed., Springer Science + Business Media LLC, New York, NY, 690 p.

Graney, J. R. & McGibbon, D.H (1991) Geological Setting and Controls on Gold Mineralization in the Marigold Mine Area, Nevada, Geological Society of Nevada, Geology and Ore Deposits of the Great Basin, vol. 2, pp. 865-874.

Gray, D.J., Wildman, J.E., & Longman, G.D., (1999), Selective and Partial Extraction Analyses of Transported Overburden for Gold Exploration, in the Yilgarn Craton, Western Australia, Journal of Geochemical Exploration, vol. 67, pp. 51-66.

Grim, R.E. (1968) Clay Mineralogy 2nd ed., McGraw Hill, New York, 362 p.

Harvey, A., Wigand, P., & Wells, S. (1999) Response of Alluvial Fan Systems to the Late Pleistocene to Holocene Climate Transition: Contrast Between Margins of Pluvial Lakes Lahontan and Mojave, Nevada and California, USA, CATENA, vol. 36, issue 4, pp. 255-281.

Hoffman, E. L., Clark, J. R., & Yeager, J.R. (1998) Gold Analysis- Fire Assaying and Alternative Methods, Canadian Institute of Mining, Metallurgy, and Petroleum, Exploring Mining Geology, vol. 7, pp. 155-160.

Hoffman, P.E. (2010) Groundwater Conditions at the Marigold Mine Site-2009 Annual, Compiled for the Marigold Mine and Bureau of Land Management, Hydro-Engineers LLC, p. 74.

Hoffman, S.J. (1986a) Ch 2: The Soil Survey-Designing an Exploration Program, Exploration Geochemistry: Design and Interpretation of Soil Surveys, Reviews in Economic Geology vol. 3, Society of Economic Geologists, pp. 19-38.

Hoffman, S. J. (1986b) Ch 3: Soil Sampling, Exploration Geochemistry: Design and Interpretation of Soil Surveys, Reviews in Economic Geology vol. 3, Society of Economic Geologists, pp. 39-79.

Jenks, J.D. (2002) Summary Report, The Gil Mineral Claims Kinross/Teryl Joint Venture Project, Teryl Resources Corporation Internal Document, 37 p.

Johnston, M.K. & Ressel, M.W. (2005) Carlin-type and Distal Disseminated Au-Ag Deposits: Related Distal Expressions of Eocene Intrusive Centers in North-Central Nevada, SEG, Economic Geology 100th Anniversary vol., pp. 451-483.

Langmuir, D. (1997) Aqueous Environmental Chemistry, Prentice-Hall, New York, 600 p.

Lee, D.E. (1982) Photointerpretive map of the surficial geology of the north Fairbanks D-1 and south Livengood A-1 quadrangles, Alaska: Alaska Division of Geological & Geophysical Surveys Alaska Open-File Report 156, 5 sheets.

Leybourne, M.I. & Cameron, E. (2007) Groundwaters in Geochemical Exploration: Methods, Applications, and Future Directions, Proceedings of Exploration 07: Fifth Decennial International Conference on Mineral Exploration, pp. 201-221.

Lide, D.R. (1995), Handbook of Chemistry & Physics 76th ed., CRC Press, Boca Raton, FL, 2576 p.

Mahlanga, T., Gudyanga, F.P., & Simba, D.J. (2009) Leaching of the Arsenopyrite/Pyrite Flotation Concentrates Using Metallic Iron in a Hydrochloric Acid Medium, Hydrometallurgy Conference, The Southern African Institute of mining and Metallurgy, 16 p.

Mann, A.W., Gray, L.M., Birrell, R.G., Webster, J.G., Brown, K.L., Mann, A.T., Humphreys, D.B., & Pedrix, J.L. (1995) Mechanism of Formation of Mobile Metal Ion Anomalies, Minerals and Energy Research Institute of Western Australia, Report 153, 407 p.

Mann, A.W., Birrell, R.D, Mann, A.T., Humphreys, D.B., & Pedrix, J.L. (1998) Application of the mobile metal ion technique to routine geochemical exploration, Journal of Geochemical Exploration, vol. 61, 87-102 pp.

Mann, A.W, Birrell, R.D, Fedikow, M.A.F., & de Souza, H.A.F. (2005) Vertical ionic migration: mechanisms, soil anomalies, and sampling depth for mineral exploration, AAG/ Geological Society of London *Geochemistry: Exploration, Environment, Analysis*, Vol. 5, pp. 201–210.

Marsden, J. O. & House, C.I., 2006, The chemistry of Gold extraction, 2nd Ed, Society for Mining, Metallurgy, and Exploration, New York, 680 p.

McCoy, D.T., Newberry, R.J., & Layer, P.W. (1995) Geological, geochemical, and geochronologic evidence for both metamorphic and intrusive metallogenesis in Alaskan gold deposits: Geological Society of America., Abstract with program, vol. 27, p. A63.

McCoy, D. T, Newberry, R.J., Layer, P.W., DiMarchi, J.J., Bakke, A., Masterman, J.S., & Minehane, D.L. (1997) Plutonic Related Gold Deposits of Interior Alaska *in* Goldfarb, R.J., ed. Ore Deposits of Alaska, Economic Geology Monograph, No. 9, Society of Economic Geologists, pp. 138-152.

McGibbon, D. (2004) Marigold summary and tour guide, Internal Report, Marigold Mine, 32 p.

Mumpton, F.A. (1977) Mineralogy and Geology of Natural Zeolites, Reviews in Mineralogy, vol. 4, Min. Soc. America, 338 p.

Newberry, R.J., Bundtzen, T.K., Clautice, K.H., Combellick, R.A., Douglas, T., Laird, G.M., Liss, S.A., Pinney, D.S., Reifenstuhl, R.R., & Solie, D.N., 1996, Preliminary geologic map of the Fairbanks mining district, Alaska: Alaska Division of Geological & Geophysical Surveys Public Data File 96-16, 17 p., 2 sheets.

Panhorst, T.L. (1996) Structural Control and Mineralization at Lone Tree Mine, Humbolt County, Nevada with Implications on Sampling Protocol, UMI, Bell and Howell information Company, Ann Arbor, MI, 304 p.

Peel, M.C., Finlayson, B.L., McMahon, T.A. (2007) Updated World Map of the Köppen-Geiger Climate Classification, Hydrology and Earth System Sciences, Discussion 4, pp. 439-473.

Robinson, M.S. (2010) Technical Report for the Gil/JV Gold Property, Fairbanks Mining District, Alaska, Teryl Resources Corp., Richmond, BC, Canada, 48 p.

SGS Minerals Services (2009) Before and After Rain, Mt. Isa Prospects, Northern Queensland, Australia, MMI Case Studies, T3 SGS 1091-CS47A, Web. February 4, 2016.

Sims, J. (2015) Fort Knox Mine 43-101 Technical Report, 167 p.

Sipos, P., Németh, T., Kis, V. K., & Mohai, I. (2008) Sorption of copper, zinc and lead on soil mineral phases, Chemosphere, v. 73, pp. 461-469.

Smee, B. (1998) A New Theory to Explain the Formation of Soil Geochemical Responses Over Deeply Covered Gold Mineralization in Arid Environments, Journal of Geochemical Exploration, vol. 61, pp. 149-172.

Stumm, W. & Morgan, J. J. (1996) Aquatic Chemistry 3rd ed., Wiley-Interscience, New York, 1040 p.

Theodore, T. (1998) Large Distal-Disseminated Precious-Metal Deposits in the Battle Mountain Mining District, Nevada, USGS Open File Report 98-338, 27 p.

Theodore, T. (1991a), Preliminary Geologic Map of the North Peak Quadrangle, Humboldt and Lander Counties, Nevada, USGS Open-File Report 91-429.

Theodore, T. (1991b) Preliminary Geologic Map of the Valmy Quadrangle, Humboldt County, Nevada, USGS Open-File Report 91-430.

Thompson, A. & Goyne, K.W. (2012) Introduction to the Sorption of Chemical Constituents in Soils, Nature Education Knowledge, vol. 4, pg. 7.

Thompson, I. (1986) Getting It Right, Exploration Geochemistry: Design and Interpretation of Soil Surveys, Reviews in Economic Geology, vol. 3, pp. 1-18.

Thurman, E.M. (1985) Organic geochemistry of natural waters, Martinus Nijhoff, Dordrecht, 497 p.

Tyler, G. (2011) ICP-OES, ICP-MS, and AAS Techniques Compared, technical note 5, HORIBA group: Longjumeau, France, 11 p.

Ziólkowska, M., Milewska-Duda, J., & Duda, J.T. (2016) A qualitative approach to adsorption mechanism identification on microporous carbonaceous surfaces, Adsorption, vol. 22, pp. 233-246.

Zumdahl, S.S., & Zumdahl, S.A. (2007) Chemistry, 7th ed., Houghton Mifflin Company, Boston, 1056 p.

Appendix 1.1: MMI analyses along line A'-B',

Analyte Detection Label	N83E	Nad83N	year	cover ft.	Ag ppb 1	As ppb 10
MMI 65-106	485776	4513180	2008	0-39	23	10
MMI 65-105	485807	4513180	2008	0-39	25	10
MMI 65-104	485837	4513180	2008	0-39	27	10
MMI 65-103	485868	4513180	2008	0-39	25	<10
MMI 65-102	485898	4513180	2008	0-39	22	30
MMI 65-101	485928	4513180	2008	0-39	29	20
MMI 65-100	485959	4513180	2008	0-39	33	10
MMI 65-99	485989	4513180	2008	0-39	23	20
MMI 65-98	486020	4513180	2008	0-39	29	<10
MMI 65-97	486050	4513180	2008	0-39	26	10
MMI 65-96	486081	4513180	2008	0-39	28	20
MMI 65-95	486111	4513180	2008	0-39	22	10
MMI 65-94	486142	4513180	2008	0-39	33	20
MMI 65-93	486172	4513180	2008	0-39	21	20
MMI 65-92	486203	4513180	2008	0-39	26	20
MMI 65-91	486233	4513180	2008	40-200	37	<10
MMI 65-90	486264	4513180	2008	40-200	31	20
MMI 65-89	486294	4513180	2008	40-200	31	40
MMI 65-88	486325	4513180	2008	40-200	31	20
MMI 65-87	486355	4513180	2008	40-200	39	40
MMI 65-86	486386	4513180	2008	40-200	30	20
MMI 65-85	486416	4513180	2008	40-200	32	50
MMI 65-84	486447	4513180	2008	40-200	32	60
MMI 65-83	486477	4513180	2008	40-200	36	20
MMI 65-82	486508	4513180	2008	40-200	30	40
MMI 65-81	486538	4513180	2008	40-200	35	30
MMI 65-80	486569	4513180	2008	40-200	26	10
MMI 65-79	486599	4513180	2008	40-200	30	10
MMI 65-78	486630	4513180	2008	40-200	22	20
MMI 65-77*	486660	4513180	2008	40-200	28	20

Marigold Mine, Northern Nevada (* soil disturbance)

Au ppb 0.1	Ba ppb 10	Cd ppb 1	Co ppb 5	Cu ppb 10	Pb ppb 10	Sm ppb 1	Y ppb 5	Zn ppb 20	Zr ppb 5
0.4	7450	21	14	800	20	<1	29	40	7
0.5	12700	23	9	980	20	<1	10	80	9
0.7	8850	20	18	720	30	<1	10	60	7
0.3	10000	22	10	940	20	<1	30	50	7
0.2	7510	25	17	1010	20	<1	7	90	10
0.3	5580	30	18	1030	30	<1	12	60	8
0.4	5460	43	36	800	30	2	21	70	13
0.6	7890	32	58	850	40	2	16	170	19
0.2	4860	32	22	620	20	<1	23	60	10
0.2	7660	24	29	800	20	5	66	200	14
0.3	8300	30	16	960	20	5	41	70	13
0.5	4920	28	41	620	20	<1	12	110	14
0.3	3810	45	23	830	20	<1	<5	90	10
0.2	4510	30	5	610	10	<1	<5	80	10
0.5	10700	26	14	1290	30	<1	31	50	5
0.5	5050	44	19	770	20	1	12	110	11
0.6	6470	66	23	1100	20	2	12	130	16
0.8	4470	48	30	1160	20	<1	17	90	11
0.3	1980	55	22	770	10	<1	11	100	10
0.7	2370	44	14	980	10	<1	6	70	7
0.6	2310	47	41	910	20	<1	6	90	11
0.9	5850	49	15	1440	20	<1	7	120	16
1.7	4460	35	33	1220	20	1	15	100	24
1.0	4390	56	47	1110	30	2	20	140	17
0.6	2210	42	22	890	10	<1	6	90	10
0.8	3710	49	39	1270	30	<1	13	90	15
0.5	3790	30	27	1290	20	<1	14	70	9
0.4	3350	29	20	910	20	<1	10	70	10
0.4	6200	40	25	1040	10	11	66	100	19
0.4	3230	35	16	1210	20	4	57	60	13

Appendix 1.1 (continued)

Analyte					Ag ppb	As ppb	Au ppb
Detection					1	10	0.1
Label	N83E	Nad83N	year	cover ft.			
MMI 65-76	486690	4513180	2008	40-200	35	20	0.6
MMI 65-75	486721	4513180	2008	40-200	43	10	0.6
MMI 65-74	486751	4513180	2008	40-200	35	20	1.2
MMI 65-73	486782	4513180	2008	40-200	44	70	3.0
MMI 65-72*	486812	4513180	2008	40-200	34	20	0.5
MMI 65-71	486843	4513180	2008	40-200	43	20	0.7
MMI 65-70	486873	4513180	2008	40-200	38	20	1.0
MMI 65-69	486904	4513180	2008	40-200	34	20	0.6
MMI 65-68	486934	4513180	2008	40-200	43	30	0.7
MMI 65-67	486965	4513180	2008	40-200	33	20	0.7
MMI 65-66*	486995	4513180	2008	40-200	33	10	0.6
MMI 65-65	487026	4513180	2008	40-200	37	20	0.9
MMI 65-64	487056	4513180	2008	40-200	43	10	1.3
MMI 65-63	487087	4513180	2008	40-200	31	20	0.6
MMI 65-62*	487117	4513180	2008	40-200	40	10	3.7
MMI 65-61	487148	4513180	2008	40-200	33	20	0.7
MMI 65-60	487178	4513180	2008	40-200	20	10	0.3
MMI 65-59	487209	4513180	2008	40-200	25	<10	0.4
MMI 65-58	487239	4513180	2008	40-200	51	30	2.2
MMI 65-57	487270	4513180	2008	40-200	30	10	0.8
MMI 65-56	487300	4513180	2008	40-200	45	20	1.8
MMI 65-55	487331	4513180	2008	40-200	32	10	0.6
MMI 65-54	487361	4513180	2008	40-200	34	10	0.7

Ba ppb 10	Cd ppb 1	Co ppb 5	Cu ppb 10	Pb ppb 10	Sm ppb 1	Y ppb 5	Zn ppb 20	Zr ppb 5
4150	27	8	1200	10	<1	27	50	9
4350	30	12	940	20	<1	24	50	8
3260	42	51	1220	20	<1	11	110	11
3750	48	85	1930	20	<1	11	120	14
4500	45	21	980	20	10	77	80	16
4650	32	15	970	20	<1	25	80	10
3530	52	34	880	20	1	14	120	18
2270	57	19	770	20	3	33	120	13
1460	25	14	560	<10	<1	<5	70	14
3350	47	20	890	20	<1	12	120	12
3200	39	12	780	20	<1	12	80	10
3880	40	18	780	10	<1	8	100	10
2830	37	19	820	20	<1	8	100	7
2930	32	23	810	20	<1	12	90	10
4950	27	41	1340	30	<1	17	90	9
6170	35	31	1100	20	9	63	90	14
4060	20	19	770	20	<1	40	40	9
3130	31	24	740	20	2	31	100	12
5450	59	88	1010	40	7	42	250	22
4670	39	24	1080	10	<1	<5	110	6
2190	41	85	900	20	<1	6	140	12
4620	43	27	1100	20	5	36	100	14
2840	45	30	800	20	<1	6	110	8

Appendix 1.2: MMI analyses along line C'-D',

Analyte					Ag ppb	As ppb
Detection					1	10
Label	N83E	Nad83N	year	cover ft.		
MMI 62-106	485776	4512722	2008	0-39	27	20
MMI 62-105	485807	4512722	2008	0-39	26	10
MMI 62-104	485837	4512722	2008	0-39	19	<10
MMI 62-103	485868	4512722	2008	0-39	24	10
MMI 62-102	485898	4512722	2008	0-39	27	10
MMI 62-101	485928	4512722	2008	0-39	24	10
MMI 62-100	485959	4512722	2008	0-39	21	10
MMI 62-99	485989	4512722	2008	0-39	22	40
MMI 62-98	486020	4512722	2008	0-39	27	20
MMI 62-97	486050	4512722	2008	0-39	23	10
MMI 62-96	486081	4512722	2008	0-39	25	20
MMI 62-95	486111	4512722	2008	0-39	31	20
MMI 62-94	486142	4512722	2008	0-39	31	60
MMI 62-93	486172	4512722	2008	0-39	26	20
MMI 62-92	486203	4512722	2008	0-39	26	20
MMI 62-91	486233	4512722	2008	0-39	29	30
MMI 62-90	486264	4512722	2008	0-39	18	20
MMI 62-89	486294	4512722	2008	0-39	19	20
MMI 62-88	486325	4512722	2008	0-39	16	20
MMI 62-87	486355	4512722	2008	0-39	23	20
MMI 62-86	486386	4512722	2008	40-200	20	20
MMI 62-85	486416	4512722	2008	40-200	27	20
MMI 62-84	486447	4512722	2008	40-200	27	30
MMI 62-83	486477	4512722	2008	40-200	57	50
MMI 62-82	486508	4512722	2008	40-200	22	20
MMI 62-81	486538	4512722	2008	40-200	33	30
MMI 62-80	486569	4512722	2008	40-200	33	30
MMI 62-79	486599	4512722	2008	40-200	39	40
MMI 62-78	486630	4512722	2008	40-200	36	70
MMI 62-77	486660	4512722	2008	40-200	21	20

Marigold Mine, Northern Nevada (* soil disturbance)

Au ppb	Ba ppb	Cd ppb	Co ppb	Cu ppb	Pb ppb	Sm ppb	Y ppb	Zn ppb	Zr ppb
0.1	10	1	5	10	10	1	5	20	5
0.9	14000	37	67	1060	30	6	70	110	16
0.5	10400	10	29	1050	30	<1	14	30	5
0.6	7860	20	29	720	40	1	76	30	6
0.9	7030	18	20	940	20	<1	28	60	8
0.9	7060	31	52	1210	40	7	105	70	8
2.5	10500	21	39	1250	30	<1	50	60	6
1.9	13700	16	115	740	40	<1	14	80	8
0.5	4870	29	95	980	40	2	29	70	21
0.2	2690	51	26	720	20	<1	6	80	10
0.2	3170	60	51	860	20	<1	9	110	11
0.5	3880	57	61	1030	20	2	17	130	17
0.5	4210	50	59	1120	20	<1	12	90	11
1.9	5820	45	47	1450	20	2	24	110	22
0.5	5440	66	47	860	20	4	27	130	17
1.3	7870	30	50	1160	20	7	56	90	16
1.7	5250	33	74	1110	20	<1	<5	150	12
0.5	4430	33	24	920	20	9	65	90	13
0.2	3930	28	22	840	20	21	138	40	13
0.6	3630	20	48	1390	30	2	88	30	6
0.4	3370	28	51	1130	20	<1	22	50	8
0.4	5410	42	38	1070	20	7	56	90	13
0.4	3310	43	36	1430	20	<1	8	80	9
1.0	6260	35	34	1580	20	7	63	70	11
4.7	8820	36	134	1760	40	2	18	120	11
0.7	3200	38	52	800	20	<1	21	90	9
1.0	3470	45	52	1340	20	<1	<5	110	10
1.0	3730	44	25	1030	20	<1	7	100	10
1.2	3210	45	51	1120	20	<1	8	90	12
1.8	4880	46	44	1740	20	<1	17	90	11
1.5	3100	36	76	1000	30	<1	15	80	10

Appendix 1.2 (Continued)

Analyte Detection Label	N83E	Nad83N	year	cover ft.	Ag ppb 1	As ppb 10
MMI 62-76	486690	4512722	2008	40-200	32	20
MMI 62-75	486721	4512722	2008	40-200	46	20
MMI 62-74	486751	4512722	2008	40-200	35	20
MMI 62-73	486782	4512722	2008	40-200	17	20
MMI 62-72	486812	4512722	2008	40-200	33	10
MMI 62-71	486843	4512722	2008	40-200	45	30
MMI 62-70	486873	4512722	2008	40-200	30	30
MMI 62-69	486904	4512722	2008	40-200	31	20
MMI 62-68	486934	4512722	2008	40-200	22	20
MMI 62-67	486965	4512722	2008	40-200	25	30
MMI 62-66	486995	4512722	2008	40-200	29	30
MMI 62-65	487026	4512722	2008	40-200	36	20

Au ppb	Ba ppb	Cd ppb	Co ppb	Cu ppb	Pb ppb	Sm ppb	Y ppb	Zn ppb	Zr ppb
0.1	10	1	5	10	10	1	5	20	5
0.9	4860	27	50	960	20	<1	30	50	7
0.6	2830	37	29	990	20	<1	<5	80	7
0.6	4860	34	22	1590	30	<1	26	50	6
0.3	2560	20	15	500	10	<1	22	40	9
0.5	2610	36	34	1060	20	<1	30	50	8
2.6	4500	38	52	1800	30	<1	31	70	5
1.1	8080	42	59	1130	20	4	27	140	18
0.8	2790	31	66	1110	30	<1	23	70	10
0.4	3500	34	43	960	30	<1	20	60	9
0.5	3910	35	22	1090	30	<1	30	50	8
0.6	2320	37	32	1210	20	<1	9	70	8
1.5	4570	39	48	1150	30	1	19	100	10

Appendix 1.3: MMI analyses along line E-F, Marigold Mine, Northern Nevada (* soil disturbance)

Analyte					Ag ppb	As ppb	Au ppb	Ba ppb	Pb ppb	Cd ppb	Co ppb	Cu ppb	Y ppb	Zn ppb	Zr ppb
Detection					1	10	0.1	10	10	1	5	10	5	20	5
Label	N83E	Nad83N	year	cover ft.											
MMI 52-26	485746	4511198	2008	40-200	37	20	0.7	790	10	27	28	1250		80	6
MMI 52-25*	485776	4511198	2008	40-200	33	20	0.7	770		27	23	1330		80	
MMI 52-24	485807	4511198	2008	40-200	26	10	0.6	720	10	30	31	1120	5	80	5
MMI 52-23	485837	4511198	2008	40-200	33	10	0.5	1340		22	12	1390	5	50	
MMI 52-22	485868	4511198	2008	40-200	23	30	2.4	1570		32	9	1340	5	110	7
MMI 52-21	485898	4511198	2008	40-200	26	30	0.8	1380		35	24	1230		120	6
MMI 52-20	485928	4511198	2008	40-200	20		1.6	1080		22	11	940		50	
MMI 52-19	485959	4511198	2008	40-200	36	10	0.5	1330		31	9	980		70	
MMI 52-18	485989	4511198	2008	40-200	25	20	1.1	2050	10	24	10	1470		60	9
MMI 52-17	486020	4511198	2008	40-200	41	20	0.7	2380		33	9	1280	6	70	8
MMI 52-16*	486050	4511198	2008	40-200	55	60	3.9	1220		17	40	1090		50	
MMI 52-15	486081	4511198	2008	40-200	47	30	3.4	3450	20	32	92	1400		100	6
MMI 52-14	486111	4511198	2008	40-200	44	20	3.4	3880	10	26	46	1210	7	70	
MMI 52-13	486142	4511198	2008	>200	38	20	1.4	1400	10	31	16	1650	6	90	
MMI 52-12	486172	4511198	2008	>200	33	20	0.5	930		31	6	1090	6	210	
MMI 52-11	486203	4511198	2008	>200	37	20	1.7	1400		41	21	1410		90	
MMI 52-10	486233	4511198	2008	>200	27	20	0.7	1820		33	8	1430	7	70	8
MMI 52-9	486264	4511198	2008	>200	35	70	12.1	3680	20	47	27	990	9	400	11
MMI 52-8	486294	4511198	2008	>200	34	30	1.1	4230		56	11	1130		150	8
MMI 52-7	486325	4511198	2008	>200	41	20	1.4	1760		39	10	1580		100	5
MMI 52-6	486355	4511198	2008	>200	37	20	1.4	1640		41	14	1460	8	90	
MMI 52-5	486386	4511198	2008	>200	51	30	2.5	1590		42	20	1430		110	
MMI 52-4	486416	4511198	2008	>200	44	30	2.5	3500		38	8	1470		80	5
MMI 52-3	486447	4511198	2008	>200	40	30	1.9	1820		51	26	1360		110	7
MMI 52-2	486477	4511198	2008	>200	34	20	1.2	2230		58	22	1270	7	120	8
MMI 52-1	486508	4511198	2008	>200	30	10	1.0	920		53	24	1120	10	110	6

Appendix 1.3 (continued)

Analyte Detection Label	N83E	Nad83N	year	cover ft.	Ag ppb 1
MMI 52-21_10	485980.1	4511021.9	2012	40-200	13
MMI 52-21_5	485981.6	4511021.9	2012	40-200	74
MMI 52-21	485983.2	4511021.9	2012	40-200	28
MMI 52-20_20	486007.5	4511021.9	2012	40-200	54
MMI 52-20_10	486010.6	4511021.9	2012	40-200	58
MMI 52-20_5	486012.1	4511021.9	2012	40-200	42
MMI 52-20	486013.6	4511021.9	2012	40-200	33
MMI52-19_20	486038.0	4511021.9	2012	40-200	33
MMI 52-19_10	486041.1	4511021.9	2012	40-200	35
MMI52-19_5	486042.6	4511021.9	2012	40-200	42
MMI 52-19	486044.1	4511021.9	2012	40-200	40
MMI 52-18_20	486068.5	4511021.9	2012	40-200	40
MMI 52-18_10	486071.6	4511021.9	2012	40-200	46
MMI 52-18_5	486073.1	4511021.9	2012	40-200	45
MMI 52-18	486074.6	4511021.9	2012	40-200	53
MMI 52-17_20	486099.0	4511021.9	2012	40-200	70
MMI 52-17_10	486102.0	4511021.9	2012	40-200	53
MMI 52-17_5	486103.6	4511021.9	2012	40-200	46
MMI 52-17	486105.1	4511021.9	2012	40-200	49
MMI 52-16_20	486129.5	4511021.9	2012	40-200	79
MMI 52-16_10	486132.6	4511021.9	2012	40-200	61
MMI 52-16_5	486134.1	4511021.9	2012	40-200	68
MMI 52-16	486135.6	4511021.9	2012	40-200	52
MMI 52-15_20	486159.9	4511021.9	2012	40-200	47
MMI 52-15_10	486163.0	4511021.9	2012	40-200	28
MMI 52-15_5	486164.5	4511021.9	2012	40-200	33
MMI 52-15	486166.0	4511021.9	2012	40-200	21
MMI 52-14_20	486190.4	4511021.9	2012	40-200	31
MMI 52-14_10	486193.5	4511021.9	2012	40-200	6
MMI 52-14_5	486195.0	4511021.9	2012	40-200	22
MMI 52-14	486196.5	4511021.9	2012	40-200	41

As ppb	Au ppb	Ba ppb	Pb ppb	Cd ppb	Co ppb	Cu ppb	Sb ppb	Sm ppb
10	0.1	10	10	1	5	10	1	1
370	8.3	7190	330	14	6	990	2	2
40	6.9	5280	460	21	157	1570	3	
20	1.3	3700	90	31	26	1900	1	
	0.7	5850	30	35	51	1210	2	
	0.9	5850	20	28	41	1570	2	
	1.4	5480	20	17	12	2000	1	
	0.7	3560	20	41	37	950	1	
	0.7	3060	20	54	32	900	1	
	0.5	2980	10	47	20	1030		
	0.6	5110	20	37	43	1070	2	
	0.5	3560	10	42	21	1150	1	
	1.7	3450	20	40	45	980	1	
10	1.5	3510	20	41	69	1070	2	
20	2.3	13900	20	31	32	1320	2	
20	3.2	10100	20	31	62	1360	2	
40	8.2	3710	20	10	151	1260	7	
	3.3	12200	40	26	112	1330	5	
20	3.6	11400	270	29	101	1540	4	
	2.0	9340	30	24	121	1190	4	
30	6.0	4750	40	23	219	1240	4	
10	4.3	9680	30	21	221	1090	6	
20	4.9	7410	40	46	387	1500	7	
20	4.0	4700	20	27	216	1300	8	
10	2.2	16300	20	63	75	1660	1	1
10	1.6	5220	20	34	56	1230	2	
20	1.8	4500	30	47	65	1330	2	
10	2.4	6800	20	23	33	960	1	
60	2.1	4160	70	43	60	1400	2	
300	9.2	4510	1230	27	69	2610	2	
420	**135**.0	2980	10**7**00	11	197	**423**0	4	
50	4.3	2380	240	48	131	1350	2	

Appendix 1.3 (continued)

Analyte Detection Label	N83E	Nad83N	year
MMI 52-21_10	485980.1	4511021.9	2012
MMI 52-21_5	485981.6	4511021.9	2012
MMI 52-21	485983.2	4511021.9	2012
MMI 52-20_20	486007.5	4511021.9	2012
MMI 52-20_10	486010.6	4511021.9	2012
MMI 52-20_5	486012.1	4511021.9	2012
MMI 52-20	486013.6	4511021.9	2012
MMI52-19_20	486038.0	4511021.9	2012
MMI 52-19_10	486041.1	4511021.9	2012
MMI52-19_5	486042.6	4511021.9	2012
MMI 52-19	486044.1	4511021.9	2012
MMI 52-18_20	486068.5	4511021.9	2012
MMI 52-18_10	486071.6	4511021.9	2012
MMI 52-18_5	486073.1	4511021.9	2012
MMI 52-18	486074.6	4511021.9	2012
MMI 52-17_20	486099.0	4511021.9	2012
MMI 52-17_10	486102.0	4511021.9	2012
MMI 52-17_5	486103.6	4511021.9	2012
MMI 52-17	486105.1	4511021.9	2012
MMI 52-16_20	486129.5	4511021.9	2012
MMI 52-16_10	486132.6	4511021.9	2012
MMI 52-16_5	486134.1	4511021.9	2012
MMI 52-16	486135.6	4511021.9	2012
MMI 52-15_20	486159.9	4511021.9	2012
MMI 52-15_10	486163.0	4511021.9	2012
MMI 52-15_5	486164.5	4511021.9	2012
MMI 52-15	486166.0	4511021.9	2012
MMI 52-14_20	486190.4	4511021.9	2012
MMI 52-14_10	486193.5	4511021.9	2012
MMI 52-14_5	486195.0	4511021.9	2012
MMI 52-14	486196.5	4511021.9	2012

cover ft.	Sr ppb 10	Y ppb 1	Zn ppb 20	Zr ppb 5	Mg ppb 1
40-200	310	14	420		11
40-200	2910	11	270	12	58
40-200	5690		270	8	116
40-200	6380	18	80	10	149
40-200	6220	12	70	9	149
40-200	7360	6	50	6	144
40-200	5540		100	7	140
40-200	4340	7	100	8	143
40-200	5410		120	10	166
40-200	5220	6	90	8	157
40-200	5470		80	8	171
40-200	5450		90	10	148
40-200	4380		120	7	126
40-200	7150		120	10	141
40-200	6670		150	10	119
40-200	6590		70	8	74
40-200	7780	9	90		142
40-200	5810	8	250	6	108
40-200	6830	17	70	6	152
40-200	4180	8	120	8	81
40-200	7240	5	90	6	117
40-200	5900	8	240	16	114
40-200	5680		150	7	138
40-200	9490	14	170	19	154
40-200	7920		160	10	127
40-200	6370	8	170	11	119
40-200	9140		80		143
40-200	4490		240	9	144
40-200	870		1120	7	35
40-200	1360		**324**0	13	92
40-200	3300	8	260	17	92

Appendix 1.3 (continued)

Analyte Detection Label	N83E	Nad83N	year	cover ft.	Ag ppb 1
MMI 52-13_20	486220.9	4511021.9	2012	>200	34
MMI 52-13_10	486224.0	4511021.9	2012	>200	17
MMI 52-13_5	486225.5	4511021.9	2012	>200	31
MMI 52-13	486227.0	4511021.9	2012	>200	50
MMI 52-1_20	486251.4	4511021.9	2012	>200	37
MMI 52-12_10	486254.4	4511021.9	2012	>200	45
MMI 52-12_5	486256.0	4511021.9	2012	>200	36
MMI 52-12	486257.5	4511021.9	2012	>200	56
MMI 52-11_20	486281.9	4511021.9	2012	>200	35
MMI 52-11_10	486284.9	4511021.9	2012	>200	46
MMI 52-11_5	486286.4	4511021.9	2012	>200	34
MMI 52-11	486288.0	4511021.9	2012	>200	40
MMI 52-10_20	486312.3	4511021.9	2012	>200	34
MMI 52-10_10	486315.4	4511021.9	2012	>200	36
MMI 52-10_5	486316.9	4511021.9	2012	>200	33
MMI 52-10	486318.4	4511021.9	2012	>200	24
MMI 52-9_20	486342.8	4511021.9	2012	>200	31
MMI 52-9_10	486345.9	4511021.9	2012	>200	38
MMI 52-9_5	486347.4	4511021.9	2012	>200	32
MMI 52-9	486348.9	4511021.9	2012	>200	39
MMI 52-8_20	486373.3	4511021.9	2012	>200	33
MMI 52-8_10	486376.4	4511021.9	2012	>200	36
MMI 52-8_5	486377.9	4511021.9	2012	>200	21
MMI 52-8	486379.4	4511021.9	2012	>200	37

As ppb	Au ppb	Ba ppb	Pb ppb	Cd ppb	Co ppb	Cu ppb	Sb ppb	Sm ppb
10	0.1	10	10	1	5	10	1	1
70	13.1	4380	70	73	100	1150	2	
380	**590**.0	2700	1770	**32**	**273**	1160	**3**	
60	28.8	4120	1890	68	64	1770	2	
80	43.2	4640	9990	30	227	3640	3	
10	0.8	2470	20	76	53	1070	2	
	0.7	2990	20	44	28	1530	1	
20	1.0	2220	20	60	34	1200	1	
30	2.2	3530	190	28	71	950	3	
20	1.8	2100	30	67	90	1070	2	
20	1.4	2230	20	48	52	2210	3	
20	0.7	1640	20	37	63	1320	2	
10	1.2	8160	20	44	46	1450	1	1
10	0.6	2590	10	39	23	1770	1	
20	1.4	5160	20	58	52	1250	1	
10	1.3	4020	20	75	48	890		2
	0.5	2610	20	53	59	1250	1	
20	0.8	1860	10	75	68	1120	2	
10	1.1	8760	40	75	270	1450	2	5
10	2.3	9740	30	70	222	1310	1	7
10	1.5	2150	20	64	77	1250	2	
10	1.2	8590	20	65	62	1570	1	6
30	1.6	2650	20	69	76	1710	2	
	1.9	3420	20	37	63	1350	1	
10	1.3	3360	20	56	68	1580	2	

Appendix 1.3 (continued)

Analyte Detection Label	N83E	Nad83N
MMI 52-13_20	486220.9	4511021.9
MMI 52-13_10	486224.0	4511021.9
MMI 52-13_5	486225.5	4511021.9
MMI 52-13	486227.0	4511021.9
MMI 52-1_20	486251.4	4511021.9
MMI 52-12_10	486254.4	4511021.9
MMI 52-12_5	486256.0	4511021.9
MMI 52-12	486257.5	4511021.9
MMI 52-11_20	486281.9	4511021.9
MMI 52-11_10	486284.9	4511021.9
MMI 52-11_5	486286.4	4511021.9
MMI 52-11	486288.0	4511021.9
MMI 52-10_20	486312.3	4511021.9
MMI 52-10_10	486315.4	4511021.9
MMI 52-10_5	486316.9	4511021.9
MMI 52-10	486318.4	4511021.9
MMI 52-9_20	486342.8	4511021.9
MMI 52-9_10	486345.9	4511021.9
MMI 52-9_5	486347.4	4511021.9
MMI 52-9	486348.9	4511021.9
MMI 52-8_20	486373.3	4511021.9
MMI 52-8_10	486376.4	4511021.9
MMI 52-8_5	486377.9	4511021.9
MMI 52-8	486379.4	4511021.9

year	cover ft.	Sr ppb 10	Y ppb 1	Zn ppb 20	Zr ppb 5	Mg ppb 1
2012	>200	4760	8	250	15	137
2012	>200	2710	14	1400	10	160
2012	>200	5010	9	650	15	153
2012	>200	3250	6	1500	21	114
2012	>200	5170	7	160	12	142
2012	>200	7490	6	100	9	186
2012	>200	6420		160	11	165
2012	>200	3410	6	200	11	66
2012	>200	3690	9	150	14	121
2012	>200	5040	8	100	10	129
2012	>200	4150	12	90	11	127
2012	>200	7850	10	110	15	180
2012	>200	6590	14	80	9	169
2012	>200	6550	8	120	14	144
2012	>200	6190	14	160	20	155
2012	>200	5470	22	100	13	165
2012	>200	4230	5	180	13	108
2012	>200	7110	37	160	24	188
2012	>200	6470	48	200	24	160
2012	>200	4840	7	190	14	152
2012	>200	8010	45	130	20	178
2012	>200	6070	15	160	15	161
2012	>200	5880	32	90	11	148
2012	>200	6300	17	120	11	165

Appendix 1.4: MMI analyses along line I-J, Marigold Mine, Northern Nevada

Analyte					Ag ppb	As ppb	Au ppb	Ba ppb	Cd ppb	Co ppb	Cu ppb	Pb ppb	Sm ppb	Y ppb	Zn ppb	Zr ppb
Detection					1	10	0.1	10	1	5	10	10	1	5	20	5
Label	N83E	Nad83N	year	cover ft.												
MMI 3-20	484421	4507601	2007	0-39	35	20	6.7	41900	17	160	2480	40	5	61	110	20
MMI 3-19	484451	4507601	2007	0-39	26	20	1.9	25100	20	104	1440	30	11	93	110	17
MMI 3-18	484482	4507601	2007	0-39	14	20	2.6	44200	7	172	1000	30		8	90	22
MMI 3-17	484512	4507601	2007	0-39	10		1.6	14700	6	57	300	40	3	28	40	7
MMI 3-16	484543	4507601	2007	0-39	29	20	2.2	37700	18	147	1650	50	19	200	160	19
MMI 3-15	484573	4507601	2007	0-39	41	20	1.0	25800	26	69	1100	40	8	81	120	25
MMI 3-14	484604	4507601	2007	0-39	34	20	2.0	25600	22	161	1450	50	3	40	170	26
MMI 3-13	484634	4507601	2007	0-39	33	20	0.7	36900	14	80	940	50	3	50	100	22
MMI 3-12	484665	4507601	2007	0-39	36	20	5.3	41200	13	83	1910	60	4	53	130	26
MMI 3-11	484695	4507601	2007	0-39	32	40	10.3	46100	13	37	1180	90	2	20	210	35
MMI 3-10	484726	4507601	2007	0-39	25	30	0.9	22500	37	96	1530	20	4	28	200	34
MMI 3-9	484756	4507601	2007	0-39	39	60	3.2	15000	50	76	2030	30	12	76	250	48
MMI 3-8	484787	4507601	2007	0-39	57	30	3.9	16500	50	128	1710	30	13	111	170	33
MMI 3-7	484817	4507601	2007	0-39	32	30	1.5	9970	62	86	1030	20	38	236	200	39
MMI 3-6	484848	4507601	2007	0-39	49	20	1.6	8600	76	26	850	20	2	26	170	22
MMI 3-5	484878	4507601	2007	0-39	55	20	1.9	10900	47	80	1370	40	20	153	150	29
MMI 3-4	484909	4507601	2007	0-39	52	30	6.0	18200	79	71	1570	30	8	80	140	28
MMI 3-3	484939	4507601	2007	0-39	52	30	5.2	20800	72	79	2140	30	12	96	200	35
MMI 3-2	484970	4507601	2007	0-39	39		0.7	21100	31	58	950	30	29	240	100	30
MMI 3-1	485000	4507601	2007	0-39	83	20	4.2	26400	47	100	2130	30	16	151	140	30

Appendix 1.5: MMI analyses along line X-Y-Z,

Analyte Detection Label	N83E	Nad83N	year	cover ft.	Ag ppb 1	As ppb 10
MMI 41-1	485715	4507145	2008	40-200	15	
MMI 41-2	485685	4507145	2008	40-200	25	30
MMI 41-3	485654	4507145	2008	40-200	17	10
MMI 41-4	485624	4507145	2008	40-200	28	10
MMI 41-5	485593	4507145	2008	40-200	15	10
MMI 41-6	485563	4507145	2008	40-200	26	30
MMI 41-7	485532	4507145	2008	0-39	42	10
MMI 41-8	485502	4507145	2008	0-39	45	10
MMI 41-9	485471	4507145	2008	0-39	47	
MMI 41-10	485441	4507145	2008	0-39	29	10
MMI 41-11	485410	4507145	2008	0-39	37	20
MMI 41-12	485380	4507145	2008	0-39	62	50
MMI 41-13	485349	4507145	2008	0-39	24	10
MMI 41-14*	485319	4507145	2008	0-39	34	20
MMI 41-15	485288	4507145	2008	0-39	35	20
MMI 41-16	485258	4507145	2008	0-39	36	10
MMI 41-17	485227	4507145	2008	0-39	13	20
MMI 41-18	485197	4507145	2008	0-39	29	20
MMI 41-19	485166	4507145	2008	0-39	37	20
MMI 41-20	485136	4507145	2008	0-39	43	20
MMI 41-21	485106	4507145	2008	0-39	85	90
MMI 41-22	485075	4507145	2008	0-39	41	10
MMI 41-23	485045	4507145	2008	0-39	49	10
MMI 41-24	485014	4507145	2008	0-39	50	
MMI 41-25	484984	4507145	2008	0-39	50	20
MMI 41-26	484953	4507145	2008	0-39	44	40
MMI 41-27	484923	4507145	2008	0-39	53	20
MMI 41-28	484892	4507145	2008	0-39	48	10
MMI 41-29	484862	4507145	2008	0-39	41	20
MMI 41-30	484831	4507145	2008	0-39	38	10

Marigold Mine, Northern Nevada (*soil disturbance)

Au ppb	Ba ppb	Cd ppb	Co ppb	Cu ppb	Pb ppb	Y ppb	Zn ppb	Zr ppb
0.1	10	1	5	10	10	5	20	5
0.5	1720	12	31	850	10	38	90	6
2.6	2170	32	26	1400	20	14	40	10
0.8	1430	18	11	1000	10	13	120	5
2.4	1310	26	28	1120	20	12	70	6
2.1	1720	20	10	540	10	29	70	19
10.1	4530	36	9	1150	10	79	50	17
32.6	2180	11	71	1540	40	11	100	8
28.8	7220	9	41	1330	30	28		
42.1	4850	7	42	1510	40	11		
3.8	3280	14	61	690	30	7	60	
3.5	1290	29	28	950	30	44	140	7
58.5	2240	7	62	2060	70	0	50	6
5.4	2350	21	19	1200	20	0	60	
12.4	5720	6	152	1700	40	13	50	
19.8	6510	6	69	1650	30	25	60	
12.2	2280	7	20	1580	30	7	30	
9.7	990	5	192	680	280	412	50	76
7.1	2130	12	17	1370	20	6	20	
11.2	5310	15	30	1310	20	12	40	6
13.8	2390	7	8	1230	20	9	0	
14.7	90	9	36	1600	60	13	60	6
5.7	2700	17	16	1080	20	10	30	8
12.6	6560	12	14	1250	20	6	60	
3.2	7000	10	44	1020	20	10	30	
3.7	3300	22	23	910	20	21	50	6
4.7	2650	53	68	1080	40	10	130	14
0.8	980	31	16	1130	10	0	60	5
1.4	2560	49	31	1360	20	16	40	6
1.4	1200	49	13	1210			130	7
1.7	1340	31	8	1490			120	

Appendix 1.5 (Continued)

Analyte					Ag ppb	As ppb
Detection					1	10
Label	N83E	Nad83N	year	cover ft.		
MMI 41-31	484801	4507145	2008	0-39	32	20
MMI 41-32	484770	4507145	2008	0-39	23	20
MMI 41-33	484740	4507145	2008	0-39	52	
MMI 41-35	484679	4507145	2008	0-39	48	20
MMI 41-36	484648	4507145	2008	0-39	26	20
MMI 41-37	484618	4507145	2008	0-39	20	10
MMI 41-38	484587	4507145	2008	0-39	25	10
MMI 41-39	484557	4507145	2008	0-39	25	20
MMI 41-40	484526	4507145	2008	0-39	17	
MMI 41-41	484496	4507145	2008	0-39	27	10
MMI 41-42	484465	4507145	2008	0-39	29	
MMI 41-43	484435	4507145	2008	0-39	29	
MMI 41-44	484404	4507145	2008	0-39	28	10
MMI 41-45	484374	4507145	2008	0-39	38	10
MMI 41-46	484344	4507145	2008	0-39	31	
MMI 41-47	484313	4507145	2008	0-39	22	
MMI 41-48	484283	4507145	2008	0-39	30	30
MMI 41-49	484252	4507145	2008	0-39	28	
MMI 41-50	484222	4507145	2008	0-39	38	

Au ppb	Ba ppb	Cd ppb	Co ppb	Cu ppb	Pb ppb	Y ppb	Zn ppb	Zr ppb
0.1	10	1	5	10	10	5	20	5
0.9	1830	56	15	1340	20	23	70	10
2.3	1070	23	71	1000	20	31	60	13
0.8	900	26	36	1670	10	8	30	5
1.8	3940	44	33	1590	20	35	70	19
0.6	4810	32	34	1170	10	7	120	13
1.1	5580	7	52	910	20	9	30	6
11.4	9400	7	60	1380	30	8	60	5
2.6	5200	15	94	1760	30	21	110	16
1.1	7200	13	31	1550	30	9	50	8
1.6	3880	11	43	2070	30	50	20	8
1.2	6380	12	13	1820	10	9	30	5
0.9	9420	24	38	1690	20	15	90	11
2.5	3430	18	164	2510	40	19	30	9
2.4	2050	27	67	2080	20	7	30	6
2.1	3280	16	76	1830	30	13		5
1.1	2990	15	77	1820	30	15		5
2.3	3860	12	55	2080	20		20	
1.5	3490	19	23	1630	20	6	50	
1.4	1970	14	53	1900	20		80	

Appendix 1.5 (Continued)

Analyte				Ag ppb	As ppb
Detection				1	10
Label	UTM N NAD27	UTM E NAD27	year		
MMI 41-1	4506968	485800.3	2012	30	30
MMI 41-1_5	4506968	485798.8	2012	20	20
MMI 41-1_10	4506968	485797.2	2012	33	20
MMI 41-1_20	4506968	485794.2	2012	34	20
MMI 41-2	4506968	485769.8	2012	27	20
MMI 41-2_5	4506968	485768.3	2012	31	30
MMI 41-2_10	4506968	485766.8	2012	28	10
MMI 41-2_20	4506968	485763.7	2012	17	20
MMI 41-3	4506968	485739.3	2012	34	20
MMI 41-3_5	4506968	485737.8	2012	23	20
MMI 41-3_10	4506968	485736.3	2012	29	20
MMI41-3_20	4506968	485733.2	2012	24	10
MMI 41-4	4506968	485708.8	2012	83	
MMI 41-4_5	4506968	485707.3	2012	47	
MMI 41-4_10	4506968	485705.8	2012	50	
MMI 41-4_20	4506968	485702.7	2012	26	10
MMI 41-5	4506968	485678.4	2012	41	30
MMI 41-5_5	4506968	485676.8	2012	55	
MMI 41-5_10	4506968	485675.3	2012	25	20
MMI 41-5_20	4506968	485672.3	2012	21	
MMI 41-6	4506968	485647.9	2012	44	
MMI 41-6_5	4506968	485646.4	2012	42	
MMI 41-6_10	4506968	485644.8	2012	46	
MMI 41-6_20	4506968	485641.8	2012	39	
MMI 41-7	4506968	485617.4	2012	27	110
MMI 41-7_5	4506968	485615.9	2012	13	190
MMI 41-7_10	4506968	485614.4	2012	19	400
MMI 41-7_20	4506968	485611.3	2012	20	460

Au ppb	Ba ppb	Cd ppb	Co ppb	Cu ppb	Hg ppb	Mg ppb	Ni ppb	Pb ppb
0.1	10	1	5	10	1	1	5	10
2.2	7580	36	63	1750		197	408	30
0.9	7100	28	31	1310	2	209	353	20
2.1	12300	16	19	1340		213	439	20
2.0	6090	27	29	1740		211	332	20
2.5	12000	31	49	1790		215	374	30
2.6	6130	43	87	1770		249	419	30
2.5	5490	17	28	1230		197	221	20
1.2	2050	18	27	1240		219	265	20
2.2	7810	39	89	1770		192	408	30
1.2	9570	29	45	1670		247	360	20
1.9	7030	36	55	1760		183	353	20
1.1	7780	41	65	1640		198	297	20
10.2	9800	16	306	1560		233	429	120
6.7	5450	18	281	1300		147	328	130
7.4	6260	23	119	1180		209	303	70
1.6	1090	21	61	570		180	181	30
16.7	710	12	176	930		245	578	100
8.6	7720	14	322	1390		160	439	140
4.0	3370	36	103	920		186	282	50
7.0	3220	21	206	1070		124	274	60
34.3	15000	17	91	1920		144	235	60
36.5	16000	22	74	1580	1	137	221	50
34.7	12300	26	107	2120		133	264	50
20.3	12200	26	140	1670		180	342	60
24.4	4320	7	288	1270	4	89	317	70
31.3	1900	5	158	890	5	77	190	70
23.5	330	9	223	1000	10	92	260	80
22.5	270	6	276	940	16	81	276	70

Appendix 1.5 (Continued)

Analyte				Sb ppb	Sm ppb	Y ppb
Detection				1	1	5
Label	UTM N NAD27	UTM E NAD27	year			
MMI 41-1	4506968	485800.3	2012	1	2	25
MMI 41-1_5	4506968	485798.8	2012		4	38
MMI 41-1_10	4506968	485797.2	2012		9	94
MMI 41-1_20	4506968	485794.2	2012			11
MMI 41-2	4506968	485769.8	2012	1	6	69
MMI 41-2_5	4506968	485768.3	2012	2	1	14
MMI 41-2_10	4506968	485766.8	2012	2		20
MMI 41-2_20	4506968	485763.7	2012	1		17
MMI 41-3	4506968	485739.3	2012	2	2	22
MMI 41-3_5	4506968	485737.8	2012	1	8	72
MMI 41-3_10	4506968	485736.3	2012	2		10
MMI41-3_20	4506968	485733.2	2012		2	14
MMI 41-4	4506968	485708.8	2012	4	1	31
MMI 41-4_5	4506968	485707.3	2012	4	2	55
MMI 41-4_10	4506968	485705.8	2012	2		11
MMI 41-4_20	4506968	485702.7	2012	1		8
MMI 41-5	4506968	485678.4	2012	2	5	155
MMI 41-5_5	4506968	485676.8	2012	4	4	111
MMI 41-5_10	4506968	485675.3	2012	1	5	57
MMI 41-5_20	4506968	485672.3	2012	3	1	27
MMI 41-6	4506968	485647.9	2012	4	4	65
MMI 41-6_5	4506968	485646.4	2012	4	3	53
MMI 41-6_10	4506968	485644.8	2012	4	1	36
MMI 41-6_20	4506968	485641.8	2012	4	4	55
MMI 41-7	4506968	485617.4	2012	9	1	14
MMI 41-7_5	4506968	485615.9	2012	7		7
MMI 41-7_10	4506968	485614.4	2012	10	1	15
MMI 41-7_20	4506968	485611.3	2012	11	1	14

Zn ppb	Zr ppb
20	5
90	20
50	19
30	8
40	9
50	18
80	18
40	6
50	14
90	21
60	14
80	19
90	18
70	6
60	
70	7
90	17
60	
70	6
90	21
80	9
60	6
60	7
70	8
80	7
50	5
40	
60	
50	

Appendix 1.5 (Continued)

Analyte Detection				Ag ppb 1	As ppb 10
Label	UTM N NAD27	UTM E NAD27	year		
MMI 41-8	4506968	485586.9	2012	35	100
MMI 41-8_5	4506968	485585.4	2012	41	20
MMI 41-8_10	4506968	485583.9	2012	38	20
MMI 41-8_20	4506968	485580.8	2012	32	10
MMI 41-9	4506968	485556.4	2012	25	20
MMI 41-9_5	4506968	485554.9	2012	22	20
MMI 41-9_10	4506968	485553.4	2012	22	20
MMI 41-9_20	4506968	485550.3	2012	28	20
MMI 41-10	4506968	485526	2012	45	10
MMI 41-10_5	4506968	485524.4	2012	30	
MMI 41-10_10	4506968	485522.9	2012	46	30
MMI 41-10_20	4506968	485519.9	2012	35	10
MMI 41-11	4506968	485495.5	2012	41	60
MMI 41-11_5	4506968	485494	2012	45	
MMI 41-11_10	4506968	485492.4	2012	48	20
MMI 41-11_20	4506968	485489.4	2012	42	10
MMI 41-12	4506968	485465	2012	31	20
MMI 41-12_5	4506968	485463.5	2012	37	20
MMI 41-12_10	4506968	485462	2012	30	30
MMI 41-12_20	4506968	485458.9	2012	30	
MMI 41-13	4506968	485434.5	2012	32	30
MMI 41-13_5	4506968	485433	2012	25	20
MMI 41-13_10	4506968	485431.5	2012	24	20
MMI 41-13_20	4506968	485428.4	2012	35	30
MMI 41-14	4506968	485404	2012	53	10
MMI 41-14_5	4506968	485402.5	2012	39	
MMI 41-14_10	4506968	485401	2012	27	10
MMI 41-14_20	4506968	485397.9	2012	43	10

Au ppb	Ba ppb	Cd ppb	Co ppb	Cu ppb	Hg ppb	Mg ppb	Ni ppb	Pb ppb
0.1	10	1	5	10	1	1	5	10
23.7	6950	12	151	2220	5	91	285	70
30.1	12800	16	307	2530	2	95	498	60
24.3	15000	20	251	2240	2	91	391	70
9.8	13300	28	130	1520		118	304	60
5.8	4540	37	103	1000		119	199	40
6.2	4230	36	138	980		138	270	40
5.3	3010	40	105	940		100	240	30
7.1	3880	46	72	1000		97	187	20
8.7	2470	21	491	1550	1	90	710	170
5.4	6780	23	289	950		102	304	120
16.9	3310	22	384	1430	1	89	315	90
6.7	4630	28	111	1100		143	227	50
5.8	2180	25	62	1440		82	272	60
8.7	7620	28	971	1670	1	156	776	280
9.9	6530	29	1120	2020	1	156	823	310
4.8	6330	36	298	1400		158	552	90
10.2	7360	38	177	1410		138	324	50
11.1	5400	42	227	1320		134	374	50
5.9	9800	33	178	1200		117	262	40
4.9	8340	37	167	1300		146	273	50
8.3	13400	51	153	2150		144	644	20
3.1	4980	29	101	1410		147	241	30
2.3	5350	30	98	1440		138	227	30
39.2	22000	11	183	2080	2	118	403	50
17.4	18400	17	221	1610	2	116	233	70
9.9	11700	23	119	1430	2	156	337	50
2.1	7970	28	57	1470		169	222	30
13.2	18500	23	390	1910	1	188	547	100

Appendix 1.5 (Continued)

Analyte				Sb ppb	Sm ppb	Y ppb
Detection				1	1	5
Label	UTM N NAD27	UTM E NAD27	year			
MMI 41-8	4506968	485586.9	2012	13	1	14
MMI 41-8_5	4506968	485585.4	2012	21	2	24
MMI 41-8_10	4506968	485583.9	2012	21	1	15
MMI 41-8_20	4506968	485580.8	2012	5	4	54
MMI 41-9	4506968	485556.4	2012	2		7
MMI 41-9_5	4506968	485554.9	2012	3	1	25
MMI 41-9_10	4506968	485553.4	2012	2		10
MMI 41-9_20	4506968	485550.3	2012	2		8
MMI 41-10	4506968	485526.0	2012	3	5	126
MMI 41-10_5	4506968	485524.4	2012	4	4	70
MMI 41-10_10	4506968	485522.9	2012	9		5
MMI 41-10_20	4506968	485519.9	2012	3		9
MMI 41-11	4506968	485495.5	2012	2	2	24
MMI 41-11_5	4506968	485494.0	2012	4	3	84
MMI 41-11_10	4506968	485492.4	2012	5	2	53
MMI 41-11_20	4506968	485489.4	2012	2		14
MMI 41-12	4506968	485465.0	2012	2		10
MMI 41-12_5	4506968	485463.5	2012	2		12
MMI 41-12_10	4506968	485462.0	2012	2		
MMI 41-12_20	4506968	485458.9	2012	4		16
MMI 41-13	4506968	485434.5	2012	1		
MMI 41-13_5	4506968	485433.0	2012	1		
MMI 41-13_10	4506968	485431.5	2012	2		
MMI 41-13_20	4506968	485428.4	2012	14	1	16
MMI 41-14	4506968	485404.0	2012	2		10
MMI 41-14_5	4506968	485402.5	2012	2	5	54
MMI 41-14_10	4506968	485401.0	2012			14
MMI 41-14_20	4506968	485397.9	2012	2	5	88

Zn ppb	Zr ppb
20	5
140	6
80	10
80	10
90	15
110	14
90	10
120	16
160	13
50	11
70	8
120	21
80	7
90	13
110	9
130	9
130	10
130	17
130	16
180	19
120	8
180	23
140	10
90	9
70	10
120	6
100	5
90	8
70	13

Appendix 1.5 (Continued)

Analyte Detection				Ag ppb 1	As ppb 10
Label	UTM N NAD27	UTM E NAD27	year		
MMI 41-15	4506968	485373.6	2012	35	30
MMI 41-15_5	4506968	485372	2012	36	
MMI 41-15_10	4506968	485370.5	2012	29	
MMI 41-15_20	4506968	485367.5	2012	31	10
MMI 41-16	4506968	485343.1	2012	26	20
MMI 41-16_5	4506968	485341.6	2012	40	20
MMI 41-16_10	4506968	485340	2012	44	20
MMI 41-16_20	4506968	485337	2012	49	
MMI 41-17	4506968	485312.6	2012	37	40
MMI 41-17_5	4506968	485311.1	2012	27	130
MMI 41-17_10	4506968	485309.6	2012	34	180
MMI 41-17_20	4506968	485306.5	2012	42	30
MMI 41-18	4506968	485282.1	2012	34	20
MMI 41-18_5	4506968	485280.6	2012	36	20
MMI 41-18_10	4506968	485279.1	2012	38	10
MMI 41-18_20	4506968	485276	2012	26	10
MMI 41-19	4506968	485251.6	2012	104	40
MMI 41-19_5	4506968	485250.1	2012	134	20
MMI 41-19_10	4506968	485248.6	2012	27	40
MMI 41-19_20	4506968	485245.5	2012	64	20
MMI 41-20	4506968	485221.2	2012	39	10
MMI 41-20_5	4506968	485219.6	2012	36	10
MMI 41-20_10	4506968	485218.1	2012	42	
MMI 41-20_20	4506968	485215.1	2012	76	10
MMI 41-21	4506968	485190.7	2012	43	10
MMI 41-21_5	4506968	485189.2	2012	73	20
MMI 41-21_10	4506968	485187.6	2012	83	540
MMI 41-21_20	4506968	485184.6	2012	245	20

Au ppb	Ba ppb	Cd ppb	Co ppb	Cu ppb	Hg ppb	Mg ppb	Ni ppb	Pb ppb
0.1	10	1	5	10	1	1	5	10
4.4	11900	28	340	2280	1	122	473	70
4.6	16500	23	273	2590	1	184	530	90
2.8	12600	16	169	1880	1	216	379	60
1.3	7620	33	190	1790	1	156	419	60
7.3	5450	34	96	1930	1	175	342	30
8.5	4560	29	235	2580		142	432	50
12.2	3210	33	525	2950	1	169	590	60
11.9	18900	25	184	2140	4	254	418	90
9.0	4510	25	256	1780	2	106	269	70
7.1	1670	44	186	2190	2	116	554	50
5.3	2180	50	202	1880	2	204	644	60
9.8	5890	26	228	1930	2	164	526	100
5.7	4920	35	206	1840	1	136	415	50
6.2	11900	29	183	1840		144	453	50
8.5	10900	21	139	2030		149	411	40
2.6	5770	32	111	1450		155	332	40
28.8	660	22	438	3930	14	136	747	180
27.3	2610	12	514	3220	8	145	646	220
26.8	860	9	340	3880	2	155	506	400
27.5	2400	18	303	1880	1	124	611	130
11.9	9460	26	106	1560		128	333	50
9.8	9070	26	146	1680		147	395	60
10.0	11900	24	128	1810		179	378	60
27.3	12400	30	249	1890	1	139	545	110
24.8	16100	4	70	800	3	185	200	30
19.7	13600	8	236	2210	5	181	348	70
18.2	530	15	246	1490	7	76	476	60
49.1	5710	15	1100	5790	10	171	1870	130

Appendix 1.5 (Continued)

Analyte Detection				Sb ppb 1	Sm ppb 1	Y ppb 5
Label	UTM N NAD27	UTM E NAD27	year			
MMI 41-15	4506968	485373.6	2012	6		9
MMI 41-15_5	4506968	485372.0	2012	4	3	58
MMI 41-15_10	4506968	485370.5	2012	2	2	74
MMI 41-15_20	4506968	485367.5	2012	3		7
MMI 41-16	4506968	485343.1	2012	2		13
MMI 41-16_5	4506968	485341.6	2012	1		15
MMI 41-16_10	4506968	485340.0	2012	2		
MMI 41-16_20	4506968	485337.0	2012	1	2	60
MMI 41-17	4506968	485312.6	2012	2		13
MMI 41-17_5	4506968	485311.1	2012	2	3	22
MMI 41-17_10	4506968	485309.6	2012	2	1	12
MMI 41-17_20	4506968	485306.5	2012	6	4	48
MMI 41-18	4506968	485282.1	2012	3		15
MMI 41-18_5	4506968	485280.6	2012	3	2	29
MMI 41-18_10	4506968	485279.1	2012	3		24
MMI 41-18_20	4506968	485276.0	2012	2		16
MMI 41-19	4506968	485251.6	2012	6	11	152
MMI 41-19_5	4506968	485250.1	2012	5	6	130
MMI 41-19_10	4506968	485248.6	2012	8	103	400
MMI 41-19_20	4506968	485245.5	2012	4	6	115
MMI 41-20	4506968	485221.2	2012	3	2	40
MMI 41-20_5	4506968	485219.6	2012	3	3	67
MMI 41-20_10	4506968	485218.1	2012	3	5	75
MMI 41-20_20	4506968	485215.1	2012	3	3	48
MMI 41-21	4506968	485190.7	2012	8	1	15
MMI 41-21_5	4506968	485189.2	2012	14		16
MMI 41-21_10	4506968	485187.6	2012	6	1	26
MMI 41-21_20	4506968	485184.6	2012	50	2	51

Zn ppb	Zr ppb
20	5
140	20
80	12
40	9
160	13
100	12
60	8
90	8
60	10
200	12
200	60
160	44
120	13
150	15
100	14
80	14
160	18
70	24
50	21
100	225
50	18
70	13
90	12
80	9
100	18
40	5
100	11
150	19
80	9

Appendix 1.5 (Continued)

Analyte Detection				Ag ppb 1	As ppb 10
Label	UTM N NAD27	UTM E NAD27	year		
MMI 41-22	4506968	485160.2	2012	84	50
MMI 41-22_5	4506968	485158.7	2012	91	60
MMI 41-22_10	4506968	485157.2	2012	83	30
MMI 41-22_20	4506968	485154.1	2012	30	3220
MMI 41-23	4506968	485129.7	2012	63	20
MMI 41-23_5	4506968	485128.2	2012	47	10
MMI 41-23_10	4506968	485126.7	2012	49	20
MMI41-23_20	4506968	485123.6	2012	53	20
MMI 41-24	4506968	485099.2	2012	45	
MMI 41-24_5	4506968	485097.7	2012	50	
MMI 41-24_10	4506968	485096.2	2012	38	
MMI 41-24_20	4506968	485093.1	2012	36	
MMI 41-25	4506968	485068.8	2012	50	20
MMI 41-25_5	4506968	485067.2	2012	39	10
MMI 41-25_10	4506968	485065.7	2012	45	10
MMI 41-25_20	4506968	485062.7	2012	53	20
MMI 41-26	4506968	485038.3	2012	45	10
MMI 41-26_5	4506968	485036.8	2012	50	30
MMI 41-26_10	4506968	485035.2	2012	48	10
MMI 41-26_20	4506968	485032.2	2012	46	20
MMI 41-27	4506968	485007.8	2012	58	10
MMI 41-27_5	4506968	485006.3	2012	58	40
MMI 41-27_10	4506968	485004.8	2012	52	20
MMI 41-27_20	4506968	485001.7	2012	51	

Au ppb	Ba ppb	Cd ppb	Co ppb	Cu ppb	Hg ppb	Mg ppb	Ni ppb	Pb ppb
0.1	10	1	5	10	1	1	5	10
12.7	3480	31	393	3080	1	128	688	100
11.7	4740	39	249	2270	2	126	553	110
13.3	5490	31	259	2510	2	137	610	80
99.3	260	4	23	610	40	18	209	20
9.7	10700	42	85	1330	3	191	592	50
5.3	19400	41	33	1510	1	135	289	30
5.0	15800	45	63	1500		149	248	30
6.9	11900	25	109	1660	1	194	481	30
1.8	7520	35	57	1050		181	289	40
2.8	8060	29	80	960		209	418	50
1.3	6270	38	113	1030		195	370	40
1.5	6830	46	109	1060		138	302	40
1.2	310	54	172	1050		98	236	30
1.6	4170	31	200	1140		173	427	70
0.9	3240	30	97	1340		170	347	40
1.3	6340	37	49	1510	1	133	299	30
5.9	6840	42	46	1220	1	128	286	20
7.0	3860	57	143	1610	2	126	440	40
3.7	4600	35	75	1190	1	143	356	30
1.5	4550	27	126	1330	1	139	310	30
1.4	3480	63	165	1430	1	139	464	40
3.6	2870	82	141	1820		209	638	30
1.4	4870	73	90	1060	1	100	232	30
0.9	4840	49	55	1450		136	258	20

Appendix 1.5 (Continued)

Analyte				Sb ppb	Sm ppb	Y ppb
Detection				1	1	5
Label	UTM N NAD27	UTM E NAD27	year			
MMI 41-22	4506968	485160.2	2012	9	2	37
MMI 41-22_5	4506968	485158.7	2012	6	3	46
MMI 41-22_10	4506968	485157.2	2012	8	3	40
MMI 41-22_20	4506968	485154.1	2012	13		
MMI 41-23	4506968	485129.7	2012	3	4	56
MMI 41-23_5	4506968	485128.2	2012	1	4	59
MMI 41-23_10	4506968	485126.7	2012	2		16
MMI41-23_20	4506968	485123.6	2012	7	2	27
MMI 41-24	4506968	485099.2	2012	1	2	42
MMI 41-24_5	4506968	485097.7	2012	2	2	47
MMI 41-24_10	4506968	485096.2	2012	2	2	49
MMI 41-24_20	4506968	485093.1	2012	2	2	30
MMI 41-25	4506968	485068.8	2012	5		13
MMI 41-25_5	4506968	485067.2	2012	3	5	118
MMI 41-25_10	4506968	485065.7	2012	1	2	57
MMI 41-25_20	4506968	485062.7	2012	1	2	34
MMI 41-26	4506968	485038.3	2012		3	51
MMI 41-26_5	4506968	485036.8	2012	3	3	35
MMI 41-26_10	4506968	485035.2	2012	2	2	31
MMI 41-26_20	4506968	485032.2	2012	4		11
MMI 41-27	4506968	485007.8	2012	4		12
MMI 41-27_5	4506968	485006.3	2012	1	2	26
MMI 41-27_10	4506968	485004.8	2012		1	15
MMI 41-27_20	4506968	485001.7	2012	1	1	35

Zn ppb	Zr ppb
20	5
110	19
130	15
120	14
40	6
70	11
70	11
160	17
80	11
80	10
60	8
80	11
120	16
90	8
100	12
70	8
70	13
70	10
180	17
80	11
70	12
180	20
160	42
200	18
90	16

Appendix 1.5 (Continued)

Analyte Detection				Ag ppb 1	As ppb 10
Label	UTM N NAD27	UTM E NAD27	year		
MMI 41-28	4506968	484977.3	2012	50	30
MMI 41-28_5	4506968	484975.8	2012	46	10
MMI 41-28_10	4506968	484974.3	2012	46	10
MMI 41-28_20	4506968	484971.2	2012	51	10
MMI 41-29	4506968	484946.8	2012	57	10
MMI 41-29_5	4506968	484945.3	2012	53	30
MMI 41-29_10	4506968	484943.8	2012	52	30
MMI 41-29_20	4506968	484940.7	2012	61	30
MMI 41-30	4506968	484916.4	2012	54	30
MMI 41-30_5	4506968	484914.8	2012	54	20
MMI 41-30_10	4506968	484913.3	2012	46	20
MMI 41-30_20	4506968	484910.3	2012	57	20
MMI 41-31	4506968	484885.9	2012	47	20
MMI 41-31_5	4506968	484884.4	2012	30	
MMI 41-31_10	4506968	484882.8	2012	51	20
MMI 41-31_20	4506968	484879.8	2012	43	30
MMI 41-32	4506968	484855.4	2012	23	180
MMI 41-32_5	4506968	484853.9	2012	31	180
MMI 41-32_10	4506968	484852.4	2012	31	220
MMI 41-32_20	4506968	484849.3	2012	44	40
MMI 41-33	4506968	484824.9	2012	55	20
MMI 41-33_5	4506968	484823.4	2012	66	10
MMI 41-33_10	4506968	484821.9	2012	45	20
MMI 41-33_20	4506968	484818.8	2012	59	20
MMI 41-35	4506968	484764.0	2012	66	30
MMI 41-35_5	4506968	484762.4	2012	69	20
MMI 41-35_10	4506968	484760.9	2012	48	20
MMI 41-35_20	4506968	484757.9	2012	41	

Au ppb	Ba ppb	Cd ppb	Co ppb	Cu ppb	Hg ppb	Mg ppb	Ni ppb	Pb ppb
0.1	10	1	5	10	1	1	5	10
2.2	4620	68	110	1700	2	215	498	30
1.7	4320	39	33	1540		184	316	20
1.9	3360	63	106	1680	1	173	371	20
2.4	3780	32	85	1560		253	386	30
1.8	8600	43	27	1730		254	462	20
1.3	3780	92	63	1580		269	473	20
1.4	4590	100	90	1700		280	472	20
2.7	3540	79	85	1760	1	244	574	20
1.9	3350	107	118	1640		241	588	20
1.3	2720	91	43	1560		232	315	10
1.5	2720	97	129	1440		208	468	20
2.4	5650	95	77	1720		260	514	20
0.8	310	91	76	1030		241	370	
0.7	1820	29	115	1090		171	399	20
1.0	4150	73	67	1690		333	457	20
1.8	8870	42	31	2040		308	414	20
18.9	2370	89	98	1530	20	419	205	30
18.8	4300	85	135	1310	27	277	194	40
8.1	4020	90	288	1660	5	186	423	40
1.6	3240	48	72	1700		222	569	20
0.9	7140	31	56	2150		242	633	20
1.5	7620	22	72	2260	1	250	585	20
1.7	11000	26	97	2340		244	631	30
0.9	7490	37	129	2330	1	257	920	40
2.8	7840	43	94	2110		187	555	30
3.0	15100	34	53	2340		249	475	20
1.2	18800	27	67	2050		281	475	30
0.6	7740	47	78	2160		259	560	30

Appendix 1.5 (Continued)

Analyte				Sb ppb	Sm ppb	Y ppb
Detection				1	1	5
Label	UTM N NAD27	UTM E NAD27	year			
MMI 41-28	4506968	484977.3	2012	1	5	48
MMI 41-28_5	4506968	484975.8	2012			34
MMI 41-28_10	4506968	484974.3	2012	2		22
MMI 41-28_20	4506968	484971.2	2012	4	2	31
MMI 41-29	4506968	484946.8	2012		4	58
MMI 41-29_5	4506968	484945.3	2012		3	26
MMI 41-29_10	4506968	484943.8	2012		1	17
MMI 41-29_20	4506968	484940.7	2012		1	18
MMI 41-30	4506968	484916.4	2012		1	15
MMI 41-30_5	4506968	484914.8	2012			7
MMI 41-30_10	4506968	484913.3	2012			9
MMI 41-30_20	4506968	484910.3	2012		1	16
MMI 41-31	4506968	484885.9	2012		4	94
MMI 41-31_5	4506968	484884.4	2012	1	3	123
MMI 41-31_10	4506968	484882.8	2012		3	33
MMI 41-31_20	4506968	484879.8	2012		1	19
MMI 41-32	4506968	484855.4	2012	1		11
MMI 41-32_5	4506968	484853.9	2012			15
MMI 41-32_10	4506968	484852.4	2012			13
MMI 41-32_20	4506968	484849.3	2012		3	35
MMI 41-33	4506968	484824.9	2012		4	44
MMI 41-33_5	4506968	484823.4	2012		4	85
MMI 41-33_10	4506968	484821.9	2012		12	97
MMI 41-33_20	4506968	484818.8	2012		13	100
MMI 41-35	4506968	484764.0	2012	1		10
MMI 41-35_5	4506968	484762.4	2012		4	39
MMI 41-35_10	4506968	484760.9	2012		9	95
MMI 41-35_20	4506968	484757.9	2012		9	123

Zn ppb	Zr ppb
20	5
110	25
80	11
150	18
70	13
70	16
140	21
170	29
140	19
190	30
170	14
170	23
160	19
70	8
40	7
120	15
60	14
330	8
170	7
160	11
150	17
60	15
40	12
50	16
60	18
120	19
70	14
50	11
50	10

Appendix 1.5 (Continued)

Analyte Detection				Ag ppb 1	As ppb 10
Label	UTM N NAD27	UTM E NAD27	year		
MMI 41-36	4506968	484733.5	2012	26	20
MMI 41-36_5	4506968	484732.0	2012	26	30
MMI 41-36_10	4506968	484730.4	2012	25	20
MMI 41-36_20	4506968	484727.4	2012	26	10
MMI 41-37	4506968	484703.0	2012	24	20
MMI 41-37_5	4506968	484701.5	2012	16	20
MMI 41-37_10	4506968	484700.0	2012	10	20
MMI 41-37_20	4506968	484696.9	2012	15	30
MMI 41-38	4506968	484672.5	2012	32	20
MMI 41-38_5	4506968	484671.0	2012	26	20
MMI 41-1_10	4506968	484669.5	2012	26	30
MMI41-1_20	4506968	484666.4	2012	11	40
MMI 41-39	4506968	484642.0	2012	42	10
MMI 41-39_5	4506968	484640.5	2012	27	
MMI 41-39_10	4506968	484639.0	2012	35	
MMI 41-39_20	4506968	484635.9	2012	36	10
MMI 41-40	4506968	484611.6	2012	27	30
MMI 41-40_5	4506968	484610.0	2012	29	20
MMI 41-40_10	4506968	484608.5	2012	28	
MMI 41-40_20	4506968	484605.5	2012	43	
MMI 41-41	4506968	484581.1	2012	41	
MMI 41-41_5	4506968	484579.6	2012	33	10
MMI 41-41_10	4506968	484578.0	2012	31	
MMI 41-41_20	4506968	484575.0	2012	36	10
MMI 41-42	4506968	484550.6	2012	30	
MMI 41-42_5	4506968	484549.1	2012	34	10
MMI 41-42_10	4506968	484547.6	2012	31	10
MMI 41-42_20	4506968	484544.5	2012	35	

Au ppb	Ba ppb	Cd ppb	Co ppb	Cu ppb	Hg ppb	Mg ppb	Ni ppb	Pb ppb
0.1	10	1	5	10	1	1	5	10
0.9	13200	33	102	1770		209	489	20
0.5	13400	27	77	2060		251	448	20
0.4	16100	36	98	1460		250	379	20
0.4	19700	35	75	1890		198	399	20
1.1	17400	28	81	1400		121	384	30
1.1	6810	16	92	960		70	186	30
1.6	5490	15	28	670	1	341	91	30
2.4	850	6	97	1060	1	75	281	10
7.0	12900	16	320	2370		100	601	80
6.0	21400	15	303	2000		70	642	90
17.0	15000	16	212	2010		77	741	50
16.0	12300	5	139	1430	2	58	543	20
4.4	37800	13	94	2750		194	505	60
3.8	22900	14	130	1980		171	437	80
2.0	20400	18	45	2870		160	272	40
2.2	20200	18	39	2270		164	228	30
1.4	32400	23	95	2630		210	424	40
1.2	9230	23	76	2190		173	384	40
2.1	50000	16	95	2660		219	507	50
4.2	34000	13	146	2250		204	449	100
5.1	33000	13	167	1940	1	177	388	130
1.6	15000	20	135	1980	1	231	684	60
1.8	13500	12	64	2140		193	419	40
3.1	31000	20	287	2420	1	191	590	120
1.1	38300	22	111	2010		171	541	30
1.4	35300	18	77	2350		179	422	30
1.0	41500	26	106	1990		143	367	30
2.6	30200	14	172	2430		91	394	60

Appendix 1.5 (Continued)

Analyte				Sb ppb	Sm ppb	Y ppb
Detection				1	1	5
Label	UTM N NAD27	UTM E NAD27	year			
MMI 41-36	4506968	484733.5	2012		2	17
MMI 41-36_5	4506968	484732.0	2012		4	33
MMI 41-36_10	4506968	484730.4	2012		2	18
MMI 41-36_20	4506968	484727.4	2012		2	16
MMI 41-37	4506968	484703.0	2012		2	16
MMI 41-37_5	4506968	484701.5	2012			
MMI 41-37_10	4506968	484700.0	2012			
MMI 41-37_20	4506968	484696.9	2012	4		8
MMI 41-38	4506968	484672.5	2012	7	7	80
MMI 41-38_5	4506968	484671.0	2012	13	5	53
MMI 41-1_10	4506968	484669.5	2012	10	2	23
MMI41-1_20	4506968	484666.4	2012	12		8
MMI 41-39	4506968	484642.0	2012	1	13	119
MMI 41-39_5	4506968	484640.5	2012	5	6	73
MMI 41-39_10	4506968	484639.0	2012	2		25
MMI 41-39_20	4506968	484635.9	2012	1		16
MMI 41-40	4506968	484611.6	2012		14	97
MMI 41-40_5	4506968	484610.0	2012	1	2	34
MMI 41-40_10	4506968	484608.5	2012		19	137
MMI 41-40_20	4506968	484605.5	2012	2	3	128
MMI 41-41	4506968	484581.1	2012	6	8	168
MMI 41-41_5	4506968	484579.6	2012	4	17	167
MMI 41-41_10	4506968	484578.0	2012	2	1	60
MMI 41-41_20	4506968	484575.0	2012	2	6	62
MMI 41-42	4506968	484550.6	2012		14	98
MMI 41-42_5	4506968	484549.1	2012		8	58
MMI 41-42_10	4506968	484547.6	2012		5	37
MMI 41-42_20	4506968	484544.5	2012	5	2	48

Zn ppb	Zr ppb
20	5
100	16
90	16
80	20
90	23
100	15
110	12
90	12
60	6
90	17
80	10
150	14
60	5
40	13
50	7
80	10
70	10
80	17
80	13
50	12
60	8
70	7
50	19
40	7
90	18
50	14
40	12
80	17
60	9

Appendix 1.5 (Continued)

Analyte Detection				Ag ppb 1	As ppb 10
Label	UTM N NAD27	UTM E NAD27	year		
MMI 41-43	4506968	484520.1	2012	31	20
MMI 41-43_5	4506968	484518.6	2012	26	20
MMI 41-43_10	4506968	484517.1	2012	30	20
MMI 41-43_20	4506968	484514.0	2012	19	10
MMI 41-44	4506968	484489.6	2012	23	10
MMI 41-44_5	4506968	484488.1	2012	26	
MMI 41-44_10	4506968	484486.6	2012	30	
MMI41-44_20	4506968	484483.5	2012	27	10
MMI 41-45	4506968	484459.2	2012	43	
MMI 41-45_5	4506968	484457.6	2012	41	10
MMI 41-45_10	4506968	484456.1	2012	48	
MMI 41-45_20	4506968	484453.1	2012	38	
MMI 41-46	4506968	484428.7	2012	38	
MMI 41-46_5	4506968	484427.2	2012	40	
MMI 41-46_10	4506968	484425.6	2012	45	
MMI 41-46_20	4506968	484422.6	2012	53	20
MMI 41-47	4506968	484398.2	2012	29	
MMI 41-47_5	4506968	484396.7	2012	28	
MMI 41-47_10	4506968	484395.2	2012	28	20
MMI 41-47_20	4506968	484392.1	2012	21	
MMI 41-48	4506968	484367.7	2012	81	50
MMI 41-48_5	4506968	484366.2	2012	68	
MMI 41-48_10	4506968	484364.7	2012	59	
MMI 41-48_20	4506968	484361.6	2012	43	
MMI 41-49	4506968	484337.2	2012	55	10
MMI 41-49_5	4506968	484335.7	2012	40	20
MMI 41-49_10	4506968	484334.2	2012	24	
MMI 41-49_20	4506968	484331.1	2012	33	20

Au ppb 0.1	Ba ppb 10	Cd ppb 1	Co ppb 5	Cu ppb 10	Hg ppb 1	Mg ppb 1	Ni ppb 5	Pb ppb 10
0.9	16900	36	187	2120		167	861	40
0.9	22500	38	124	1580		133	461	30
0.7	17300	26	102	1780		180	539	20
0.5	19400	36	105	1320		141	366	20
1.4	36700	28	240	2570		264	686	60
2.3	37300	24	600	2360		280	904	100
2.3	28500	19	77	2730		258	555	40
1.6	30800	26	94	2430		251	498	50
2.5	18100	31	75	2110		181	501	50
2.2	24700	31	132	2160		163	621	50
2.3	16700	22	60	2300		198	576	30
1.2	12100	25	104	2070		192	578	40
1.6	12800	20	95	2380		156	570	30
2.3	25500	22	225	2690		232	789	80
3.1	21700	27	1020	2430		237	1420	160
2.9	42300	32	1360	2960		252	1360	150
1.2	21000	15	61	2620		219	560	30
1.2	25300	20	147	2420		227	618	50
1.0	27500	17	131	2480		232	633	40
0.5	17000	37	139	1780		190	505	30
5.3	17600	29	985	4870	14	211	1610	100
5.5	20300	12	536	1450	4	263	1190	50
3.9	23100	19	438	1890	2	225	1010	80
2.6	39500	18	782	2020		265	1460	100
4.4	44900	19	613	2410	2	227	804	80
2.0	35800	31	163	2420		189	652	60
1.7	36700	15	73	1740		259	472	40
1.0	25400	36	140	2750		174	585	40

Appendix 1.5 (Continued)

Analyte Detection				Sb ppb 1	Sm ppb 1	Y ppb 5
Label	UTM N NAD27	UTM E NAD27	year			
MMI 41-43	4506968	484520.1	2012	1	8	52
MMI 41-43_5	4506968	484518.6	2012		9	57
MMI 41-43_10	4506968	484517.1	2012		8	72
MMI 41-43_20	4506968	484514.0	2012		22	139
MMI 41-44	4506968	484489.6	2012		15	127
MMI 41-44_5	4506968	484488.1	2012	1	15	166
MMI 41-44_10	4506968	484486.6	2012		11	100
MMI41-44_20	4506968	484483.5	2012		11	109
MMI 41-45	4506968	484459.2	2012		1	74
MMI 41-45_5	4506968	484457.6	2012	1	9	78
MMI 41-45_10	4506968	484456.1	2012	1	4	70
MMI 41-45_20	4506968	484453.1	2012	2	1	62
MMI 41-46	4506968	484428.7	2012		1	33
MMI 41-46_5	4506968	484427.2	2012	1	10	127
MMI 41-46_10	4506968	484425.6	2012	6	3	112
MMI 41-46_20	4506968	484422.6	2012	3	9	95
MMI 41-47	4506968	484398.2	2012	1	5	66
MMI 41-47_5	4506968	484396.7	2012	1	4	81
MMI 41-47_10	4506968	484395.2	2012	1	10	88
MMI 41-47_20	4506968	484392.1	2012		29	189
MMI 41-48	4506968	484367.7	2012	8	3	76
MMI 41-48_5	4506968	484366.2	2012	3	4	129
MMI 41-48_10	4506968	484364.7	2012	3	4	133
MMI 41-48_20	4506968	484361.6	2012	2	2	86
MMI 41-49	4506968	484337.2	2012	5	4	56
MMI 41-49_5	4506968	484335.7	2012	2	5	50
MMI 41-49_10	4506968	484334.2	2012		24	189
MMI 41-49_20	4506968	484331.1	2012	1	4	28

Zn ppb	Zr ppb
20	5
110	24
140	39
50	18
110	34
50	21
50	16
20	11
30	13
30	8
50	20
20	7
40	9
30	7
40	12
60	9
80	16
20	7
40	13
30	11
90	37
820	8
40	7
70	11
30	8
40	12
60	19
	14
70	19

Appendix 1.5 (Continued)

Analyte Detection				Ag ppb 1	As ppb 10
Label	UTM N NAD27	UTM E NAD27	year		
MMI 41-50	4506968	484306.8	2012	44	
MMI 41-50_5	4506968	484305.2	2012	33	
MMI 41-50_10	4506968	484303.7	2012	21	
MMI 41-50_20	4506968	484300.7	2012	30	20

Analyte Detection				Sb ppb 1	Sm ppb 1
Label	UTM N NAD27	UTM E NAD27	year		
MMI 41-50	4506968	484306.8	2012	3	4
MMI 41-50_5	4506968	484305.2	2012	3	2
MMI 41-50_10	4506968	484303.7	2012		7
MMI 41-50_20	4506968	484300.7	2012	1	8

Au ppb	Ba ppb	Cd ppb	Co ppb	Cu ppb	Hg ppb	Mg ppb	Ni ppb	Pb ppb
0.1	10	1	5	10	1	1	5	10
1.7	21000	13	1030	1990		277	1110	160
1.5	14700	29	1680	2050		332	1390	260
0.8	13800	19	91	1970		242	492	40
1.1	28600	31	195	2100		188	623	60

Y ppb	Zn	Zr ppb
5	20	5
141	40	10
113	100	15
110	20	17
53	70	27

Appendix 1.6: MMI analyses along line K-L, Marigold Mine,

Analyte					Ag ppb	As ppb	Au ppb	Ba ppb
Dectection					1	10	0.1	10
Label	N83E	Nad83N	year	cover ft.				
MMI 29-73	482562	4506534	2008	0-39				80
MMI 29-72	482592	4506534	2008	0-39	35		1.9	1000
MMI 29-71	482623	4506534	2008	0-39	24		0.8	3270
MMI 29-70	482653	4506534	2008	0-39	21		0.5	4680
MMI 29-69	482684	4506534	2008	0-39	31	10	2.2	5730
MMI 29-68	482714	4506534	2008	0-39	84		9.3	7350
MMI 29-67	482745	4506534	2008	0-39	30	30	1.3	6100
MMI 29-66	482775	4506534	2008	0-39	37	10	2.9	14700
MMI 29-65	482805	4506534	2008	0-39	26		6.7	6560
MMI 29-64	482836	4506534	2008	0-39	60		5.7	1680
MMI 29-63	482866	4506534	2008	0-39	26		1.3	5100
MMI 29-62	482897	4506534	2008	0-39	20		0.9	6630
MMI 29-61	482927	4506534	2008	0-39	36		1.1	4370
MMI 29-60	482958	4506534	2008	0-39	30	10	0.8	8240
MMI 29-59	482988	4506534	2008	0-39	31		0.5	2410
MMI 29-58*	483019	4506534	2008	0-39	162	20	1.6	4930
MMI 29-56	483080	4506534	2008	0-39	34	20	1.1	6780
MMI 29-55	483110	4506534	2008	0-39	43	20	2.7	8260
MMI 29-54	483141	4506534	2008	0-39	25		0.4	3780
MMI 29-53	483171	4506534	2008	0-39	19		0.3	4470
MMI 29-52	483202	4506534	2008	0-39	37	20	1.1	4850
MMI 29-51	483232	4506534	2008	0-39	25	10	0.4	3170
MMI 29-50	483263	4506534	2008	0-39	31	20	1.1	4160
MMI 29-49	483293	4506534	2008	0-39	49	60	3.3	2670
MMI 29-48	483324	4506534	2008	0-39	55	40	1.8	3970
MMI 29-47	483354	4506534	2008	0-39	51	30	2.3	7200
MMI 29-46	483385	4506534	2008	0-39	68	40	2.9	5890
MMI 29-45	483415	4506534	2008	0-39	130		7.4	5550
MMI 29-44	483446	4506534	2008	0-39	20		0.5	5590
MMI 29-43*	483476	4506534	2008	0-39	74	40	5.3	4320

, Northern Nevada (*soil disturbance)

Cd ppb 1	Co ppb 5	Cu ppb 10	Pb ppb 10	Sm ppb 1	Y ppb 5	Zn ppb 20	Zr ppb 5
2	7	110				30	
20	1250	1140	180		41	70	
23	72	910	40		22	30	6
26	113	1200	50	39	247	50	34
22	102	1130	60	3	46	40	13
18	324	1590	160	3	144	30	
33	86	1120	50		11	40	7
41	335	1680	130	3	52	80	19
30	435	1700	100	5	90	70	17
16	289	1620	120		105	20	5
30	433	1100	120	28	207	110	19
29	119	1010	50	32	211	240	19
19	121	920	80		18	60	8
42	148	1380	60	17	118	100	21
18	50	750	20		9	50	6
27	105	890	40	1	16	110	10
37	107	1050	40	5	41	70	15
20	78	2320	40	3	40	30	14
24	23	870	20	6	50	50	12
28	42	780	20	20	114	100	17
38	26	730	10	4	29	70	8
37	70	1080	20	15	100	60	24
91	240	1630	50	16	120	180	31
59	482	1160	50	3	29	160	35
109	288	1240	40	10	77	170	36
85	222	1430	60	12	78	300	31
46	119	1780	30	3	35	50	9
9	362	1740	150		13	40	
21	61	700	30	26	168	60	16
39	225	1600	60		10	90	11

Appendix 1.6 (Continued)

Analyte Dectection Label	N83E	Nad83N	year	cover ft.	Ag ppb 1	As ppb 10	Au ppb 0.1
MMI 29-40*	483567	4506534	2008	0-39	31		0.8
MMI 29-39	483598	4506534	2008	0-39	45	40	2.6
MMI 29-38	483628	4506534	2008	40-200	64	20	23.8
MMI 29-37	483659	4506534	2008	40-200	25		0.8
MMI 29-36	483689	4506534	2008	40-200	35	10	1.1
MMI 29-35	483720	4506534	2008	40-200	26	10	0.4
MMI 29-34	483750	4506534	2008	40-200	27		1.1
MMI 29-33	483781	4506534	2008	40-200	48	20	1.5
MMI 29-32	483811	4506534	2008	40-200	35	10	0.9
MMI 29-31	483842	4506534	2008	0-39	79		3.3
MMI 29-30	483872	4506534	2008	0-39	138		7.1
MMI 29-29	483903	4506534	2008	0-39	37		1.0
MMI 29-28	483933	4506534	2008	0-39	68		2.2
MMI 29-27	483964	4506534	2008	0-39	20	10	1.1
MMI 29-26	483994	4506534	2008	0-39	26	20	1.1
MMI 29-A	485000	4506534	2008	40-200	37		1.2
MMI 29-B	485031	4506534	2008	40-200	23		0.5
MMI 29-C	485061	4506534	2008	40-200	16		0.2
MMI 29-D*	485091	4506534	2008	40-200	11		0.1
MMI 29-E*	485122	4506534	2008	40-200	21		4.1
MMI 29-F	485152	4506534	2008	40-200	20		1.1
MMI 29-G	485183	4506534	2008	40-200	29		0.8
MMI 29-H	485213	4506534	2008	40-200	46		2.1
MMI 29-I	485244	4506534	2008	40-200	35	20	16.3
MMI 29-J	485274	4506534	2008	40-200	26	20	2.6
MMI 29-K	485305	4506534	2008	40-200	24	10	1.1
MMI 29-L	485335	4506534	2008	40-200	66		6.5
MMI 29-M	485366	4506534	2008	40-200	38	10	2.8

Ba ppb 10	Cd ppb 1	Co ppb 5	Cu ppb 10	Pb ppb 10	Sm ppb 1	Y ppb 5	Zn ppb 20	Zr ppb 5
3920	31	43	1380	20	1	43	50	8
4340	13	156	1260	40			60	9
10700	5	98	930	30		18	30	
18200	22	85	1290	50	42	277	90	14
18000	30	124	1310	50	16	109	80	13
17900	30	114	1660	40	32	207	70	21
13800	21	118	2020	50	10	101	50	13
15100	25	68	1760	40	10	83	70	19
12700	48	186	880	50	43	267	100	35
7010	20	110	1630	50		55	50	0
15500	21	456	1960	160	27	262	30	12
22400	49	212	1440	70	30	230	180	23
8200	11	43	1450	50		97	0	
11200	15	115	940	20		12	30	8
9470	29	216	2000	40	10	84	90	14
5690	17	48	1340	40		13	60	
2440	26	41	1090	20		30	60	8
4620	26	44	1100	30	25	163	70	13
2690	18	28	740	20	7	104	40	10
5970	19	68	1310	30	2	22	60	9
5350	18	42	1130	30		21	40	6
6620	21	56	850	50		37	70	9
5950	15	87	1600	80		96	40	6
9040	15	257	1360	90	2	31	80	11
3910	37	69	1030	30	3	25	90	20
6980	32	65	1060	30	26	121	70	23
7390	17	138	2370	80	2	137	40	
5500	15	97	1030	40		21	50	8

Appendix 1.6 (Continued)

Analyte					Ag ppb	As ppb	Au ppb	Ba ppb	Cd ppb	Co ppb	Cu ppb	Pb ppb	Sm ppb	Y ppb	Zn ppb	Zr ppb
Dectection					1	10	0.1	10	1	5	10	10	1	5	20	5
Label	N83E	Nad83N	year	cover ft.												
MMI 29-N	485396	4506534	2008	40-200	19	30	8.1	7880	34	68	1100	40	16	85	90	24
MMI 29-O	485427	4506534	2008	40-200	28	20	2.2	8180	30	59	1600	30	24	150	80	16
MMI 29-P	485457	4506534	2008	40-200	16	30	2.5	3500	49	103	830	40	23	104	190	47
MMI 29-Q	485488	4506534	2008	40-200	18	20	2.0	4640	25	133	1020	30	18	92	80	26
MMI 29-R	485518	4506534	2008	40-200	27	50	5.6	2210	38	70	1390	20	25	162	110	14

Appendix 1.7: MMI analyses along line M-N, Marigold Mine, Northern Nevada

Analyte Detection Label	N83E	Nad83N	year	cover ft.	Ag ppb 1	As ppb 10	Au ppb 0.1	Ba ppb 10	Cd ppb 1	Co ppb 5	Cu ppb 10	Pb ppb 10	Zn ppb 20	Zr ppb 5
MMI 27-25	483842	4505620	2007	40-200	31		4.9	6570	30	450	370	90	60	
MMI 27-24	483872	4505620	2007	40-200	32		3.3	7100	39	265	1190	90	80	
MMI 27-23	483903	4505620	2007	40-200	32		4.6	6120	33	414	420	90	70	
MMI 27-22	483933	4505620	2007	40-200	32		5.0	6680	30	412	350	90	70	
MMI 27-21	483964	4505620	2007	40-200	16	20	0.6	8320	36	126	970	50	100	16
MMI 27-20	483994	4505620	2007	40-200	42		4.3	8730	28	563	810	160	60	
MMI 27-19	484025	4505620	2007	40-200	27		2.7	10800	33	232	1150	80	70	
MMI 27-18	484055	4505620	2007	40-200	24		2.0	9520	55	523	390	170	130	
MMI 27-17	484086	4505620	2007	40-200	19		1.5	16700	46	414	710	170	110	
MMI 27-16	484116	4505620	2007	40-200	27		2.3	12800	38	333	770	100	60	
MMI 27-15	484147	4505620	2007	40-200	22		1.8	17100	39	263	1080	180	70	15
MMI 27-14	484177	4505620	2007	40-200	36		4.2	3620	38	386	520	130	110	
MMI 27-13	484208	4505620	2007	40-200	16	10	1.1	14800	59	255	1110	70	170	35
MMI 27-12	484238	4505620	2007	>200	33		5.3	12400	44	240	1680	70	80	
MMI 27-11	484269	4505620	2007	40-200	24		3.5	15700	42	227	830	100	130	
MMI 27-10	484299	4505620	2007	40-200	33		5.4	10600	24	234	1300	70	60	
MMI 27-9	484329	4505620	2007	40-200	65		18.0	7050	21	337	1170	100	20	
MMI 27-8	484360	4505620	2007	40-200	42		5.3	4200	27	819	600	180	30	
MMI 27-7	484390	4505620	2007	40-200	18	20	0.7	7320	135	240	990	110	540	49
MMI 27-6	484421	4505620	2007	40-200	21	10	1.2	12000	123	297	1180	80	340	11
MMI 27-5	484451	4505620	2007	>200	30	10	1.3	13400	60	217	1010	90	220	
MMI 27-4	484482	4505620	2007	>200	24	10	0.8	17300	72	250	1270	60	170	10
MMI 27-3	484512	4505620	2007	>200	23		1.1	4380	44	93	970	30	130	
MMI 27-2	484543	4505620	2007	>200	46	30	1.2	3870	70	153	1470	30	130	5
MMI 27-1	484573	4505620	2007	40-200	33	50	1.2	1990	68	263	1000	60	200	15

Appendix 2: Total Organic Carbon and MMI analyses of two soil profiles from the Gil prospect, Alaska

ANALYTE	Depth	TOC	Ag	As	Au	Ba	Bi	Ca	Cd	Co	Cs	Cu	Fe	Ga	K	Li	Mg	Mn	Ni
DETECTION			1	10	0.1	10	1	10	1	5	0.5	10	1	1	0.1	5	1	0.001	5
UNITS	cm	%	ppb	ppb	ppb	ppb	ppb	ppm	ppb	ppb	ppb	ppb	ppm	ppb	ppm	ppb	ppm	ppm	ppb
W9825 : 0-2	1	15.6	0.5	5	0.05	3810	12	230	11	1000	0.3	30	227	7	76.5	23	99	1.58	151
W9825 : 2-4	3	5.6	5	20	0.6	2760	14	120	30	430	0.7	180	177	7	40.2	8	48	1.69	574
W9825 : 4-6	5	3.0	6	5	2.7	4340	11	130	17	503	0.8	290	129	4	32.3	6	66	0.841	758
W9825 : 6-8	7	2.2	7	20	8.3	4600	20	140	15	458	1.4	350	136	4	29.9	5	62	0.799	779
W9825 : 8-10	9	2.8	8	5	3.6	6370	10	140	19	482	3.2	640	126	3	21.7	2	65	0.405	1180
W9825 : 10-12	11	1.8	10	10	5.3	8380	8	180	19	462	5.3	820	119	3	18.8	2	71	0.398	1350
W9825 : 12-14	13	1.9	10	10	6.4	7160	9	200	19	432	5.3	1000	114	3	14.5	2	68	0.402	1480
W9825 : 14-16	15	1.5	11	5	9.3	9600	7	260	21	380	3.8	1140	98	2	14.2	2	97	0.312	1890
W9825 : 16-18	17	2.0	9	5	12.1	9030	6	270	19	300	3.2	1060	89	2	11.9	2	95	0.215	1880
W9825 : 18-20	19	1.9	9	5	5.9	8070	6	250	20	324	3.1	1020	94	2	10.9	2	89	0.241	2190
W9825 : 20-22	21	1.7	11	5	6.8	7150	6	260	20	361	4.6	1120	102	2	11.1	2	94	0.317	2200
W9825 : 22-24	23	1.3	10	5	7.9	7890	4	300	17	263	3.7	1190	74	2	10.4	2	105	0.213	2070
W9825 : 24-26	25	1.5	10	5	6.9	5290	5	280	19	416	4.5	1310	85	2	10.3	2	108	0.406	2100
W9825 : 26-28	27	1.3	10	5	10.1	4780	7	280	18	351	4	1040	73	2	8.5	2	99	0.387	1750
W9825 : 28-30	29	1.4	16	5	12.3	7390	6	310	19	256	2.6	1370	65	2	9.3	2	114	0.221	2100
W9825 : 30-32	31	1.1	13	5	9.9	9790	3	320	13	134	2.9	1350	52	2	9.1	2	107	0.109	1750

			Ag	As	Au	Ba	Bi	Ca	Cd	Co	Cs	Cu	Fe	Ga	K	Li	Mg	Mn	Ni
W9829: 0-2	1	10.1	0.5	140	0.8	4300	3	640	181	1180	0.2	600	107	4	130	86	174	4.81	527
W9829: 2-4	3	10.7	1	50	0.2	3880	22	220	124	1210	0.2	580	279	9	87.8	52	84	0.974	648
W9829: 4-6	5	5.7	4	5	0.1	3060	4	90	25	637	0.2	330	136	6	43.2	2	43	0.143	804
W9829: 6-8	7	3.2	8	5	0.5	3530	2	80	15	399	0.2	440	115	6	29.4	2	36	0.082	772
W9829: 8-10	9	1.3	10	30	4.3	3780	7	70	14	258	2.2	580	104	8	23.9	2	31	0.182	884
W9829: 10-12	11	1.3	11	40	3.3	4650	8	70	11	200	2.9	800	89	8	18	6	30	0.136	735
W9829: 12-14	13	0.9	13	40	3	5830	7	110	13	266	3.7	1120	89	7	13.9	2	37	0.23	880
W9829: 14-16	15	1.0	14	40	4.8	6390	5	130	12	239	3.7	1450	68	5	11.7	2	41	0.178	884
W9829: 16-18	17	1.0	16	20	5.8	5910	3	120	12	198	3	1760	59	4	9.9	2	40	0.092	1070
W9829: 18-20	19	1.0	13	20	3.1	5310	3	130	10	162	3.2	1510	63	5	8.9	2	39	0.082	1030
W9829: 20-22	21	1.0	15	20	3.5	5220	3	140	9	134	3.1	1540	56	4	8.8	2	43	0.079	963
W9829: 22-24	23	0.8	28	10	4.1	5360	2	160	7	112	2.6	1550	50	3	8.2	2	52	0.062	926
W9829: 24-26	25	1.5	17	5	2.4	4370	2	120	11	117	2.2	1650	65	3	5.8	2	47	0.046	1200

Appendix 2 (continued)

ANALYTE	Depth	TOC	P	Pb	Rb
DETECTION			0.1	10	5
UNITS	cm	%	ppm	ppb	ppb
W9825 : 0-2	1	15.6	3.3	20	22
W9825 : 2-4	3	5.6	4.3	250	28
W9825 : 4-6	5	3.0	1.4	250	48
W9825 : 6-8	7	2.2	1.9	260	80
W9825 : 8-10	9	2.8	1	290	117
W9825 : 10-12	11	1.8	0.9	260	167
W9825 : 12-14	13	1.9	1.1	230	160
W9825 : 14-16	15	1.5	0.7	240	141
W9825 : 16-18	17	2.0	0.7	190	119
W9825 : 18-20	19	1.9	0.6	210	117
W9825 : 20-22	21	1.7	0.7	230	156
W9825 : 22-24	23	1.3	0.4	200	133
W9825 : 24-26	25	1.5	0.6	210	141
W9825 : 26-28	27	1.3	0.5	190	132
W9825 : 28-30	29	1.4	0.3	200	106
W9825 : 30-32	31	1.1	0.3	130	110

			P	Pb	Rb
W9829: 0-2	1	10.1	7.7	500	13
W9829: 2-4	3	10.7	8.8	540	17
W9829: 4-6	5	5.7	1.9	240	12
W9829: 6-8	7	3.2	1	200	26
W9829: 8-10	9	1.3	1.6	350	87
W9829: 10-12	11	1.3	1.2	350	111
W9829: 12-14	13	0.9	1.6	330	141
W9829: 14-16	15	1.0	1	320	159
W9829: 16-18	17	1.0	0.6	310	148
W9829: 18-20	19	1.0	0.8	300	151
W9829: 20-22	21	1.0	0.6	300	154
W9829: 22-24	23	0.8	0.5	270	147
W9829: 24-26	25	1.5	0.4	310	119

Sc	Sr	Th	Ti	U	Zn	Zr
5	10	0.5	3	1	20	5
ppb	ppb	ppb	ppb	ppb	ppb	ppb
45	1870	10.5	192	9	880	8
54	910	36.4	463	18	1410	26
52	1170	36.5	259	19	410	26
58	1000	44.6	315	22	400	39
77	1230	46.4	205	31	310	34
98	1460	52.2	174	41	280	43
113	1300	60.4	220	51	220	57
133	1870	59.4	94	62	270	50
132	1830	54.7	104	58	210	49
129	1830	55.3	81	57	180	46
127	1820	61.9	93	61	170	55
136	2080	58.8	65	67	170	53
137	1960	64.3	58	70	190	57
124	1800	61.9	88	65	230	57
152	2110	56	48	82	180	54
121	2150	54	92	74	110	64

Sc	Sr	Th	Ti	U	Zn	Zr
38	3850	16.4	71	62	8400	17
58	1910	20.3	239	41	3790	17
39	1070	13.7	156	14	460	7
42	990	17.4	268	14	200	11
68	780	42	797	23	170	38
102	760	68	1210	36	60	64
143	860	95	1210	52	90	87
166	940	103	850	58	40	76
165	920	85.6	549	61	40	56
142	870	81.6	580	50	30	58
133	950	82.3	463	54	40	56
124	1080	82.3	304	54	40	48
136	1020	75.4	231	59	30	38

Appendix 2 (continued)

ANALYTE	Depth	TOC	Ce
DETECTION			5
UNITS	cm	%	ppb
W9825 : 0-2	1	15.6	12
W9825 : 2-4	3	5.6	128
W9825 : 4-6	5	3.0	161
W9825 : 6-8	7	2.2	280
W9825 : 8-10	9	2.8	489
W9825 : 10-12	11	1.8	933
W9825 : 12-14	13	1.9	1130
W9825 : 14-16	15	1.5	1180
W9825 : 16-18	17	2.0	1310
W9825 : 18-20	19	1.9	1110
W9825 : 20-22	21	1.7	940
W9825 : 22-24	23	1.3	1220
W9825 : 24-26	25	1.5	1020
W9825 : 26-28	27	1.3	1110
W9825 : 28-30	29	1.4	1420
W9825 : 30-32	31	1.1	1560
			Ce
W9829: 0-2	1	10.1	161
W9829: 2-4	3	10.7	72
W9829: 4-6	5	5.7	41
W9829: 6-8	7	3.2	65
W9829: 8-10	9	1.3	432
W9829: 10-12	11	1.3	900
W9829: 12-14	13	0.9	1220
W9829: 14-16	15	1.0	1400
W9829: 16-18	17	1.0	1170
W9829: 18-20	19	1.0	951
W9829: 20-22	21	1.0	845
W9829: 22-24	23	0.8	884
W9829: 24-26	25	1.5	699

Dy	Er	Eu	Gd	La	Nd	Pr	Sm	Tb	Y	Yb
1	0.5	0.5	1	1	1	1	1	1	1	1
ppb	ppb	ppb	ppb	ppb	ppb	ppb	ppb	ppb	ppb	ppb
6	11	0.8	3	6	8	2	2	0.5	25	23
45	27	7.4	34	52	102	19	27	5	195	20
60	30	10.2	47	59	142	25	36	8	255	21
61	30	13.4	58	117	209	40	50	8	265	20
108	53	22.1	100	151	343	62	82	15	541	35
141	65	32.1	142	323	547	105	120	20	742	43
160	73	39	172	374	652	125	151	22	812	49
187	93	44.1	199	469	676	126	165	26	959	62
179	89	44.9	201	508	717	139	167	25	939	61
177	86	42.2	184	434	658	123	155	25	914	61
157	79	36	160	313	559	104	135	21	850	56
165	80	39.8	178	480	651	126	154	23	831	57
165	81	37.6	169	375	582	110	141	23	877	57
141	66	34.6	153	457	593	116	133	20	715	47
198	99	49.2	221	522	776	147	187	28	1030	68
162	77	46.1	198	571	798	152	179	24	808	54

Dy	Er	Eu	Gd	La	Nd	Pr	Sm	Tb	Y	Yb
28	18	6.9	29	60	105	21	26	4	119	18
41	37	5	23	27	56	10	16	4	184	33
39	31	3.5	16	13	39	7	11	4	174	25
42	32	4.4	21	22	59	10	15	4	188	25
79	37	16.6	76	146	286	54	65	11	341	26
129	55	28.8	129	326	542	106	113	18	625	37
189	88	45.3	203	505	789	147	179	27	954	59
214	106	51.8	232	625	889	168	204	30	1090	76
229	115	50.8	233	481	818	148	196	31	1180	82
171	85	40.5	183	369	655	119	157	24	914	64
151	75	35.5	162	307	567	105	137	21	763	54
147	71	36.4	165	316	589	109	143	21	747	50
169	85	35.1	162	235	531	93	134	22	880	61

Appendix 3: MMI analyses of soil from the Gil prospect, interior Alaska

ANALYTE	Ag	Al	As	Au	Ba	Bi	Ca	Cd	Ce	Co	Cs	Cu
METHOD	MMI-M											
DETECTION	1	1	10	0.1	10	1	10	1	5	5	0.5	10
UNITS	ppb	ppm	ppb	ppb	ppb	ppb	ppm	ppb	ppb	ppb	ppb	ppb
W9816	6	86	100	0.5	2750	2	50	15	142	436	1.5	**4480**
W9817	4	89	40	0.7	2080	3	30	2	41	201	2.4	2820
W9818	4	90	40	0.9	2300	6	40	2	35	178	2.2	2000
REP-W9818	3	83	50	0.8	2160	7	30	2	42	167	2.4	2260
W9819	2	102	5	0.5	1470	8	40	9	20	269	0.8	610
W9820	4	69	40	0.7	2430	2	70	5	53	233	1.3	1830
W9821	29	91	5	0.3	5240	<1	330	17	543	36	<0.5	2580
W9822	2	69	50	0.05	1720	2	60	4	38	218	0.9	1850
W9823	9	125	5	0.7	2770	6	80	20	206	513	1.4	620
W9824	4	189	5	0.4	2350	3	110	5	21	385	1	90
W9825	10	182	5	6.2	4970	8	150	20	866	510	5.6	820
W9827	8	>200	5	1	2460	4	40	13	103	224	2	200
W9828	9	>200	60	3.6	5030	8	100	12	647	191	4.1	350
W9829	16	193	40	3.1	4580	5	100	9	791	214	3.8	1270
W9830	13	>200	30	1.6	3980	3	50	11	722	161	4.6	1080
W9864	15	141	20	6.4	6820	6	210	14	734	109	3.9	910
W9865	11	126	10	6.4	9810	2	400	11	731	138	2	510
W9866	**16**	74	5	**10.2**	**10300**	<1	**570**	13	538	88	0.8	1230
W9867	16	125	40	3.4	4710	1	230	17	420	64	2.5	650
W9868	13	>200	160	5.9	4250	8	100	7	489	123	6	510
W9869	10	195	60	2.7	4220	3	90	18	593	179	3.3	670
W9870	9	>200	70	1.8	3130	4	20	18	380	307	4.3	860
REP-W9870	9	>200	80	1.7	3170	4	20	16	304	288	4	810

Appendix 3 (continued)

ANALYTE	Dy	Er	Eu	Fe	Ga	Gd
METHOD	MMI-M					
DETECTION	1	0.5	0.5	1	1	1
UNITS	ppb	ppb	ppb	ppm	ppb	ppb
W9816	27	17.5	5.4	396	3	24
W9817	8	5.8	1.3	320	2	6
W9818	7	6.2	1.3	309	2	6
REP-W9818	7	5.2	1.2	349	2	6
W9819	15	14.2	1.4	217	4	7
W9820	7	4.2	1.6	344	2	7
W9821	110	65.6	24	53	1	119
W9822	5	2.7	1	354	3	5
W9823	77	41.6	13.2	188	3	63
W9824	15	14.7	1.8	166	4	8
W9825	171	86.6	38.1	123	4	178
W9827	49	29.4	7.2	149	5	35
W9828	60	27.4	16	128	9	70
W9829	146	73	33.1	87	7	152
W9830	120	54.1	26.3	95	7	117
W9864	120	61.2	28.7	66	3	126
W9865	83	39.6	24.4	48	3	107
W9866	71	38.2	19.5	20	<1	87
W9867	72	37	15.4	77	2	74
W9868	85	43	19.3	92	8	89
W9869	126	63.7	25.7	123	4	121
W9870	118	66.6	18.8	185	4	93
REP-W9870	102	58.3	15.4	182	4	78

K	La	Mg	Mn	Nb	Nd	Ni	P
0.1	1	1	10	0.5	1	5	0.1
ppm	ppb	ppm	ppb	ppb	ppb	ppb	ppm
7.3	57	15	5870	3.3	83	1250	3.3
6.1	18	17	1700	2.1	21	696	1.9
4.5	14	26	900	1.7	18	626	1.8
4.4	19	22	790	2.4	21	660	2.3
3.6	8	24	1110	0.8	15	201	1.2
4.8	23	53	1190	1.4	28	805	1.7
7.5	179	71	680	0.25	344	1940	0.2
10.2	17	36	5380	2.6	19	340	3.1
7.9	59	39	560	1.1	168	792	1.2
15.7	7	57	180	0.8	19	509	0.9
12.3	302	67	2510	1.1	574	1730	1.4
17.4	32	30	180	0.8	94	605	1.7
8.6	324	39	2020	3.1	309	592	2.7
11.4	337	40	1590	2.5	530	785	1.1
8.2	276	26	610	1.9	463	637	1.4
7.1	310	60	650	0.5	463	751	0.4
6.8	356	94	480	0.25	457	601	0.1
8.3	165	103	860	0.25	283	837	<.1
7.3	146	57	730	0.25	238	694	0.5
8.7	182	31	980	1.9	305	388	1.6
6.7	188	29	840	0.9	385	763	1.9
5.1	110	9	630	2.3	267	797	3.4
5.2	88	10	630	2.3	215	764	3.5

Appendix 3 (continued)

ANALYTE	Pb	Pr	Rb	Sb	Sc	Sm
METHOD	MMI-M					
DETECTION	10	1	5	1	5	1
UNITS	ppb	ppb	ppb	ppb	ppb	ppb
W9816	50	19	88	7	88	21
W9817	20	5	99	2	26	5
W9818	30	4	80	2	27	5
REP-W9818	30	5	80	3	28	5
W9819	380	3	38	3	34	5
W9820	10	6	49	3	30	6
W9821	160	69	46	2	101	92
W9822	30	5	43	3	23	5
W9823	260	32	50	1	54	47
W9824	20	3	125	<1	39	6
W9825	240	121	177	<1	109	143
W9827	220	18	76	<1	46	25
W9828	230	74	128	2	65	62
W9829	330	115	149	2	127	127
W9830	350	103	160	2	118	100
W9864	230	101	138	1	111	109
W9865	150	103	75	<1	80	99
W9866	80	59	68	<1	75	71
W9867	160	51	91	<1	79	58
W9868	350	65	166	2	81	73
W9869	270	80	99	<1	95	97
W9870	370	54	119	1	103	72
REP-W9870	350	42	115	1	96	59

Sr	Tb	Th	Ti	U	Y	Yb	Zn	Zr
10	1	0.5	3	1	1	1	20	5
ppb	ppb	ppb	ppb	ppb	ppb	ppb	ppb	ppb
470	4	51.1	803	41	158	17	160	140
340	1	16	448	13	39	5	60	40
460	1	19.2	456	18	39	6	90	37
400	1	20.6	603	20	36	4	80	42
410	2	19.2	433	20	75	11	420	23
590	1	19.2	377	23	35	3	110	34
1790	18	36.3	70	76	708	52	170	79
430	0.5	16.9	810	13	23	2	70	40
700	12	23.8	227	25	411	28	470	22
950	2	14.6	168	15	79	21	50	17
1120	28	58.4	180	55	999	61	160	58
430	7	21.7	200	14	255	23	200	17
620	11	71	1070	28	297	18	180	59
700	24	91.8	1100	56	780	51	50	78
470	20	64.1	778	42	611	34	80	68
1270	20	70.3	279	61	674	47	60	54
2030	15	60.4	181	54	464	29	50	40
2440	12	64.4	8	76	397	30	30	49
1240	12	30.7	134	57	410	25	130	39
630	14	65.3	786	39	456	30	190	76
800	20	42.2	219	41	692	44	300	45
260	17	56.4	347	42	624	46	410	67
260	15	54.9	331	39	541	43	390	67

Appendix 3 (continued)

ANALYTE	Ag	Al	As	Au	Ba
METHOD	MMI-M				
DETECTION	1	1	10	0.1	10
UNITS	ppb	ppm	ppb	ppb	ppb
W9871	7	>200	**920**	3.7	3330
W9872	8	>200	310	2.2	2970
W9873	10	198	360	3.4	1980
W9874	6	188	420	1	1920
W9875	7	>200	160	2.8	3130
W9876	9	104	30	3.3	4800
W9877	7	179	80	1	2220

ANALYTE	Dy	Er	Eu	Fe	Ga	Gd
METHOD	MMI-M					
DETECTION	1	0.5	0.5	1	1	1
UNITS	ppb	ppb	ppb	ppm	ppb	ppb
W9871	28	14.2	7.3	223	7	31
W9872	131	65	29	135	7	135
W9873	81	42.4	16.8	183	5	77
W9874	54	31.4	10.2	221	7	49
W9875	211	114	36.6	147	5	185
W9876	66	36	12.7	75	1	62
W9877	98	53	14.6	187	5	77

Bi	Ca	Cd	Ce	Co	Cs	Cu
1	10	1	5	5	0.5	10
ppb	ppm	ppb	ppb	ppb	ppb	ppb
5	60	8	273	133	4.8	220
2	40	10	889	129	4.4	750
4	40	16	404	156	3	820
5	50	8	277	186	1.7	330
4	60	14	1080	229	2.1	790
<1	310	12	259	24	1.7	210
3	40	17	373	195	1.5	640

K	La	Mg	Mn	Nb	Nd	Ni	P
0.1	1	1	10	0.5	1	5	0.1
ppm	ppb	ppm	ppb	ppb	ppb	ppb	ppm
9.5	112	15	2910	4	133	246	5.8
6.8	273	9	1350	3.3	481	636	5
10.5	125	13	1100	3.5	257	668	4.9
7.7	76	16	2200	4.2	145	427	5.7
5.2	219	19	2330	1.7	533	953	3.1
5.3	88	40	290	0.25	161	440	0.3
5.7	72	10	1290	1.4	189	484	2.9

Appendix 3 (continued)

ANALYTE	Pb	Pr	Rb	Sb	Sc	Sm
METHOD	MMI-M					
DETECTION	10	1	5	1	5	1
UNITS	ppb	ppb	ppb	ppb	ppb	ppb
W9871	250	32	131	5	47	30
W9872	250	105	138	2	104	114
W9873	330	53	112	2	80	65
W9874	320	31	73	2	62	39
W9875	380	107	86	1	120	139
W9876	110	33	78	<1	57	45
W9877	360	36	84	1	87	52

Sr	Tb	Th	Ti	U	Y	Yb	Zn	Zr
10	1	0.5	3	1	1	1	20	5
ppb	ppb	ppb	ppb	ppb	ppb	ppb	ppb	ppb
320	5	55.4	969	16	139	10	520	94
200	22	63.6	778	39	735	41	240	113
280	13	69	598	37	414	29	270	110
420	9	51.6	898	19	294	23	350	63
570	32	59.8	310	51	1200	77	350	52
1080	10	16	36	51	376	23	120	17
280	14	45.7	336	42	507	36	590	55